# ASSESSMENT OF THE VISUAL THALAMIC CIRCUITRY IN HALLUCINATIONS IN DEMENTIA WITH LEWY BODIES


Daniel Erskine

Thesis submitted in candidature for the degree of Doctor of Philosophy

Newcastle University

Institute of Neuroscience

December 2016

## Abstract

Background

Visual hallucinations occur in 70-90% of patients with dementia with Lewy bodies (DLB) and are related to decreased quality of life for patients. However, the underlying neuropathological changes that promote the manifestation of visual hallucinations in DLB are not known. Several hypotheses of visual hallucinations in DLB have either directly implicated the lateral geniculate nucleus (LGN), pulvinar and superior colliculus or suggested impairments in their putative functions.

Methods

*Post-mortem* LGN, pulvinar and superior colliculus tissue was obtained from DLB cases with a clinical history of visual hallucinations and compared to cognitively normal control and Alzheimer's disease (AD) cases without visual hallucinations. Neuropathological lesions were quantified in individual cases using densitometry and neuronal and glial cell populations were quantified with stereology. RNA sequencing and subsequent bioinformatics analysis of biological pathway alterations was performed by a collaborator on pulvinar tissue from DLB and non-hallucinating control cases. The bioinformatics data was used to identify protein targets based on pathway alterations, which were then investigated using western blot analysis.

Results

Lewy body pathology and neuronal loss was specifically found in the pulvinar and superior colliculus of DLB cases, particularly in regions implicated in visual attention and target selection. In contrast, AD cases had more widespread degenerative changes. Molecular analysis of the pulvinar demonstrated reduced expression of several synaptic markers, concomitant with elevated expression of several astrocytic markers in DLB.

Conclusion

The relative specificity of changes in visual thalamic regions may contribute to the occurrence of visual hallucinations in DLB. Synaptic degeneration in the pulvinar likely further impedes visual attentional function in DLB. The present results may indicate DLB patients have impairments in directing visual attention to external stimuli, thus facilitating visual hallucinations by an over-reliance upon expectations and experience rather than stimulus-driven perception.

# Acknowledgements

As with any scientific study, this work would not have been possible without the help and advice of many people. My first thanks must go to those individuals who kindly donated their brain tissue for research purposes, whose donation makes this work possible. I hope they would be proud of what we have learned as a result of their generous gift. I would also like to express my thanks to Yvonne Emily Mairy, whose generous donation to the National Institute for Health Research Biomedical Research Unit in Lewy body dementia at Newcastle University funded this project.

I am particularly indebted to my supervisors, Ahmad Khundakar, Chris Morris and Alan Thomas, who have each aided my development enormously with their different, but mutually complimentary, areas of expertise. I am very grateful for their encouragement and enthusiasm, and for giving me the opportunity to carry out this project.

A special note of thanks must go to Johannes Attems and Ian McKeith, who have contributed immensely to helping me develop as a researcher and encouraged me in developing my future career plans. I would also like to thank John-Paul Taylor and Paul Donaghy, who facilitated my meeting patients in the clinic to discuss visual hallucinations from the viewpoint of the person experiencing them. No amount of reading could have given me such a wonderful insight into this phenomenon, so I am deeply grateful for this experience.

I must give special thanks to Mary Johnson, Ros Hall and Lynne Ramsay, who have taught me a lot about histological staining techniques (as an art as well as a science, Mary!) and answered my unending questions about often obscure techniques and optimisation of protocols. I would also like to thank Peter Hanson and Preeti Singh, who instructed me in conducting immunoassays, particularly in development and optimisation, and helped immensely with troubleshooting when things did not go to plan.

Science does not just work by research in a lab, but by the mutual support and collaboration amongst colleagues/friends (this line becomes blurred). I would like to express my deepest thanks to my friends Kirsty McAleese, Lauren Walker, Steph Meyer, Eliona Tsefou, Lina Patterson and Israa Al-Banaa, for their support and friendship throughout my studies.

Lastly, but by no means least, I would like to give special thanks to my partner, Rachel. She has had to endure my preoccupation with this project, often involving me working over weekends and at inconvenient times, meaning that plans had to be continually changed. However, she has supported me immensely throughout this endeavour, for which I am greatly appreciative, and it has undoubtedly contributed greatly to this work. I would also like to thank my families and friends, in Northern Ireland and Newcastle, who encouraged me to follow my dreams, cheered my successes, commiserated when things did not go according to plan, and helped motivate me when I needed it.

The RNA sequencing and subsequent bioinformatics analysis in Chapter 5 was conducted at the laboratory of Mark Cookson at the National Institutes of Health, Bethesda, MD, USA. I had no role in the generation of this data, beyond extracting RNA and sending it to our collaborator, from which we were provided with the results of the pathway analysis.

Sub-dissection of frozen tissue for transcriptomic/proteomic analysis was performed by Dr Chris Morris. Sectioning of fixed tissue was carried out by Dr Ahmad Khundakar and my only role was to mount cut sections onto slides from the water bath. As the superior colliculus is contained on the upper midbrain block that is used for routine diagnostics, approximately 75% of tau and α-synuclein sections were already stained so I did not perform staining on these sections. Amyloid-β stained sectioned were only available for six upper midbrain sections, therefore, I stained the remainder.

Daniel Erskine

December 2016

*“To strive, to seek, to find, and not to yield”*

- *Alfred, Lord Tennyson, “Ulysses”*

## Papers published during PhD studies

**Erskine, D.**, Thomas, A.J., Attems, J., Taylor, J.P., McKeith, I.G. *et al* (2016). Specific patterns of neuronal loss in the pulvinar nucleus in dementia with Lewy bodies. *Movement Disorders*, in press.

McAleese, K.E., Walker, L., **Erskine, D.**, Thomas, A.J., McKeith, I.G., Attems, J. (2016). TDP-43 pathology in Alzheimer's disease, dementia with Lewy bodies, and ageing. *Brain Pathology*. DOI: 10.1111/bpa.12424.

**Erskine, D.** and Khundakar, A.A. (2016). Stereological approaches to dementia research using human brain tissue. *Journal of Chemical Neuroanatomy*. DOI: 10.1016/j.jchemneu.2016.01.004.

Khundakar, A.A., Hanson, P.S., **Erskine, D.**, Lax, N.Z. Roscamp, J., Karyka, E. *et al*. (2016). Analysis of primary visual cortex in dementia with Lewy bodies indicates GABAergic involvement associated with recurrent complex visual hallucinations. *Acta Neuropathologica Communications*, 4:66. DOI: 10.1186/s40478-016-0334-3.

**Erskine, D.**, Taylor, J.P., Firbank, M.J., Patterson, L., Onofrj, M., O'Brien, J.T. *et al*. (2016). Changes to the lateral geniculate nucleus in Alzheimer's disease but not dementia with Lewy bodies. *Neuropathology and Applied Neurobiology*, 42, 366-376. DOI: 10.1111/nan.12249.

## Author’s declaration

This thesis is submitted for the degree of Doctor of Philosophy to Newcastle University. The research described within this thesis was performed by me at the Ageing Research Laboratories or the Medical Toxicology Centre within the Institute of Neuroscience, and is my own work unless otherwise stated. The research was carried out under the supervision of Ahmad Khundakar, Chris Morris and Alan Thomas between September 2013 and September 2016.

I certify that none of the material within this thesis has been previously submitted by me for a degree or any other qualification at this or any other university.

# Table of contents

# List of figures

# List of tables

# List of abbreviations

| | |
|---|---|
| AD | Alzheimer’s disease |
| ALDH1L1 | Aldehyde dehydrogenase 1 family member L1 |
| ANCOVA | Analysis of covariance |
| ANOVA | Analysis of variance |
| C3 | Complement component C3 |
| CAA | Cerebral amyloid angiopathy |
| CBD | Corticobasal degeneration |
| CBS | Charles Bonnet syndrome |
| CD68 | Cluster of differentiation 68 |
| CHI3L1/YKL-40 | Chitinase 3-like protein 1/YKL-40 |
| CSF | Cerebrospinal fluid |
| CE | Coefficient of error |
| DAB | 3, 3’ diaminobenzidine |
| DAT | Dopamine transporter |
| DLB | Dementia with Lewy bodies |
| DTI | Diffusion tensor imaging |
| EDTA | Ethylenediamine tetra-acetic acid |
| ELISA | Enzyme-linked immunosorbent assay |
| GABA | Gamma-aminobutyric acid |
| GABARAP | GABA type A receptor-associated protein |
| GAD65/67 | Glutamic acid decarboxylase 65/67 |

| | |
|---|---|
| GAD67 | Glutamic acid decarboxylase 67 |
| GAP43 | Growth-associated protein 43 |
| GAPDH | Glyceraldehyde 3-phosphate dehydrogenase |
| GFAP | Glial fibrillary acidic protein |
| GO | Gene ontology |
| HRP | Horseradish peroxidase |
| HSD | Honest significant difference |
| HSPA1A | Heat shock 70 kDa protein 1A |
| HSPA1B | Heat shock 70 kDa protein 1B |
| HSP70 | Heat shock protein 70 kDa |
| I-MIBG | l-metaiodobenzylguanidine |
| KLK6 | Kallikrein related peptidase 6 |
| LB | Lewy body |
| LGN | Lateral geniculate nucleus |
| MAG | Myelin associated glycoprotein |
| MAP2 | Microtubule-associated protein 2 |
| MCI | Mild cognitive impairment |
| MMSE | Mini-mental state examination |
| MRI | Magnetic resonance imaging |
| mRNA | Messenger ribonucleic acid |
| MSA | Multiple systems atrophy |
| NBIA1 | Neurodegeneration with brain iron accumulation type 1 (formerly Hallervorden-Spatz disease) |
| NBTR | Newcastle Brain Tissue Resource |

| | |
|---|---|
| NFT | Neurofibrillary tangle |
| NPI | Neuropsychiatric inventory |
| NSF | *N*-ethylmalemide-sensitive factor |
| OCT | Optical coherence tomography |
| PAD | Perceptual and attention deficit model |
| PD | Parkinson’s disease |
| PDD | Parkinson’s disease dementia |
| PET | Positron emission tomography |
| PM | Post-mortem |
| PSD-95 | Post-synaptic density protein 95 |
| PSP | Progressive supranuclear palsy |
| REM | Rapid eye movement |
| RGB | Red-green-blue |
| RGC | Retinal ganglion cell |
| RNA | Ribonucleic acid |
| RNAseq | Ribonucleic acid sequencing |
| SDS-PAGE | Sodium dodecyl sulphate polyacrylamide gel electrophoresis |
| SERPINH7/HSP47 | Serine (or cysteine) proteinase inhibitor, clade H (heat shock protein 47), member 1 |
| SGI | Stratum griseum intermedium of the superior colliculus |
| SGP | Stratum griseum profundum of the superior colliculus |
| SGS | Stratum griseum superficiale of the superior colliculus |
| SNAP-25 | Synaptosomal associated protein 25 |

| | |
|---|---|
| SNARE receptor | Soluble *N*-ethylmalemide-sensitive factor attachment protein |
| SPECT | Single-photon emission computerised tomography |
| SV2B | Synaptic vesicle glycoprotein 2B |
| TBST | Tris-buffered saline with Tween20 |
| TDP-43 | TAR domain binding protein 43 |
| TEAB | Tetraethyl ammonium bicarbonate |
| UPDRS | Unified Parkinson's disease rating scale |
| VaD | Vascular dementia |
| V1 | Visual area 1/primary visual cortex/striate cortex |
| V5/MT | Visual area 5/mediotemporal visual area |
| VEGF | Vascular endothelial growth factor |

# Chapter 1: Introduction

## 1.1 Dementia

People are living longer than at any previous point in human history, contributing to sustained global population ageing. According to the United Nations, there were 205 million people aged over 60 years old in 1950. In 2009, this number had risen to 737 million, and is projected to rise to up to 2 billion by 2050 (United Nations. Department of, 2010). The global elderly population is increasing, and will surpass child and adolescent numbers by 2045 (Sosa-Ortiz *et al.*, 2012). As a result of this demographic shift, diseases for which increasing age is the greatest risk factor are expected to rise.

Dementia refers to a group of conditions characterised by the progressive and irreversible decline in cognitive functions, with a corresponding impact upon autonomous living (American Psychiatric, 2013). Dementia can result from one of several conditions, including Alzheimer's disease (AD), vascular dementia (VaD) and dementia with Lewy bodies (DLB), the primary focus of this project. Dementia disorders increase in incidence and prevalence with advancing age (World Health, 2012). Global population ageing has contributed to an increased number of people diagnosed with dementia. In 2010 there were 36 million people living with dementia worldwide, by 2013 this rose to 44 million and is projected to reach 76 million by 2030 (Prince *et al.*, 2013). The rise in the global incidence and prevalence of dementia disorders has contributed to an increased financial burden on health services, as well as social costs to family members, who often provide care without financial compensation (Hurd *et al.*, 2013; DaDalt and Coughlin, 2016).

### 1.1.1. Epidemiology

In higher-income countries, dementia occurs in 5-10% of those aged over 65 years old and the incidence of dementia increases with advancing age (Hugo and Ganguli, 2014), ranging from 0.1% at 65 to 8.6% at 95 of age (Jorm and Jolley, 1998). Although prevalence is higher amongst females, incidence is not, suggesting that higher prevalence reflects longer life expectancy amongst females (Hugo and Ganguli, 2014). Clinically and pathologically, AD is the most prevalent form of dementia, accounting for 60-70% of all dementia cases (Jellinger *et al.*, 1990;

Neuropathology Group. Medical Research Council Cognitive and Aging, 2001; Plassman *et al.*, 2007).

DLB is the second most prevalent primary degenerative dementia after AD (Heidebrink, 2002). The incidence of DLB is 3.8% of new dementia cases and its prevalence is 4.2% of dementia diagnoses in the community, 7.5% in secondary care (Vann Jones and O'Brien, 2014), and further increases up to three-fold when 'possible DLB' is included (Boot, 2013). A prevalence study in 40 Swedish nursing homes found that 16% of residents had two or more core symptoms of DLB (Zahirovic *et al.*, 2016). At autopsy, DLB accounts for 20% of all dementia cases suggesting an over-representation at autopsy or clinical under-diagnosis (McKeith, 2000). DLB may be initially clinically under-recognised as it is characterised by motor and cognitive impairments, meaning patients can initially present to different medical specialists. DLB patients may, for example, be treated by a neurologist for motor symptoms or a dementia specialist (psychiatrist or geriatrician) for the cognitive aspects of the disorder. The medical specialist to whom DLB patients first present may influence their diagnosis as neurologists are more likely to underestimate the presence of dementia in patients with movement disorders (Hely *et al.*, 2008), with dementia specialists often under-recognising motor features (Schneider *et al.*, 2007).

## 1.2 Dementia with Lewy bodies

### 1.2.1 Overview of clinical diagnostic criteria for DLB

DLB is characterised by three core clinical features: cognitive fluctuations, parkinsonism and visual hallucinations, in the presence of progressive cognitive decline (McKeith, 2006). Additionally, several suggestive and supportive features can aid clinical diagnosis of DLB. A diagnosis of 'probable DLB' may be made if two or more core features, or one core feature plus a suggestive feature, are present. 'Possible DLB' may be diagnosed if one core or suggestive feature is present in isolation. Probable DLB cannot be diagnosed on the basis of suggestive features alone (McKeith *et al.*, 2005). The consensus diagnostic criteria have high levels of specificity for DLB (~95%), but lower levels of sensitivity (32-83%) (McKeith *et al.*, 2000; Nelson *et al.*, 2010).

### 1.2.2 Core clinical features of DLB

Cognitive fluctuations are a core symptom of DLB and are defined as variations in cognitive ability and alertness over time (McKeith *et al.*, 2004). This may be observed as changes in responsiveness to an individual's surroundings, marked by periods of reduced attentiveness or awareness to external stimuli (McKeith, 2006). The fluctuating nature of this phenomenon means that the individual experiences transient periods of normal, or near-normal, functioning (McKeith *et al.*, 1996). Although cognitive fluctuations may also occur in AD and VaD they tend to occur in more severe dementia, whilst DLB patients show the greatest variations in attention, independent of dementia severity and parkinsonism (Walker *et al.*, 2000b). DLB patients typically have spontaneous episodes of interruptions in awareness or attention whilst AD patients describe difficulties in dealing with the cognitive demands of their situation (Bradshaw *et al.*, 2004). Ratings of cognitive fluctuations based on clinician impression are also higher in DLB compared to AD patients (Walker *et al.*, 2012). DLB patients have impaired performance on cognitive reaction time tasks, identified as predictors of other measures of cognitive fluctuations (Walker *et al.*, 2000a), in comparison to AD, Parkinson's disease (PD) and older cognitively normal individuals (Ballard *et al.*, 2002).

Parkinsonian extra-pyramidal symptoms also represent a core symptom of DLB and consist of slowness of movement (bradykinesia), tremor in the absence of voluntary muscle contraction (rest tremor), mask-like face, rigidity, stooped posture and shuffling gait (McKeith *et al.*, 2005). Parkinsonian signs are the predominant clinical features of PD (Gibb and Lees, 1988) and occur in approximately 68% of DLB patients (Aarsland *et al.*, 2001). The phenotypic similarities between PD and DLB likely result from both being pathologically characterised by the intracytoplasmic aggregation of the protein α-synuclein into deposits termed Lewy bodies within vulnerable neurons (Spillantini *et al.*, 1997; Attems *et al.*, 2013). PD dementia is differentiated from DLB on the basis of motor symptoms preceding cognitive symptoms by one year or more (McKeith, 2006), though this arbitrary distinction has been challenged (Berg *et al.*, 2014). However, DLB patients may have subtle differences in motor symptoms, specifically less rest tremor and more rigidity than PD patients (Gnanalingham *et al.*, 1997). PDD patients have more severe motor symptoms than DLB, as assessed by Hoehn and Yahr staging, a clinical rating scale

of the severity of parkinsonian features (Petrova *et al.*, 2015). Another study has found greater rigidity, gait impairment, bradykinesia and tremor during voluntary muscle contraction (action tremor) but no difference in rest tremor or abnormal posture in DLB compared to PD cases (Aarsland *et al.*, 2001). Overall, DLB cases have a motor phenotype where gait and postural difficulties, rather than tremor, are the most prominent features (Burn *et al.*, 2003). Gait and postural predominant motor phenotypes in DLB indicate involvement of non-dopaminergic neurotransmitter loss in motor impairment, with cholinergic loss implicated (Burn *et al.*, 2003; Burn *et al.*, 2006). AD patients can also experience parkinsonian symptoms. However, neuropathological examination has shown AD cases with extrapyramidal features more frequently have pathological similarities to PD and DLB than those who do not (Tosto *et al.*, 2015). Motor symptoms in DLB may contribute to the greater functional impairment found in DLB compared to AD patients (McKeith *et al.*, 2006).

A third core clinical feature of DLB is recurrent complex visual hallucinations which occur in 60-80% of patients (Burghaus *et al.*, 2012). Whilst visual hallucinations are sometimes found in other neurodegenerative disorders, such as AD and PD, they are more prevalent (Ballard *et al.*, 1997; Fenelon *et al.*, 2000), appear earlier (Fenelon *et al.*, 2000), are more severe (Chiu *et al.*, 2016), and are more likely to persist over time (Ballard *et al.*, 1997) in DLB. Hallucinations in DLB patients are typically complex, involving objects, such as people, animals, insects or disembodied faces, whilst in AD they are simple and brief, such as seeing shadows (Mosimann *et al.*, 2006). There may be gender differences in the content of hallucinations, with men more likely to hallucinate machines, and women more likely to hallucinate family members or children (Urwyler *et al.*, 2016). Hallucinations may be frightening (Burghaus *et al.*, 2012) and DLB patients have less insight into the unreality of these perceptions compared to non-demented PD patients (Bertram and Williams, 2012). If they hallucinate, DLB and AD patients have a similar level of reduced insight into the unreality of their perceptions (Ballard *et al.*, 1997). Hallucinations in DLB are related to decreased quality of life and are associated with higher rates of institutionalisation (Bostrom *et al.*, 2007). Additionally, visual hallucinations contribute to increased distress amongst caregivers of DLB patients (Ricci *et al.*, 2009). Other visual symptoms, such as abnormalities in saccadic and pursuit eye movements, pupil reactivity and visual perception are also frequently observed in DLB (Armstrong,

2012), and may result from shared visual system pathology with that inducing visual hallucinations (Diederich *et al.*, 2014). Despite the prevalence and impact of visual hallucinations on DLB patients, the underlying pathological changes promoting their occurrence are unknown (Diederich *et al.*, 2014), thus limiting the development of targeted treatments.

### 1.2.3 Suggestive clinical features of DLB

In addition to the three core features, rapid eye movement (REM) sleep behaviour disorder, neuroleptic sensitivity and low dopamine transporter uptake in the basal ganglia on single-photon emission computerised tomography (SPECT) or positron emission tomography (PET) are considered suggestive symptoms of DLB (McKeith *et al.*, 2005).

REM sleep behaviour disorder is characterised by an individual abnormally acting out dreams by vocalising and moving, often against a perceived attacker (Boeve, 2013). REM sleep behaviour disorder is more commonly found in synucleinopathies than in AD or mild cognitive impairment (MCI, an intermediate state between normal cognitive functioning and AD (Morris and Cummings, 2005)) (Boeve *et al.*, 2001). REM sleep behaviour disorder is also found in progressive supranuclear palsy (PSP), a disorder marked by parkinsonism without α-synuclein pathology (Munhoz and Teive, 2014) but is strongly associated with α-synuclein pathology when it precedes the onset of other neurological symptoms (Boeve *et al.*, 2013). As PSP is a tauopathy rather than an α-synucleinopathy, the topography of pathological changes may be important in eliciting REM sleep behaviour disorder (Munhoz and Teive, 2014).

Neuroleptic sensitivity is characterised by the exacerbation of parkinsonian motor features and/or impaired consciousness following administration of neuroleptic drugs (McKeith *et al.*, 2005). Neuroleptic medications are a class of pharmaceuticals that inhibit dopaminergic D2 receptors primarily used in the treatment of schizophrenia (Madras, 2013). The proposed efficacy of neuroleptics in schizophrenia is based on a hypothesised increase in D2 receptors in the striatum of schizophrenic patients, with pharmacological antagonism reducing dopaminergic activity to normal levels (Nordstrom *et al.*, 1995; Corripio *et al.*, 2011). D2 receptors are reduced in the

striatum of DLB patients, thus administration of neuroleptic agents may further exacerbate striatal dopaminergic deficits (Walker *et al.*, 1997; Piggott *et al.*, 1999). Approximately 50% of DLB patients have a severe adverse reaction to neuroleptics, and a greater proportion have milder adverse reactions (McKeith *et al.*, 1992; Aarsland *et al.*, 2005). As a result of early reports on the sensitivity of DLB patients to neuroleptics (e.g. (McKeith *et al.*, 1992)), there are few modern studies on rates of neuroleptic sensitivity in DLB. Some studies have assessed the efficacy of atypical antipsychotics, that interact with the serotonergic system and have a more transient effect on D2 receptors, for treating psychotic symptoms in DLB (Kusumi *et al.*, 2015). Despite early promise from a positive case report (Allen *et al.*, 1995), a randomised controlled trial suggested that risperidone, an atypical antipsychotic, is poorly tolerated by the majority of DLB patients and can lead to a worsening of scores on some neuropsychological tests (Culo *et al.*, 2010).

Neuroimaging of the dopamine transporter (DAT) with PET or SPECT shows reduced binding in the nigrostriatal dopaminergic system in DLB (Piggott *et al.*, 1999; McKeith *et al.*, 2005). A large multicentre trial has shown that SPECT imaging of DAT is a reliable method for segregating DLB from AD (McKeith *et al.*, 2007). As there is some overlap in clinical presentations between AD and DLB, particularly in early stages (McKeith *et al.*, 2016), additional tools to differentiate these two diseases are of particular importance.

### 1.2.4 Supportive clinical features of DLB

Supportive features incorporate symptoms often occurring in DLB but lack the specificity to include them in a scheme designed to improve diagnostic accuracy (McKeith *et al.*, 2005). Supportive features of DLB include repeated falls and syncope, transient loss of consciousness, severe autonomic dysfunction, non-visual hallucinations, delusions, depression, medial temporal preservation on structural magnetic resonance imaging (MRI), reduced occipital perfusion, low uptake of I-metaiodobenzylguanidine (I-MIBG) on cardiac scintigraphy and low wave activity on electroencephalogram with transient, sharp waves in the temporal lobe (McKeith *et al.*, 2005).

### 1.2.5 Non-hallucinatory visual features of DLB

Although visual hallucinations are a core clinical feature (McKeith *et al.*, 2005), other visual deficits commonly occur in DLB (Armstrong, 2012). Visual acuity does not differ significantly in DLB patients compared to age-matched controls, though impairments have been found in other visual functions such as eye movement difficulties, visuospatial perception and visual attention (Metzler-Baddeley *et al.*, 2010). Although visual perceptual and oculomotor difficulties are commonly encountered amongst DLB patients, they are not considered to be core or supportive features necessary for rendering a clinical diagnosis (McKeith *et al.*, 2005).

Eye movement deficits occur in several neurodegenerative dementia disorders, prominently in PSP, but are thought to be more significant in DLB and PDD than AD (Armstrong and Kergoat, 2015). Saccades are fast eye movements that serve to move the eye so that the fovea centralis, the retinal area corresponding to the central visual field, is centred upon the region of the visual field to which the observer wishes to attend (Schall, 1995). Saccadic eye movements take longer to execute and are more likely to fall short of their target in DLB compared to control and AD patients (Mosimann *et al.*, 2005).

Complex visual functions are thought to be particularly impaired in DLB (Armstrong, 2012). DLB patients perform poorly on tasks involving size or length estimation of observed objects, overlapping figures and spatial localisation, indicating visuospatial dysfunction (Mosimann *et al.*, 2004). When presented with a battery of cognitive tasks, DLB patients consistently show poorer performance on sub-scales with a substantial visuospatial component than AD or PD (Scharre *et al.*, 2016). Despite not being a core clinical feature, visuospatial impairment is often a presenting feature of DLB and may be useful in the differentiation from AD (Tiraboschi *et al.*, 2006; Yoshizawa *et al.*, 2013).

Visual attention is also impaired in DLB (Collerton *et al.*, 2003). DLB patients perform more poorly on tests of attentional/executive function, including the trail-making and Stroop tasks, than PDD (Mondon *et al.*, 2007). DLB patients show impaired filtering of distracting visual information (Perriol *et al.*, 2005) and make more frequent saccades to distractors during pursuit eye movements (Henderson *et al.*, 2011). The manifestation of visual hallucinations has been related to visual attentional deficits

(Cagnin *et al.*, 2013), and focused attention upon hallucinated objects has been demonstrated to promote their cessation in PD (Diederich *et al.*, 2003).

### 1.2.6 Phenotypic overlaps between DLB and other parkinsonian motor disorders

PD is a movement disorder characterised by slowness of movement, rigidity, and rest tremor, typically referred to as a parkinsonian motor phenotype (Postuma *et al.*, 2015). A spectrum of cognitive features occur in PD, ranging from subtle cognitive impairment to PDD (Litvan *et al.*, 2012). Approximately 20% of PD patients experience complex visual hallucinations, though approximately 40% experience 'simple' hallucinations involving the perception of movement or a presence in the peripheral visual field (passage and presence hallucinations, respectively) (Fenelon *et al.*, 2000). Subtle features of impaired cognition are a risk factor for PDD, which occurs in up to 80% of PD patients (Aarsland *et al.*, 1996; Aarsland *et al.*, 2003).

PSP is a progressive parkinsonian disorder characterised by postural instability with falls and slow vertical saccadic eye movements (Respondek *et al.*, 2013). Corticobasal degeneration (CBD) has a variable presentation, with asymmetrical rigidity, dysfunctional voluntary movement and unintentional movements (Armstrong *et al.*, 2013). Both PSP and CBD are pathologically characterised by tau pathology, as further described in section 1.3.2. PSP and CBD patients rarely experience visual hallucinations (Armstrong and Kergoat, 2015).

Multiple systems atrophy (MSA) is characterised by autonomic dysfunction, particularly urinary incontinence and erectile dysfunction in males, in addition to either parkinsonism non-responsive to levodopa and/or a syndrome of unsteadiness and discoordination, termed ataxia (Gilman *et al.*, 2008). MSA is pathologically characterised by the presence of Papp-Lantos bodies, as further described in section 1.2.8. The topography of Papp-Lantos bodies is related to several distinct clinical phenotypes of MSA (Kim *et al.*, 2015). Visual hallucinations may occur in 5-9% of MSA patients but their presence is considered to be more strongly predictive of DLB, PD or PDD (Bertram and Williams, 2012).

### 1.2.7 Cognitive profile of DLB vs other neurodegenerative diseases

Even at early stages, DLB patients typically have greater impairments in visuo-spatial processing than AD (Yoshizawa *et al.*, 2013). In contrast to PD, PDD and MSA, DLB patients have more severe impairment on attentional/executive functioning tasks, particularly those with a high visuo-spatial processing component (Kao *et al.*, 2009; Petrova *et al.*, 2015). Although encoding and retrieval of memory is more impaired in AD (Yoshizawa *et al.*, 2013), DLB patients have more memory domain impairments than MSA or PD (Kao *et al.*, 2009). The overall cognitive profile of DLB patients suggests prominent attentional and executive dysfunction, particularly tasks with a substantial visuo-spatial component, and relative preservation of memory when compared to AD.

### 1.2.8 α-synuclein pathology

Many neurodegenerative dementia disorders are characterised by aberrant misfolding and aggregation of highly-expressed tissue proteins (Taipa *et al.*, 2012). DLB cases have midbrain, limbic and neocortical neuronal cytoplasmic inclusions consisting of ubiquitinated α-synuclein termed Lewy bodies (Perry *et al.*, 1990b; Spillantini *et al.*, 1997). Lewy bodies are also the characteristic neuropathological feature of PD and PDD and, as a result, the three conditions are collectively considered to lie on the Lewy body disease spectrum (Kovari *et al.*, 2009; Attems *et al.*, 2013). Mild Lewy body pathology is occasionally found in aged cases without cognitive or motor impairment, and may be more prevalent with increasing age in such individuals (Saito *et al.*, 2004).

α-synuclein is thought to be central to the pathogenesis of Lewy body disease (Kalia and Kalia, 2015) due to the involvement of α-synuclein mutations in familial PD (Polymeropoulos *et al.*, 1997) and its presence within Lewy bodies (Spillantini *et al.*, 1997). In Lewy bodies, α-synuclein is aggregated into insoluble assemblies (Baba *et al.*, 1998) which are thought to follow a stereotypical temporal and topographic course, originating in the brainstem and spreading to the neocortex through the limbic system (Braak *et al.*, 2003; McKeith *et al.*, 2005). Limbic or neocortical Lewy body pathology is necessary for a pathological diagnosis of DLB (McKeith *et al.*, 2005).

α-synuclein-positive inclusions in astrocytes and oligodendrocytes have also been described in brainstem and midbrain regions in PD (Wakabayashi *et al.*, 2000; Seidel *et al.*, 2015). More recently, an antibody against aggregated α-synuclein has demonstrated astrocytic and 'dot-like' profiles in cortical regions in DLB (Kovacs *et al.*, 2012). However, the role of glial α-synuclein pathology in the aetiology of Lewy body disease, and its relationship to clinical features, is not yet known.

Neuropathological staging schemes have been devised to chart the topographical distribution of Lewy body pathology in PD/PDD (Braak *et al.*, 2004) and DLB (McKeith *et al.*, 2005). Both the PD and DLB schemes describe Lewy body pathology spreading in a stereotypical manner, originating in the brainstem before affecting limbic regions and, ultimately, vulnerable regions of the neocortex (Braak *et al.*, 2004; McKeith *et al.*, 2005). Based purely on the topography of Lewy body pathology, DLB and PDD are indistinguishable (Ruffmann *et al.*, 2016). However, Lewy body pathology is higher in the neocortex than the brainstem of individuals who present with dementia; in contrast, brainstem pathology is greater than neocortical pathology in individuals who present with parkinsonism (Yamamoto *et al.*, 2005). A diagnosis of DLB or PDD is based upon the sequence of symptom onset, with the requirement that parkinsonism precedes cognitive symptoms by one or more years to qualify for a diagnosis of PDD (McKeith *et al.*, 2005). Why some Lewy body disorders present with cognitive or motor symptoms has not been satisfactorily explained in the literature. However, it is possible the initial sequence of Lewy body deposition is different between DLB and PDD patients, but the same distribution is observed at terminal stages.

The stereotypical spread of Lewy body pathology in DLB, PD and PDD has prompted speculation that aggregated α-synuclein may spread through the brain in a manner reminiscent of the mode of transmission described previously for prion protein in transmissible spongiform encephalopathies such as variant Creutzfeldt-Jakob disease, kuru and bovine spongiform encephalopathy (Prusiner and Kingsbury, 1985; Seidel *et al.*, 2015). This hypothesis suggests misfolded species of α-synuclein protein, when introduced to normal physiological α-synuclein, have the capacity to induce misfolding into the pathogenic conformation, gaining toxic qualities (Goedert, 2015).

α-synuclein aggregates within oligodendroglia, termed Papp-Lantos bodies or glial cytoplasmic inclusions, are the characteristic neuropathological feature of MSA (Barker and Williams-Gray, 2016). Why α-synuclein affects oligodendroglia rather than neurons in MSA, and its role in neurodegeneration, remains unknown (Burn and Jaros, 2001). Lewy bodies and occasional α-synuclein-positive neuroaxonal spheroids have been previously described in neurodegeneration with brain accumulation type 1 (NBIA1, formerly Hallervorden-Spatz disease) (Wakabayashi *et al.*, 1999; Galvin *et al.*, 2000; Neumann *et al.*, 2000; Saito *et al.*, 2000). However, the underlying pathophysiology of NBIA1 is not well understood, thus limiting knowledge on whether α-synuclein is a primary pathology and how it contributes to the disease process (Jellinger, 2003).

### 1.2.9 Concomitant pathologies in DLB

The aged brain often manifests more than one type of age-related neurodegenerative pathology (Kovacs *et al.*, 2008; Jellinger and Attems, 2015). However, the presence of multiple pathologies within an aged brain does not, by necessity, mean that the individual has more than one type of dementia (i.e. mixed dementia). A diagnosis of mixed dementia is typically only given when the full pathological diagnostic criteria for more than one disorder have been met (Jellinger and Attems, 2007).

Intermediate AD-type pathology, in the form of neurofibrillary tangles and amyloid-β plaques (as discussed in section 1.3.2), is often observed, but not invariant, in DLB brains (McKeith *et al.*, 1996). Rather than being incidental, AD-type pathology may contribute to the disease process and exacerbate cognitive decline in DLB (Howlett *et al.*, 2015). However, the presence of neurofibrillary tangles and/or amyloid-β plaques is not necessary for a neuropathological diagnosis of DLB (McKeith *et al.*, 2005). Imaging of amyloid-β using positron emission tomography *intra vitam* is an attractive method to assess changes previously only identifiable *post-mortem*. However, amyloid-β imaging has not been consistently demonstrated to improve accuracy of DLB diagnosis (Donaghy *et al.*, 2015). Imaging suggests amyloid-β is higher in DLB than PDD (Gomperts, 2014), and may be useful in identifying PD patients at risk of cognitive decline (Donaghy *et al.*, 2015). Furthermore, elevated

expression of amyloid-β in cerebrospinal fluid has been identified as a predictor of cognitive decline in PD (Yarnall *et al.*, 2014), and may predict more rapid cognitive decline in DLB (Abdelnour *et al.*, 2016). It is unclear how amyloid-β may contribute to elevated rates of cognitive decline, but it has been demonstrated to enhance the aggregation of α-synuclein *in vivo*, suggesting it may accelerate the progression of Lewy body disease (Masliah *et al.*, 2001).

Vascular pathologies increase in frequency with ageing, and may also be found in DLB. DLB cases have significantly more severe cerebrovascular lesions than PD cases, ranging from nothing to mild/moderate lacunes and/or white matter lesions (Jellinger and Attems, 2008). Cerebral amyloid angiopathy (CAA) has been demonstrated to be significantly higher in DLB than PD cases, and correlates with the global burden of tau and α-synuclein. However, one study investigating cerebrovascular lesions reported no significant difference in the severity of white matter changes or cortical micro-infarcts, but did find increased total mini-bleeds, in DLB compared to control cases (De Reuck *et al.*, 2013).

TAR DNA-binding protein (TDP)-43 pathology, the characteristic neuropathological feature of amyotrophic lateral sclerosis and a subtype of frontotemporal dementia, has been reported in aged individuals without cognitive impairment, AD and DLB cases (Higashi *et al.*, 2007). In AD cases, TDP-43 follows a distinct topographical sequence of deposition (Josephs *et al.*, 2014; Josephs *et al.*, 2016), which has also been observed in normal ageing and DLB (McAleese *et al.*, 2016). However, TDP-43 pathology in DLB, whilst variable, is not significantly more advanced than that observed in aged control cases and seems to show a greater association with AD-type than α-synuclein pathology (McAleese *et al.*, 2016). However, one study has demonstrated significant relationships between α-synuclein and TDP-43 burden within the amygdala (Yokota *et al.*, 2010).

## 1.3 Alzheimer's disease

### 1.3.1 Clinical features

AD is clinically characterised by progressively declining cognition which substantially impairs the ability to conduct normal daily activities (McKhann *et al.*, 2011). Although commonly considered to be an amnestic disorder, there are non-amnestic

presentations that can result from AD pathology, such as posterior cortical atrophy (Alladi *et al.*, 2007) and logopenic progressive aphasia (Rabinovici *et al.*, 2008). Amnestic AD is the most common presentation of AD, and is characterised by impairment in the learning and recall of recently acquired information due to deficient episodic memory (McKhann *et al.*, 2011; Dubois *et al.*, 2014).

### 1.3.2 Amyloid-β and tau pathology

AD-type pathology consists of senile plaques, neurofibrillary tangles, neuropil threads and neuritic plaques (Hyman *et al.*, 2012). Neurofibrillary tangles and neuropil threads consist of microtubule-associated protein tau, a protein normally localised to axons that binds to, and stabilises, the microtubule network (Mandelkow and Mandelkow, 2012). Under pathological conditions, tau becomes abnormally phosphorylated, detaches from microtubules and accumulates in vulnerable neurons (Bancher *et al.*, 1989; Mandelkow and Mandelkow, 2012). Variants of tau pathology are found in several disorders known as tauopathies, which include AD, PSP and CBD (Irwin, 2016). As with Lewy body pathology, staging schemes have been developed to chart the temporal sequence of these pathologies in AD. Tau neurofibrillary tangles are thought to originate in the transentorhinal cortex, prior to spreading to the fusiform and lingual gyri, and ultimately affecting wider neocortical regions (Braak *et al.*, 2006).

Amyloid-β is a peptide cleaved from the amyloid precursor protein by β- and γ-secretases and accumulates in the parenchyma into neurotoxic plaques (Kuruva and Reddy, 2016). Senile plaques largely consist of extracellular deposits of amyloid-β peptide and originate in cortical regions prior to deposition in sub-cortical structures, ultimately affecting midbrain and brainstem regions (Thal *et al.*, 2002). The presence of focal amyloid-β deposits with a distended halo of tau-positive neurites, termed neuritic plaques, are necessary for a neuropathological diagnosis of AD (Attems *et al.*, 2013).

Stereological studies have typically reported neurofibrillary tangles to be a more robust correlate of neuronal loss than amyloid-β plaques (Erskine and Khundakar, 2016). However, it is thought that both pathologies interact to elicit the neuronal dysfunction and death that contributes to the clinical phenotype of AD (Attems *et al.*,

2013). AD-type pathology is frequently observed in aged, cognitively intact individuals. A *post-mortem* study of 39 cognitively intact, elderly subjects identified only one case without neurofibrillary tangle pathology. However, tau pathology was milder in cognitively intact individuals than AD, predominantly corresponding to the first three stages of the Braak staging scheme (Knopman *et al.*, 2003). Therefore, although AD-type pathology may be encountered in the cognitively intact elderly, it is typically less severe than in individuals with AD.

### 1.3.3 Concomitant pathologies in AD

Vascular pathologies, such as atherosclerosis, small vessel disease and CAA, occur commonly with ageing, particularly alongside AD-type pathology (Grinberg and Thal, 2010; Attems *et al.*, 2013). Rather than incidental findings, vascular pathologies may contribute to cerebral hypoperfusion in AD (Love and Miners, 2016), and hasten the rate of cognitive decline (Pachalska *et al.*, 2015).

TDP-43 pathology has been identified in AD, where it follows a distinct sequence of deposition and is related to an accelerated rate of cognitive decline (Josephs *et al.*, 2014; Josephs *et al.*, 2016). TDP-43 pathology shows a greater association with AD than with DLB or normal ageing (McAleese *et al.*, 2016).

## 1.4 The molecular function of α-synuclein

### 1.4.1 Synaptic function

Synapses are the primary medium for neuronal communication and comprise the axon of the presynaptic neuron, the dendrite of the postsynaptic neuron and the space between them, termed the synaptic cleft (Hudspeth *et al.*, 2013). The majority of synapses within the human central nervous system are chemical synapses, which facilitate neuronal communication via neurotransmitters (Sudhof, 2013). Prior to release into the synaptic cleft, neurotransmitters are stored in synaptic vesicles (Hudspeth *et al.*, 2013), which are required to quickly fuse with a special area of the plasma membrane, termed the ‘active zone’, in response to the influx of calcium ions into the presynaptic neuron as the result of action potential generation (Sudhof, 2013). Synaptic vesicle exocytosis is mediated by the N-ethylamide sensitive factor

attachment protein receptor (SNARE) family which include synaptobrevin, syntaxin-1 and synaptosomal-associated protein 25 (SNAP-25) (Rizo and Xu, 2015).

The SNARE family of proteins facilitate the exocytotic release of neurotransmitters into the synaptic cleft by mediating the fusing of the presynaptic vesicle to the cell membrane. SNARE proteins carry out this function by assembling into a stable four-helix bundle known as the SNARE complex, which provides energy for the synaptic vesicle (Weber *et al.*, 1998). The SNARE complex interacts with a variety of other proteins to facilitate synaptic vesicle exocytosis (Sudhof, 2013), including chaperones such as α-synuclein, which are thought to support exocytosis by maintaining the SNARE complex assembly (Burre *et al.*, 2010; Sharma *et al.*, 2011).

### 1.4.2 α-synuclein structure

α-synuclein, the major protein component of Lewy bodies, is thought to predominantly exist as an unfolded monomeric protein with a propensity to aggregate (Spillantini *et al.*, 1997; Tofaris and Spillantini, 2007). However, the N-terminal region of α-synuclein adopts a helical conformation in the presence of lipid membranes (Eliezer *et al.*, 2001), which may facilitate membrane binding to aid ion-channel formation, a putative role for α-synuclein (Zakharov *et al.*, 2007). When isolated from red blood cells α-synuclein has been reported to exist as a tetramer with a helically folded structure that is resistant to aggregation (Bartels *et al.*, 2011). However, the tetrameric structure of α-synuclein has been contested by other studies which have reported α-synuclein to be an unfolded monomer when isolated from human and murine brain, or human-derived neuronal cell lines (Fauvet *et al.*, 2012).

### 1.4.3 α-synuclein aggregation

The factors predisposing α-synuclein aggregation in Lewy body disease are not well understood but the monomeric form may be particularly vulnerable to assemble into the β-pleated sheet rich structures comprising Lewy bodies and neurites (Bartels *et al.*, 2011; Eugene *et al.*, 2014). The ratio of different α-synuclein conformations may be perturbed in Lewy body disorders, leading to a relative increase in aggregation-prone monomeric α-synuclein (Gurry *et al.*, 2013). Polymorphisms in the α-synuclein promoter have been identified as a potential risk factor for idiopathic PD (Kruger *et*

*al.*, 1999). This is consistent with the suggestion that increased expression levels of α-synuclein may promote self-aggregation into an intermediate stage characterised by oligomeric species before further aggregation into the fibrils comprising Lewy bodies and neurites (Giasson *et al.*, 1999; Conway *et al.*, 2000a; Conway *et al.*, 2000b). However, whilst most oligomers likely aggregate further into fibrils, some oligomers stabilise and aggregate into 'stacks' of oligomers (Paslawski *et al.*, 2014). Oligomers are thought to be more neurotoxic than fibrillar or monomeric forms of α-synuclein, and may be a major causative agent in the neuronal dysfunction that characterises α-synucleinopathies (Winner *et al.*, 2011; Cremades *et al.*, 2012).

Aggregation of α-synuclein is thought to be an important pathogenic event in the natural history of Lewy body disorders (Bendor *et al.*, 2013); however, it is not clear whether aggregation elicits toxic effects through a loss- or gain- of function (Cookson, 2006). α-synuclein aggregates may induce a loss of function by binding the membrane-bound monomeric form, removing it from the membrane, thus inhibiting its normal function (Chaudhary *et al.*, 2014). However, α-synuclein aggregation may lead to a gain of cytotoxic function as oligomeric α-synuclein interacts with cellular membranes and induces the influx of substances from the extracellular milieu into the neuron, critically impairing neuronal functioning (Danzer *et al.*, 2007). Additionally, fibrillar α-synuclein may inhibit microtubule formation by inducing the fibrillisation of tau protein, potentially inhibiting the microtubule transport network (Oikawa *et al.*, 2016). Neuronal dysfunction as a result of α-synuclein aggregation may result from both a loss of normal function and a gain of toxic function, with aggregation impeding the normal physiological role of α-synuclein but also leading to the creation of aggregates with cytotoxic qualities.

## 1.5 Human visual system and visual thalamic structures

### 1.5.1 An overview of the human visual system

Visual perception begins in the eye, where light is transduced by the photoreceptors of the retina and transmitted along the optic nerve (Masland, 2012). Retinal ganglion cells (RGC), whose axons comprise the optic nerve, transmit the neural representation of the observed visual field to the lateral geniculate nucleus (LGN) of the thalamus, the primary subcortical relay centre between the retina and visual cortex (Reese, 2011) (Fig. 1.1). The visual cortex then sends ascending visual

information to one of two parallel post-striate pathways: one projecting dorsally, which is involved in spatial and movement perception, and one projecting ventrally, which is implicated in object perception (Ungerleider LG, 1982) (Fig. 1.2).

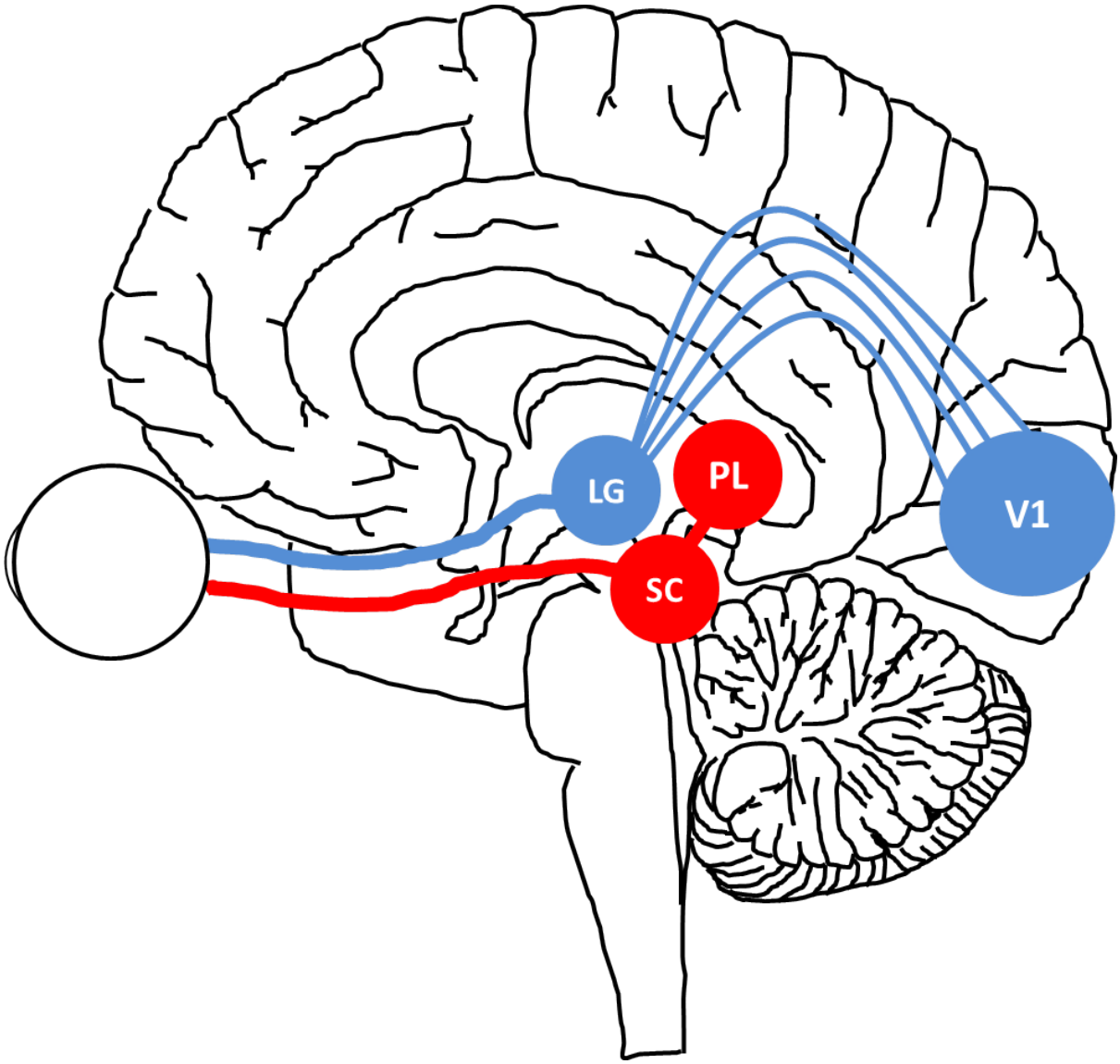


*Figure 1.1: The afferent visual pathways.*

*The primary visual pathway (blue) projects from the retina to the lateral geniculate nucleus (LG) prior to the primary visual cortex (V1). The secondary visual pathway (red) projects from the retina to the superior colliculus (SC) and the pulvinar (PL).*

An additional ‘secondary’ visual pathway originates in the retina, running parallel to the ‘primary’ retina-LGN-primary visual cortex pathway. The secondary visual pathway projects from the retina to the superior colliculus and then innervates the pulvinar nucleus of the thalamus (Fig. 1.1) (Diederich *et al.*, 2014). From the pulvinar, one pathway continues to visual area V5/MT and is thought to serve motion processing (Stepniewska *et al.*, 1999; Stepniewska *et al.*, 2000). Another pathway from the pulvinar projects to widespread targets, including the cingulate gyrus, amygdala and insular cortex (Romanski *et al.*, 1997), and is thought to integrate sensory inputs with limbic influences (Benarroch, 2015).

The primary and secondary visual pathways are not completely segregated. The superior colliculus of the secondary visual pathway has reciprocal connectivity with the LGN and visual cortex (Krauzlis *et al.*, 2013). Similarly, the pulvinar directly innervates the primary visual cortex, and can modulate its activity (Zhou *et al.*, 2016). Therefore, the two subcortical visual pathways could be considered to be separate but synergistic.

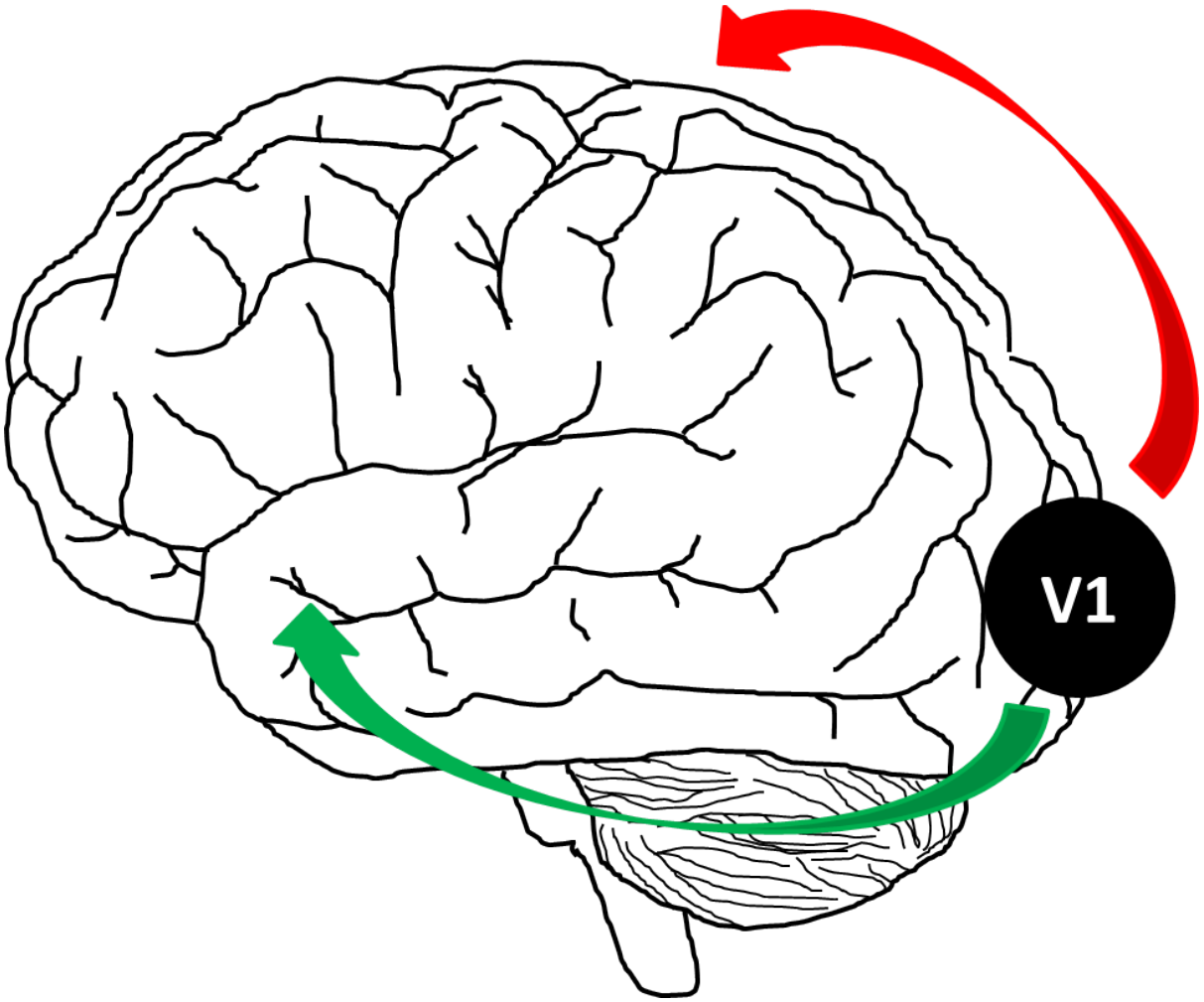


*Figure 1.2: The human post-striate visual systems.*

*Two streams are demonstrated projecting from the primary visual cortex (V1). One stream travels ventrally along the occipito-temporal region (green arrow; ventral stream), from V1 to the association visual cortical areas V2 and V4, before projecting down the inferior temporal lobe. Another stream projects dorsally along the occipito-parietal region (red arrow; dorsal stream), from V1 to the V5/MT area, travelling further to the inferior parietal lobule.*

### 1.5.2 The lateral geniculate nucleus

The LGN is a laminar structure on the inferolateral aspect of the thalamus, enveloped by the optic tract (Jones, 2007). The LGN is composed of six laminae, each containing lamina-specific cell types: the magnocellular laminae comprising larger cells and parvocellular laminae containing smaller cells (Clark, 1932). The two ventral laminae are composed of magnocellular neurons, whilst the remaining four dorsal laminae are parvocellular. Laminae four and six are innervated by processes originating in the contralateral retina, whilst afferent input to laminae 3 and 5 emanates from the ipsilateral retina (Steriade M, 1997). As each retina encodes information from both the right and left visual hemi-fields, each LGN processes information from the contralateral visual hemi-field from both eyes (Jones, 2007). A third cell type, koniocellular, exist in the LGN and are present on the ventral surface of each lamina and within intralaminar regions (Hendry and Reid, 2000).

The primary innervation of the LGN comes from the retina through RGC and its main efferent connection is with the primary visual cortex through the optic radiations (Steriade M, 1997). However, input also comes to the LGN from the midbrain superior colliculus and is thought to suppress LGN activity during fast saccadic eye movements, a phenomenon known as ‘saccadic suppression’ (Harting *et al.*, 1991). The LGN also receives modulatory inputs from the thalamic reticular nucleus, a top-down regulator of thalamic activity that forms part of activity-dependent inhibitory loops with efferent targets of the LGN (Crick, 1984). The LGN also has considerable reciprocal connectivity with the targets of its efferent projections, especially the primary visual cortex, which sends feedback modulation to the LGN and reticular thalamus (Jones, 2007). LGN excitability is modulated by inputs from the brainstem reticular formation through pontogeniculo-occipital waves, which occur during sleep and can create spurious visual activity in the absence of visual input (Steriade, 1996).

The segregation of the LGN into magnocellular and parvocellular laminae reflects the organisation of the primate visual system into functionally distinct but mutually complimentary and interacting pathways. Studies of non-human primates have demonstrated that parvocellular neurons, which are predominantly innervated by RGC from the fovea centralis of the retina, have lower contrast sensitivity but higher spatial frequency than magnocellular neurons, which are rarely innervated by RGC from the fovea centralis (Derrington and Lennie, 1984). Parvocellular neurons

receive inputs from retinal cells that respond to red-green colour, whereas magnocellular neurons receive input from retinal cells that are achromatic (Martin *et al.*, 2011). The differences in response properties between magnocellular and parvocellular neurons reflect differences in their functional roles in visual perception: the magnocellular pathway is implicated in spatial and motion perception and the parvocellular pathway is involved in form recognition (Merigan and Maunsell, 1993). A neuroimaging study has indicated that similar functional distinctions exist between magnocellular and parvocellular laminae in the human LGN (Zhang *et al.*, 2015).

Unlike magnocellular and parvocellular neurons, koniocellular cells of the LGN survive following ablation of the primary visual cortex (Cowey and Stoerig, 1989) as they directly innervate the cortical motion processing region V5/MT (Sincich *et al.*, 2004). Koniocellular neurons show slower rhythmic patterns of activity than magnocellular or parvocellular neurons (Cheong *et al.*, 2011) and are innervated by retinal cells that are sensitive to the blue-yellow colour spectrum (Jeffries *et al.*, 2014). Koniocellular neurons are a heterogenous neuronal class suggesting that individual sub-classes are implicated in divergent physiological processes (Xu *et al.*, 2001). Koniocellular neurons project to the visual area V5/MT indicating a role in the perception of movement (Diederich *et al.*, 2014). However, the pathway in which koniocellular neurons participate may also aid visuo-spatial attention (Jayakumar *et al.*, 2013), as visual attention can be better directed by blue-yellow than red-green stimuli (Li *et al.*, 2007).

### 1.5.3 The pulvinar nucleus

The pulvinar is a large nucleus at the posterior part of the thalamus, lying on the superior aspect of the LGN (Jones, 2007). The pulvinar has four morphologically and physiologically distinct regions: anterior, medial, lateral and inferior (Burton and Jones, 1976). However, these regions can be further sub-divided on the basis of the neurochemical composition of individual neurons (Jones and Hendry, 1989). Although the pulvinar is often considered to be a predominantly visual structure, the anterior and medial aspects do not project to regions that are specifically involved in visual perception (Jones, 2007). The anterior pulvinar projects to somatosensory

regions whilst the medial pulvinar may support vision through its interaction with regions involved in sensory processing and attention (Benarroch, 2015).

The primary pulvinar inputs relating to visual perception originate in the visual regions of the midbrain, such as the superior colliculus (Lysakowski *et al.*, 1986). The superior colliculus is thought to primarily innervate the inferior pulvinar due to its degeneration following collicular lesions (Benevento and Fallon, 1975) but functional studies also show innervation of the medial and lateral pulvinar, with both regions sending afferent fibres to the medial temporal region (area V5/MT) of the dorsal visual stream (Benevento and Standage, 1983; Berman and Wurtz, 2010). Some retinal innervation of the inferior pulvinar is also present (Nakagawa and Tanaka, 1984), though these afferents are relatively small and proximal to the LGN (Jones, 2007). Cortical regions directly connected to each other are typically also connected through the pulvinar, contributing to its putative role in modulating cortico-cortical interactions (Benarroch, 2015). Of particular relevance to the visual system, the secondary visual area V2 (Ungerleider *et al.*, 2014) and the fourth visual area V4 (Gattass *et al.*, 2014) innervate relay neurons in the inferior and lateral pulvinar.

Thalamocortical output from the pulvinar generally innervates primary and association sensory cortices (Jones, 2007), suggesting a role as an association nucleus (Benarroch, 2015). The lateral pulvinar projects to the primary visual cortex, innervating laminae 1, 2 and 3, and the association visual cortex. These connections may be directly reciprocal (Ogren and Hendrickson, 1976), though the descending pathway may be routed through the reticular thalamic nucleus (Jones, 2007). The inferior pulvinar also innervates the primary and association visual cortices, as well as area V5/MT in the dorsal visual stream (Cusick *et al.*, 1993).

Functionally, the pulvinar is hypothesised to play a role in visual attention (Jones, 2007). Physiological studies have shown changes in the excitability of pulvinar neurons based on the behavioural relevance of stimuli in the visual field (Kastner *et al.*, 2004). Lesions of the pulvinar often lead to deficits of visual attention, such as spatial neglect, a phenomenon where an individual cannot perceive a region of the visual field (Karnath *et al.*, 2002). Pulvinar lesions can induce difficulties in localising stimuli, including spatially combining separate visual features, indicating a role in visuospatial perception (Ward *et al.*, 2002).

### 1.5.4 The superior colliculus

The superior colliculus is a laminar structure on the dorsal aspect of the midbrain (May, 2006). Although the superior colliculus has traditionally been considered an important structure for oculomotor functions (Gandhi and Katnani, 2011), it is becoming increasingly clear that it contributes to more complex components of visual perception, such as visual target selection (Krauzlis *et al.*, 2013) and attention (Muller *et al.*, 2005). Anatomically, the superior colliculus has alternative strata consisting of white and grey matter, broadly arranged into three grey matter laminae: *stratum griseum superficiale* (SGS; superficial grey lamina), *stratum griseum intermedium* (SGI, intermediate grey lamina) and *stratum griseum profundum* (SGP, deep grey lamina) (Krauzlis *et al.*, 2013).

The SGS is an exclusively visual lamina of the superior colliculus and receives direct retinal input (Perry and Cowey, 1984). Modulatory cholinergic afferents to the SGS have been described in cats, emanating from the parabigeminal nucleus (Sherk, 1979). The efferent projections from the SGS innervate primary visual pathway structures, such as the LGN and primary visual cortex (Benevento and Fallon, 1975), where they are thought to suppress activity during eye movements (Wurtz *et al.*, 2011). The SGS may also contribute to non-conscious motion perception, through its connectivity with area V5/MT in the dorsal visual stream through the inferior pulvinar (Stepniewska *et al.*, 1999; Stepniewska *et al.*, 2000).

The SGI and SGP are considered to be functionally and anatomically independent from the SGS (Krauzlis *et al.*, 2013). In contrast to the predominantly retinal input of the SGS, the SGI and SGP receive afferents from wide-ranging cortical and sub-cortical regions. Inputs to the SGI and SGP include motor and association sensory cortices, the hypothalamus, zona incerta, substantia nigra pars reticulata, locus coeruleus, dorsal raphe, pedunclopontine and deep cerebellar nuclei (Sparks and Hartwich-Young, 1989). Functionally, the SGI and SGP have traditionally been viewed as having a predominantly motor function (Gandhi and Katnani, 2011). However, these laminae, which contain retinotopic maps of the visual field, are also thought to support the selection of visual targets (Sparks, 1999). Neurons within the retinotopic area corresponding to the target of an upcoming saccade show

heightened activity prior to the initiation of the saccade, suggesting the SGI and SGP are involved in the selection of saccadic targets (Glimcher and Sparks, 1992). Outputs from the SGI to the mediodorsal nucleus of the thalamus, which projects to the frontal eye fields, may serve to stabilise the visual field during saccadic eye movements (Wurtz *et al.*, 2011). Auditory and somatosensory maps have been demonstrated in the deeper laminae of the cat superior colliculus, in addition to multi-sensory neurons that respond to input from more than one sensory modality, indicating a role in the integration of sensory inputs (Wallace *et al.*, 1993).

## 1.6 Visual hallucinations

### 1.6.1 Cortical release hypothesis

Charles Bonnet syndrome (CBS) is a hallucinatory disorder defined by the presence of visual hallucinations in a cognitively intact elderly individual (Ffytche, 2005). Visual hallucinations are a common feature of eye disease, occurring in up to 40% of cases, particularly when visual dysfunction has occurred in late life (ffytche, 2009). The association between eye disease and hallucinations prompted the development of the 'cortical release' hypothesis of visual hallucinations (Manford and Andermann, 1998). This suggests impairments between the retina and the primary visual cortex may be important in the manifestation of complex visual hallucinations. This phenomenon is postulated to result from a reduction in inhibition, particularly in association visual areas, as a compensatory mechanism for impaired or degraded visual input. This hypothesis is supported by the observation that complex visual hallucinations occur in epileptiform disorders, which are also marked by altered excitatory/inhibitory activity, particularly when the focus of aberrant activity is the visual association regions (Josephson and Kirsch, 2006).

The cortical release hypothesis suggests reduced inhibition occurs as a response to reduced input to the visual cortex. Lesions of the LGN have been demonstrated to induce defects in acuity in the visual field corresponding to the area lesioned, though normal functioning usually resolves in the case of small focal lesions (Gunderson and Hoyt, 1971), (Luco *et al.*, 1992). However, although one study has demonstrated visual acuity deficits as a function of disease duration in individuals with Lewy body disease (Archibald *et al.*, 2011), another study has not demonstrated visual impairments exceeding those observed in neurologically unimpaired controls

(Metzler-Baddeley *et al.*, 2010). Visual acuity impairments in PD are related to the onset of minor hallucinatory phenomena, such as passage and presence hallucinations, where an individual may erroneously perceive movement or a presence in their peripheral visual field (Urwyler *et al.*, 2014). No difference has been found in visual acuity on ophthalmological assessment between hallucinating and non-hallucinating PD patients (Gallagher *et al.*, 2011). Visual hallucinations have been previously described in non-demented PD cases with normal visual acuity but deficient colour vision and contrast sensitivity (Diederich *et al.*, 1998). This could suggest that higher visual functional impairment, rather than ocular dysfunction, contributes to visual hallucinations in some cases.

If ocular changes are not responsible for visual cortical compensation, this may suggest that visual cortical input is altered through another mechanism, if cortical release underlies the manifestation of visual hallucinations in DLB. The LGN and pulvinar may be functionally altered in Lewy body disease, creating conditions that contribute to cortical release (Manford and Andermann, 1998). Brainstem regions modulating visual thalamic activity, such as the dorsal raphe and pedunculopontine nucleus, can alter visual thalamic activity between sleep-wake cycles (Monti, 2011). Degeneration of brainstem regions projecting to the visual thalamus may alter activity in the LGN and pulvinar, which has a corresponding effect upon activity in the association visual cortex (Manford and Andermann, 1998). One study has demonstrated an absence of visual acuity deficits but a relationship between visual hallucinations and sleep-wake cycle dysfunction (Gallagher *et al.*, 2011). This may suggest shared mechanisms, such as brainstem degeneration, underlying both sleep dysfunction and visual hallucinations.

### 1.6.2 Perception and attention deficit

Normal object perception is thought to be the result of the complex interplay between external ‘bottom-up’ visual input, and internal ‘top-down’ representations of objects and scenes, termed ‘proto-objects’, formed as a result of visual experience, and deployed on the basis of expectations (Wolfe *et al.*, 2003). Competition is thought to exist between both bottom-up visual input and top-down expectations to bias perception. The perceptual and attention deficit (PAD) model suggests that

dysfunctional sensory input processing biases toward top-down expectations and contributes to the selection of incorrect proto-objects (Collerton *et al.*, 2005b). Crucially, scene perception remains intact, so the perceived proto-object is congruous with the observed scene but incorrect. Under normal conditions, attention affixes proto-objects into the observed visual scene, and this process is also thought to be perturbed in the PAD model (Lu and Dosher, 1998). Therefore, under the PAD model, impairments in object perception contribute to incorrect proto-object selection, and attentional dysfunction fixes incorrect, though contextually congruous objects, into the subjective visual scene, which are perceived as visual hallucinations (Collerton *et al.*, 2005a). The authors of the PAD hypothesis have tested this model by assessing perception and attention in patients with a dementia diagnosis and controls (Makin *et al.*, 2013). They found attention, but not visual acuity, was significantly deficient in dementia cases with visual hallucinations, offering some support for the PAD hypothesis. Lower scores of sustained attention in hallucinating PD patients (Meppelink *et al.*, 2008) and the disappearance of visual hallucinations following focused attention (Diederich *et al.*, 2003) further indicate a role for attention in the aetiology of visual hallucinations in Lewy body disease.

The PAD hypothesis and subsequent experimental work have implicated dysfunctional attentional processes in the aetiology of complex visual hallucinations (Collerton *et al.*, 2005b; Meppelink *et al.*, 2008; Makin *et al.*, 2013). Therefore, dysfunction or degeneration of regions implicated in visual attentional mechanisms may contribute to the manifestation of visual hallucinations in DLB. The LGN receives widespread inputs from regions that modulate visual activity, such as the superior colliculus and thalamic reticular nucleus (Jones, 2012). As it is an early relay structure for afferent visual processing, the LGN is ideally placed to modulate visual input in response to attentional and behavioural demands. Increased activity has been reported in the LGN as a consequence of focused attention, indicating that attention modulates activity in the LGN (O'Connor *et al.*, 2002). However, attention-mediated activity changes in the LGN are likely the result of modulatory feedback from the primary visual cortex to the reticular thalamic nucleus, which gates LGN activity patterns (Montero, 2000; Jones, 2012).

The pulvinar is thought to have an important role in visual attentional mechanisms (Jones, 2012; Benarroch, 2015) and its widespread cortical connections are thought

to underlie its putative function in modulating cortico-cortical activity based on attentional demands (Saalmann *et al.*, 2012). Lesions of the pulvinar lead to deficits in filtering distracting visual stimuli (Fischer and Whitney, 2012) and in attending to specific features of an observed stimulus (Ward *et al.*, 2002). Taken together, this indicates a functional role for the pulvinar in visual attention.

The Sprague effect, where spatial neglect occurs as a result of lesions to the occipital or parietal lobe, is recovered following superior colliculus lesioning, suggesting its contribution to visual attention (Sprague, 1966; Weddell, 2004). Like the LGN, the superior colliculus shows increased activity when the observer is attending to a visual stimulus, albeit with substantially higher attention-mediated activity than the LGN (Schneider and Kastner, 2009). Stimulation of collicular regions bias eye and head/neck movements toward spatial locations corresponding to the retinotopic area stimulated, indicating a role in target selection (Corneil *et al.*, 2002; Gandhi and Katnani, 2011). Microstimulation of the superior colliculus can also spatially focus attention without eye movements toward the area of attention, a phenomenon known as covert attention (Muller *et al.*, 2005).

Perception and attentional deficits in DLB are thought to be the result of cholinergic dysfunction (Collerton *et al.*, 2005b). *Post-mortem* studies have demonstrated cholinergic deficits in DLB, often exceeding those found in AD (Perry *et al.*, 1990a; Perry *et al.*, 1994; Tiraboschi *et al.*, 2002), and these have been suggested to contribute a vulnerability to visual hallucinations (Perry and Perry, 1995). The major cholinergic nuclei, such as the nucleus basalis of Meynert (Lippa *et al.*, 1999; Kim *et al.*, 2011; Grothe *et al.*, 2014) and pedunculopontine nucleus (Schmeichel *et al.*, 2008; Hepp *et al.*, 2013), typically manifest Lewy body pathology in DLB. A physiological study that measured activity as an analogue of cholinergic activity has demonstrated changes in DLB which are commensurate with visual hallucination frequency and severity (Marra *et al.*, 2012). An imaging study targeting cholinergic receptors *in vivo* has also suggested alterations in cholinergic uptake associated with visual hallucinations (O'Brien *et al.*, 2008). A relationship between cholinergic dysfunction and visual hallucinations is further implied by reports of acetylcholinesterase inhibitor efficacy in their treatment (Burghaus *et al.*, 2012).

### 1.6.3 ‘Blind’ to blindsight

Blindsight is the ability of blind individuals to utilise facets of observed visual scenes without conscious awareness of perception (Barbur, 2004). Specifically, individuals with blindsight often accurately locate or identify presented stimuli within their peripheral visual field, react to moving stimuli and perform eye movements to follow and move between presented objects, despite an inability to consciously perceive them (Stoerig and Cowey, 1997). More recent work indicates that emotion-laden images may be perceived in an analogous manner termed ‘affective blindsight’ (Tamietto and de Gelder, 2010). PD patients often inappropriately guess objects in their peripheral visual fields, have difficulty perceiving motion, exhibit eye movement deficiencies and have impairments in recognising emotional facial stimuli, suggesting they have the converse of blindsight (Diederich *et al.*, 2014). The ‘blind’ to blindsight syndrome is thought to contribute to the occurrence of presence and passage hallucinations, simple hallucinations where an object or movement is incorrectly perceived in the peripheral visual field. Deficient blindsight pathways in Lewy body disease may also force reliance upon the longer-latency primary visual pathway for information normally carried along the faster secondary visual pathways (Diederich *et al.*, 2014). It is possible that slowed transfer of supportive visual information could lead to an over-reliance upon top-down processing in visual perception, particularly in circumstances of changing visual conditions, and bias the individual towards expected, rather than experienced, visual stimuli. This could contribute toward visual hallucination if top-down processes are also dysfunctional.

The hypothesis that Lewy body disorder patients are ‘blind’ to blindsight suggests brain structures with functional roles in motion perception, eye movements and perception of emotional stimuli will be pathologically dysfunctional. Four brain structures, the LGN, pulvinar, superior colliculus and amygdala, have been directly implicated in these functions and in blindsight pathways hypothesised to be dysfunctional in Lewy body disease (Diederich *et al.*, 2014). Koniocellular neurons of the LGN directly innervate the cortical motion perception area, V5/MT, in a pathway thought to contribute to the blindsight phenomenon (Sincich *et al.*, 2004; Schmid *et al.*, 2010). However, magnocellular and parvocellular neurons of the LGN, which are not part of putative blindsight pathways and primarily innervate the primary visual cortex, also show sensitivity to motion (Lee *et al.*, 1979).

The SGS of the superior colliculus is thought to have a role in motion perception as it contains motion sensitive neurons (Inayat *et al.*, 2015). Additionally, the SGS receives direct retinal input and projects to the motion area V5/MT through the inferior aspect of the pulvinar, in a pathway with a putative role in the non-conscious perception of motion (Lanyon *et al.*, 2009) and may, therefore, contribute to motion perception deficits in Lewy body disorders (Diederich *et al.*, 2014). The SGI of the superior colliculus also has an important role in selecting the targets of upcoming saccadic and pursuit eye movements (Glimcher and Sparks, 1992; Krauzlis and Dill, 2002), which are deficient in Lewy body disorders (Mosimann *et al.*, 2005; Diederich *et al.*, 2014). In particular, DLB patients have increased saccadic latency and a tendency to perform saccades that fall short of their target (Mosimann *et al.*, 2005), an identical pattern of deficits to that observed when the SGI of non-human primates is chemically inactivated (Aizawa and Wurtz, 1998).

In addition to the role of the pulvinar in relaying motion information from the superior colliculus to V5/MT, the medial aspect of the pulvinar has substantial connectivity with the amygdala (Romanski *et al.*, 1997), in which high levels of Lewy body pathology have been associated with visual hallucinations (Harding *et al.*, 2002). PD patients show impaired perception of fear in observed faces (Sprengelmeyer *et al.*, 2003), and lesions specifically affecting the medial pulvinar lead to impaired fear perception, particularly in observed faces (Ward *et al.*, 2007), indicating the medial pulvinar may contribute to affective blindsight (Diederich *et al.*, 2014).

### 1.6.4 Difficulty in engaging the dorsal attentional network

Dysfunctional connectivity and activity across brain networks has been proposed as a contributor to the occurrence of visual hallucinations across numerous disease-states (Onofrj *et al.*, 2013). This hypothesis, when specifically applied to DLB/PD, has indicated dysfunction contributing to altered activity in response to observed visual stimuli and may lead to the manifestation of visual hallucinations. Under normal conditions, the ventral attentional network monitors incoming sensory information and engages the dorsal attentional network, which directs attention to visual stimuli, on the basis of salience and behavioural relevance (Corbetta and Shulman, 2002; Asplund *et al.*, 2010). In DLB/PD, it has been suggested that the

brain has difficulty in activating the dorsal attentional network in response to ambiguous visual stimuli (Shine *et al.*, 2014). This leads to an overreliance on the default mode network, which is involved in self-referential thought that manipulates and retrieves memories (Mazoyer *et al.*, 2001). The default mode network has previously been related to ‘mind wandering’ and may bias perceptual systems toward ‘top-down’ influences based on memory or experience of visual perception (Shine *et al.*, 2014).

In DLB/PD patients, a dysfunctional default mode network may lead to difficulty in engaging the dorsal attentional network. The dorsal attentional network involves dorsolateral prefrontal, posterior parietal and striatal regions interconnected with the superior colliculus (Bisley and Goldberg, 2010). The dorsal attentional network is implicated in directing attention toward stimuli on the basis of salience of behavioural goals (Shine *et al.*, 2014). The superior colliculus has an important role in target selection, orienting and visual attention (Krauzlis *et al.*, 2013), suggesting the pattern of deficient activity is consistent with known roles of the superior colliculus. The pulvinar has not been directly implicated in the shifting between default mode network and dorsal attention network. However, the pulvinar has a strong influence on visual cortical activity in response to observed stimuli, and can influence attention-mediated enhanced cortical activity (Purushothaman *et al.*, 2012; Zhou *et al.*, 2016). This role is functionally similar to that suggested for the dorsal attentional network and may indicate interaction with the pulvinar.

## 1.7 The thalamus and superior colliculus in neurodegenerative disorders

### 1.7.1 Thalamic pathology in Lewy body disorders

The thalamus consists of over 40 anatomically and physiologically distinct sub-nuclei and is a central hub for relaying and modulating activity across the brain (Jones, 2012). Dysfunction in highly-interconnected hubs, such as the thalamus, has previously been implicated in dysfunctional network activity in dementia disorders (Pievani *et al.*, 2011). As a result, the thalamus has been the subject of several studies aiming to elucidate its pathological vulnerability and relevance to the clinical features of dementia.

Neuropathological studies have demonstrated that Lewy body pathology is most frequently encountered in the central lateral, central medial, limitans-suprageniculate, paracentral, paraventricular and reuniens nuclei in PD (Rub *et al.*, 2002). However, cell counting methods across all thalamic nuclei have demonstrated no neuronal loss in any region in PD but significant loss in the anterodorsal nucleus in AD compared to control cases (Xuereb *et al.*, 1991). Neuronal loss has not been demonstrated in the limbic thalamic nuclei but has been reported in the intralaminar nuclei in PD and PSP compared to control cases (Henderson *et al.*, 2000). Reductions in neuronal number were reported in the parafascicular and centre-median nuclei in PD and PSP when compared to control (Henderson *et al.*, 2000). Examination of the intralaminar nuclei in DLB and PDD has demonstrated the paraventricular, central lateral and central medial nuclei are most severely affected by Lewy body pathology in DLB and PDD (Brooks and Halliday, 2009). However, neuronal loss was only observed in the parataenial, central lateral and centre-median/parafascicular nuclei of DLB, PD and PDD cases compared to control.

Autoradiographic studies have been used to investigate the expression of post-synaptic receptors or pre-synaptic transporters, which may indicate neurochemical abnormalities in the thalamus across disease states. Nicotinic cholinergic (alpha 3 and alpha 6) receptor expression labelled by the [(125)I]alpha-conotoxin MII ligand is reduced in the centre-median, parafascicular and ventral lateral nuclei in DLB (Ray *et al.*, 2004; Bohr *et al.*, 2005). The LGN and pulvinar were not analysed in this study as they were only present on sections from a small number of cases but, when present, the LGN had among the highest levels of receptor expression. Studies employing a different cholinergic receptor ligand (α-bungarotoxin, labelling alpha 7, 8 and 9 receptors) have demonstrated cholinergic receptor reductions in the reticular thalamic nucleus, a key regulator of thalamic activity in DLB, which exceed those found in schizophrenia cases (Court *et al.*, 1999). Muscarinic M2 and M4 cholinergic receptors labelled by the ligand [$^{3}$H]AFDX384 were specifically reduced in the mediodorsal nucleus in DLB compared to control cases (Warren *et al.*, 2007). The LGN and pulvinar were not assessed in this study but the mediodorsal nucleus is a key target of the cholinergic pedunculopontine nucleus, where atrophy has been identified in hallucinating PD cases compared to those without hallucinations (Janzen *et al.*, 2012). Acetylcholine may contribute to enhanced cortical neuronal

activity, thus increasing the probability that signals are differentiated from noise. Cholinergic reductions may create ambiguity in discriminating signals from background neural activity, which may corrupt and alter information transfer throughout the cortex, and may therefore contribute to the development of visual hallucinations (Perry and Perry, 1995). Autoradiographic studies of dopaminergic D2 receptors in the thalamus have identified changes in the lateral dorsal and ventrointermedius nuclei in DLB cases with extrapyramidal features but these changes were unrelated to visual hallucinations (Piggott *et al.*, 2007).

### 1.7.2 Neuroimaging studies in the thalamus in DLB

Until recently, neuroimaging studies have mostly studied the thalamus as a unitary structure due to inability to resolve small thalamic sub-nuclei. One study that employed PET with ligands to detect glucose metabolism has demonstrated no change to glucose metabolism in the thalamus in DLB (Ishii *et al.*, 1998). Structural MRI has demonstrated bilateral reductions in thalamic volume in DLB compared to control cases (Beyer *et al.*, 2007). Diffusion tensor MRI, a neuroimaging technique that detects tissue damage through increased diffusivity of tissue, has found increased mean diffusivity in DLB but this was not significantly different from AD (Watson *et al.*, 2012).

SPECT imaging has been employed to assess regional perfusion changes in DLB as a method to clinically differentiate from AD. These studies have validated previous findings of occipital hypoperfusion in DLB but have also demonstrated this occurs alongside thalamic hyperperfusion in comparison to AD cases (Sato *et al.*, 2007; Shimizu *et al.*, 2008). Compared to controls, DLB patients have reduced perfusion in the thalamus at early stages of the disease (Chang *et al.*, 2008). This may indicate that physiological changes in the thalamus and occipital lobe act in concert to contribute to visual manifestations in DLB.

### 1.7.3 Pathological and neuroimaging studies in the thalamus in Alzheimer's disease

MRI data in familial AD has shown volumetric losses in the thalamus when it is assessed as a unitary structure (de Jong *et al.*, 2008). Total thalamic volume loss has also been demonstrated on MRI in sporadic cases that have been clinically

assessed as having prodromal AD (Eustache *et al.*, 2016), and in amnestic MCI cases, compared to controls (Yi *et al.*, 2016). The anterior nuclei of the thalamus are particularly vulnerable to AD-type histopathological changes, with the anterodorsal nucleus showing complete loss of neurons in some cases (Braak and Braak, 1991; Xuereb *et al.*, 1991). The dorsomedial nucleus also shows neuronal loss and AD-type pathology in AD (Paskavitz *et al.*, 1995).

On histological examination, the LGN shows widespread amyloid-β deposition, in the absence of neurofibrillary and neuritic plaque pathology, in AD cases (Price *et al.*, 1991; Leuba and Saini, 1995). However, another study reported very low levels of tau pathology in the LGN (Dugger *et al.*, 2011). Cytochrome oxidase levels are also reduced on histological analysis of the LGN in AD, and this has been suggested to contribute to visual dysfunction in AD (Wong-Riley *et al.*, 1997).

The pulvinar has widespread plaque and tangle pathology in AD cases compared to controls (Kuljis, 1994). Although psychotic symptoms are relatively uncommon in AD compared to DLB, AD patients with psychotic features have reduced pulvinar perfusion on SPECT compared to AD patients without psychotic features (Mega *et al.*, 2000). AD cases may have increased iron in the pulvinar as demonstrated by T2*-weighted MRI but its contribution to the clinical phenotype requires further investigation (Moon *et al.*, 2012; Langkammer *et al.*, 2014).

The superior colliculus exhibits lower levels of tau pathology than the inferior colliculus in AD, and is milder than that observed in the superior colliculus in PSP (Dugger *et al.*, 2011). Another study has described tau and amyloid-β pathology across all laminae of the superior colliculus, though amyloid-β was relatively more severe than tau pathology (Leuba and Saini, 1995).

## 1.8 The visual system in Lewy body disorders

### 1.8.1 The retina

An early case report of the retina in a DLB patient showed reduced density of cone cells and pale inclusion bodies in the outer plexiform lamina, which were not immunoreactive for any known markers of Lewy bodies in the brain, with α-synuclein homologues β-synuclein and γ-synuclein expressed in different laminae to those

observed in control retinae (Maurage *et al.*, 2003). A later study using six PD/PDD cases failed to demonstrate retinal pathology beyond diffuse cytoplasmic α-synuclein immunoreactivity within isolated cells (Ho *et al.*, 2014). Retinal α-synuclein immunoreactivity was not considered to be typical of Lewy body pathology observed in the brain. However, another study demonstrated sparsely distributed fibres in the inner retinal surface of 7/9 PD and 1/3 DLB cases, with no immunoreactivity observed in cases without α-synucleinopathy (Beach *et al.*, 2014). A further study in three PD cases reported lamina-specific deposition of α-synuclein-immunoreactive intracellular inclusions present in the nuclear, plexiform and the ganglion cell laminae of the inner retina, and these were morphologically similar to Lewy bodies in the brain (Bodis-Wollner *et al.*, 2014).

Visual acuity has been assessed using the Snellen chart in probable DLB patients and demonstrated no significant difference compared to control or PD, irrespective of visual hallucination status (Devos *et al.*, 2005). However, in the same study, electroretinograms demonstrated photoreceptor abnormalities in the retina of DLB patients, which the authors speculate are more likely to contribute to simple than complex visual hallucinations. Another study demonstrated no change in visual acuity in PD patients diagnosed less than three years previously compared to controls (Nowacka *et al.*, 2015). Retinal functional abnormalities have been speculated to result from dopaminergic reductions, possibly as a result of diminished dopaminergic input to the retina (Nowacka *et al.*, 2015). Retinal dopaminergic deficits have been suggested to be due to the presence of dopaminergic neurons and fibres, predominantly in the inner retinal laminae (Frederick *et al.*, 1982), and the descriptions of α-synuclein pathology occurring within these strata in Lewy body disorders (Bodis-Wollner *et al.*, 2014).

Optical coherence tomography (OCT), a technique for obtaining high-resolution images of the eye, has been used to determine thinning of the retinal nerve fibre lamina in DLB, PDD and AD as an analogue of neuronal or axonal loss in the retina (Moreno-Ramos *et al.*, 2013). This study reported significant retinal nerve fibre thinning in all disease groups compared to control and this was related to general cognitive decline, as determined by lower mini-mental state examination (MMSE) score (Moreno-Ramos *et al.*, 2013). A further study using OCT to determine the thickness of individual retinal laminae in a larger cohort of 101 PD compared to 46

control eyes has described volumetric reductions in the total macula, inner plexiform lamina, inner nuclear lamina and outer nuclear lamina (Chorostecki *et al.*, 2015). However, PD patients had volumetric increases in the outer plexiform lamina. Not all studies employing OCT have demonstrated retinal lamina thinning. One study using recently diagnosed PD patients failed to replicate findings of reduced retinal and retinal nerve fibre lamina thickness (Nowacka *et al.*, 2015). OCT studies of the retinal vasculature have demonstrated venous morphological changes but no arterial abnormalities in PD (Kromer *et al.*, 2016).

### 1.8.2 The LGN

The LGN has been pathologically investigated only once in DLB, with an absence of Lewy pathology reported in 19 cases, irrespective of visual hallucination status (Yamamoto *et al.*, 2006). However, all DLB cases were qualitatively assessed as having very mild or mild neuronal loss in the LGN. Another study reported α-synuclein immunoreactivity in the form of neurites and dot-like structures present in 15/16 PD cases (Rahimi *et al.*, 2015). No study has yet determined whether neuronal loss occurs in the LGN in DLB using quantitative methods.

No imaging or physiological studies have been carried out in the LGN in DLB. However, in PD, the magnocellular visual pathway showed greater impairment on assessment of event-related potentials compared to controls than the parvocellular pathway (Arakawa *et al.*, 1999). Another study employed a psychophysical approach to determine the functional integrity of magnocellular, parvocellular and koniocellular pathways, based on assessment of their known visual functions (Silva *et al.*, 2005). This study reported impaired performance on a contrast sensitivity task to evaluate magnocellular performance in PD patients compared to controls. PD patients were also impaired on tasks forcing them to use chromatic information to determine a gap in a ring with red/green and blue/yellow spectra, as markers of parvocellular and koniocellular pathways, respectively. The patterns of impairment were independent of one another, and only magnocellular task performance was related to age.

### 1.8.3 The occipital lobe

The primary visual cortex within the occipital lobe was initially described as being frequently spared Lewy pathology in DLB (Perry *et al.*, 1990b). Subsequent studies have reported low (Yamamoto *et al.*, 2006; Yamamoto *et al.*, 2007; Mukaetova-Ladinska *et al.*, 2013) or absent (Khundakar *et al.*, 2016) Lewy pathology in the primary visual cortex in DLB. Occipital visual association cortices are typically reported to have more severe α-synuclein pathology than the primary visual cortex (Yamamoto *et al.*, 2006; Mukaetova-Ladinska *et al.*, 2013). Qualitative assessment reported very mild or mild neuronal loss (Yamamoto *et al.*, 2006), whilst a quantitative study found no significant change in neuronal number in any primary visual cortical lamina in DLB (Khundakar *et al.*, 2016). α-synuclein pathology has been reported in lamina 6 of the visual cortex in 7/16 PD cases, and was more severe than the Lewy pathology in the LGN reported in the same study (Rahimi *et al.*, 2015). The synaptic proteins synaptophysin, SNAP-25, syntaxin and γ-synuclein were found in one study to be significantly reduced in the visual cortex in DLB, as determined by enzyme-linked immunosorbent assay (ELISA), and this was related to cholinergic activity, as determined by a choline acetyltransferase activity assay (Mukaetova-Ladinska *et al.*, 2013).

An increase in α4β2 nicotinic cholinergic receptor binding has been reported in the occipital lobe of hallucinating DLB cases and this increase was especially marked in patients that had recently hallucinated (O'Brien *et al.*, 2008). Cholinergic receptor upregulation in DLB may be due to hyperactive cholinergic afferents from the LGN as a result of heightened excitation. A study employing transcranial magnetic stimulation to generate phosphenes, the elicitation of basic perceptual phenomena as a result of occipital stimulation, has reported the threshold of stimulation necessary to induce their occurrence is lower in DLB cases with more severe visual hallucinations, indicating occipital hyperexcitation (Taylor *et al.*, 2011). Transcriptomic and proteomic assessment of *post-mortem* visual cortex tissue obtained from hallucinating DLB patients has suggested an altered gene expression profile and proteomic changes indicating impaired gamma-aminobutyric acid (GABA) -ergic transmission (Khundakar *et al.*, 2016). Changes to GABA, the major inhibitory neurotransmitter (Jembrek and Vlainic, 2015), may alter the excitability of the primary visual cortex in DLB (Desgent and Ptito, 2012).

Structural MRI studies have demonstrated atrophy in the occipital lobe in DLB cases compared to PDD and control (Beyer *et al.*, 2007). However, another study failed to find occipital changes in DLB compared to PDD (Burton *et al.*, 2004). However, this study considered visual hallucinations necessary for a diagnosis of PDD, thus increasing phenotypic similarities between the DLB and PDD groups (Watson *et al.*, 2009). Another study with a large cohort and carefully matched participants failed to show significant occipital atrophy in DLB compared to control (Whitwell *et al.*, 2007).

Arterial spin-labelling MRI and PET/SPECT studies have consistently reported occipital hypoperfusion in DLB patients (Donnemiller *et al.*, 1997; Lobotesis *et al.*, 2001; Colloby *et al.*, 2002; Ceravolo *et al.*, 2003; Sato *et al.*, 2007; Shimizu *et al.*, 2008; Armstrong, 2012; Taylor *et al.*, 2012; Robertson *et al.*, 2016). Bilateral perfusion deficits have been related to the occurrence of visual hallucinations (Pasquier *et al.*, 2002; Nagahama *et al.*, 2010) and have been suggested to relate to visuospatial deficits in DLB (Colloby *et al.*, 2002). A study using ELISA to quantify molecular markers of occipital microvasculature and perfusion in tissue obtained from the primary and secondary visual cortices has demonstrated specific reductions in the vascular endothelial growth factor (VEGF) and myelin-associated glycoprotein (MAG), putative markers of microvasculature and hypoperfusion, respectively, in DLB compared to control and AD cases (Miners *et al.*, 2014b). VEGF and MAG were significantly positively correlated with each other and negatively correlated with total α-synuclein and phosphorylated α-synuclein. Therefore, hypoperfusion in the occipital lobe in DLB may occur due to microvascular changes as a result of α-synuclein pathology. Although previous studies have demonstrated an absence, or very low levels, of Lewy body pathology in DLB (Khundakar *et al.*, 2016), the sensitivity of ELISA may have detected low levels of pathology that cannot be observed by immunohistochemical methods.

PET studies have reported glucose hypometabolism in the occipital lobe in DLB compared to control and AD (Imamura *et al.*, 1997; Ishii *et al.*, 2015), and MSA patients (Claassen *et al.*, 2011). Occipital hypoperfusion has been reported to be a marker of prodromal DLB, though this was based on a study which assessed a relatively small number of patients (Fujishiro *et al.*, 2013). A study using autopsy-confirmed cases demonstrated occipital hypometabolism as a unique feature of DLB, particularly in the primary visual cortex, and was able to identify cases clinically

diagnosed as AD but retrospectively diagnosed with DLB following neuropathological assessment (Minoshima *et al.*, 2001). Occipital hypometabolism, in combination with preserved glucose metabolism in temporal and parietal cortices, may contribute to the manifestation of visual hallucinations in DLB (Imamura *et al.*, 1999). The number of times non-demented PD patients experience pareidolia, the misidentification of visual stimuli, has been significantly correlated with hypoperfusion of the occipital, temporal and parietal cortices (Uchiyama *et al.*, 2015). The authors suggest paradoelia is a marker for visual hallucinations, thus indicating that posterior cortical hypometabolism may create a vulnerability to hallucinogenesis. However, no difference in occipital glucose metabolism was previously found between hallucinating and non-hallucinating DLB cases (Metzler-Baddeley *et al.*, 2010).

Studies employing diffusion tensor imaging (DTI) have reported white matter damage in the occipital lobe in DLB, particularly in occipito-parietal tracts (Watson *et al.*, 2012), which exceeds that observed in AD and control patients (Nedelska *et al.*, 2015). DLB patients have a similar pattern of global white matter impairment to that observed in PDD but the association visual areas of the lateral occipital cortex are more severely affected in DLB than in PDD (Lee *et al.*, 2010). The authors speculate this may contribute to the greater vulnerability to visual hallucinations in DLB than PDD. However, another study has reported that occipital white matter damage is associated with an absence of visual hallucinations in DLB (Barber *et al.*, 1999).

### 1.8.4 The pulvinar

Neuropathological examination of the pulvinar, association visual cortex and inferior temporal cortex, components of the secondary visual pathway, has demonstrated Lewy body pathology is more severe than that observed in the primary pathway routed through the LGN and primary visual cortex (Yamamoto *et al.*, 2006). The pulvinar has been demonstrated to exhibit variable Lewy body pathology in DLB, ranging from absent to severe, which is independent of disease duration and concomitant AD-type pathology. In a comprehensive study of the pulvinar in PD, no sub-region of the pulvinar was found to exhibit neuronal or volumetric reductions compared to control or AD cases (Xuereb *et al.*, 1991). An ELISA study has demonstrated a reduction in the expression of kallikrein related peptidase 6 (KLK6)

in the pulvinar in DLB compared to control cases (Miners *et al.*, 2014a). KLK6 is a protease with a putative function in the cleavage of α-synuclein within its most fibrillogenic region, suggesting it may inhibit aggregation of α-synuclein (Kasai *et al.*, 2008). However, there was no relationship between KLK6 levels and α-synuclein pathology (Miners *et al.*, 2014a).

DTI MRI has been used to assess thalamic sub-nuclei on the basis of connectivity. DLB patients have increased mean diffusivity, as a putative marker of tissue damage, in thalamic regions projecting bilaterally to the prefrontal and parieto-occipital cortices (Delli Pizzi *et al.*, 2015b). Using the same approach but specifically framed around visual hallucinations, the same research team have demonstrated increased mean diffusivity in posterior thalamic regions projecting to occipital and parietal cortical regions, which is significantly related to the severity and frequency of visual hallucinations in DLB (Delli Pizzi *et al.*, 2014). The anatomy of the posterior thalamus does not map perfectly onto sub-regions delineated as a result of connectivity studies (Shipp, 2003). However, posterior thalamic projections to occipital and parietal regions reflect known pathways emanating from the pulvinar in non-human primates (Soares *et al.*, 2001; Kaas and Lyon, 2007). Neuroimaging analysis of connectivity has demonstrated disconnect between the thalamus and occipital cortex in DLB (Caminiti *et al.*, 2016), which could have relevance to the LGN and pulvinar as both are strongly interconnected with the occipital lobe (Jones, 2012).

### 1.8.5 The superior colliculus

Neuropathology in the superior colliculus has only been investigated in DLB in one study, which found moderate Lewy body pathology (Sierra *et al.*, 2016). However, this study did not assess neuronal density or the vulnerability of individual laminae to Lewy body pathology, nor were the findings related to visual hallucinations.

Structural connectivity studies have reported decreased white matter integrity in the anterior thalamic radiation, which is related to microstructural damage in the mediodorsal thalamic nucleus (Delli Pizzi *et al.*, 2015a). The mediodorsal thalamus receives input from the superior colliculus (Erickson *et al.*, 2004) in a pathway that ultimately projects to the frontal eye fields (Sommer and Wurtz, 2004), perhaps indicating that this pathway is dysfunctional in DLB.

### 1.8.6 Brain regions beyond the primary and secondary visual pathways

A DTI study of white matter pathways has demonstrated increased diffusivity of the inferior longitudinal fasciculus, a white matter tract projecting from the occipital lobe to the temporal cortex, associated with visual hallucinations in DLB (Kantarci *et al.*, 2010). Consistent with the proposal that occipito-temporal abnormalities may contribute to visual hallucinations, hypometabolism in the right occipito-temporal junction is greater in DLB patients with visual hallucinations compared to those without (Perneczky *et al.*, 2008).

SPECT studies of cerebral perfusion have demonstrated hypoperfusion in the right inferior temporal lobe and bilateral perfusion in the anterior cingulate (Heitz *et al.*, 2015), and the left midcingulate gyrus (Blanc *et al.*, 2014), are significantly correlated with the intensity of visual hallucinations in DLB. A combined study using MRI and PET has reported atrophy and reduced perfusion of the right anterior insula is significantly related to the intensity of visual hallucinations (Blanc *et al.*, 2014).

Temporal lobe Lewy body pathology burden has been correlated with the presence of visual hallucinations, especially in the amygdala and parahippocampal gyrus (Harding *et al.*, 2002). In the temporal lobe, hallucinating PD cases have higher densities of Lewy bodies in the middle temporal gyrus, entorhinal cortex and anterior cingulate compared to those with no history of visual hallucinations (Gallagher *et al.*, 2011).

Higher Lewy body pathology has also been found in the amygdala, frontal, temporal and parietal cortices in PD patients with visual hallucinations compared to those without hallucinations (Papapetropoulos *et al.*, 2006). However, the group with visual hallucinations predominantly had neocortical Lewy body pathology, compared to the non-hallucinating group who generally had brainstem and transitional types. As visual hallucinations typically occur later in the time course of PD (Fenelon *et al.*, 2000; Richard *et al.*, 2002), and neocortical Lewy body pathology is thought to be the final stage of α-synuclein deposition (Braak *et al.*, 2004; McKeith, 2006), these findings may simply reflect changes resulting from longer disease duration.

Visual hallucinations in DLB have been related to reduced nicotinic α-bungarotoxin binding in the temporal lobe, possibly due to the loss of alpha 7 nicotinic receptor markers (Court *et al.*, 2001). Increased binding of ligands for M2 and M4 muscarinic receptors in the cingulate has been related to the presence of visual hallucinations and may be involved in their pathophysiology (Teaktong *et al.*, 2005).

## 1.9 Summary and overview

DLB is a common neurodegenerative dementia disorder marked by the presence of complex and recurring visual hallucinations (McKeith, 2006). Despite being a core symptom of DLB, there is a paucity of evidence regarding the pathological aetiology of visual hallucinations (Burghaus *et al.*, 2012). There is some evidence to support the hypothesis that cortical excitability changes could contribute to visual hallucinations in DLB (Ffytche, 2005; Taylor *et al.*, 2011; Makin *et al.*, 2013). The visual thalamus contains nuclei involved in ascending connections to the cortex through the LGN, as well as structures involved in visual attentional functions such as the pulvinar. The superior colliculus is proximal to the LGN and pulvinar, functionally interacting with both, and has previously been directly related to processes implicated in visual hallucinations in DLB (Diederich *et al.*, 2014; Shine *et al.*, 2014). A number of hypotheses directly implicate subcortical visual thalamic structures, or predict dysfunctional activity consistent with the known function of these structures, in the manifestation of visual hallucinations in DLB. The present study therefore quantitatively assessed cellular populations in structures within, or interacting with, the visual thalamic circuitry. Additionally, proteomic assessment was conducted on the pulvinar to evaluate whether it manifests changes at the molecular level. The overall goal of this study was thus to evaluate whether subcortical visual structures manifest changes that could create a vulnerability to visual hallucination in DLB.

## 1.10 Research aims

The present study aimed to assess the vulnerability of the visual thalamic structures to neurodegenerative changes in DLB. Such changes, if present, may provide insights into the pathological aetiology of visual hallucinations in DLB.

The hypothesis for this study was that some or all assessed subcortical visual structures, the LGN, pulvinar and superior colliculus, possess a distinct pattern of neurodegenerative pathology and/or alterations to neuronal/glial populations in DLB compared to AD and control cases. Additionally, the pulvinar nucleus was hypothesised to have an altered gene and protein expression profile that may create a vulnerability to visual hallucinations in DLB compared to control cases.

This study aimed to:

1) Assess the burden of α-synuclein, tau and amyloid-β pathology in the sub-regions of the LGN, pulvinar and superior colliculus in DLB, AD and control cases using quantitative histological techniques.
2) Calculate neuronal and glial cell populations in the sub-regions of the LGN, pulvinar and superior colliculus in DLB, AD and control cases using three-dimensional stereological analysis.
3) Identify proteins to target based on gene expression analysis using RNA sequencing data from pulvinar tissue in DLB compared to control cases.
4) Assess targeted proteins in the pulvinar in DLB compared to control cases, using molecular techniques.

# Chapter 2: Methods

## 2.1 Introduction

This chapter describes the sampling and staining of histological specimens and the biochemical assay protocols performed on fixed and frozen brain tissue. These will be separated into histopathological analysis using fixed human tissue and biochemical analysis using frozen human tissue. Histopathological analysis incorporates the dissection methods and storage of fixed tissues, the histological and immunohistochemical methods to stain tissues and the stereological and densitometric analyses to assess pathological and morphological changes. Biochemical analyses will outline the acquisition of frozen tissue specimens, the RNA isolation techniques for RNA sequencing, the bioinformatics techniques used to assess pathway changes and the proteomic assays used to quantify protein expression in tissue.

## 2.2 Study cohort

DLB and AD cases were selected for inclusion in the present study on the basis of fulfilling clinical and neuropathological criteria for DLB or AD, respectively (McKeith *et al.*, 2005; Montine *et al.*, 2012). AD cases were included as a group with well-defined cognitive impairment and neurodegenerative pathology but an absence of complex visual hallucinations (Burghaus *et al.*, 2012). Clinico-pathological diagnosis was reached following a case note review by senior clinicians and consideration of neuropathological findings by a senior neuropathologist. In most cases, DLB cases were included on the basis of a clinical history of recurrent complex visual hallucinations. Control cases were included on the basis of an absence of neurological and psychiatric disorders during life and absent or low neurodegenerative pathology on *post-mortem* assessment. The individual characteristics of the individual study cohorts are detailed in each chapter.

## 2.3 Tissue acquisition and preparation

### 2.3.1 Tissue preparation at the Newcastle Brain Tissue Resource

All brain tissue was acquired from the NBTR, a United Kingdom Human Tissue Authority approved research tissue bank. Ethical approval was granted by the Local Research Ethics Committee of Newcastle and North Tyneside Health Authority (ref: 08/H0906/136). Tissue was obtained at autopsy, with the interval from death to freezing and fixation noted. Tissue from the left hemisphere was sliced coronally at approximately 1 cm intervals, prior to rapid freezing at -80°C between copper blocks. The right hemisphere was fixed in 10% neutral-buffered formalin for five weeks before dissection into 7 mm coronal sections. From the 7 mm coronal slices, a pre-defined number of sections were sub-dissected into blocks used for diagnosis and research (Fig. 2.1). All fixed brain tissue sections were then processed by paraffin wax embedding, including the remaining tissue following sub-dissection of diagnostic tissues.

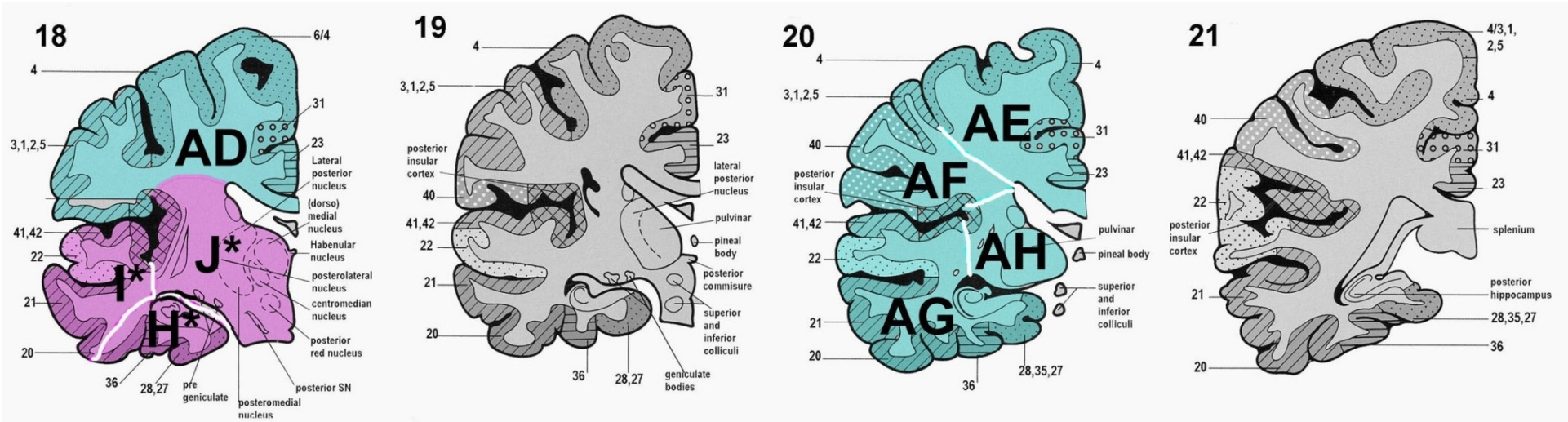


*Figure 2.1: Brain map of dissection protocol at NBTR.*

*Brain regions with letters indicate the code for the individual blocks that are used for neuropathological diagnosis. The LGN and pulvinar were typically found, in entirety, between coronal levels 18 and 21. Purple and cyan coloured blocks indicate blocks that are obtained for diagnostic and research purposes, respectively. Blocks J and AH from the NBTR dissection protocol were usually sampled for analysis.*

### 2.3.2 The lateral geniculate nucleus

The LGN is a small structure located on the ventrolateral aspect of the surface of the posterior thalamus and is easily identified on coronal sections by its distinctive shape and laminar structure (Fig. 2.2A). The LGN was serially sectioned from the start of the first tissue block on which it was not present based on gross examination, typically corresponding to coronal levels 16-17 or block F on the NBTR brain dissection protocol, until its disappearance (Fig. 2.1).

### 2.3.3 The pulvinar nucleus

The pulvinar is the largest of the thalamic nuclei and occupies the majority of the posterior aspect of the thalamic complex (Jones, 2012) (Fig. 2.2B). The pulvinar was identified at its anterior pole, situated on the lateral posterior aspect of the centromedian thalamic nucleus (Fig. 2.2A) (Popken *et al.*, 2002; Mai *et al.*, 2016). Sectioning commenced from the presence of the centromedian nucleus without any pulvinar present, to ensure that the complete antero-posterior extent of the pulvinar was sampled through the z-axis. On the NBTR brain dissection protocol, sectioning typically commenced at coronal level 16-17 (block F; Fig. 2.1).

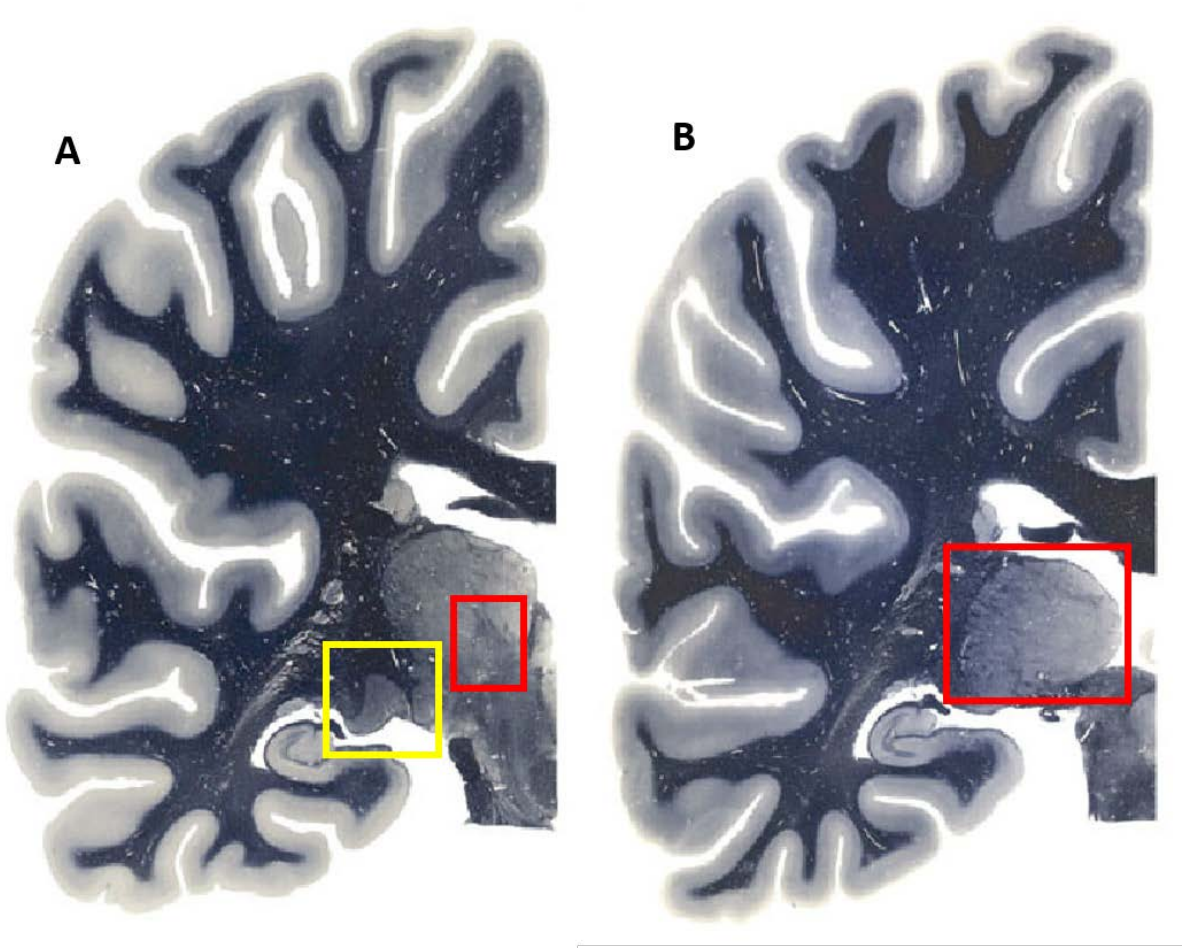


*Figure 2.2: Coronal brain sections illustrating the LGN and pulvinar.*

*Sections are stained with Loyez's haematoxylin and illustrate the anatomical location of the LGN and pulvinar. A demonstrates the LGN (yellow) and the centromedian thalamic nucleus (red). B illustrates the pulvinar complex (red). Images courtesy of (Mai et al., 2016), plates 44 and 46.*

### 2.3.4 The superior colliculus

Under the NBTR brain dissection protocol, the midbrain was cut from the cerebrum at the level of the third cranial nerve, along a line from the junction of the mammillary body running posteriorly to the upper part of the superior colliculus. The superior colliculus was identified based on its location on the dorsal aspect of the midbrain, proximal to the periaqueductal grey (Krauzlis *et al.*, 2013) (Fig. 2.3).

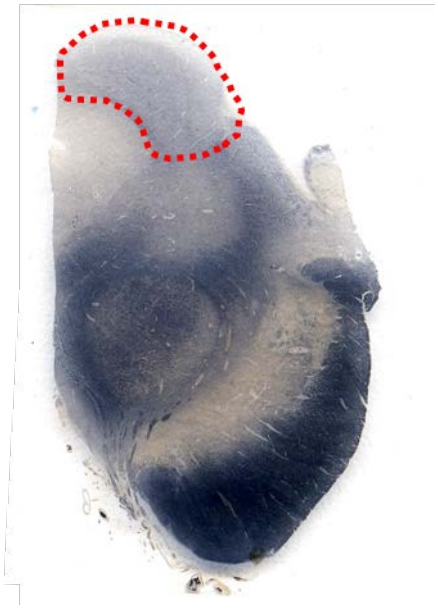

*Figure 2.3: Left upper midbrain stained with Loyez's haematoxylin.*

*The superior colliculus is outlined in red. This is a photomicrograph of a control case.*

### 2.3.5 Cutting and preparation of tissues

Blocks containing the entire structure of interest were sectioned on a HM340E rotary microtome with a *z*-axis monitor (Thermo Scientific, Waltham, MA, USA), with 5x 30 µm and 10x 10 µm sections taken at every 0.5 mm interval (Fig. 2.4).

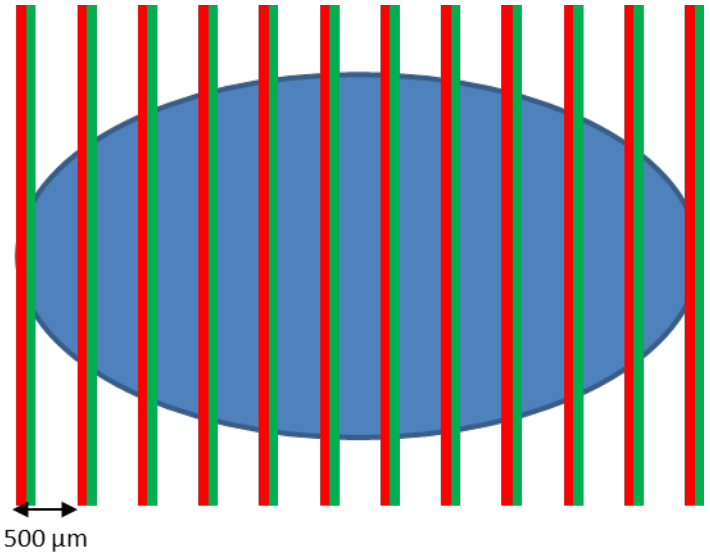


*Figure 2.4: Sampling strategy used for stereological analysis.*

*From a random starting point, 5x 30 µm sections (red) and 10x 10 µm (green) were taken, the tissue (blue) was then cut through for approximately another 250 µm, until 500 µm from the initial start of that interval was reached.*

Sections were mounted onto Histobond (CellPath, Newtown, UK) charged slides using a water bath and dried for 48 hours at 30 °C. Once dried, sections were stored at room temperature prior to staining.

### 2.3.6 Histological staining with cresyl violet

Cresyl violet staining was conducted on 30 µm sections at intervals using the sampling scheme noted in Fig. 2.4. Sections were first heated in a 60°C oven for 30 minutes prior to dewaxing by immersion in absolute xylene, then rehydrated through a graded series of ethanol solutions from absolute ethanol to 95% ethanol. Sections were then placed in 1% hydrochloric acid in 70% ethanol for five minutes then

washed in distilled water, prior to incubation in pre-heated 60°C cresyl fast violet solution in a 60°C oven for five minutes and removed from the oven to cool for a further five minutes in solution. Sections were differentiated in 95% ethanol solution until pallor of the internal capsule was evident on thalamic sections or the red nucleus and periaqueductal grey were visible on upper midbrain sections, before being dehydrated through a graded series of progressively less dilute ethanol solutions, cleared in xylene and mounted using DPX (CellPath, Newtown, UK).

### 2.3.7 Immunohistochemistry

Immunohistochemistry was conducted on 6-10 μm formalin-fixed tissue sections. Paraffin-embedded sections were first heated in a 60°C oven for 30 minutes prior to dewaxing by immersion in absolute xylene. Sections were then rehydrated through a graded series of progressively more dilute ethanol solutions, beginning with absolute ethanol and progressing through 95%, 90%, 70%, 50% and 30% solutions until water. Antigen retrieval protocols were conducted on tissue sections to unmask epitopes that have been cross-linked as a result of tissue fixation. The optimal technique used to unmask the epitopes was empirically determined and differed for the individual antibodies employed. Antigen retrieval using citrate buffer used trisodium citrate pH 6.0 pre-heated for 10 minutes at full power in an 800 watt microwave (SLS, Hessle, UK), then heated on full power in the microwave with the slides for 10 minutes and cooled in the solution for 20 minutes at room temperature. The formic acid method involved immersing slides in room temperature absolute formic acid for a pre-determined period of time. Ethylenediamine tetra-acetic acid (EDTA) pH 8.0 antigen retrieval was performed in a pressure cooker. EDTA buffer was heated in a pressure cooker until boiling and sections were then placed in boiling EDTA for two minutes. Sections were then washed in flowing water. Trypsin antigen retrieval used trypsin working solution pH 7.8 consisting of 0.5% trypsin in water mixed with 1% calcium chloride in water and diluted to 0.05% trypsin with water. Trypsin working solution was heated to 37ºC and sections were placed into the solution and incubated for 15 minutes at 37ºC, prior to washing in running water.

Endogenous peroxidase activity in tissues was blocked in 3% hydrogen peroxide in water for 20 minutes. Sections were thoroughly washed after quenching, firstly in

water and then in three washes of 10 mM tris-buffered saline and Tween20 pH 7.6 (TBST).

Tissue sections were outlined using an ImmEdge hydrophobic barrier pen (Vector Laboratories, Burlingame, CA, USA) and primary antisera, suspended in TBST, were pipetted onto the section and incubated for one hour at room temperature. Following three washes in TBST, the universal probe from the Menarini MenaPath kits (Menarini, diagnostics, Berkshire, UK) was placed onto the section for 30 minutes incubation at room temperature. Sections were then washed three times in TBST before polymer solution conjugated to horseradish peroxidase (Menarini MenaPath) was placed onto sections and incubated for 30 minutes, prior to three washes in TBST. To visualise antibody binding, 3, 3' diaminobenzidine (DAB) chromogen in DAB substrate buffer (Menarini MenaPath) was made up as per manufacturer's instructions and applied to sections for four minutes. Sections were then washed in running water for ten minutes.

Sections were counterstained by placing them in Mayer's haematoxylin solution for 30 seconds. They were then washed in water, differentiated with 1% hydrochloric acid in 70% ethanol, and blued with 1% ammonia in water.

Sections were then dehydrated through a series of progressively more concentrated ethanol solutions until absolute ethanol, before clearing in xylene and being mounted with DPX (CellPath, Newtown, UK). Sections were carefully checked by the unaided eye and under a microscope to ensure quality and consistency of staining.

## 2.4 Stereological analysis

### 2.4.1 Introduction to stereology

Stereological methods enable one to estimate three-dimensional attributes of a structure, such as volume, based on its two-dimensional profile on sections taken at uniform intervals throughout the entire structure (Mouton, 2013). This differs from traditional neuropathological methods, which typically use a single section from a brain structure and calculate the density of a particular object within a defined region of interest. This approach assumes that a section obtained from an arbitrary point within a brain structure is representative of the whole region, and that objects within the structure are expressed in a homogeneous distribution throughout. Neuronal

counts within a single structure are dependent upon the structure being cut at the same plane in every case, to ensure a similar area is sampled in every case.

To overcome issues with two-dimensional analysis of the brain, stereological protocols enable greater inference to be drawn regarding three-dimensional characteristics of individual structures (Mouton, 2011). Using this method, assumptions regarding the homogeneous distribution of particles within a structure and sectioning on the same plane do not have to be made as the whole structure is sampled. For small structures, such as those to be assessed in the present project, this typically involves serially sectioning the entire structure from its anterior to posterior pole (Mouton, 2013). As a result, this is a labour-intensive approach typically only employed in a research setting and is often at odds with the efficient reporting of cases conducted in a brain storage facility. However, several studies have been conducted using stereological methodology to investigate changes to neuronal populations that occur in various dementias (Erskine and Khundakar, 2016). Previously, stereological studies have demonstrated important relationships between neuronal loss and cognitive decline in AD (Gomez-Isla *et al.*, 1996; von Gunten *et al.*, 2006).

In the present studies, stereological methodology has been employed to investigate whether total neuronal or glial number differs in the subcortical visual structures across the individual experimental groups. Total cell number is estimated by determining volume on the basis of the two-dimensional profile of the structure of interest obtained at known intervals analysed serially throughout the entire structure. As a result of the whole structure being evaluated, it is not affected by artefacts such as the plane on which the object is cut or the distribution of the sampled object within the structure (Mouton, 2011). Cellular density is calculated by counting the object of interest within randomly sampled areas of the region of interest, inside a frame of known size. Total number is then estimated as a product of the mean density of the cellular population of interest per area, and the total volume of the structure.

### 2.4.2 Sampling method

Stereologer software (Stereologer, Bethesda, MD, USA) was used on a computer coupled to a Zeiss AxioVision Z.1 microscope (Zeiss, Oberkochen, Germany) with a

motorised stage. As outlined in section 2.3.5 on cutting and preparation of tissues, the LGN and pulvinar were serially sectioned, beginning at a random point within the first interval, and then at systematic 0.5 mm intervals through the antero-posterior extent of the structure (z-axis) until the posterior pole, as outlined in Fig. 2.4. As the starting point was random, and the intervals between sampled sections were uniform, this meant that the every part of the structure had an equal probability of being sampled for analysis. On the basis of this sampling method, the entire structure was sampled throughout its z-axis.

On each coronal section, a region of interest corresponding to the boundary of the structure (x-y axis), was drawn at low magnification (Fig. 2.5A). Within the delineated region of interest, a systematic, randomly-oriented point grid was superimposed over the observed image (Fig. 2.5B). The imposition of a randomly-oriented point grid means that every area within the region of interest has an equal probability of being sampled for analysis. As a result of this sampling method, a representative sample of the coronal profile of each structure was obtained across its x-y axis on each section. This meant that the structure was sampled in a systematic and random manner through its x-y and z axis.

The number of sections analysed per case, and the interval between the individual points on the grid, were empirically determined for each structure based on an initial pilot study, prior to the collection of data. Initial pilot studies consisted of analysis of a minimum of two complete cases. On the completion of the pilot cases, coefficient of error (CE) values were calculated with the aim of assessing whether each case had been sampled to a sufficient degree to ensure that sampling error was within acceptable boundaries. CE values were determined by the Gundersen-Jensen method (Gundersen and Jensen, 1987), as described by the following equation:

$$CE^2 = \left(\frac{\Sigma\,(I^2)}{(\Sigma\,I)^2} + \frac{\Sigma\,(Volume^2)}{\Sigma\,(Volume^2)} - \frac{2\Sigma(1 \cdot Volume)}{(\Sigma\,I \cdot \Sigma\,Volume)}\right) \cdot \left(\frac{n}{n-1}\right)$$

Where $I$ = objects counted, $Volume$ = reference area x (sampling frame density)$^2$ x section depth, and $n$ = number of fields.

CE values between 0.01 and 0.15 are considered to contain acceptable levels of error (Herculano-Houzel *et al.*, 2015).

### 2.4.3 Estimation of the volume of structures

The present series of studies were designed to estimate the total number of neurons within the specified brain regions across different disease states. Therefore, in each individual case, the parameters to be assessed were the total volume of the structure and the mean number of neurons within a defined volume of tissue. The product of the mean number of neurons per volume, combined with the total volume of the structure, gives an estimation of the total number of neurons within each structure per case.

A systematic and random counting grid was superimposed onto the image, as outlined in the previous section, and Cavalieri's method was used to determine the volume of the structure. Cavalieri's principle allows estimation of the total volume of a structure of interest based on the intersection distance (*T*), the area per point on the counting grid (*a*) and the sum of the number of counted points (*p*):

$$V := T \cdot a \cdot \Sigma p$$

As outlined in section 2.4.2 on the sampling of tissues, a region of interest was drawn around the border of the structure in the x-y axis at low magnification of 2.5x objective. A counting grid was then super-imposed over this image on the screen of the computer coupled to the microscope. The distance between points on the counting grid was empirically determined, based on the result of pilot studies. All points within the defined region of interest were clicked to count them as within the region of interest. This was repeated for every section at equally-spaced intervals for the entirety of the structure through the *z* axis per case. On the basis of the information input to the programme, the software calculated an estimate of the total volume of the structure, according to the Cavalieri principle.

### 2.4.4 Estimation of neuronal number

To determine the mean density of cells within a given structure, the x-y axis was randomly sampled, as outlined in section 2.4.2 on the sampling of tissues. Similar to the point-grid that was used for determination of volume using the Cavalieri method, a grid of randomly-oriented points was used to sample the x-y axis. In this instance, each point corresponded to an area that was then viewed at high magnification. The number of points per area of tissue was empirically determined on the basis of pilot studies. Within each area viewed at high magnification, a frame of known size was superimposed onto the observed image (Fig. 2.5C). The frame size employed for each structure was empirically determined based on pilot studies. The thickness of the section was determined, then the number of cells within each frame was counted, excluding cells that transected the border of the frame on its left and bottom border. The known size of the frame and the thickness of the section enabled the volume of tissue sampled to be determined and, therefore, the mean density of cells per volume were calculated. This procedure was repeated for every section at equally-spaced intervals for the entirety of the structure through the *z* axis, yielding the numerical density, i.e. the mean number of cells in a given volume of tissue.

The numerical density was calculated per case as follows:

$$Nv = \frac{\sum^{p-} Q^{-}}{P \cdot V}$$

Where $Nv$ = numerical density, $p-$ = disector samples, $Q^{-}$ = *Q*-weighted number of objects counted, $P$ = total number of disectors, and $V$ = disector volume.

Although point grids were used to determine volume and to select regions in which to count cells at high magnification, these two steps were conducted sequentially by the software programme. Therefore, it was possible for the interval between points for determination of volume to be different from the interval used for selecting the frame in which to count cells at high magnification. For each parameter, the interval between points in counting grids was kept the same for all cases per structure.

An overall estimate of the number of cells present within a structure of interest was determined automatically by the Stereologer software by calculating the mean

number of cells in a given area, with consideration of the volume estimate provided by the Cavalieri method.

In practice, a series of sections for each structure per case was obtained. On each section, a region of interest was drawn around the structure at 2.5x objective (Fig. 2.5A). A grid of points was then superimposed over the region of interest, points on the region of interest had to be clicked to turn green, thus providing data to determine volume using the Cavalieri principle (Fig. 2.5B). As before, another point grid was superimposed, the size of which was empirically determined by pilot studies, to sample the x-y axis to determine areas that will be viewed at 63x objective to determine cellular density (Fig. 2.5B). Neurons were then counted within disector frames of known dimensions at 63x oil immersion objective (Fig. 2.5C). At each point, the top and bottom of the section were established through the z-axis, thus determining the thickness of the section. Cells were counted if their nucleolus was present within the frame, or if they were on the right or top border of the frame (Fig. 2.5C). Neurons were differentiated from glia based on the presence of Nissl substance within the cytoplasm, a pale nucleus and a single, identifiable, nucleolus (Khundakar *et al.*, 2009).

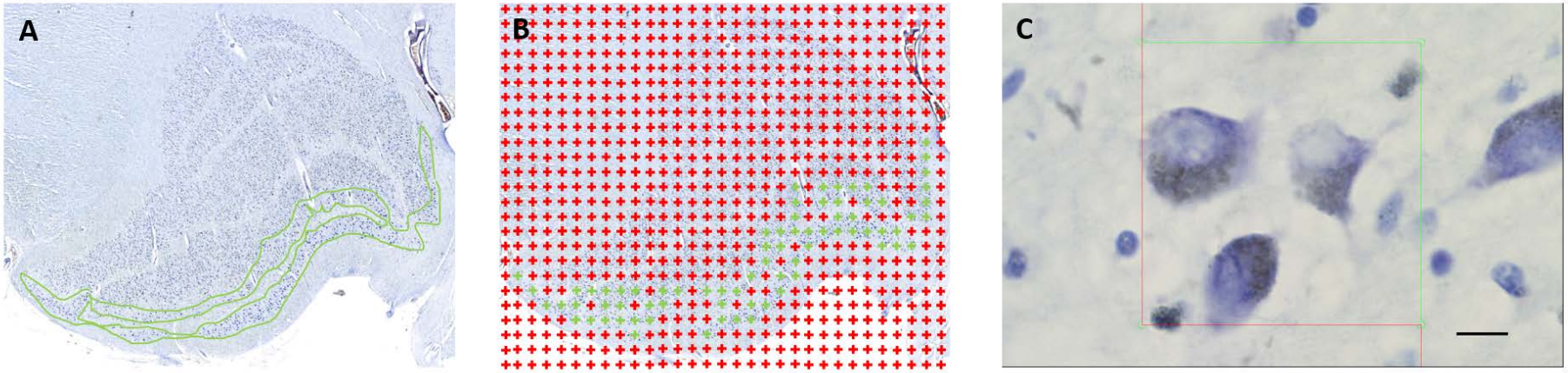


*Figure 2.5: Stereological methods.*

*A region of interest was drawn around the structure to be assessed, in this instance the magnocellular laminae of the LGN (A). A point grid was superimposed over the structure, points were clicked to turn green if they were within the region to be sampled (B). The points clicked were used to determine volume using the Cavalieri method, and neurons were counted within randomly-sampled frames in the x-y axis. Randomly sampled points within the region of interest were viewed at high magnification, and neurons were counted within a disector frame of known dimensions (C).*

## 2.5 Densitometric analysis of immunoreactivity

Densitometric analysis assessed the percentage area stained by an antibody in a particular region of interest.

For the LGN, images of the entire the region of interest on coronal sections throughout the z-axis of the structure were captured on a microscope using a camera coupled to a computer. The images were imported into NIS elements (Nikon, Tokyo, Japan) or ImagePro (Media Cybernetics Plus v.4.1 (Bethesda, MD, USA) image analysis software and standardised red-blue-green (RGB) thresholds were determined separately for each antibody. To exclude intracellular amyloid-β from analysis of 4G8 antibody, size restrictions were also employed based on empirical observations of size. Intracellular amyloid-β was not counted as it is present in most cells and may then be affected by factors such as neuronal loss. This allowed analysis of the immunopositive signals without detection of non-specific background staining, as it did not reach the intensity threshold for detection. The percentage area stained was recorded for every image taken and a mean generated across all images per case.

For the pulvinar and superior colliculus, the Stereologer programme was used to draw a region of interest at 2.5x objective, from which randomly sampled points were analysed on higher-magnification, either 10x, 20x or 40x objective, dependent upon the size and distribution of the objects being analysed. For consistency, the objective at which objects were analysed was the same for each antibody per region across all cases. The randomly sampled frames were photographed, using the microscope camera, and imported to ImagePro or NIS elements analysis software to conduct analysis of the percentage area stained (Fig. 2.6). RGB thresholds were empirically determined and applied per antibody. Size thresholds were employed for 4G8 amyloid-β analysis to prevent counting of intracellular amyloid-β.

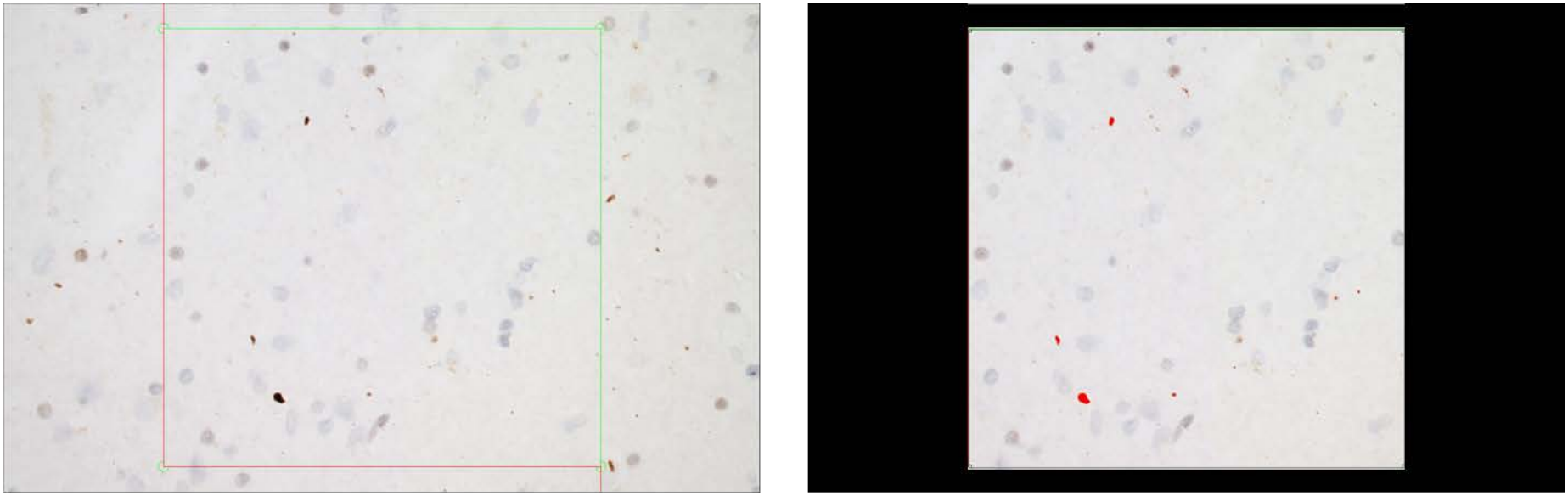

*Figure 2.6: Densitometric analysis of immunoreactivity.*

*Images of sections stained with α-synuclein at 20x magnification have a region of interest drawn around the disector frame. A colour threshold is then applied which detects immunoreactivity labelled by the DAB chromogen within the region of interest only but does not detect non-specific background staining.*

## 2.6 Molecular techniques

### 2.6.1 RNA isolation and sequencing

Frozen tissue was placed in 5-10 volumes of pre-cooled RNA*later* solution (Ambion, Warrington, UK) and stored at -80°C. Tissue was removed from RNA*later* and rapidly homogenised in TRI-reagent (Ambion, Warrington, UK) and stored at -80°C. RNA was extracted using a spin column method as per manufacturer's instructions (Ribopure, Ambion, Warrington, UK), and 1 µg of RNA DNase-treated (Turbo-DNase free, Ambion, Warrington, UK). The RNA concentration was determined using a Nanodrop ND 1000 Spectrophotometer (Nanodrop Technologies, DE, USA) and RNA integrity number examined with an Agilent 2100 Bioanalyzer RNA 6000 Nano Assay (Agilent Technologies, Stockport, UK) according to manufacturer's instructions.

### 2.6.2 Western blotting

Frozen tissue was brought to -20°C in a freezing cabinet and relevant regions removed. Approximately 20 mg tissue was homogenised using a rotor-stator type homogeniser in ice cold lysis buffer containing 0.2 M tetraethyl ammonium bicarbonate, pH 7.2 (TEAB; Sigma-Aldrich, MO, USA), 1 mM EDTA and protease inhibitor tablets (Complete, Roche, Burgess Hill, UK). Samples were made to 0.02% sodium dodecyl sulphate and sonicated on ice in a sonicating water bath for 20 minutes and with a sonic probe for five seconds. Protein quantification was then performed using Bradford assay (Sigma-Aldrich, MO, USA).

Samples were prepared for sodium dodecyl sulphate polyacrylamide gel electrophoresis (SDS-PAGE) by adding sample buffer (Novex NuPAGE LDS sample buffer, Invitrogen, Waltham, MA, USA), a reducing agent (NuPAGE sample reducing agent, Invitrogen, Waltham, MA, USA) and made up to 1 µg/µl with TEAB. Prepared samples were then denatured by heating at 70 ºC to reveal primary protein structure. Prepared tissue samples were then loaded onto NuPAGE 12% Bis-Tris gel (Invitrogen, Waltahm, MA, USA), 10 µg per well, with 1x SDS NuPAGE MOPS Running Buffer containing NuPAGE Antioxidant (Invitrogen, Waltham, MA, USA). Proteins were transferred to a nitrocellulose membrane using an iBlot transfer device (Invitrogen, Waltham, MA, USA) and stained with Ponceau S solution (Sigma-Alrich, MO, USA) to ensure successful transfer and equal protein loading. Membranes were

destained with 1x TBST (Sigma-Aldrich, MO, USA) and stored in TBST at 4°C overnight.

Membranes were incubated in 5% dried milk (Marvel, Premier Foods, Griffiths Way, UK) in TBST for 60 minutes at room temperature to block non-specific protein binding sites. Primary antibody incubation was conducted for one hour at room temperature diluted in 5% dried milk in TBST with agitation. Membranes were washed in TBST for 10 minute intervals two times, and then incubated for a further 30 minutes with horseradish peroxidase conjugated secondary antibodies at room temperature under agitation. Membranes were washed for 15 minutes four times in TBST prior to visualisation with Enhanced Chemiluminescence (GE, Amersham, Buckinghamshire, UK) and detected using x-ray film (Fuji, Fisher Scientific, Loughborough, UK). Size and intensity of protein bands was quantified using ImageJ software (NIH, Bethesda, MA, USA) with target protein expression normalised to glyceraldehyde 3-phosphate dehydrogenase-horseradish peroxidase conjugate (GAPDH-HRP conjugate; 1:4000, Santa Cruz, TX, USA) expression. Although concerns have been raised about the reliability of using highly-expressed housekeeping proteins as western blot loading controls (Goasdoue *et al.*, 2016), GAPDH has been demonstrated to be less variable across different biological conditions than other commonly used loading controls such as β-tubulin and β-actin (Goasdoue *et al.*, 2016; Lee *et al.*, 2016).

### 2.7 Statistical analysis

All data were assessed for normality by the Shapiro-Wilk test and inspection of histograms and Q-Q plots. Homogeneity of variance was assessed by Levene's f-test. Homogeneity of regression slopes was determined by inspection of co-regression of variables on a scatterplot.

If all assumptions were met, analysis of covariance (ANCOVA) was employed for all variables, using age and *post-mortem* interval as covariates. This enabled the effects of age and different degrees of *post-mortem* autolysis to be statistically controlled and has been used in similar stereological studies (Dorph-Petersen *et al.*, 2009). If all parameters excluding homogeneity of regression slopes were satisfied, analysis of variance (ANOVA) was used. This allows significant main effects to be identified in

data but does not enable one to control for covariates influencing the main effect. If data were not normally distributed, non-parametric Kruskal-Wallis tests were used.

Post-hoc analysis of ANCOVA was conducted using pairwise comparisons. For ANOVA, Tukey's honest significant difference (HSD) test was used. Kruskal-Wallis tests were followed by Mann-Whitney *U* tests. Corrections for multiple comparisons were not employed on Mann-Whitney tests. By convention, the Bonferroni correction (α/n, where n is the number of independent tests performed) is employed to attenuate for multiple comparisons. This correction is one of the most conservative multiple comparisons adjustments, as the α value falls markedly with higher numbers of tests, leading to increased probability of performing a type two error (i.e. a false negative) (Streiner and Norman, 2011). The premise of multiple comparisons testing has been criticised on the basis that it assumes chance is the first order explanation for observations, undermining the key tenet of empirical research that assumes regularities of nature which may explain observations (Rothman, 1990). Additionally, the relatively small samples employed in the present series of studies would likely mean that these studies would be under-powered to detect a significant difference if multiple comparisons corrections were employed. However, to determine the importance of statistically significant alterations, and to guard against potential type one errors (i.e. false positives), effect sizes were calculated using Cohen's d and considered for all observed changes.

# Chapter 3: Histological studies in the lateral geniculate nucleus

## 3.1 Introduction

Although visual hallucinations are a core clinical diagnostic feature of DLB, the pathological changes that give DLB patients a vulnerability to hallucination remain largely unknown (McKeith *et al.*, 2005; Diederich *et al.*, 2014). Physiological studies have demonstrated thinning of the retinal nerve (Moreno-Ramos *et al.*, 2013) and electroretinogram alterations in DLB (Devos *et al.*, 2005). Neuropathological studies have also demonstrated sparse neuritic α-synuclein pathology in the retina of nine PD and three DLB patients (Beach *et al.*, 2014) though another study, using six PD cases, has noted that retinal α-synuclein differs from Lewy pathology in the brain (Ho *et al.*, 2014). However, this has been contested with another study reporting retinal α-synuclein pathology to be similar to that observed in the brain (Bodis-Wollner *et al.*, 2014). Despite the high prevalence of visual perceptual abnormalities, the afferent visual system remains relatively under-studied in DLB.

The LGN relays incoming visual information from the retina to the primary visual cortex (Jones, 2012). Although it is a crucial structure for visual sensation, few studies have assessed how the LGN is affected by neurodegenerative disease. Sparse tau pathology has been recorded in AD and PSP (Dugger *et al.*, 2011), whilst amyloid-β pathology has been observed in the LGN in AD and some aged control cases (Leuba and Saini, 1995). Two studies have used qualitative methods to investigate the LGN in Lewy body diseases. One study found cell loss but an absence of Lewy body pathology in DLB (Yamamoto *et al.*, 2006) and another described α-synuclein pathology in the LGN and visual cortex in PD (Rahimi and Kovacs, 2014). The role of the LGN in visual hallucinations in DLB has not yet been investigated using quantitative neuropathological techniques, despite an opinion paper expressing the need for such studies (Diederich *et al.*, 2014). The aim of the present study, therefore, was to investigate whether pathological abnormalities exist in the LGN that may contribute to the generation of complex visual hallucinations in DLB.

### 3.1.1 Aims

Using *post-mortem* LGN tissue taken from DLB patients who had experienced visual hallucinations, compared with aged cognitively normal controls and disease-control AD patients with no visual hallucinations, this study aimed to:

1) Use stereological methods to estimate the total number of neurons and glial cells in the LGN.
2) Quantify the burden of neurodegenerative pathological lesions, labelled by antibodies against amyloid-β, phosphorylated tau and α-synuclein.
3) Assess whether there are changes to sub-populations of neurons labelled by antibodies against the calcium-binding proteins calbindin, calretinin and parvalbumin, and the GABA-ergic neuron marker glutamic acid decarboxylase 65/67 (GAD65/67).

## 3.2 Methods

### 3.2.1 Tissue acquisition

The LGN lies on the bank of the lateral ventricle, on the ventral surface of the posterior thalamus (Jones, 2007). The LGN is easily identified in coronal sections, even to the unaided eye, due to its distinctive striated architecture (Fig. 3.1) (Jones, 2012).

Three groups were included in the LGN study: DLB patients who had experienced complex visual hallucinations during life, AD patients who had not experienced complex visual hallucinations during life and aged controls showing none, or very low, age-associated neurodegenerative pathology and no clinical history of psychiatric disease. Cases with severe degenerative opthalmological conditions, such as glaucoma and macular degeneration, were excluded due to previously documented degeneration of the LGN in these disorders (Hernowo *et al.*, 2011; Zikou *et al.*, 2012). Within these criteria, cases were included based on whether the LGN was complete both coronally and along its antero-posterior extent. The cases meeting the criteria consisted of six DLB, seven AD and seven control cases (Table 3.1).

From a random starting point, fixed tissue blocks containing the entire LGN were serially sectioned from the anterior to the posterior pole to ensure that the entire structure was sampled. 30 μm sections were obtained at each 1 mm interval and

stained with cresyl violet for stereological analyses. 10 μm sections were obtained at approximately alternate intervals to those obtained for stereology were stained with antibodies against a range of protein targets (Table 3.2) using Menarini MenaPath Polymer kits (Menarini, Berkshire, UK), as described in Methods.

*Table 3.1: Demographic information for cases used in the LGN study.*

*'PM interval' represents the interval between death and post-mortem examination, 'Braak NFT' represents global neurofibrillary pathology stage as outlined in (Braak et al., 2006), 'McKeith LB' represents global Lewy body pathology stage, as outlined in (McKeith et al., 2005), 'clinico-path diagnosis' represents the overall diagnosis, as decided upon by case-note review and neuropathological examination by senior clinicians, in accordance with consensus criteria (McKeith et al., 2005; Montine et al., 2012).*

| Case ID | Gender | Age at death (years) | PM interval (hours) | Braak NFT | McKeith LB | Clinico-path diagnosis | Hallucinations |
|---|---|---|---|---|---|---|---|
| C1 | F | 78 | 23 | 2 | None | Control | None reported |
| C2 | F | 74 | 45 | 2 | None | Control | None reported |
| C3 | F | 85 | 99 | 2 | None | Control | None reported |
| C4 | M | 77 | 83 | 2 | None | Control | None reported |
| C5 | M | 73 | 25 | 0 | None | Control | None reported |
| C6 | M | 80 | 16 | 2 | Brainstem | Control | None reported |
| C7 | M | 85 | 57 | 2 | None | Control | None reported |
| Mean±SD | | 81.4±8. | 43.6±33 | 1.8±1 | | | |
| D1 | M | 84 | 56 | 2 | Neocortical | DLB | Complex visual hallucinations |
| D2 | M | 89 | 88 | 3 | Neocortical | DLB | Complex visual hallucinations |
| D3 | M | 71 | 8 | 3 | Neocortical | DLB | Complex visual hallucinations |
| D4 | M | 71 | 68 | 3 | Neocortical | DLB | Complex visual hallucinations |
| D5 | M | 78 | 83 | 1 | Neocortical | DLB | Complex visual hallucinations |

| | | | | | | | |
|---|---|---|---|---|---|---|---|
| D6 | F | 78 | 96 | 3 | Neocortical | DLB | Complex visual hallucinations |
| Mean±SD | | 78.5±7 | 66.5±32 | 2.5±1 | | | |
| A1 | M | 76 | 6 | 6 | None | AD | None reported |
| A2 | M | 91 | 22 | 5 | None | AD | None reported |
| A3 | F | 85 | 32 | 5 | None | AD | None reported |
| A4 | F | 77 | 63 | 6 | None | AD | None reported |
| A5 | F | 81 | 73 | 5 | None | AD | None reported |
| A6 | F | 93 | 34 | 5 | None | AD | None reported |
| A7 | F | 86 | 51 | 6 | None | AD | None reported |
| Mean±SD | | 84.1±7 | 40.1±24 | 5.4±1 | | | |

### 3.2.2 Stereology

The LGN has a distinctive laminar structure that enables delineation of functionally and anatomically distinct sub-populations of cells. The LGN is typically divided, based on laminae and cellular populations, into two ventral 'magnocellular' and four dorsal 'parvocellular' laminae (Dorph-Petersen *et al.*, 2009). Magnocellular neurons are optimised for detecting motion and rapidly changing visual information, in contrast to parvocellular neurons, which are better suited to detailed form and colour processing (Jones, 2012; Denison *et al.*, 2014). As a result of the functional differences between magnocellular and parvocellular neurons, separate stereological counts were made of both populations to help interpret the likely physiological effects of any specific changes. As shown in Fig. 3.1, neuronal and glial populations were determined by their anatomical location within laminae of LGN. However, as noted previously (Hickey and Guillery, 1979), some magnocellular neurons are present outside the two ventral laminae. Therefore, these 'islands' of magnocellular neurons were identified based on staining intensity and size (as in (Dorph-Petersen *et al.*, 2009)) and included in estimations of magnocellular neuron number, as in Fig. 3.1.

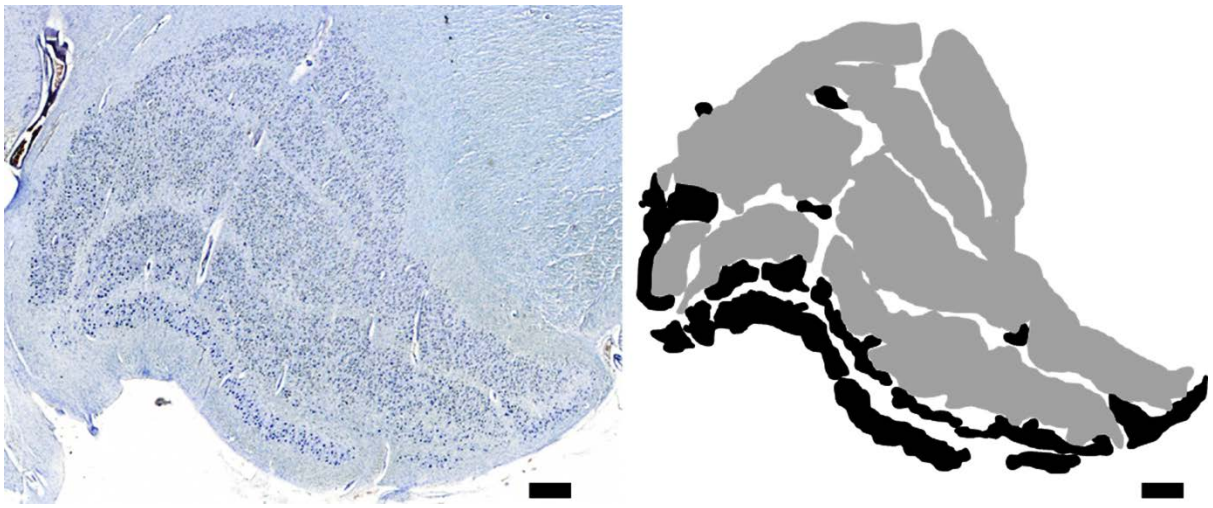

*Figure 3.1: Anatomy of the LGN.*

*This section is taken from approximately the midpoint through the coronal plane and stained with cresyl violet. Lamination is evident on the photomicrograph and the schematic illustrates how the LGN was divided into magnocellular (black) and parvocellular (grey). Bar = 1 mm.*

A third sub-type of LGN neuron, koniocellular cells, are distributed on the ventral aspect of some laminae, rather than being lamina-specific (Jones, 2012). A previous report suggested that koniocellular neurons are labelled by calbindin antibodies (Munkle *et al.*, 2000). However, no specific labelling was located in the LGN using

various methods of epitope unmasking and antibody titrations with two calbindin antibodies (Sigma Aldrich, MO, USA and Merck Millipore, Germany).

Stereological methodology was used to estimate the total number of neurons and glia within the LGN, as outlined in section 2.4. Cell counts were conducted at 63x oil-immersion objective using the optical disector probe. Glial cell counts were calculated in both LGN sub-regions in disector frames of 1900 $\mu m^2$, with neuron counts calculated in disector frames of 3500 $\mu m^2$. Section thickness did not significantly vary across disease groups in the magnocellular or parvocellular laminae. Mean CE values suggested that the analysis reached an acceptable level of accuracy, as all cases had CE values <0.10. A mean of 7 (range of 5-9) sections were analysed per case.

### 3.2.3 Densitometry

Sections from alternate intervals to those used for stereological analysis were stained with AT8, 4G8 and 5G4 antibodies to label phosphorylated tau, amyloid-β and aggregated α-synculein, respectively. To determine the percentage area immunoreactive for individual antibodies, images were taken of the entire LGN using a Nikon 90i microscope (Nikon, Tokyo, Japan) with a 20x magnifying objective and DsFi1 camera (Nikon, Tokyo, Japan). Images were then imported into NIS elements software and RGB thresholds determined individually for AT8, 4G8 and 5G4 antibodies, as described previously (Mandler *et al.*, 2014). As in section 2.5, individual thresholds were set based on colour and intensity to ensure that non-specific background staining was not included. Size thresholds were employed for sections stained with the 4G8 antibody to ensure that intracellular amyloid-β was not included in analyses.

To determine the percentage area immunoreactive for GAD65/67, calretinin and parvalbumin, sampled images were taken of the entire the LGN from sections throughout the structure, using a Zeiss AxioPlan 2 microscope (Zeiss, Oberkochen, Germany) with a 20x magnifying objective and 3-chip CCD true colour camera (JVC, Yokohama, Japan). Images were imported into the ImagePro Plus v.4.1 image analysis system and RGB thresholds determined individually for each antibody, as

described previously (Perry *et al.*, 2012). Individual thresholds were set based on colour and intensity to ensure that non-specific background staining was not included.

Cholinergic dysfunction is well described in DLB and may contribute to visual hallucinations (Perry and Perry, 1995). The LGN receives cholinergic afferents which directly modulate its excitability (Kodama and Honda, 1996), suggesting cholinergic dysfunction may alter visual system activity and potentially contribute to visual hallucinations. The LGN was stained with antibodies against choline acetyltransferase, a cholinergic marker, and the cholinergic pre-synaptic transporter to determine whether changes were observed in DLB compared to control and AD. However, no immunoreactivity was observed in the LGN with either antibody, despite numerous titrations and epitope retrieval steps being used. Choline acetyltransferase immunoreactivity was observed in the corpus striatum as expected but not immunoreactivity was observed in the LGN, implying that the antibody worked but the epitope recognised by the antibody was not present within the LGN. In the case of the vesicular cholinergic transporter, no immunoreactivity was visible anywhere, implying the antibody did not work.

### 3.2.4 Statistical analyses

Inspection of Q-Q plots, and Shapiro-Wilk and Levine's F tests suggested that LGN stereological data were normally distributed and had homogeneity of variance. Additionally, visual inspection of regression lines of stereological data with age and PM interval indicated that homogeneity of regression slopes could also be assumed. Therefore, ANCOVA was conducted on LGN stereological data, followed by post-hoc pairwise comparisons. However, neuropathological and densitometric data were not normally distributed, so Kruskal-Wallis and post-hoc Mann-Whitney tests were conducted.

*Table 3.2: Antibodies used in the LGN study.*

| Antibody | Manufacturer | Dilution | Antigen retrieval |
|---|---|---|---|
| 5G4 α-synuclein | Analytik Jena, Germany | 1:4500 | Formic acid + citrate pH 6.0 |
| AT8 phospho-tau | Autogen, MA, USA | 1:4000 | Citrate pH 6.0 |
| 4G8 amyloid-β | Covance, NJ, USA | 1:15000 | Formic acid |
| GAD65/67 | Sigma Aldrich, MO, USA | 1:12000 | Citrate pH 6.0 |
| Parvalbumin | Sigma Aldrich, MO, USA | 1:8000 | Citrate pH 6.0 |
| Calretinin | Sigma Aldrich, MO, USA | 1:1000 | Citrate pH 6.0 |

## 3.3 Results

### 3.3.1 Demographics

There was no significant difference in age at death ($F=0.92$, $p=0.415$), *post-mortem* delay ($F=1.486$, $p=0.253$) or gender ($\chi^2=3.935$, $p=0.140$) between experimental groups (Table 3.1).

### 3.3.2 Stereology

Stereological data are summarised in Fig. 3.2. A significant main effect of diagnosis on parvocellular neuron number was found ($F=5.845$, $p=0.013$), with a significant decrease in AD cases compared to DLB ($p=0.004$, $d=1.18$) and a trend towards a significant reduction in AD compared to control ($p=0.064$, $d=0.80$). A significant main effect of diagnosis on parvocellular glia cell number was found ($F=4.118$, $p=0.038$), with a significant decrease in AD cases compared to DLB ($p=0.012$, $d=1.17$). No significant main effect of diagnosis on neuronal or glial cell number was found in the magnocellular laminae.

There was no significant main effect of diagnosis on the ratio of glial cells to neurons in the parvocellular laminae of the LGN. However, a significant main effect of diagnosis on the ratio of glial cells to neurons was found in the magnocellular

laminae (F=7.733, p=0.005), with the ratio of glial cells to neurons increased in magnocellular laminae in AD compared to control (p=0.001, d=1.67) and in AD compared to DLB (p=0.035, d=1.15).

Braak stage was negatively correlated with the number of parvocellular neurons (rho=-0.473, p=0.035; Fig. 3.3) and the number of magnocellular neurons (rho=-0.444, p=0.050; Fig. 3.3) across all subjects.

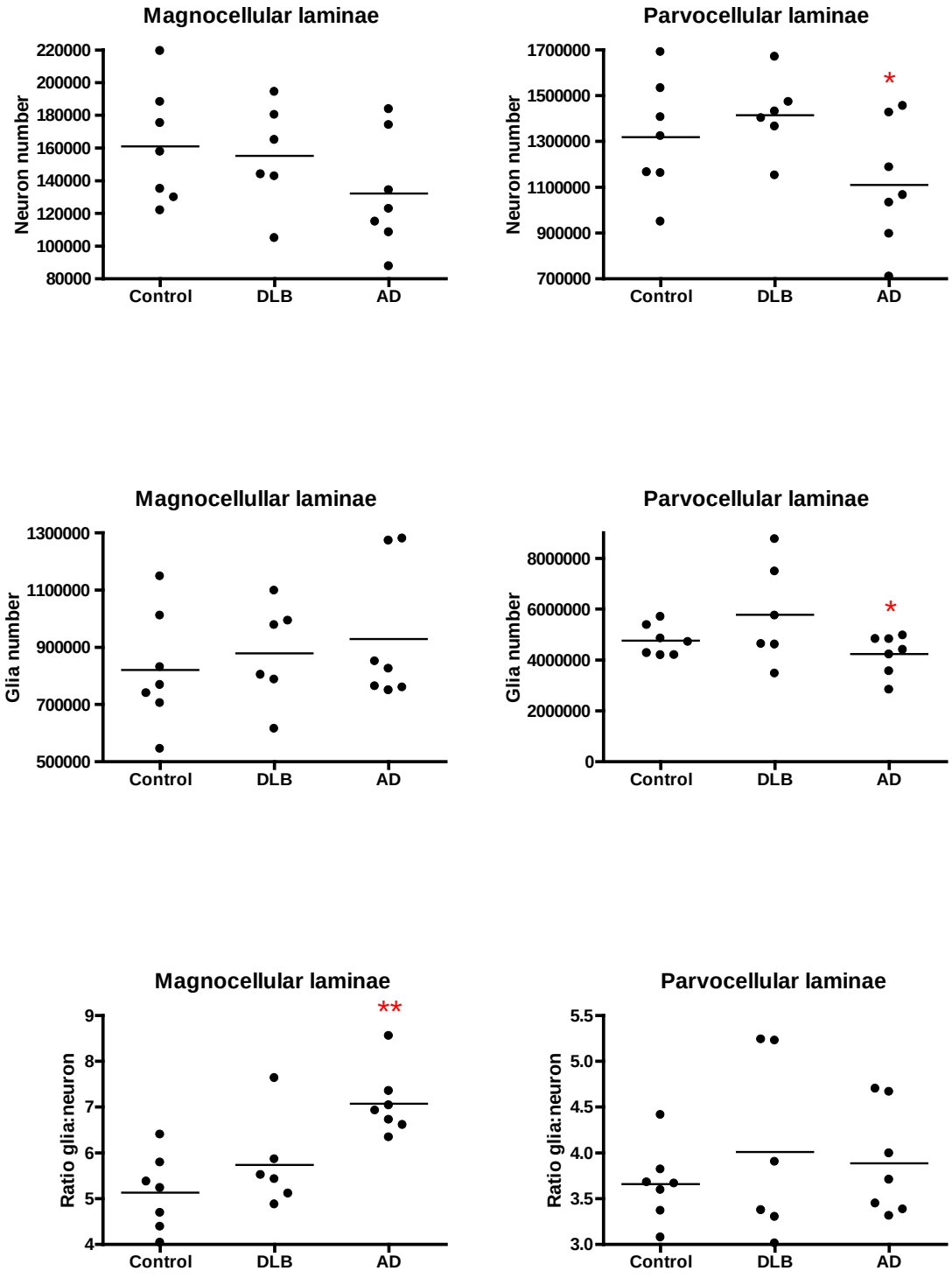


*Figure 3.2: Dot plots illustrating stereological estimates in the LGN.*

*Lines demonstrate the mean; *p<0.05 compared to DLB, **p<0.05 compared to control and DLB.*

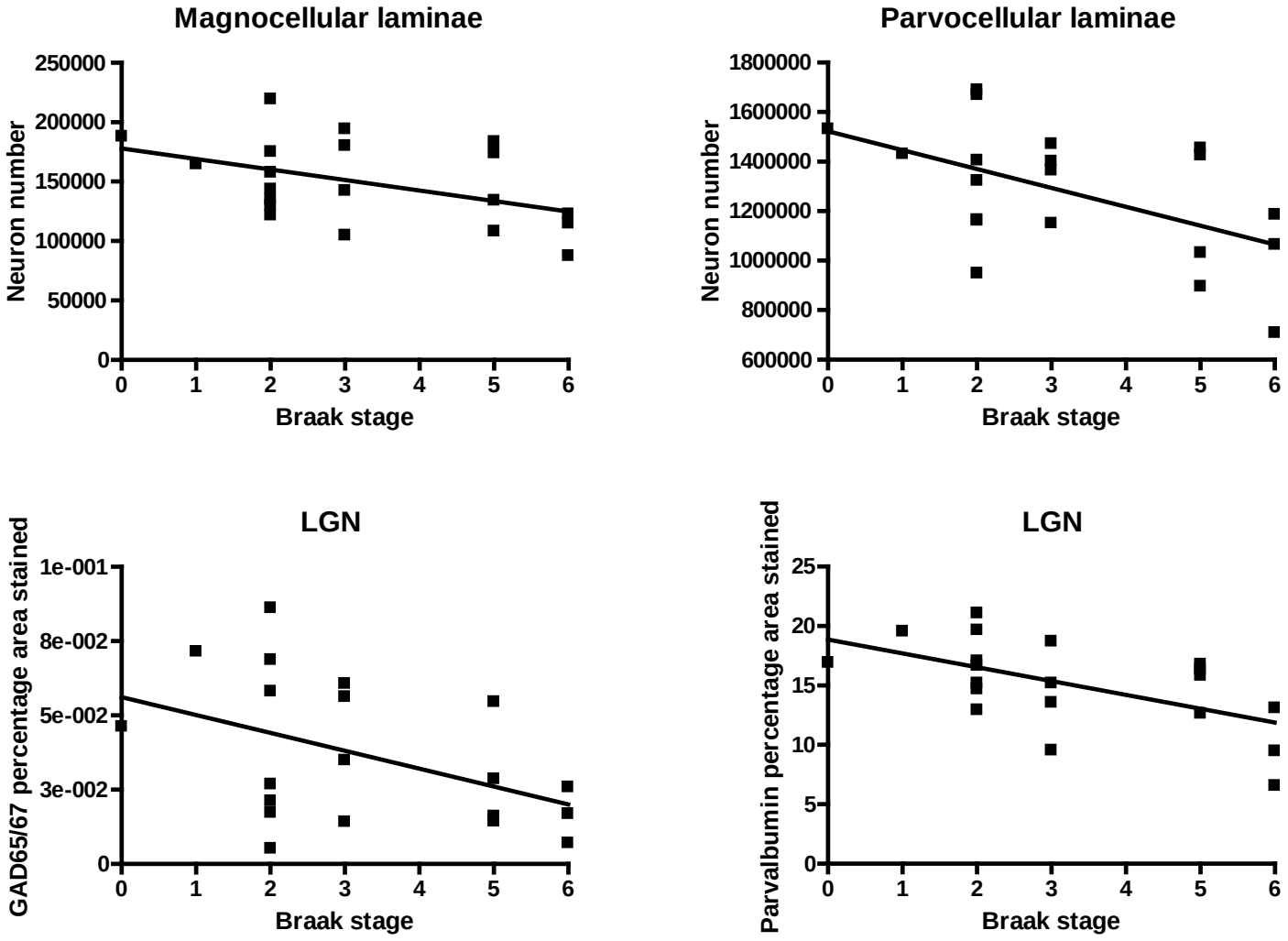


*Figure 3.3: Scatterplots demonstrating correlations between Braak stage and stereological and densitometric data.*

### 3.3.3 Densitometry

An absence of Lewy body pathology was found in all cases (Fig. 3.4A), despite immunoreactivity in the insula, present on the same slides of the cases with DLB (Fig. 3.4B) but not AD or control. Tau pathology was absent in most cases, except for occasional sparse AT8-immunoreactive neuropil threads, which were seen in the AD cases with a Braak neurofibrillary pathology stage of 6 (Fig. 3.4C and 4D). 4G8 immunoreactivity, as an indicator of amyloid-β pathology, was present in all cases but to varying degrees (Fig. 3.4E and 3.4F). A significant main effect of diagnosis on amyloid-β percentage area stained was found ($\chi^2$=9.599, p=0.008), with a significant 7.9 fold increase found in AD cases, when compared to control (U=4.0, p=0.004, d=1.49). No significant difference was found between DLB and control subjects or between AD and DLB.

GABAergic interneurons were identified in the LGN by staining for GAD65/67. The distribution and morphology of the GAD65/67-labelled cells was consistent with those identified in a previous study of interneuron populations in the human LGN (Zinner-Feyerabend and Braak, 1991) (Fig. 3.5A). The percentage area of GAD65/67 immunostaining did not differ significantly between DLB, control and AD. Within cases, there was no significant difference in GAD65/67 density across sections.

Calcium-binding proteins were used to identify neuronal sub-populations present within the LGN (Munkle *et al.*, 2000). Calcium-binding proteins were used to identify neuronal sub-populations up-regulated following diminished visual input (Arai *et al.*, 1992; Gonzalez *et al.*, 2006), and project to the visual cortex (Yucel *et al.*, 2000). As described in a previous study (Munkle *et al.*, 2000), parvalbumin staining was widespread within the LGN, with some neurons intensely labelled, and a proliferation of dark terminal-like boutons (Fig. 3.5B). Percentage area of parvalbumin immunostaining did not significantly differ between DLB, control and AD (Fig. 3.6). Calretinin showed a homogeneous pattern of staining, with magnocellular neurons stained more intensely than parvocellular neurons (Fig. 3.4C and 3.4D), as demonstrated previously (Munkle *et al.*, 2000). No significant main effect of diagnosis on percentage area stained for calretinin was found between DLB, control and AD (Fig. 3.6). Parvalbumin and calretinin expression did not significantly differ across sections from within individual cases.

GAD65/67 immunoreactivity was negatively correlated with Braak stage (rho=-0.440, p=0.046; Fig. 3.3). Parvalbumin percentage area stained was negatively correlated with Braak stage (rho=-0.562, p=0.008; Fig. 3.3). Calretinin was not significantly correlated with any neuropathological variables.

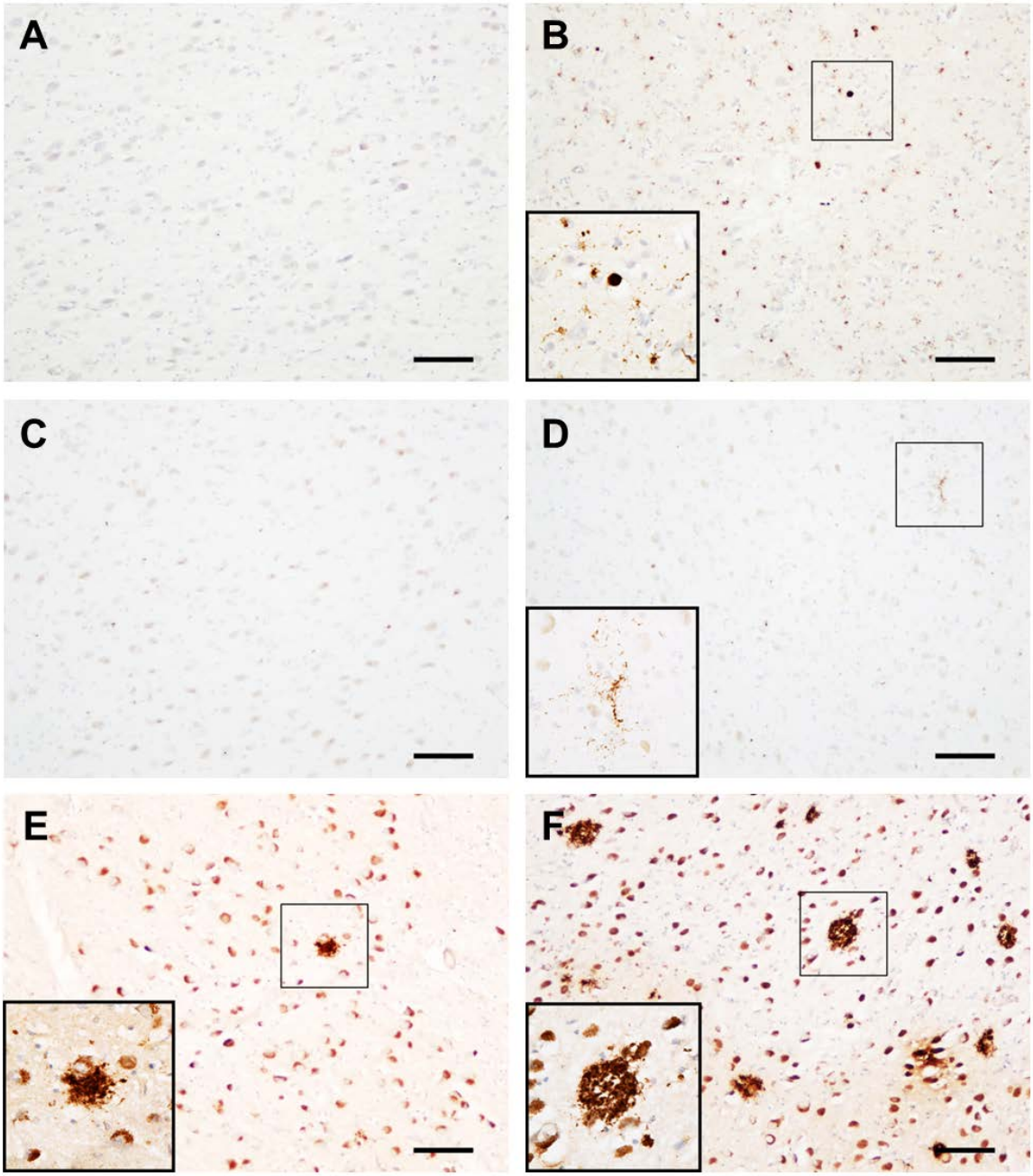


*Figure 3.4: Neuropathology in the LGN.*

*Photomicrographs demonstrating the absence of α-synuclein staining in the LGN of a DLB case (A), in contrast to the insula (B), on the same slide of the same case, with Lewy bodies and neurites observed (B, inset); absence of tau pathology in a Braak stage 5 AD case (C), sparse tau pathology in a Braak stage 6 case (D); amyloid-β pathology in a DLB (E) and AD (F) case. Scale bar = 100 μm, inset images are x4 the original image.*

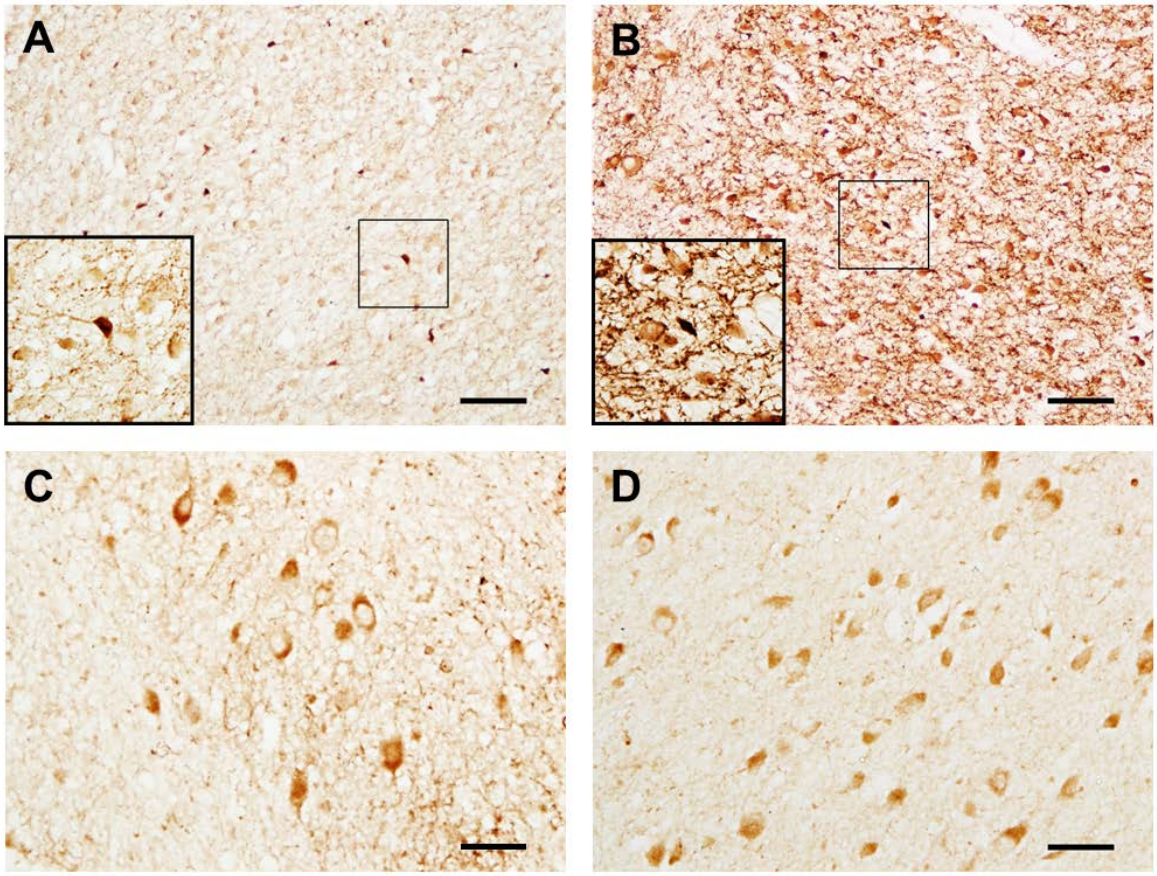


*Figure 3.5: Neuronal subpopulations in the LGN.*

*Photomicrographs illustrating the distribution of GAD65/67 immunoreactive cells in the LGN (A) with interneuronal morphologies (A inset), consistent with (Zinner-Feyerabend and Braak, 1991); parvalbumin immunostaining showing numerous stained processes and synapses, in addition to intensely labelled cells (inset; B), consistent with (Munkle et al., 2000); calretinin immunostaining revealing more intense staining of magnocellular (C) than parvocellular (D) neurons in one case, consistent with (Munkle et al., 2000). A+B scale bars = 100 µm, C+D scale bars = 50 µm. Inset images are x4 the original image.*

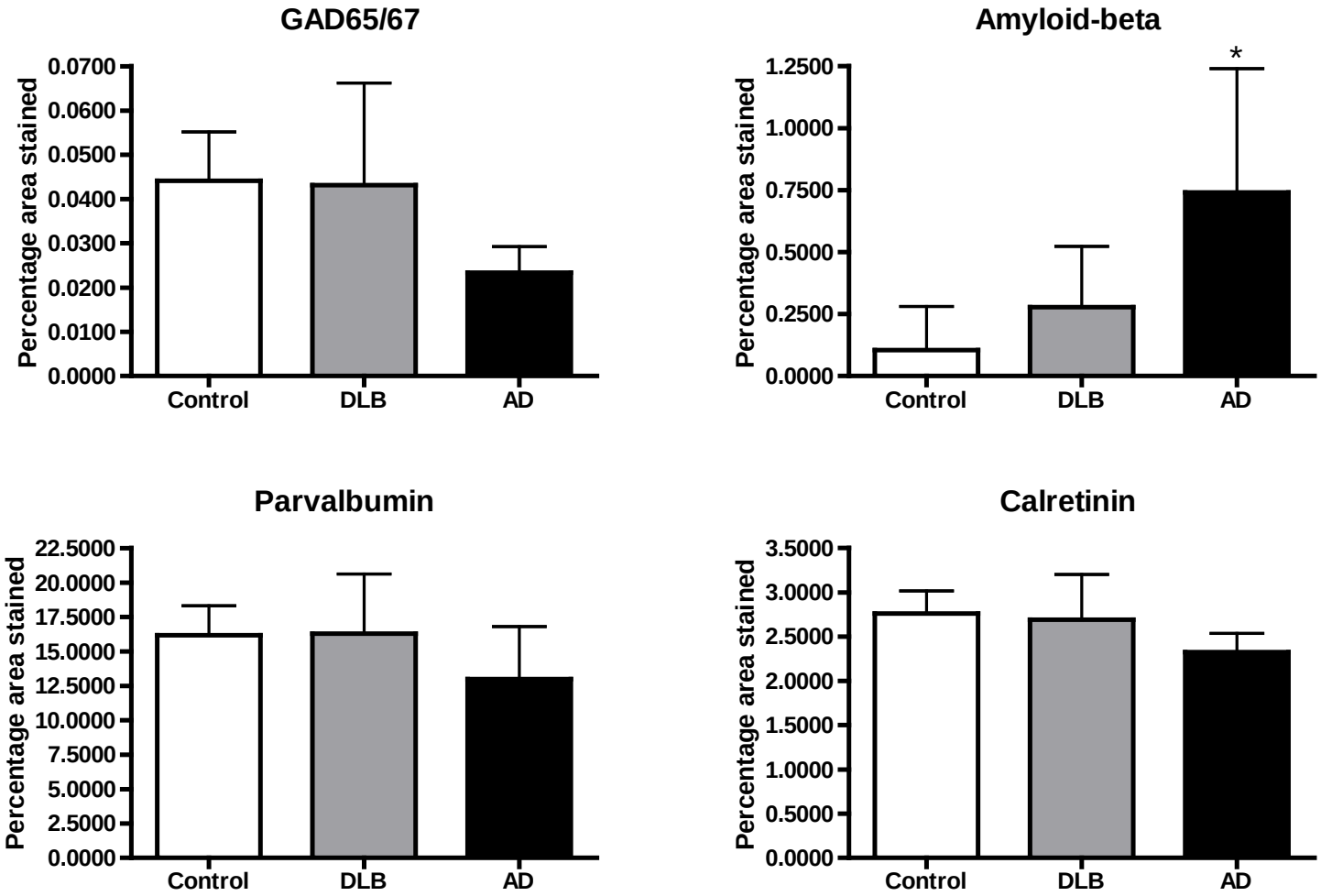


*Figure 3.6: Bar charts illustrating densitometric data in the LGN.*

*Bars symbolise means and standard deviation; *p<0.05 compared to control.*

## 3.4 Discussion

The present results suggest the number of neuronal and glial cells does not significantly differ from that of aged controls in the LGN of DLB patients. However, the severity of gliosis was higher in AD cases, compared to DLB and control subjects. These changes were accompanied by increased amyloid-β pathology in AD cases and a moderate loss of parvocellular neurons and glia in AD, when compared to DLB cases.

Although the LGN is a vital part of the afferent visual pathway (Jones, 1998), and visuoperceptual changes are a frequent occurrence in DLB (Armstrong, 2012), few studies have investigated how the LGN is affected in DLB. The only pathological studies conducted in LGN in DLB have focused on the magnitude of neuropathological lesions, and one study on neuronal loss, but based entirely on qualitative assessment (Yamamoto *et al.*, 2006; Rahimi and Kovacs, 2014).

The present study found cellular populations of the LGN apparently spared in DLB and not subject to substantial neurodegeneration. In contrast, AD cases exhibited increased gliosis and moderate cell loss. Previous work has shown there are retinal abnormalities in Lewy body diseases (Maurage *et al.*, 2003; Devos *et al.*, 2005; Moreno-Ramos *et al.*, 2013; Beach *et al.*, 2014). However, the relative sparing of the LGN in DLB demonstrated in the present study is unprecedented. Whilst this finding implies the manifestation of visual symptoms in DLB is likely the result of degenerative changes elsewhere in the brain, one may speculate that the relative intactness of the LGN, in the context of degeneration elsewhere, may be an important factor the pathophysiology of visual hallucinations in DLB.

In DLB, retinal changes may lead to an incomplete representation of the visual scene being relayed to the LGN. As the LGN is seemingly intact, it may then relay the incomplete visual scene to higher visual structures. In a somewhat analogous fashion to the ‘filling in’ of the blind spot created by the optic nerve emanating from the retina, this incomplete or distorted visual information may then require completion by higher visual structures. Pathological alterations to higher visual structures involved in the process of ‘filling in’ may mean that the process of correcting for the missing information is not carried out correctly. This could result in the generation of images that are additional to the input that has been conveyed to

the brain, i.e. hallucinations, perception without sensory input. In AD cases, the mild degeneration of the LGN may be commensurate with retinal and/or cortical changes, thus preventing incomplete visual information being faithfully relayed to the higher visual system.

Consistent with the findings of the present study, Lewy body pathology has previously been described as absent from the LGN in DLB (Yamamoto *et al.*, 2006). However, another study in PD has shown that the LGN is frequently affected by α-synuclein pathology, albeit to a minor degree (Rahimi and Kovacs, 2014). Whilst a different clinical entity from DLB, there are some similarities between the two conditions in terms of the neuropathological lesions present (Spillantini *et al.*, 1997). It is not clear why α-synuclein pathology was identified in PD but not in DLB. One explanation may be that as DLB typically has a shorter disease duration than PD, there is a shorter period of time for pathology to spread to the LGN. Impaired antigenicity or a dysfunctional antibody may be ruled out, considering the strong immunostaining observed in the insula on the same slides of the same cases (Fig. 3.4B).

It is possible the difference in vulnerability of the LGN to α-synuclein pathology reflects idiosyncratic differences between PD and DLB. The LGN has substantial connectivity with the pedunculopontine nucleus of the brainstem (Rye, 1997), a structure more severely affected by Lewy body pathology in PD compared to DLB (Hepp *et al.*, 2013). An emerging view suggests misfolded α-synuclein spreads throughout the brain in a transsynaptic manner, reminiscent of prion protein (Herva and Spillantini, 2015; McCann *et al.*, 2016). Thus the presence of α-synuclein pathology in the LGN in PD may be the result of a greater pathological burden at brainstem sites interconnected with the structure. The LGN receives input from brain regions other than the pedunculopontine nucleus but brainstem sites may be of particular relevance in this regard as the brainstem is thought to be a key predilection site for α-synuclein pathology in the brain in PD (Braak *et al.*, 2003).

Although previous studies in neurodegenerative diseases disagree on whether the LGN is affected by neurofibrillary pathology (Leuba and Saini, 1995; Dugger *et al.*, 2011), the present study did show some sparse neuropil threads in three cases that had been neuropathologically classified as having the highest global burden of

neurofibrillary pathology. Additionally, Braak neurofibrillary pathology stage was related to the amount of amyloid-β in the LGN and inversely related to the number of neurons within the LGN. The primary cortical target of the LGN, the primary visual cortex, is affected at the most advanced stage of tau pathology (Braak *et al.*, 2006). This raises the possibility that degeneration of the LGN observed in Braak stage 6 AD cases is the result of degeneration of the primary visual cortex (Hof and Morrison, 1990), and the reciprocal connectivity between both structures (Jones, 1998). The primary visual cortex is not typically affected by tau pathology in DLB (Perry *et al.*, 1990b; Khundakar *et al.*, 2016). Therefore, the sparing of the LGN may reflect the preservation of its primary afferent target. Tau pathology is observed in the visual cortex during in the most advanced stages of AD (Braak *et al.*, 2006) and the degeneration observed in the LGN is relatively mild, which raises the suggestion this may represent a late event in the progression of AD. If changes to the LGN occur at late stages of AD it is difficult to estimate how much of an influence this has upon the clinical phenotype.

As reported in a previous study (Leuba and Saini, 1995), increased amyloid-β was found in the LGN of AD cases. DLB typically had comparable amyloid-β pathology to control, though two DLB cases did exhibit high amyloid-β expression. Though possibly coincidental, the two DLB cases with high amyloid-β pathology were the oldest in the DLB group. As amyloid-β turnover is increasingly impaired with advancing age (Patterson *et al.*, 2015), it is possible that this is an age-related phenomenon in DLB.

This study showed no significant changes in GAD65/67, parvalbumin and calretinin immunoreactivity between groups. However, significant correlations were observed between Braak stage and several variables, including the percentage area stained for calcium-binding protein parvalbumin and amyloid-β peptide, and cell numbers from stereology. Whilst these findings may reflect the relationship of these variables to global tau pathology burden, they may also reflect the composition of the groups used. Control cases all had Braak stage 0-2, AD cases had Braak stage 5-6 and DLB cases were between both. Therefore, based on the present data, it is not possible to establish whether the correlations reflect increasing global tau burden or simply the distinct conditions of each group, or both.

Two previous studies using stereological approaches to estimate the number of neurons have been conducted in the LGN in tissue from people who had schizophrenia and were generally of lower age (Selemon and Begovic, 2007; Dorph-Petersen *et al.*, 2009). Whilst the numerical estimates presented here are broadly similar to one study (Dorph-Petersen *et al.*, 2009), they are over three times smaller in magnitude than reported in another (Selemon and Begovic, 2007). The slight disparity in numerical estimates in the present study compared to Dorph-Peterson and colleagues (Dorph-Petersen *et al.*, 2009) is possibly due to slight variations in the sampled region of interest within the LGN. Dorph-Peterson and colleagues included the intralaminar regions in their analysis of the LGN, which would have increased the volume of the structure. Though these laminae contain fewer neurons than the magnocellular or parvocellular laminae, counting them would likely have increased the estimated number of neurons by increasing the volume estimate of the region of interest, whilst only moderately reducing the measures of neuronal density. This is especially true of the magnocellular laminae, which have much wider intralaminar laminae and contain more intralaminar neurons than parvocellular intralaminar regions (Percival *et al.*, 2014). Correspondingly, a greater magnitude of difference was found between magnocellular compared to parvocellular counts in the present study and that by Dorph-Peterson and colleagues (Dorph-Petersen *et al.*, 2009).

As described earlier, greater differences were found between the present results and those reported by Selemon and colleagues, who recorded greater numbers of neurons in the LGN than the present study (Selemon and Begovic, 2007). The previous study (Selemon and Begovic, 2007) calculated the volume of the LGN using the thickness of sections without adjusting for shrinkage as a result of staining. In contrast, the present study, and that by Dorph-Peterson and colleagues (Dorph-Petersen *et al.*, 2009), measured section thickness after the staining of tissue sections. It is possible, therefore, that the Selemon study over-estimated the volume of the LGN in their study, which would correspondingly overestimate neuronal number.

AD patients have previously been shown to exhibit a pattern of perceptual deficits, when tested using electroretinograms and visual evoked potentials, suggesting magnocellular pathway dysfunction (Sartucci *et al.*, 2010). It is possible that the

magnocellular gliosis observed in the present study is the neuropathological analogue of these symptoms. However, as perceptual data from the cohort during life is incomplete or absent, it is not possible to establish the relationship between these phenomena by relating the neuropathological findings from the present study to physiological data from life.

This study was limited by a relatively small sample size, which was the result of tissue availability and sampling restrictions, limiting the power of the study. As some changes in the AD group were approaching statistical significance, such as magnocellular neuron number, it is possible that a larger sample size may have yielded a significant result. However, the DLB group showed no indication or trend towards reductions in any of the assessed variables. Therefore, if the DLB group are representative of DLB cases generally, it is less likely that a larger group would have yielded a significant difference from controls. Small group sizes are a persistent feature of human *post-mortem* studies, especially those which employ correctly applied stereological methodology, which necessitates whole, intact structures (Erskine and Khundakar, 2016). This study was conducted using the most unbiased approach possible. However, shrinkage following formalin fixation is well-understood (Haug *et al.*, 1984) and it is impossible to exclude the possibility that bias was unwittingly introduced by a differential rate of shrinkage across disease groups.

In summary, the present study has shown that the LGN is relatively preserved in hallucinating DLB cases, in comparison to mild increases in pathology and degeneration observed in non-hallucinating AD cases. The preservation of the LGN may contribute to the phenomenon of visual hallucinations in DLB by faithfully relaying the features of a fragmented or distorted visual scene. However, it is unlikely that the preservation of the LGN is itself sufficient to cause hallucinations, which likely result from dysfunction in other areas of the visual system. Changes to the LGN in AD are speculated to be a late feature of neuropathological change, so it is difficult to assess the importance of the present findings in understanding clinico-pathological correlative relationships in AD.

# Chapter 4: Histological studies in the pulvinar nucleus

## 4.1 Introduction

The pulvinar nucleus of the thalamus is thought to play an important role in visual attentional mechanisms (Benarroch, 2015; Zhou *et al.*, 2016). Pulvinar lesions can cause deficits in filtering distracting stimuli (Fischer and Whitney, 2012) and feature binding of visual objects (Ward *et al.*, 2002). The pulvinar, which has widespread cortical connections, is thought to play a general role in modulating cortico-cortical activity based on attentional demands (Saalmann *et al.*, 2012). The widespread cortical connections of the pulvinar seem to mirror the connectivity of cortico-cortical pathways, suggesting that the pulvinar plays a crucial role in modulating activity across the cortex (Benarroch, 2015). The pulvinar is traditionally parcellated into four anatomical sub-regions based on histological staining: anterior, medial, lateral and inferior (Munkle *et al.*, 2000). However, these histological sub-regions do not map perfectly onto sub-regions that have been segregated based on functionality or connectivity (Shipp, 2003).

Recent evidence has suggested degeneration of particular sub-regions of the pulvinar, as assessed by mean diffusivity on functional MRI, predicts clinical markers of visual hallucination frequency and severity (Delli Pizzi *et al.*, 2014). Despite such findings, no neuropathological studies have investigated the role of different pulvinar sub-regions in visual hallucinations in DLB. Therefore, the present study aimed to assess potential degenerative morphometric and/or neuropathological changes to the pulvinar nucleus that may contribute a vulnerability to visual hallucinations, using unbiased stereological and quantitative neuropathological methods.

### 4.1.1 Aims

Using *post-mortem* pulvinar tissue taken from hallucinating DLB patients, compared with aged cognitively normal individuals and disease-control non-hallucinating AD patients, this study aimed to:

1) Use stereological methods to evaluate the number of neurons and glia in the sub-regions of the pulvinar.
2) Quantify and compare the burden of neuropathological lesions in the different sub-regions of the pulvinar.

3) Quantify and compare the degree of astrogliosis and microgliosis in the sub-regions of the pulvinar, based on indications from RNA sequencing results in Chapter 5.

## 4.2 Methods

### 4.2.1 Tissue acquisition

The pulvinar is the most posterior of the thalamic nuclei and protrudes into the lateral ventricle (Jones, 2007). In the fixed tissue dissection protocol used at NBTR, two or three blocks corresponding to the posterior thalamus typically contain the extent of the pulvinar through the z-axis.

Three groups of cases were included in this study: DLB patients who had experienced complex visual hallucinations during life, AD patients without a clinical history of visual hallucinations and aged control subjects with low or absent levels of neurodegenerative pathology and no history of psychiatric disorders. Cases were included based on whether the pulvinar was intact along its antero-posterior extent. The cases meeting these criteria consisted of eight DLB, eight AD and eight control subjects (Table 4.1).

From a random starting point, fixed tissue blocks containing the entire pulvinar were exhaustively serially sectioned, with 30 µm sections obtained at each 1 mm interval and stained with cresyl fast violet for stereological analyses. 10 µm sections were stained with antibodies against a range of protein targets (Table 4.2) using Menarini Menapath Polymer detection kits (Menarini, Berkshire, UK), as described in Methods. Protein targets included cluster of differentiation 68 (CD68) and glial fibrillary acidic protein (GFAP), putative markers of activated microglia and astrocytes, respectively. This was due to RNA sequencing data (detailed in Chapter 5) suggesting changes indicative of gliosis.

*Table 4.1: Demographic information for cases used in the pulvinar study.*

*'PM interval' is the interval between death and post-mortem examination, 'Braak NFT' represents global neurofibrillary pathology stage as outlined in (Braak et al., 2006), 'McKeith LB' represents global Lewy body pathology stage, as outlined in (McKeith et al., 2005), 'clinico-path diagnosis' represents the overall diagnosis, as decided upon by case-note review and neuropathological examination by senior clinicians, in accordance with consensus criteria (McKeith et al., 2005; Montine et al., 2012).*

| Case ID | Gender | Age at death (years) | PM interval (hours) | Braak NFT | McKeith LB | Clinico-path diagnosis | Hallucinations |
|---|---|---|---|---|---|---|---|
| C1 | F | 78 | 23 | 2 | None | Control | None reported |
| C4 | M | 77 | 83 | 2 | None | Control | None reported |
| C5 | M | 73 | 25 | 0 | None | Control | None reported |
| C6 | M | 80 | 16 | 2 | Brainstem | Control | None reported |
| C7 | M | 85 | 57 | 3 | None | Control | None reported |
| C8 | F | 99 | 5 | 2 | None | Control | None reported |
| C9 | F | 65 | 47 | 1 | Amygdala | Control | None reported |
| C10 | F | 76 | 86 | 2 | None | Control | None reported |
| Mean±SD | | 79.1±10 | 42.8±31 | 1.8±1 | | | |
| D2 | M | 89 | 88 | 3 | Neocortical | DLB | Frequent complex visual hallucinations |
| D6 | F | 78 | 96 | 3 | Neocortical | DLB | Frequent complex visual hallucinations |
| D7 | F | 73 | 99 | 3 | Neocortical | DLB | Infrequent complex visual |

| | | | | | | | |
|---|---|---|---|---|---|---|---|
| | | | | | | | hallucinations |
| D8 | M | 81 | 81 | 3 | Neocortical | DLB | Frequent complex visual and auditory hallucinations |
| D9 | M | 77 | 46 | 3 | Neocortical | DLB | Infrequent complex visual hallucinations |
| D10 | F | 81 | 44 | 4 | Neocortical | DLB | Frequent complex visual hallucinations |
| D11 | F | 91 | 10 | 3 | Neocortical | DLB | Frequent complex visual hallucinations |
| D12 | M | 73 | 47 | 2 | Neocortical | DLB | Frequent complex visual hallucinations |
| Mean±SD | | 80.4±7 | 63.9±32 | 3.1±1 | | | |
| A1 | M | 76 | 6 | 6 | None | AD | None reported |
| A2 | M | 85 | 32 | 5 | None | AD | None reported |
| A5 | F | 81 | 73 | 5 | None | AD | None reported |
| A8 | M | 89 | 61 | 6 | None | AD | None reported |
| A9 | M | 68 | 24 | 6 | None | AD | None reported |
| A10 | F | 86 | 123 | 6 | Brainstem | AD | None reported |
| A11 | F | 95 | 23 | 6 | Amygdala | AD | None reported |
| A12 | M | 85 | 39 | 6 | None | AD | None reported |
| Mean±SD | | 83.1±8 | 47.6±37 | 5.8±1 | | | |

### 4.2.2 Stereology

The primate pulvinar has traditionally been parcellated into four cytoarchitectonically defined regions: the anterior, medial, lateral and inferior pulvinar nuclei (Hirai and Jones, 1989). GAD65/67 immunohistochemistry was used to delineate the pulvinar into sub-regions, based on a previous report (Popken *et al.*, 2002) (Fig. 4.1). The inferior pulvinar was incomplete on all sections due to its location at a point where the upper midbrain is dissected from the diencephalon, thus precluding stereological analysis of this sub-region. The lateral pulvinar was differentiated from other structures based on its striated appearance (Fig. 4.1) (Jones, 2012).

The border between the anterior and medial pulvinar could not be reliably identified through the z-axis. As stereological protocol requires the entire structure to be sampled for analysis, the anterior and medial pulvinar were grouped together and will subsequently be referred to as the 'anteromedial pulvinar' when referring to stereological analyses.

Stereological methods were used to estimate the total number of neurons and glia within the pulvinar nuclei. Cell counts were conducted at 63x oil-immersion objective using the optical disector probe. Glial cell counts were calculated in both pulvinar sub-regions in disector frames of 1900 $\mu m^2$, with neuron counts calculated in disector frames of 3500 $\mu m^2$. Section thickness did not vary across disease groups in anteromedial or lateral pulvinar. CE values had acceptable levels of accuracy, with CE values <0.10. A mean of 9 sections (range 7-12) were analysed for the anteromedial pulvinar and a mean of 8 sections (range 6-9) for the lateral pulvinar.

*Table 4.2: Antibodies used in the pulvinar study.*

| Antibody | Manufacturer | Dilution | Antigen retrieval |
|---|---|---|---|
| 5G4 α-synuclein | Analytik Jena, Germany | 1:4500 | Formic acid + citrate pH 6.0 |
| AT8 phospho-tau | Autogen, MA, USA | 1:4000 | Citrate pH 6.0 |
| 4G8 amyloid-β | Covance, NJ, USA | 1:15000 | Formic acid |
| GAD65/67 | Sigma Aldrich, MO, USA | 1:12000 | Citrate pH 6.0 |
| GFAP | Dako, Denmark | 1:10000 | Citrate pH 6.0 |
| CD68 | Dako, Denmark | 1:350 | Trypsin |

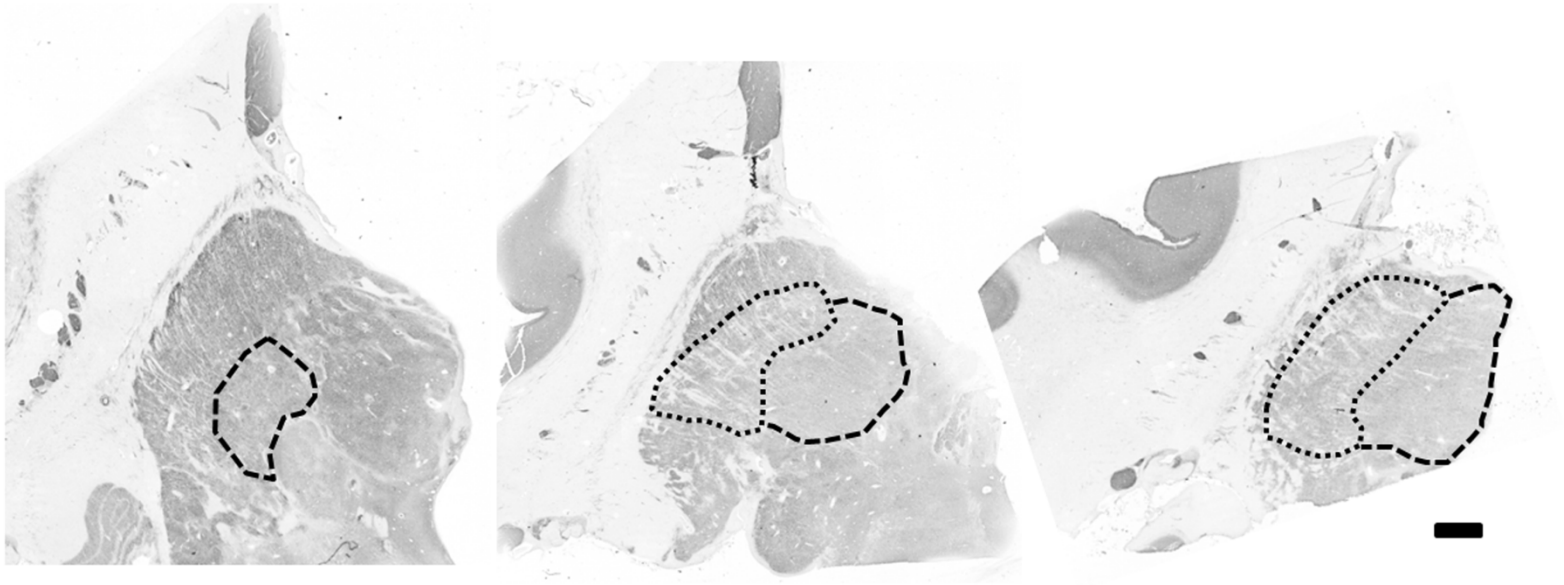

*Figure 4.1: Anatomy of the pulvinar.*

*The anteromedial (dashes) and lateral (dots) pulvinar are illustrated in successive coronal sections. Scale bar = 3 mm.*

### 4.2.3 Densitometry

The anterior, medial and lateral nuclei were analysed using quantitative neuropathological techniques. Although the anterior and medial pulvinar border could not be reliably identified for stereological analysis, where the entire structure along its antero-posterior extent is required, it was possible to identify the individual structures for analysis of neuropathology if the section which contained the emergence of the anterior pole of the pulvinar was used to represent the anterior pulvinar. The medial and lateral pulvinar were assessed by densitometric analysis of the region at which both structures were at their maximal area on coronal section, as the anterior pulvinar is not present at this point (Mai *et al.*, 2016), combined with the section prior to the last section coronally on which they were present, to better represent the whole structure than a single section.

To quantify neuropathological lesions, images of the sub-nuclei of the pulvinar were taken on a Zeiss AxioVision Z.1 microscope using a JVC 3-chip CCD true colour camera. Stereologer software was used to delineate a region of interest with a 2.5x objective, prior to placement of disector frames in a uniform, random arrangement. This method prevented the introduction of sampling bias by giving every area of the region of interest an equal probability of being analysed. Disector frames were captured at 10x objective for amyloid-β and tau, and at 20x objective for α-synuclein pathology, CD68 and GFAP, on the basis of the relative particle size and distribution of the structures measured. Images were taken within the disector frames and analysed using ImagePro Plus v.4.1 image analysis system. Using previously published techniques (Perry *et al.*, 2012), the mean percentage area of immunoreactivity was determined by standardizing RGB thresholds per antibody and applying to all sections per case. Each case thus had a mean value generated per antibody across all sections analysed.

### 4.2.4 Statistical analyses

Inspection of Q-Q plots and Shapiro-Wilk tests suggested that a normal distribution could be assumed for the stereological data. However, visual inspection of regression lines of stereological data with age and PM interval indicated that homogeneity of regression slopes could not be assumed for all analyses. Therefore, ANOVA was conducted on stereological data, with Tukey's HSD as the post-hoc test

if data had homogeneity of variance. Data that did not have homogeneity of variance were assessed using Games-Howell. Densitometric data were not normally distributed so Kruskal-Wallis tests with post-hoc Mann-Whitney U tests were used for these data.

## 4.3 Results

### 4.3.1 Demographics

There was no significant difference in age ($F=0.478$, $p=0.627$), *post-mortem* interval ($F=0.881$, $p=0.429$) or gender ($\chi^2=0.336$, $p=0.845$) between experimental groups (Table 4.1).

Final MMSE scores were available for 14/24 cases (five control, five DLB, four AD) and there was no significant difference between groups in the interval from last MMSE assessment to death. As expected, MMSE scores were significantly lower in DLB ($p<0.01$, $d=1.80$) and AD ($p<0.01$, $d=1.74$) patients, compared to controls, but there was no significant difference between AD and DLB.

### 4.3.2 Stereology

In the anteromedial pulvinar, no significant main effect of diagnosis on neuronal or glial number was found, and the volume of the structure was not significantly different across groups (Fig. 4.2).

In the lateral pulvinar, a significant main effect of diagnosis on neuronal number was found ($F=14.219$, $p<0.01$). Post-hoc tests using Tukey's HSD showed a significant decrease in neuronal number in DLB cases compared to controls ($p<0.01$, $d=1.82$) and a significant decrease in AD cases compared to controls ($p=0.02$, $d=0.99$). There was a trend toward a significant reduction in neuronal number in DLB versus AD cases ($p=0.06$, $d=0.83$). No significant differences in glial cell number or lateral pulvinar volume were found across groups (Fig. 4.2).

In the anteromedial pulvinar, there was a trend towards a significant main effect of diagnosis on the ratio of glia to neurons but was not statistically significant ($F=3.432$, $p=0.051$). In the lateral pulvinar, a significant main effect of diagnosis on the ratio of glia to neurons was found ($F=7.855$, $p=0.003$). DLB cases had a significant increase

in glia relative to neurons compared to control ($p=0.002$) and AD ($p=0.038$). There was no significant difference between control and AD.

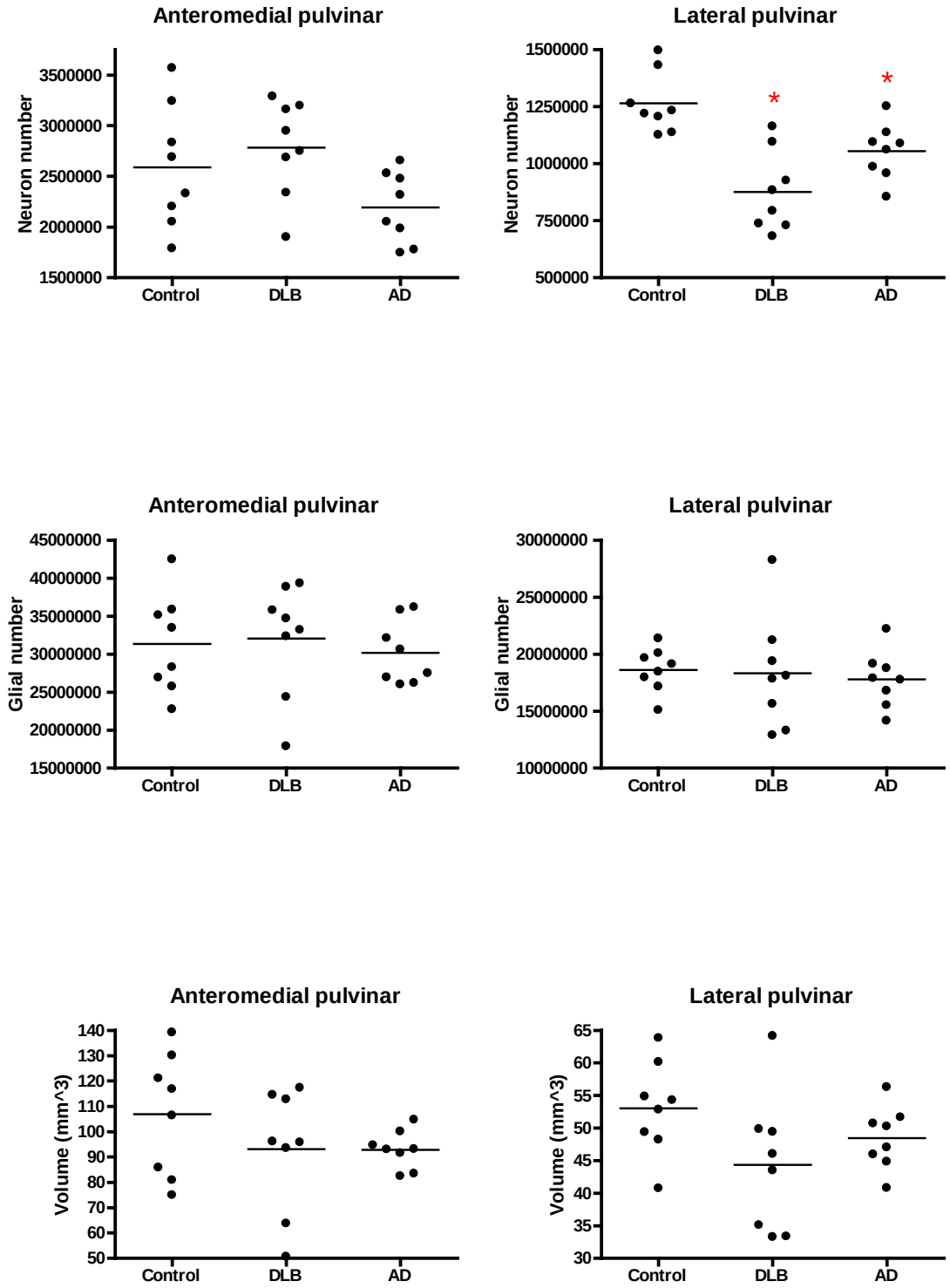


Figure 4.2: Stereological data.

Dot plots illustrate stereological data from the pulvinar nuclei, lines represent the mean, *p<0.05 compared to control.

### 4.3.3 Densitometry

Graphical summaries of densitometric data can be found in Fig. 4.3.

α-synuclein pathology was found in the pulvinar of all DLB cases, more frequently as Lewy neurites and dot-like profiles (dot-like profiles have been identified previously with the 5G4 antibody (Kovacs *et al.*, 2012)), than as Lewy bodies (Fig. 4.4A). There was a significant main effect of diagnosis on α-synuclein pathology in the anterior ($\chi^2$=15.53, p<0.001), medial ($\chi^2$=15.54, p<0.001) and lateral ($\chi^2$=14.37, p=0.001) pulvinar. DLB cases had greater α-synuclein pathology in the anterior pulvinar than control (U=1.0, p=0.001, d=1.47) and AD cases (U=1.0, p=0.001, d=1.47). DLB cases had greater α-synculein pathology in the medial pulvinar than control (U=0.0, p=0.001, d=1.66) and AD cases (U=0.0, p=0.001, d=1.65). DLB cases had greater α-synuclein pathology in the lateral pulvinar than control (U=1.0, p=0.001, d=1.55) and AD cases (U=3.0, p=0.002, d=1.47).

In all three regions analysed, α-synuclein was significantly higher in DLB cases when compared to control and AD cases (Fig. 4.3). In DLB cases, the medial pulvinar was invariably more severely affected by α-synuclein pathology than the lateral (Z=2.524, p=0.012, d=0.62) or anterior nuclei (Z=2.857, p=0.004, d=0.48), and no significant difference in expression was found between anterior and lateral nuclei.

Tau pathology was rarely present as neurofibrillary tangles in the pulvinar in non-AD cases. DLB cases typically had small patches of neuropil threads (Fig. 4.4B). There was a significant main effect of diagnosis on tau pathology in the anterior ($\chi^2$=15.83, p<0.001), medial ($\chi^2$=11.60, p=0.003) and lateral ($\chi^2$=14.60, p=0.001) pulvinar. AD had greater tau pathology in the anterior pulvinar than control cases (U=0.0, p=0.001, d=1.20) and DLB (U=3.0, p=0.002, d=1.18). There was no significant difference in tau pathology between DLB and control cases in the anterior pulvinar. AD had greater amyloid-β pathology in the medial pulvinar than control cases (U=2.0, p=0.002, d=1.24) and DLB (U=12.0, p=0.04, d=1.17). There was no significant difference in tau pathology between DLB and control cases in the medial pulvinar. AD cases had greater amyloid-β pathology in the lateral pulvinar than control (U=1.0, p=0.001, d=1.31) and DLB (U=7.0, p=0.008, d=1.23). There was no significant difference in tau pathology between DLB and control cases in the lateral pulvinar.

Amyloid-β pathology was variable in the pulvinar, with diffuse and focal deposits observed in varying quantities between the disease groups (Fig. 4.4C). There was a significant main effect of diagnosis on amyloid-β pathology in the anterior (F=5.571, p=0.011), medial (F=5.206, p=0.015) and lateral (F=7.379, p=0.004) pulvinar. AD had greater amyloid-β pathology in the anterior pulvinar than control cases (p=0.003, d=1.31) and DLB (p=0.040, d=1.12). There were no significant differences in amyloid-β levels in the anterior pulvinar between DLB and control cases. AD cases had greater amyloid-β pathology in the medial pulvinar than control (p=0.011, d=1.38). There was no significant difference between amyloid-β levels in the medial pulvinar between DLB and control cases or AD and DLB cases. AD cases had greater amyloid-β pathology in the lateral pulvinar than control (p=0.003, d=1.50). There was no significant difference between amyloid-β levels in the lateral pulvinar between DLB and control or AD and DLB cases.

The GFAP antibody intensely labelled astrocytic profiles and processes throughout the pulvinar nuclei in all cases (Fig. 4.4D). There was a significant main effect of diagnosis on GFAP expression in the anterior (F=10.23, p=0.001), medial (F=6.26, p=0.008) and lateral (F=6.19, p=0.008) pulvinar. DLB cases had greater GFAP expression in the anterior pulvinar than control cases (p=0.009, d=1.27). AD cases had greater GFAP expression in the anterior pulvinar than control cases (p=0.001, d=1.58). There was no significant difference in GFAP expression between DLB and AD in the anterior pulvinar. DLB had greater GFAP expression in the medial pulvinar than control cases (p=0.038, d=1.13). AD had greater GFAP expression in the medial pulvinar than control cases (p=0.009, d=1.37). There was no significant difference in GFAP expression between DLB and AD in the medial pulvinar. DLB had greater GFAP expression in the lateral pulvinar than control cases (p=0.045, d=1.10). AD had greater GFAP expression in the lateral pulvinar than control cases (p=0.009, d=1.38). There was no significant difference in GFAP expression between DLB and AD cases in the lateral pulvinar.

The CD68 antibody labelled microglial profiles in the pulvinar nuclei (Fig. 4.4E). No significant differences were found between groups in the microglial marker CD68 in any pulvinar sub-region (Fig. 4.3).

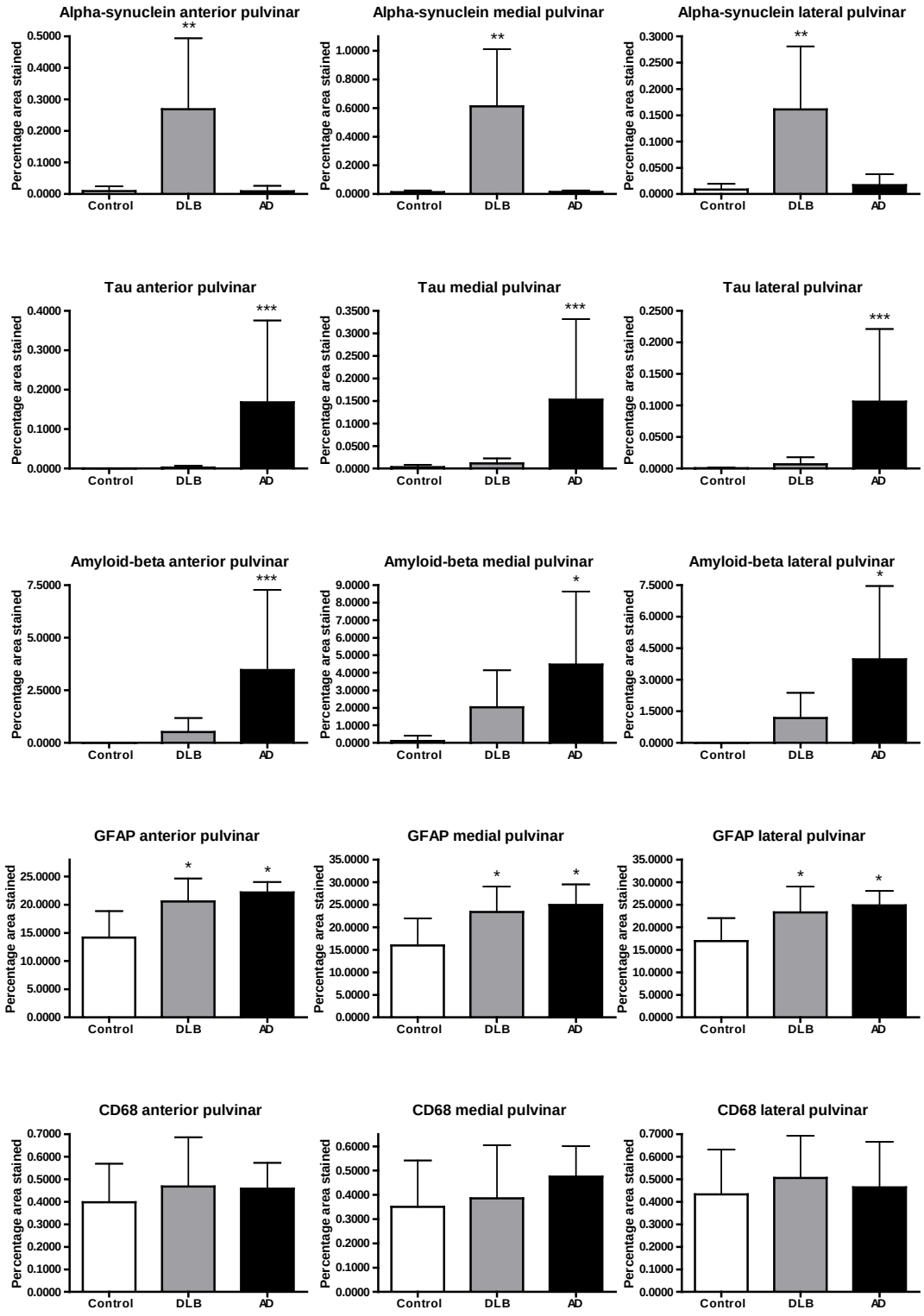


Figure 4.3: Densitometric analysis of the pulvinar nuclei.

Bars represent mean and error bars represent standard deviation. *p<0.05 compared to control, **p<0.05 compared to control and AD, ***p<0.05 compared to control and DLB.

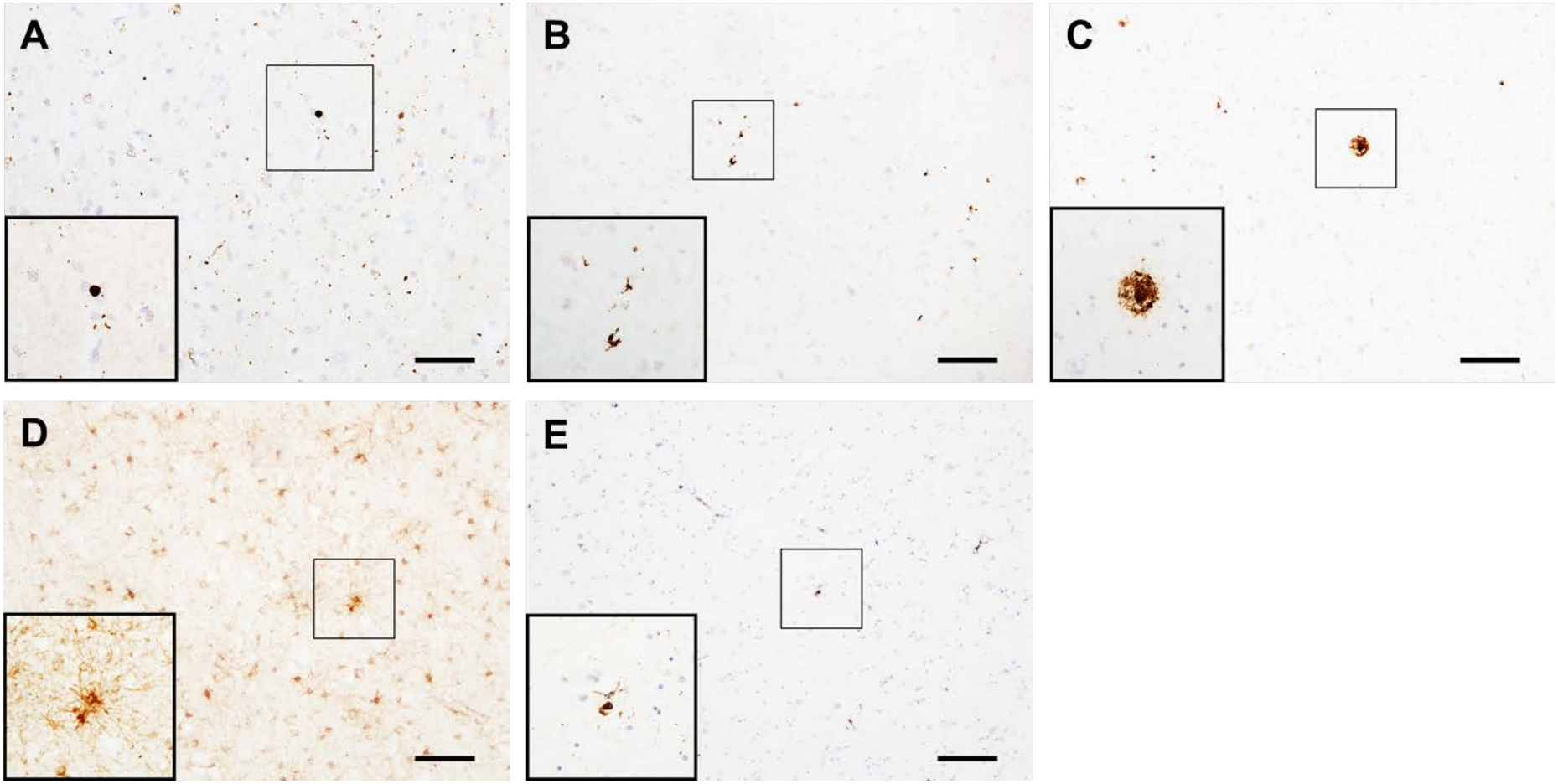


*Figure 4.4: Pathology in the lateral pulvinar.*

*Photomicrographs of the lateral pulvinar of a DLB case stained with 5G4 anti-α-synuclein (A), AT8 anti-phosphorylated tau (B), 4G8 anti-amyloid-β peptide (C), anti-GFAP (D) and anti-CD68 (E). Bar (A) = 50 µm, (B-E) = 100 µm, inset picture (A) is x2 the original image, (B-E) are x4 the original image.*

### 4.3.4 Relationships between stereological and densitometric data

There was a negative relationship between tau and neuronal number in the anteromedial pulvinar of DLB cases (rho=-0.98, $p<0.01$; Fig. 4.5). There was a negative relationship between α-synuclein and neuronal number in the lateral pulvinar of DLB cases (rho=-0.88, $p<0.01$; Fig. 4.5).

There was a negative relationship between GFAP and neuronal number in the lateral pulvinar of AD cases (rho=-0.76, $p=0.02$; Fig. 4.5). There was no relationship between neuronal number and any densitometric variable in the anteromedial pulvinar of AD cases.

No relationships were found between any neuropathological and stereological variables in the anteromedial or lateral pulvinar in control cases. Age was not significantly correlated with any neuropathological or stereological variable in any region. No significant correlations were found between GFAP percentage area stained and total glial number or mean glial density in any pulvinar sub-region.

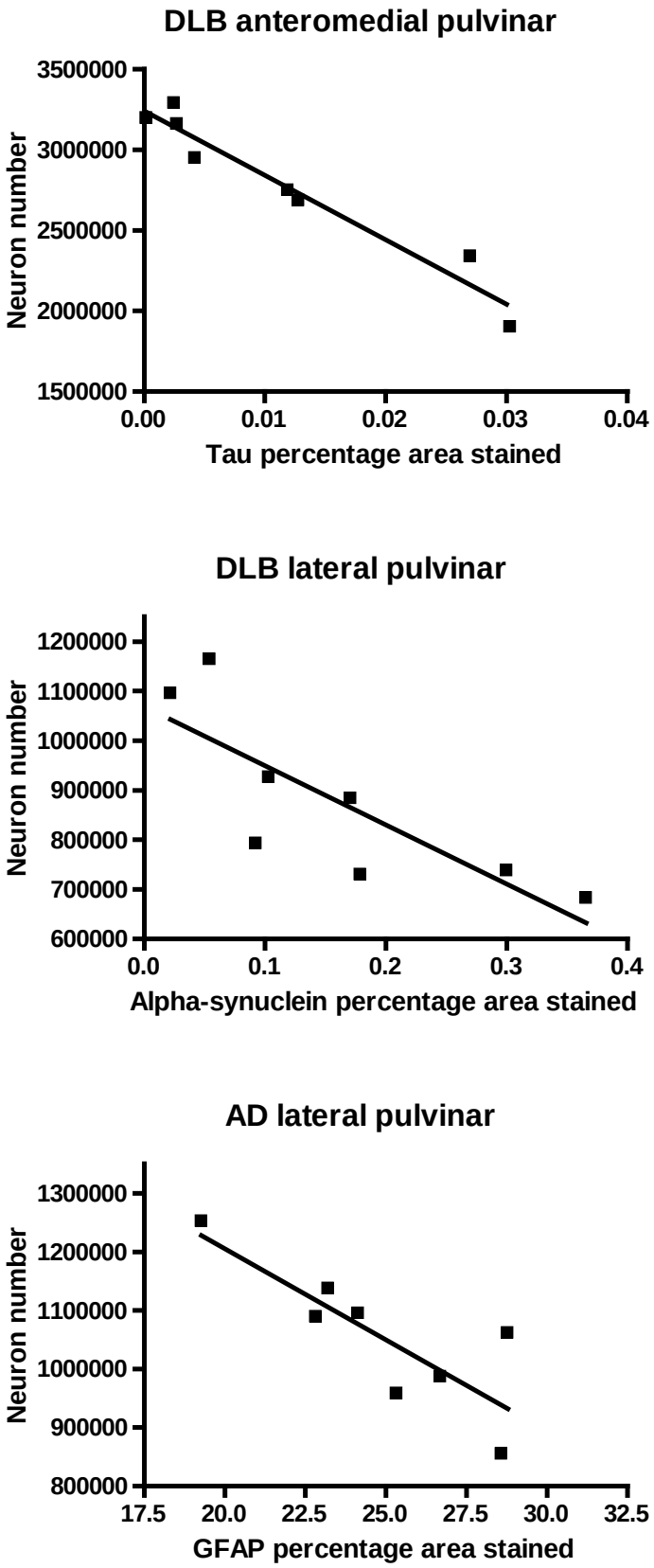


*Figure 4.5: Correlations between stereological and densitometric variables.*

## 4.4 Discussion

The present study found a significant reduction in neuronal number in the lateral but not anteromedial pulvinar in DLB, compared to control, and a trend toward a decrease in neuronal number in DLB, compared to AD, cases. A significant increase in α-synuclein pathology and astrocyte immunoreactivity was also found in the pulvinar in DLB compared to control cases but no significant difference in astrocyte expression was found in DLB compared to AD cases.

A previous study has shown the pulvinar nucleus is vulnerable to Lewy body pathology, in comparison to another visual region of the thalamus, the LGN (Yamamoto *et al.*, 2006). This is in broad agreement with the findings outlined in this study, as well as our previous findings in Chapter 3. However, the present study extended these findings by demonstrating a specific pattern of neuronal loss in the lateral pulvinar, and no change in neuronal number in the anteromedial pulvinar mirroring the findings in the LGN. In contrast, AD cases had significant neuronal loss in the LGN (Chapter 3) and less marked loss in the lateral pulvinar, when compared to DLB. Taken together, these findings suggest that neuronal loss in the visual thalamus in DLB is specific to the lateral pulvinar, where neuronal loss is more severe than that observed in AD. This is a notable finding as it is not common for stereological studies conducted in regions outside of the mid-brain to find neuronal reductions in DLB that exceed those in AD (for a review see (Erskine and Khundakar, 2016)).

The lateral pulvinar is known to receive prominent innervation from visual cortical areas (Kaas and Lyon, 2007) and to be functionally involved in regulating cortical activity in vision-related pathways (Bridge *et al.*, 2015). As the lateral pulvinar has been shown to have a strong regulatory influence on the functioning of the primary visual cortex (Purushothaman *et al.*, 2012), its degeneration in DLB may lead to altered functioning of the visual cortex and contribute to hallucinogenesis. In primate visual area V4, deactivation of the lateral pulvinar leads to reduced frequency of cortical oscillations similar to those observed during inattention or sleep (Zhou *et al.*, 2016). Lesion studies of the lateral pulvinar in non-human primates have demonstrated behavioural changes indicative of perceptual neglect, such as reluctance to grasp target stimuli with the contralateral limb (Wilke *et al.*, 2010). As impaired visual attentional function is thought to contribute to the manifestation of

visual hallucinations in DLB (Collerton *et al.*, 2005b; Diederich *et al.*, 2005), neuronal loss observed in the lateral pulvinar in the present study may contribute to visual attentional dysfunction, which may relate to the occurrence of visual hallucinations.

Previous neuroimaging findings have shown increased mean diffusivity in posterior thalamic regions that project to occipital and parietal regions in DLB (Delli Pizzi *et al.*, 2014). The degree of increased diffusivity in the posterior thalamic regions corresponding to the pulvinar have been demonstrated to relate to clinical markers of visual hallucination frequency and severity, suggesting a relationship between degeneration of pulvinar sub-nuclei that project to occipital regions and the occurrence of visual hallucinations (Delli Pizzi *et al.*, 2014). Whilst the cytoarchitectonic parcellation of the pulvinar into anterior, medial, lateral and inferior sub-regions is not fully compatible with segregation based on physiology and connectivity (Shipp, 2003), areas corresponding to the lateral pulvinar project to occipital and parietal regions (Soares *et al.*, 2001; Kaas and Lyon, 2007). This suggests the present finding of neuronal loss in the lateral pulvinar shares some consistencies with that reported from neuroimaging studies and may provide independent neuropathological verification of these findings (Delli Pizzi *et al.*, 2014).

The medial pulvinar, which possessed the greatest burden of α-synuclein pathology among the pulvinar nuclei examined in DLB cases (Fig. 4.2), has substantial reciprocal connectivity with the amygdala (Romanski *et al.*, 1997). Despite its higher burden of Lewy body pathology, the medial pulvinar did not evidence neuronal loss in DLB, suggesting neuronal loss is not the result of Lewy body pathology in isolation. The pathway from the medial pulvinar to the amygdala may underlie affective blindsight, where blind individuals respond appropriately to emotional facial expressions, without conscious perception. Lesioning of the medial pulvinar leads to impairments in emotional facial processing (Ward *et al.*, 2007). This pathway has been suggested to be dysfunctional in PD and may relate to impaired perception of fear in observed faces in Lewy body disease (Saenz *et al.*, 2013). Deficits in affective blindsight have previously been discussed in the context of wider impairments to blindsight pathways that may contribute to visual hallucinations in Lewy body disease (Diederich *et al.*, 2014).

The lateral and anterior pulvinar receive input from early visual (Benarroch, 2015) and somatosensory cortical areas (Jones *et al.*, 1979), respectively. These regions are often affected at later stages of Lewy body pathology than the amygdala and cingulate which connect with the medial pulvinar (McKeith *et al.*, 2005) and may be consistent with the emerging view suggesting α-synuclein pathology may spread in a manner reminiscent of prion protein (Herva and Spillantini, 2015; McCann *et al.*, 2016).

GFAP is an astrocytic intermediate filament protein that serves as an astrocytic marker that is up-regulated in neurodegenerative diseases and ageing (Middeldorp and Hol, 2011). Activated astrocytes may have a role in neuroprotection and repair and may be present in higher levels in tissues undergoing degenerative changes (Sofroniew, 2009). Therefore, the present finding of increased GFAP immunoreactivity throughout the pulvinar complex in DLB and AD may reflect a reactive, compensatory response to neurodegenerative insults. Although one study has demonstrated elevated GFAP in the cerebrospinal fluid of DLB patients (Ishiki *et al.*, 2016), another study did not, and also found no significant increase in GFAP-immunoreactive astrocytes in the frontal cortex in DLB, nor a relationship with Lewy body pathology (van den Berge *et al.*, 2012). Therefore, the present finding of reactive astrogliosis in the pulvinar in DLB may not simply reflect a stereotyped response seen throughout the brain in DLB. In contrast, astrogliosis is observed in many brain regions in AD and it is related to AD-type pathology (Garwood *et al.*, 2016).

Microglial activation, as seen by CD68 staining, was not found to differ from control cases in the hippocampus of DLB cases (Bachstetter *et al.*, 2015). Therefore, it is perhaps unsurprising the present study did not demonstrate changes in CD68 immunoreactivity in DLB cases. Previous studies have suggested microglia show less of a tendency to co-localise with Lewy body pathology (Mackenzie, 2000) than they do with AD-type pathology (Arends *et al.*, 2000). However, enrichment of proteins implicated in inflammation were found in transcriptomic analysis of the pulvinar (detailed in Chapter 5). Therefore, an activated microglial marker was used in the present study to investigate whether microglial activation is related to the inflammatory changes identified in a different group of DLB cases. Considering the relationship between microglia and AD-type pathology, it is more surprising that the

present study did not reveal changes in CD68 immunoreactivity in AD cases. However, one study has shown CD68 immunoreactivity is regionally variable, even in AD, with low levels of CD68 found in some brain regions, even when high AD-type pathology is present (Henstridge *et al.*, 2015). This suggests microglial activation is not a uniform response across all brain regions, even in conditions such as AD.

The negative relationship between α-synuclein immunoreactivity in the lateral pulvinar and neuronal number may indicate neuronal losses reflect more advanced levels of α-synuclein pathology. Such an effect may reflect an inherent maladaptive effect of α-synuclein aggregation, either through a loss of normal α-synuclein function or a toxic gain of function, or both (Cookson, 2006). Alternatively, α-synuclein level within the lateral pulvinar may increase as a product of increasing global α-synuclein burden. Therefore, neuronal loss in the lateral pulvinar may be the result of global degenerative influences, of which local α-synuclein levels are a proxy measure. Relating these findings to quantitative measures of α-synuclein pathology throughout the brain would allow further investigation of these proposals.

The negative relationship between tau levels in the medial pulvinar and neuronal number in DLB indicates local tau levels increase at a level commensurate with neuronal loss. As with α-synuclein in the lateral pulvinar, this may reflect global neuropathological burden. However, AD cases which had more widespread tau pathology throughout the brain, and were found to have higher levels of tau pathology in the anterior and medial pulvinar, did not have significant neuronal loss in the anteromedial pulvinar. Therefore, it is difficult to understand how tau pathology and neuronal loss could be directly related in the pulvinar in DLB.

The specific pattern of neuronal loss seen in the lateral pulvinar in DLB patients has also been demonstrated in stereological studies of schizophrenic patients (Highley *et al.*, 2003). Although visual hallucinations are relatively uncommon in schizophrenia (Mueser *et al.*, 1990), schizophrenic and DLB patients often experience visual attentional deficits (Luck and Gold, 2008; Armstrong, 2012) and impairments in smooth pursuit eye movements (Armstrong, 2012; Gracitelli *et al.*, 2015), which can occur as a result of attentional dysfunction (Yee, 1983). Considering the putative role of the lateral pulvinar in modulating visual cortical activity based on attentional demands (Purushothaman *et al.*, 2012; Bridge *et al.*, 2015; Zhou *et al.*, 2016), these

findings may highlight a common neurodegenerative change that promotes attentional dysfunction in both disorders. In DLB, visual attentional deficits may act in concert with dysfunction or degeneration of other brain regions to elicit hallucinations. Considering the clinical and pathological overlap between PD and DLB, and the potential involvement of pulvinar dysfunction in blindsight pathways implicated in PD (Diederich *et al.*, 2014), this may be a shared pattern of degeneration with PD. Future studies may investigate whether Lewy body pathology and neuronal loss also occur in the pulvinar in PD.

In summary, the present study has shown specific patterns of degeneration in the DLB pulvinar and that these changes are of greater magnitude than those observed in AD. Whilst speculative, the putative role of the lateral pulvinar in modifying the response properties of visual cortical neurons may suggest its degeneration contributes to alterations in cortical activity, which has previously been related to visual hallucinations in DLB (Taylor *et al.*, 2011). Additionally, the results of the current study offer broad neuropathological support for neuroimaging findings implicating the degeneration of particular pulvinar sub-regions in visual hallucinations in DLB (Delli Pizzi *et al.*, 2014).

# Chapter 5: Molecular studies in the pulvinar nucleus

## 5.1 Introduction

The previous chapter detailed the results of a histological study of the pulvinar in DLB which reported Lewy body pathology and astrogliosis in all pulvinar sub-regions, with neuronal loss restricted to the lateral pulvinar. The pulvinar has a role in visual attention and target selection (Benarroch, 2015), and exerts a powerful modulatory influence on visual cortical functioning (Kaas and Lyon, 2007; Purushothaman *et al.*, 2012). As visual attentional mechanisms (Collerton *et al.*, 2005b; Diederich *et al.*, 2005) and altered activity in the primary visual cortex (Taylor *et al.*, 2011; Khundakar *et al.*, 2016) have both been postulated to create a vulnerability to visual hallucination, these results may indicate a pathological basis for visual hallucinations in DLB.

The neuronal loss identified in the lateral pulvinar, and the higher levels of α-synuclein pathology in the medial pulvinar, suggest that these two large pulvinar sub-regions are functionally altered in DLB. Whilst histological analysis is valuable in ascertaining gross cellular morphometric changes and vulnerability to Lewy body formation, little information was provided regarding intracellular processing or neuronal functioning. Fixed-brain *post-mortem* tissue precludes the assessment of potential physiological changes that may have occurred as a result of morphological and pathological changes to neurons. Proteomic information could enable greater understanding of the potential impact of structural changes in visual thalamic circuitry and how they contribute to the clinical phenotype of DLB.

This chapter therefore aimed to elaborate on the findings of the previous chapter by identifying potential changes at the molecular level. Firstly, tissue from the pulvinar was homogenised for RNA isolation and sent to a collaborator for sequencing and bioinformatics analysis to ascertain whether gene expression changes occur in DLB compared to aged control cases. Relative RNA expression levels were compared to identify significantly altered transcripts between groups. Gene ontology (GO) software was employed by our collaborator to identify biological processes, molecular function and cellular component annotations to establish systems associated with DLB in the pulvinar. Based on the resulting list of altered transcripts and pathways, this chapter outlines a series of western blot experiments used to assess levels of protein expression in the pulvinar.

### 5.1.1 Aims

These studies used frozen *post-mortem* pulvinar tissue obtained from hallucinating DLB cases compared to cognitively normal, non-hallucinating, control cases. This study aims to:

1) Investigate significantly altered transcripts to compile a list of protein targets.
2) Assess protein expression changes based on identified changes in transcription and in specific biological pathways.

## 5.2 Methods

### 5.2.1 Tissue acquisition

The pulvinar was identified as approximately the most posterior 5 mm of the thalamus, protruding into the lateral ventricle (Jones, 2007). 14 control and 14 DLB were included in the present study based on the intial criteria of low *post*-mortem interval and preserved pH for optimal neurochemical analysis (Table 5.1). However, since conducting this study, it has become apparent that low *post-mortem* interval is less important than tissue pH in selecting frozen brain tissue (Robinson *et al.*, 2016). DLB cases were selected due to the presence of well-formed visual hallucinations, and a clinical and pathological diagnosis of DLB. Approximately 50 mg of tissue was removed from the posterior pole of the thalamus using a cooled scalpel and homogenised in 0.2M TEAB buffer, combined with protease inhibitor tablets (see Section 2.6.2).

*Table 5.1: Demographic information for cases used in the molecular pulvinar study.*

*'PM interval' is the interval between death and post-mortem examination, 'Braak NFT' represents global neurofibrillary pathology stage as outlined in (Braak et al., 2006), 'McKeith LB' represents global Lewy body pathology stage, as outlined in (McKeith et al., 2005), 'clinico-path diagnosis' represents the overall diagnosis reached by case-note review and neuropathological examination by senior clinicians and a consultant neuropathologist. 'ND' means 'not determined'.*

| Case ID | Gender | Age at death (years) | Tissue pH | PM interval (hours) | Braak NFT | McKeith LB | Clinico-path diagnosis |
|---|---|---|---|---|---|---|---|
| C5 | M | 73 | 6.45 | 25 | 0 | None | Control |
| C11 | F | 84 | 6.55 | 7 | 3 | None | Control |
| C12 | F | 88 | 6.39 | 21 | 3 | None | Control |
| C13 | F | 74 | ND | 28 | 1 | None | Control |
| C14 | F | 76 | 6.07 | 10 | 1 | None | Control |
| C15 | M | 72 | 6.25 | 31 | 2 | None | Control |
| C16 | M | 71 | ND | 15 | ND | ND | Control |
| C17 | M | 67 | ND | 38 | 1 | None | Control |
| C18 | M | 85 | ND | 24 | 2 | None | Control |
| C19 | M | 66 | 6.66 | 9 | ND | ND | Control |
| C20 | F | 79 | ND | 26 | 3 | None | Control |
| C21 | F | 82 | 6.57 | 26 | 0 | None | Control |
| C6 | M | 80 | ND | 16 | 3 | Brainstem | Control |
| Mean±SD | | 76.7±7 | 6.4±0.2 | 21.2±9 | 1.8±1 | | |
| D13 | M | 75 | 6.45 | 18 | 3 | Neocortical | DLB |

| | | | | | | | |
|---|---|---|---|---|---|---|---|
| D14 | M | 78 | 6.40 | 8 | 4 | Neocortical | DLB |
| D15 | M | 69 | 6.65 | 27 | 5 | Neocortical | DLB |
| D16 | M | 78 | 6.46 | 23 | 4 | Neocortical | DLB |
| D17 | M | 79 | 6.83 | 30 | 4 | Neocortical | DLB |
| D18 | F | 77 | 6.24 | 23 | 3 | Neocortical | DLB |
| D19 | M | 79 | 6.66 | 26 | 3 | Neocortical | DLB |
| D20 | M | 77 | 6.50 | 38 | ND | ND | DLB |
| D21 | M | 76 | ND | 13 | 3 | Neocortical | DLB |
| D22 | F | 81 | 6.02 | 4 | 5 | Neocortical | DLB |
| D23 | M | 79 | 6.65 | 16 | 3 | Neocortical | DLB |
| Mean±SD | | 77.1±3 | 6.5±0.2 | 20.5±10 | 3.7±1 | | |

### 5.2.2 RNA sequencing

To investigate relative changes in RNA transcription in the pulvinar, RNA was extracted using a spin column method and treated with DNase. RNA concentration and integrity was subsequently determined before samples were dispatched to the laboratory of Professor Mark Cookson at the National Institutes of Health (NIH), Bethesda, MD, USA for RNA sequencing and bioinformatics analyses.

Samples were analysed using DSEQ2 software with a general linear model assessing differences based on disease, with tissue pH, age, gender and PM interval used as covariates. Adjustments for multiple testing were employed with standard filters (Cook's cutoff and automatic filters within the program). RNA sequencing data was analysed using GO software to assess pathways that may be dysfunctional or altered using a bioinformatics approach for large datasets. A detailed summary of analysis methods can be found in (Love *et al.*, 2014).

### 5.2.3 SDS-PAGE and Western blotting

Protein homogenates of pulvinar tissue from control and DLB were prepared as described in Section 2.6.2. The total protein content of each sample was determined using the Bradford assay (Sigma-Aldrich, MO, USA). 10 µg of 1 µg/µl total protein was loaded into each well, with each well representing one case, of a polyacrylamide gel. The constituent proteins within the samples were separated using SDS-PAGE and transferred to nitrocellulose membranes for western blot analysis. Protein targets were identified from GO enrichment analysis of RNA sequencing data, and probed using antibodies (Tables 5.2 and 5.3). Relative protein expression was determined between groups using semi-quantitative densitometric methods outlined in methods, and normalised relative to the housekeeping protein GAPDH.

### 5.2.4 Statistics

Variable changes, such as substrate exposure time, create difficulties in comparison between individual membranes. Densitometric analysis is a relative, independent, measure and, as a result, independent t-tests were performed on each protein target.

## 5.3 Results

### 5.3.1 Demographics

There was no significant difference in age at death ($F=0.031$, $p=0.862$), *post-mortem* interval ($F=0.030$, $p=0.863$) or gender ($\chi^2=2.098$, $p=0.211$) between experimental groups (Table 5.1).

### 5.3.2 RNA sequencing

One control and three DLB cases were excluded from the analysis due to low RNA integrity. The remaining group, 13 control and 11 DLB, showed some degree of separation in RNA profile between experimental groups but this was not absolute (Fig. 5.1).

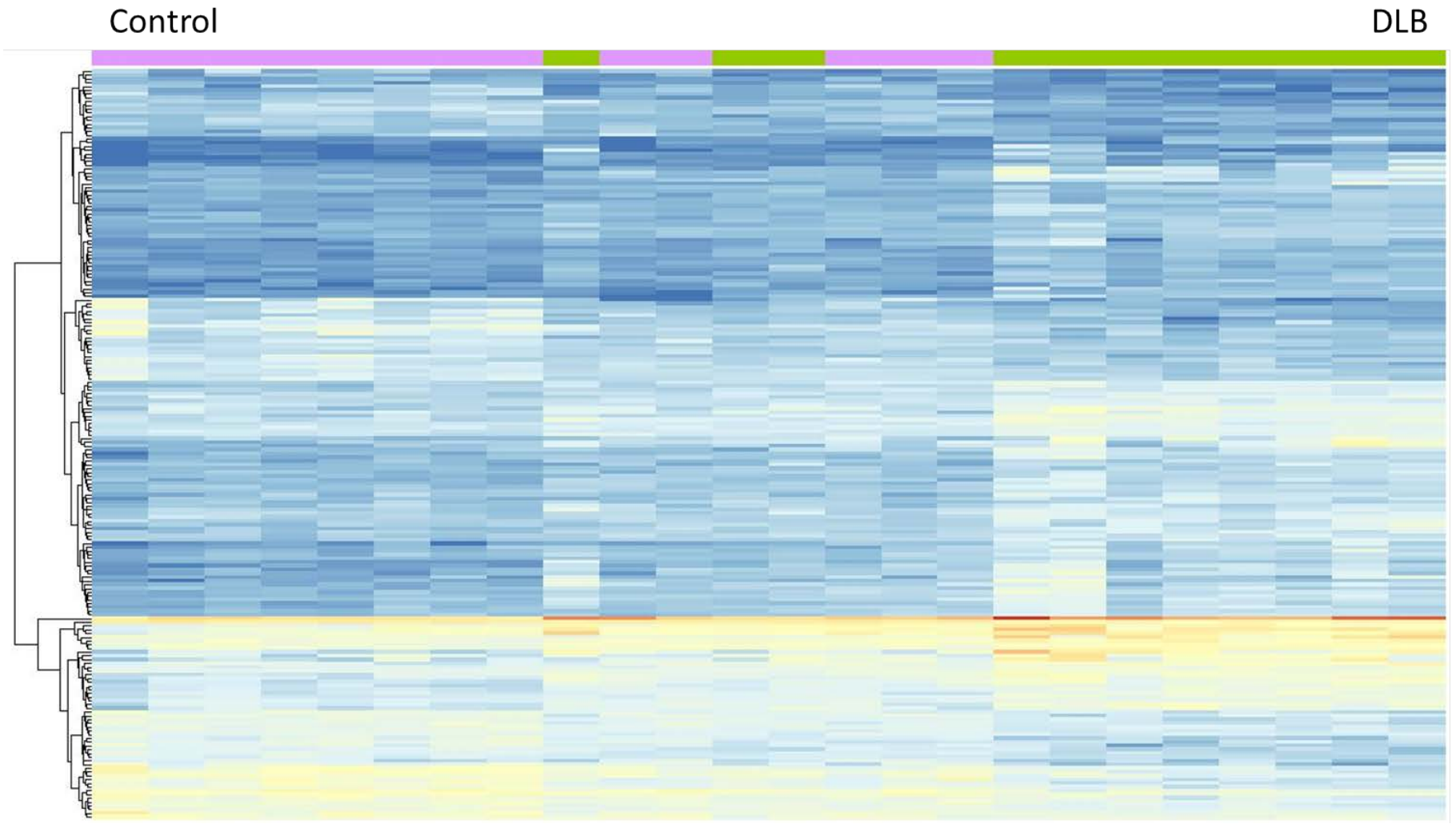


*Figure 5.1: Heat map of RNA sequencing data.*

*Whilst many cases show clear separation from controls, there is overlap visible in the middle.*

### 5.3.3 Selection of protein targets

GO enrichment was conducted in the pulvinar samples following RNA sequencing. This showed significant enrichment for synaptic proteins and proteins involved in positive regulation of immune system process.

Protein targets relating to synaptic functioning and immune system regulation were further investigated based on the identification of these pathways as altered in the GO analysis. Antibodies were often not available for altered protein targets identified using RNA sequencing analysis. In other cases, the expression of the protein was hypothesised to be low, based on relatively low levels of transcription. The pulvinar is a small region of the brain and, as a result, there was a limited amount of tissue available following RNA extraction. Work on previous studies has indicated that obtaining antibodies recognising their target epitope in human tissue is difficult, and optimisation of such antibodies often consumes large amounts of tissue (Khundakar *et al.*, 2016). Therefore, the present study aimed to use antibodies that had previously been demonstrated to work in human *post-mortem* tissue.

As a result, the choice of protein targets was based on:

A) Availability of antibodies demonstrated to work in human tissue.
B) A hypothetical link to synaptic or immune system functioning based on GO consortium pathways data.
C) A significant quantity of the protein to make detection likely (a base mean > 100 was used as an arbitrary cut-off point).

Based on these criteria, the antibodies against synaptic proteins used in the present study are listed in Table 5.2.

The antibodies against positive regulators of immune system functioning are listed in Table 5.3. GO analysis indicated that several markers of astrocytic sub-populations were elevated, such as GFAP and chitinase-3-like 1 (CHI3L1/YKL-40). Aldehyde dehydrogenase 1 family member L1 (ALDH1L1) is thought to be a more general marker of astrocytes and was therefore also included in this analysis (Cahoy *et al.*, 2008).

In addition to the synaptic and immune system regulatory proteins listed, two GABAergic markers (glutamic acid decarboxylase 67; GAD67 and GABA type A

receptor-associated protein; GABARAP) were also assessed due to a previous finding of specific molecular GABAergic changes in the visual system in DLB, which occurred in the absence of histological GABAergic changes (Khundakar *et al.*, 2016).

*Table 5.2: Synaptic antibodies used in the present study, with the two additional GABAergic markers (GAD67 and GABARAP).*

*In the instance of the protein having several transcript variants, the fold change and p-value are the isoform that showed the greatest change, as this was the justification for looking at the protein.*

| Antibody | Manufacturer | Catalogue number | Dilution | Log2 fold change on RNAseq | p value on RNAseq |
|---|---|---|---|---|---|
| Gephyrin | Synaptic systems | 147111 | 1:1000 | -0.8332 | 0.0105 |
| PSD-95 | Santa Cruz | sc-32290 | 1:500 | -0.8392 | 0.0020 |
| Synaptophysin | Millpore | MAB368 | 1:20,000 | -0.7153 | 0.0142 |
| SNAP-25 | Santa Cruz | sc-20038 | 1:2000 | -0.8810 | 0.0054 |
| GAP43 | Santa Cruz | sc-135915 | 1:500 | -0.8835 | 0.0056 |
| SV2B | ProteinTech | 14624-1-AP | 1:500 | -1.7425 | <0.0001 |
| MAP2 | Sigma Aldrich | M4403 | 1:500 | -0.7013 | 0.0104 |
| NSF | Santa Cruz | sc-15339 | 1:4000 | -0.9992 | 0.0140 |
| GAD67 | Santa Cruz | sc-58531 | 1:1000 | -0.6815 | 0.0160 |
| GABARAP | Abcam | ab109364 | 1:1000 | +0.0318 | 0.8136 |

*Table 5.3: Antibodies against positive regulators of immune system functioning.*

*In the instance of the protein having several transcript variants, the fold change and p-value are the isoform that showed the greatest change, as this was the justification for looking at the protein.*

| Antibody | Manufacturer | Catalogue number | Dilution | Log2 fold change on RNAseq | p value on RNAseq |
|---|---|---|---|---|---|
| ALDH1L1 | Millipore | MABN461 | 1:1000 | +0.3893 | 0.1865 |
| SERPINH1/HSP47 | Santa Cruz | sc-13150 | 1:25 | +1.9451 | <0.0001 |
| HSPA1A | GeneTex | GTX111088 | 1:10,000 | +1.4714 | 0.0002 |
| HSPA1B | GeneTex | GTX106148 | 1:5000 | +1.2800 | 0.0005 |
| GFAP | Santa Cruz | sc-33673 | 1:500 | +0.8315 | 0.0048 |
| CHI3L1/YKL-40 | Abcam | ab77528 | 1:1000 | +2.0865 | <0.0001 |
| C3 | Abcam | ab11862 | 1:2000 | +1.2742 | <0.0001 |

### 5.3.4 Western blotting of synaptic and GABAergic proteins

Western blot analysis of synaptic proteins showed that, in comparison to control, DLB had several significant reductions.

A single band at approximately 80 kDa was demonstrated for gephyrin (Fig. 5.2A), which corresponds with the canonical sequence (Uniprot: Q9NQX3). Gephyrin was significantly reduced in DLB compared to control ($t=2.35$, $p=0.0350$, $d=0.78$; Fig. 5.2A).

A single band at approximately 80 kDa was demonstrated for post-synaptic density protein 95 (PSD-95; Fig. 5.2B), which corresponds with the canonical sequence (Uniprot: P78352). PSD-95 was significantly reduced in DLB compared to control ($t=2.63$, $p=0.0153$, $d=0.96$; Fig. 5.2B).

Two bands were demonstrated at approximately 39 kDa and 37 kDa for synaptophysin, subsequently described as isoforms 1 and 2, respectively (Fig. 5.2C). The canonical sequence of synaptophysin is 39 kDa (Jahn *et al.*, 1985) but the only described variant of the canonical sequence of synaptophysin is 21 kDa (Uniprot: P08247-2). Synaptophysin isoform 1 was significantly reduced in DLB compared to control ($t=2.62$, $p=0.0212$, $d=0.90$; Fig. 5.2C). No significant difference was found in isoform 2 between DLB and control (Fig. 5.2C).

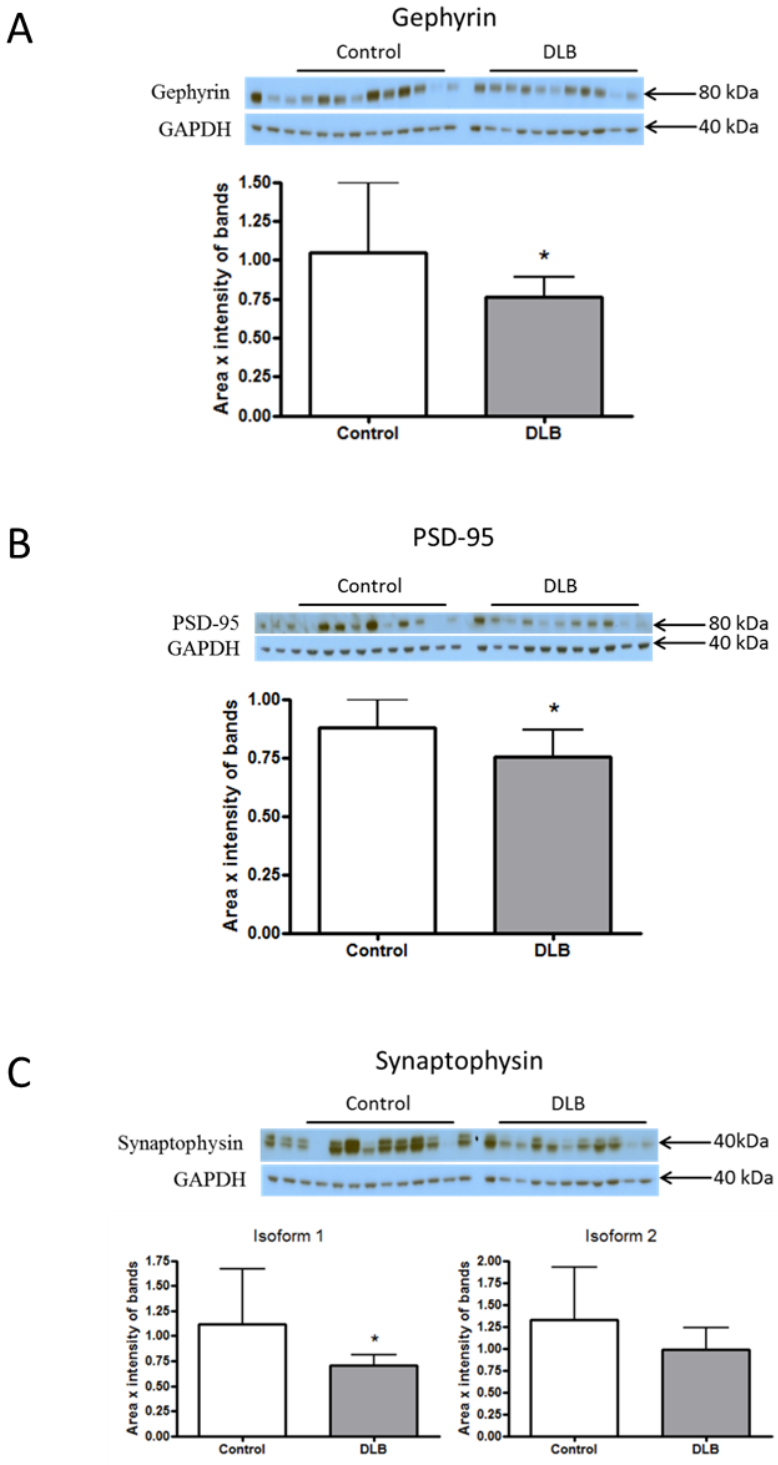


*Figure 5.2: Western blotting of gephyrin, PSD-95 and synaptophysin.*

*Gephyrin (A), PSD-95 (B) and synaptophysin (C) expression is compared between control and DLB. Bars demonstrate the mean and error bars represent standard deviation. *p<0.05.*

A single band at approximately 24 kDa was demonstrated for SNAP-25 (Fig. 5.3A), which corresponds with the canonical sequence (Uniprot: P60880). SNAP-25 was not significantly different between DLB and control (p=0.0846; Fig. 5.3A).

A single band at approximately 50 kDa was demonstrated for growth-associated protein 43 (GAP43; Fig. 5.3B), which does not correspond with the canonical sequence (Uniprot: P17677). The canonical sequence of GAP43 has a molecular mass of 25 kDa. As the observed bands are approximately twice the known molecular mass of the canonical sequence, one may speculate this is a dimer. GAP43 was not significantly different between DLB and control (p=0.1308; Fig. 5.3B).

A single band at approximately 78 kDa was demonstrated for synaptic vesicle glycoprotein 2B (SV2B; Fig. 5.3C), which corresponds with the canonical sequence (Uniprot: Q7L1I2). SV2B was not significantly different between DLB and control (p=0.8770; Fig. 5.3C).

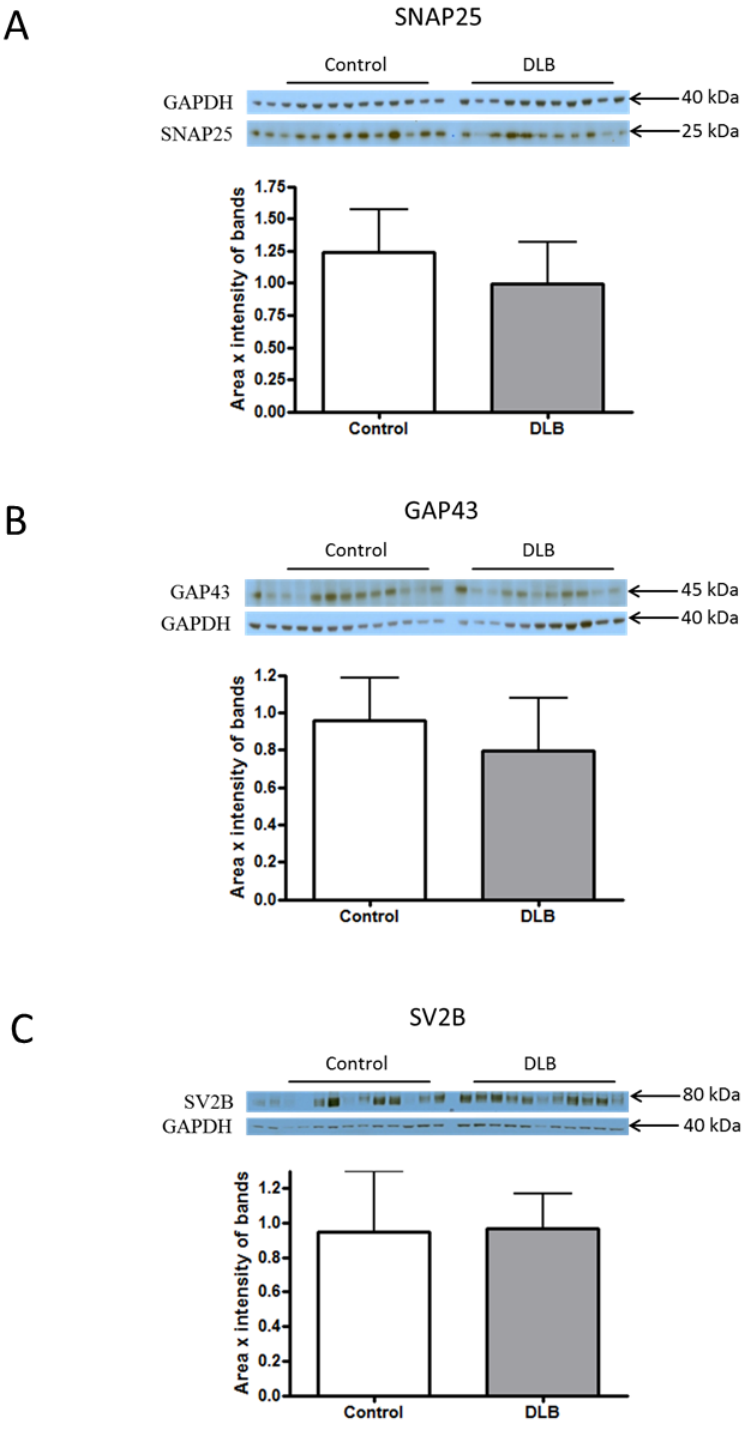


*Figure 5.3: Western blotting of SNAP-25, GAP43 and SV2B.*

*SNAP-25 (A), GAP43 (B) and SV2B (C) expression is compared between control and DLB. Bars demonstrate the mean and error bars represent standard deviation.*

A single band at approximately 50 kDa was demonstrated for microtubule-associated protein 2 (MAP2; Fig. 5.4A), which does not correspond with the canonical sequence. It was not possible to detect the canonical sequence of MAP2, which has a relatively high molecular weight of 200 kDa (Uniprot: P11137). Instead, a known variant of the canonical sequence, isoform 2 (Uniprot: P11137-2), was detected at 50 kDa. MAP2 was significantly reduced in DLB compared to control ($t=2.40$, $p=0.0256$, $d=0.89$; Fig. 5.4A).

A single band at approximately 82 kDa was demonstrated for N-ethylmaleimide sensitive fusion protein (NSF; Fig. 5.4B), which corresponds with the canonical sequence (Uniprot: P46459). NSF was significantly reduced in DLB compared to control ($t=2.97$, $p=0.0070$, $d=1.04$; Fig. 5.4B).

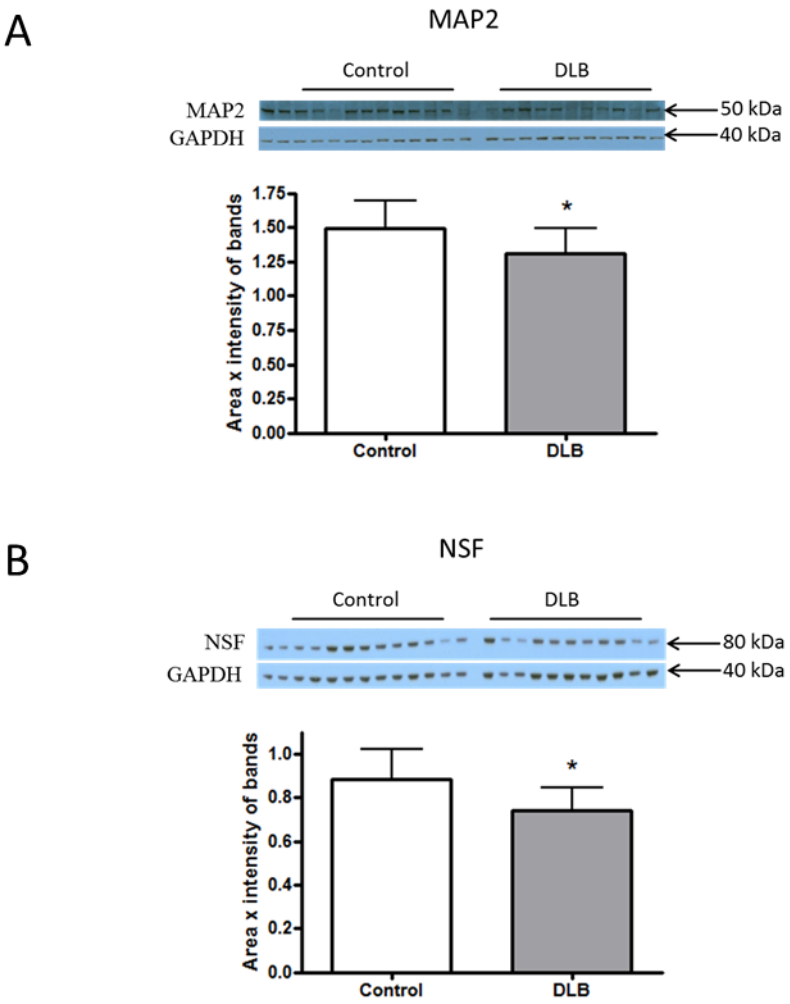


*Figure 5.4: Western blotting of MAP2 and NSF.*

*MAP2 (A) and NSF (B) expression is compared between control and DLB. Bars demonstrate the mean and error bars represent standard deviation. *p<0.05.*

A single band at approximately 67 kDa was demonstrated for GAD67 (Fig. 5.5A), which corresponds with the canonical sequence (Uniprot: Q99259). GAD67 was significantly reduced in DLB compared to control (t=2.68, p=0.0171, d=0.92; Fig. 5.5A).

Two bands were demonstrated at approximately 16 kDa and 14 kDa for GABARAP (Fig. 5.5B), which will be subsequently referred to as GABARAP isoform 1 and GABARAP isoform 2, respectively. The only described sequence of GABARAP is 14 kDa (Uniprot: O95166). The band at 16 kDa, which is qualitatively smaller, may represent a previously undescribed isoform of GABARAP. GABARAP isoform 1 was significantly reduced in DLB compared to control (t=2.20, p=0.0430, d=0.86; Fig. 5.5B). However, GABARAP isoform 2 was not significantly different between DLB and control (p=0.0545; Fig. 5.5B).

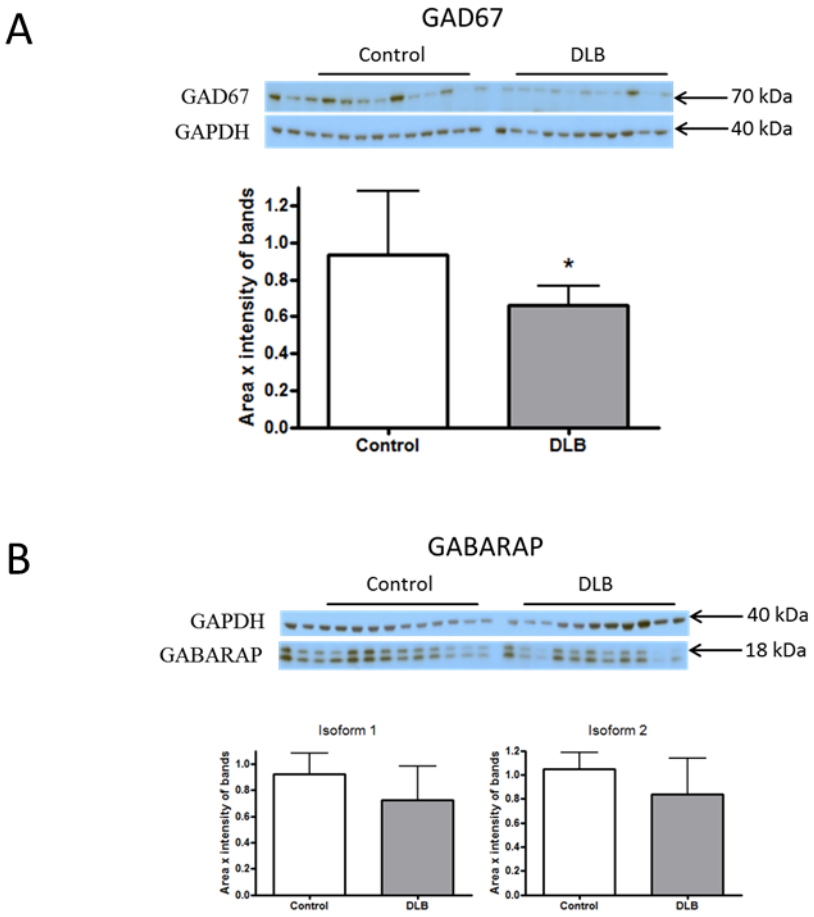


*Figure 5.5: Western blotting of GAD67 and GABARAP.*

*GAD67 (A) and GABARAP (B) expression is compared between control and DLB. Bars demonstrate the mean and error bars represent standard deviation. *p<0.05.*

### 5.3.5 Western blotting of proteins that regulate immune system functioning

Two bands were demonstrated at approximately 100 kDa and 90 kDa for ALDH1L1, which will be subsequently described as isoforms 1 and 2, respectively (Fig. 5.6A). The former corresponds with the canonical sequence (Uniprot: O75891) and a known isoform has a molecular mass of 88 kDa (Uniprot: O75891-2), suggesting that isoform 2 is a known variant of ALDH1L1. ALDH1L1 isoform 1 was significantly increased in DLB compared to control ($t=3.93$, $p=0.0007$, $d=1.25$; Fig. 5.6A). No significant difference was found in isoform 2 between DLB and control (Fig. 5.6A). Isoform 1 was relatively increased, compared to isoform 2, in DLB compared to control ($t=3.92$, $p=0.001$, $d=1.26$).

A single band at approximately 70 kDa was demonstrated for heat shock 70 kDa protein 1B (HSPA1B; Fig. 5.6B), which corresponds with the canonical sequence (Uniprot: P0DMV9). HSPA1B was significantly increased in DLB compared to control ($t=2.99$, $p=0.0112$, $d=1.11$; Fig. 5.6B).

A single band at approximately 43 kDa was demonstrated for CHI3L1/YKL-40 (Fig. 5.6C), which corresponds with the canonical sequence (Uniprot: P36222). CHI3L1/YKL-40 was significantly increased in DLB compared to control ($t=2.40$, $p=0.0300$, $d=0.93$; Fig. 5.6C).

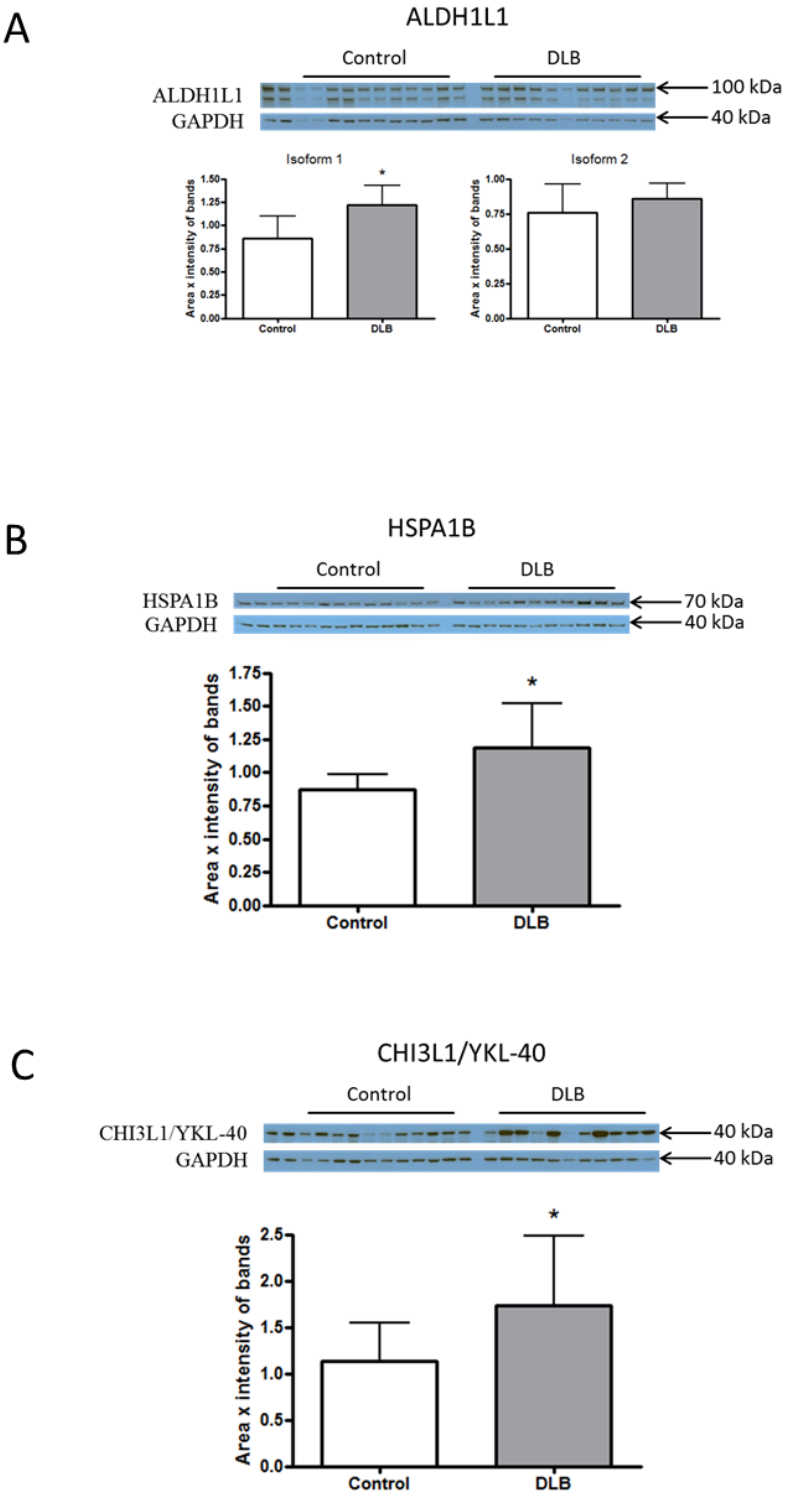


*Figure 5.6: Western blotting of ALDH1L1, HSPA1B and CHI3L1/YKL-40.*

*ALDH1L1 (A), HSPA1B (B) and CHI3L1/YKL-40 (C) expression is compared between control and DLB. Bars demonstrate the mean and error bars represent standard deviation.*p<0.05*

A single band at approximately 47 kDa was demonstrated for serine (or cysteine) proteinase inhibitor, clade H (heat shock protein 47), member 1 (SERPINH1/HSP47; Fig. 5.7A), which corresponds with the canonical sequence (Uniprot: P50454). SERPNH1/HSP47 was not significantly different between DLB and control (p=0.6368; Fig. 5.7A).

A single band at approximately 70 kDa was demonstrated for heat shock protein 70 kDa protein 1 (HSPA1A; Fig. 5.7B), which corresponds with the canonical sequence (Uniprot: P0DMV8). HSPA1A was not significantly different between DLB and control (p=0.6140; Fig. 5.7B).

A single band was detected at approximately 100 kDa for complement component 3 (C3; Fig. 5.7C), which does not correspond with the canonical sequence which has a molecular mass of 187 kDa (Uniprot: P01024). However, a molecular mass of 187 kDa would not be detectable using the method employed and, therefore, the band at 100 kDa was quantified. The 100 kDa band of C3 was not significantly different between DLB and control (p=0.1499; Fig. 5.7C).

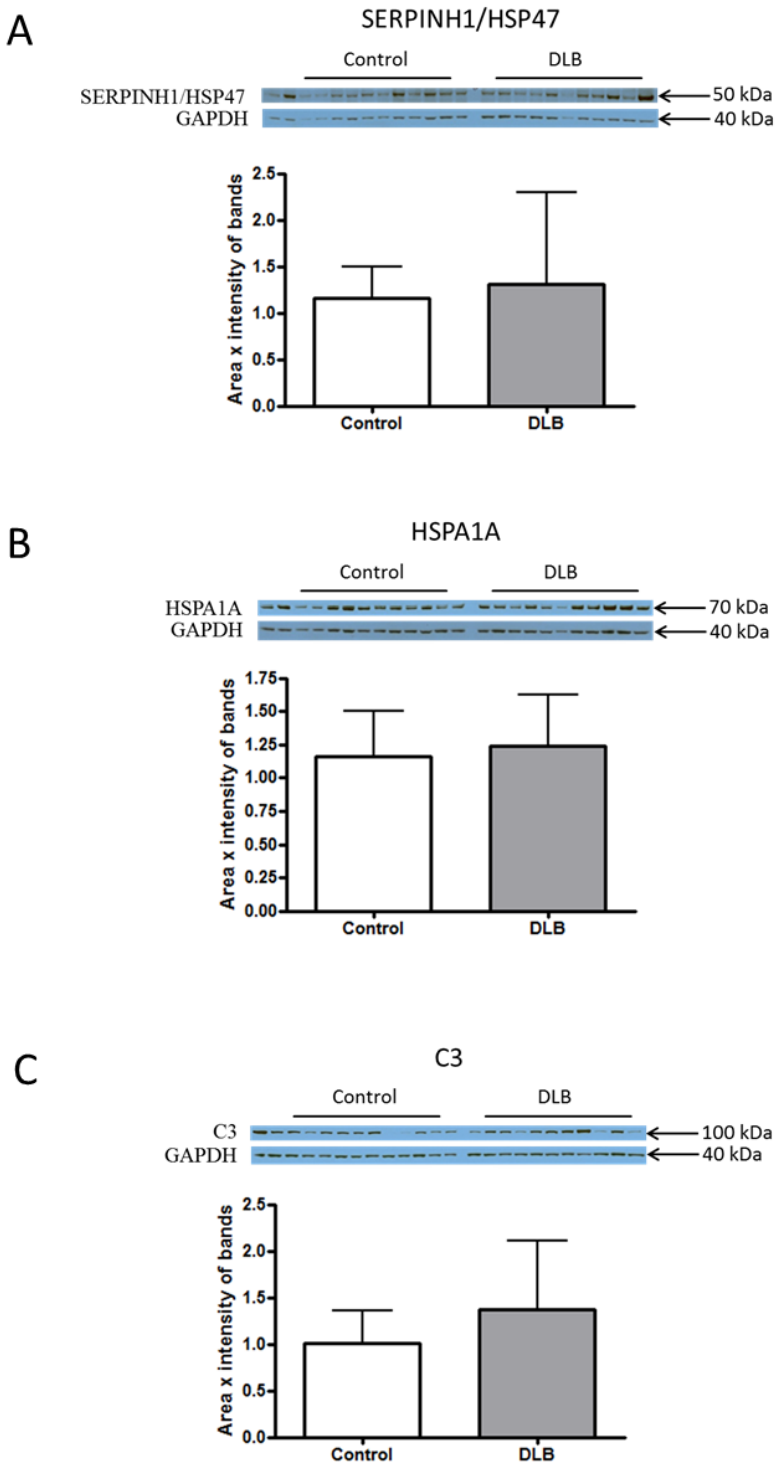


*Figure 5.7: Western blotting of SERPINH1/HSP47, HSPA1A and C3.*

*SERPINH1/HSP47 (A), HSPA1A (B) and C3 (C) is compared between control and DLB. Bars demonstrate the mean and error bars represent standard deviation.*

Several bands were demonstrated between 40 and 50 kDa for GFAP (Fig. 5.8), though all previously described isoforms of GFAP have an approximate molecular mass of 50 kDa (Uniprot: P14136). The additional bands below 50 kDa may reflect degradation products. The top, middle and bottom bands were analysed and will subsequently be referred to as GFAP isoforms 1, 2 and 3, respectively. GFAP isoform 1 was not significantly different between DLB and control ($p=0.5107$; Fig. 5.8). GFAP isoform 2 was not significantly different between DLB and control ($p=0.7234$; Fig. 5.8). GFAP isoform 3 was not significantly different between DLB and control ($p=0.1122$; Fig. 5.8).

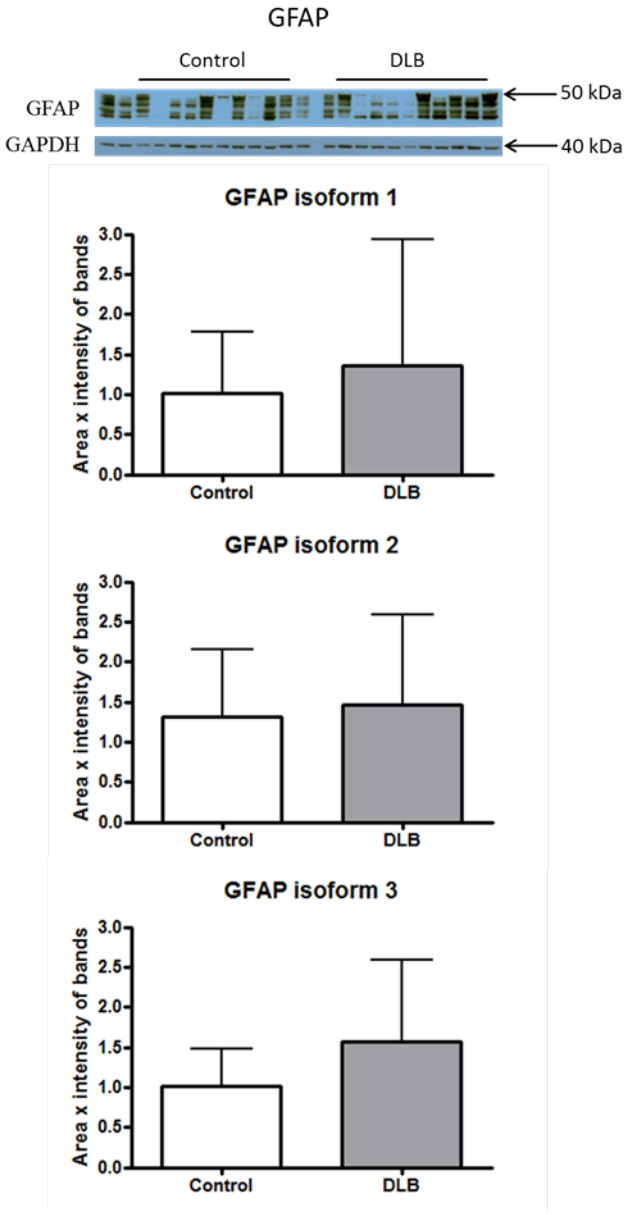


*Figure 5.8: Western blotting of GFAP.*

*GFAP isoform expression is compared between control and DLB. Bars demonstrate the mean and error bars represent standard deviation.*

### 5.3.6 Relationships between synaptic markers

*Post-mortem* interval was previously demonstrated to relate to decreases in some synaptic proteins, such as PSD-95 (Siew *et al.*, 2004; Sinclair *et al.*, 2015). However, a study published subsequent to the completion of this work has demonstrated *post-mortem* interval has little impact on proteomic analysis, with most changes driven by tissue pH (Robinson *et al.*, 2016). For this reason, *post-mortem* interval and tissue pH (when available) were related to all synaptic proteins. The only significant correlation was between tissue pH and SNAP-25 (rho=0.486, p=0.048).

A correlation matrix was constructed between presynaptic markers (Table 5.4). This matrix suggested similar patterns of expression between synaptophysin, NSF, SNAP-25, GAP43 and dynamin. However, SV2B showed no significant correlations with other presynaptic markers.

A correlation matrix was constructed between postsynaptic markers (Table 5.5). This matrix suggested similar patterns of expression between PSD-95, gephyrin and GABARAP. However, MAP2 was only significantly correlated with GABARAP isoform 2.

*Table 5.4: Correlation matrix demonstrating correlations between presynaptic markers.*

*All cases were used for this analysis. *p<0.05.*

| | SYP | NSF | SNAP-25 | GAP43 | SV2B |
|---|---|---|---|---|---|
| Synaptophysin | | 0.69* | 0.46* | 0.59* | 0.31 |
| NSF | 0.69* | | 0.25 | 0.57* | 0.13 |
| SNAP-25 | 0.46* | 0.25 | | 0.52* | -0.10 |
| GAP43 | 0.59* | 0.57* | 0.52* | | 0.11 |
| SV2B | 0.31 | 0.13 | -0.10 | 0.11 | |

*Table 5.5: Correlation matrix demonstrating correlations between postsynaptic markers.*

*All cases were used for this analysis. *p<0.05.*

| | PSD-95 | Gephyrin | GABARAP1 | GABARAP2 | MAP2 |
|---|---|---|---|---|---|
| PSD-95 | | 0.55* | 0.79* | 0.77* | 0.27 |
| Gephyrin | 0.55* | | 0.61* | 0.53* | 0.27 |
| GABARAP1 | 0.79* | 0.61* | | 0.94* | 0.40 |
| GABARAP2 | 0.77* | 0.53* | 0.94* | | 0.44* |
| MAP2 | 0.27 | 0.27 | 0.40 | 0.44* | |

*Table 5.9: Correlation matrix demonstrating correlations between astrocytic markers.*

*All cases were used for this analysis. *p<0.05.*

| | ALDH1L1 1 | ALDH1L1 2 | GFAP 1 | GFAP 2 | GFAP 3 | CHI3L1 |
|---|---|---|---|---|---|---|
| ALDH1L1 1 | | 0.79* | 0.17 | 0.31 | 0.39 | 0.47* |
| ALDH1L1 2 | 0.79* | | -0.17 | 0.00 | 0.16 | 0.32 |
| GFAP 1 | 0.17 | -0.16 | | 0.65* | 0.16 | 0.06 |
| GFAP 2 | 0.31 | 0.00 | 0.65* | | 0.71* | 0.26 |
| GFAP3 | 0.39 | 0.16 | 0.16 | 0.71* | | 0.36 |
| CHI3L1 | 0.47* | 0.32 | 0.06 | 0.26 | 0.36 | |

### 5.3.7 Relationships between inflammatory markers

A correlation matrix was constructed between all astroglial markers (Table 5.6). ALDH1L1 did not correlate with GFAP but positively correlated with CHI3L1/YKL-40. No GFAP isoform was related to ALDH1L1 or CHI3L1/YKL-40.

### 5.3.8 Relationships between astroglial and synaptic markers

To investigate potential relationships between synaptic and astroglial markers, the synaptic markers synaptophysin, NSF, SNAP-25, GAP43, dynamin, PSD-95, gephyrin and GABARAP were correlated with the astroglial markers ALDH1L1, GFAP and CHI3L1/YKL-40. The synaptic markers were selected based on the substantial interrelationships with other synaptic markers. The three astroglial markers were selected based on the evidential base linking them to astrocytic patterns of expression, and the previous observation of astrocytic increases in the pulvinar in DLB described in Chapter 4. As these analyses were not directly hypothesis-driven, Bonferroni corrections were applied to these results.

ALDH1L1 isoform 1 was significantly negatively correlated with GAP43 (rho=-0.576, corrected p=0.033) and dynamin (rho=-0.623, corrected p=0.011). No significant correlations were found between ALDH1L1 isoform 1 and synaptophysin, NSF, SNAP-25, PSD-95, gephyrin, GABARAP isoform 1 and GABARAP isoform 2. All significant correlations between ALDH1L1 isoform 1 and synaptic markers are illustrated in Fig. 5.10.

All GFAP isoforms and the ALDH1L1 isoform 2 were not significantly correlated with any synaptic markers after Bonferroni correction.

CHI3L1/YKL-40 was significantly negatively correlated with NSF (rho=-0.578, p=0.033), GAP43 (rho=-0.612, p=0.011), PSD-95 (rho=-0.599, p=0.022), GABARAP isoform 1 (rho=-0.712, p=0.001) and GABARAP isoform 2 (rho=-0.672, p=0.001). No significant correlations were found between CHI3L1/YKL-40 and synaptophysin, SNAP-25 and gephyrin. Scatterplots of all significant correlations between CHI3L1/YKL-40 and synaptic markers are illustrated in Fig. 5.10.

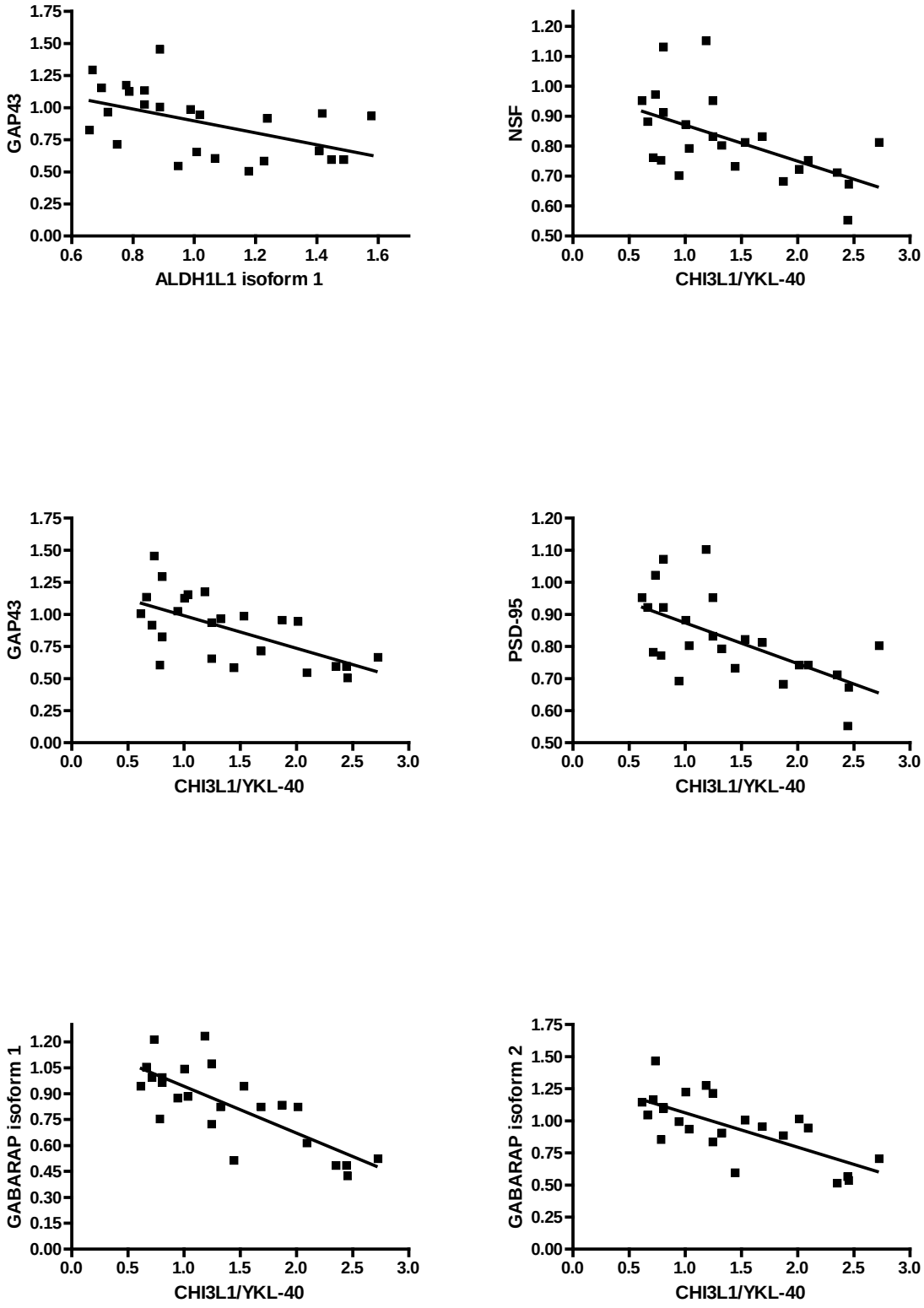


*Figure 5.10: Correlations between synaptic and astrocytic markers.*

*Scatterplots illustrating significant correlations between ALDH1L1 and CHI3L1/YKL-40 with synaptic markers.*

## 5.4 Discussion

RNA sequencing data provided by a collaborator demonstrated synaptic and inflammatory changes in the pulvinar nucleus in DLB at the transcriptional level. The present study elaborated on these findings by demonstrating corresponding alterations in protein expression. Previous studies have shown that the pulvinar is vulnerable to Lewy body pathology (Yamamoto *et al.*, 2006) unlike other thalamic visual structures, such as the LGN (Erskine *et al.*, 2016). However, this is the first study to investigate the pulvinar at the molecular level in DLB. These findings indicate that beyond neuronal loss and astrogliosis identified using histopathological approaches in the previous chapter, the pulvinar undergoes molecular changes suggestive of synaptic loss and inflammation in DLB. Furthermore, there was a significant negative relationship between some astroglial markers and synaptic loss, indicating reductions in synaptic marker expression are commensurate with increases in astroglial markers.

### 5.4.1 Selective reductions in synaptic markers

Information transfer between neurons in the central nervous system is predominantly carried out at chemical synapses by neurotransmitters, which enable the fast passage of information between neurons (Hudspeth *et al.*, 2013). Secretion of neurotransmitters into the synapse is induced by the opening of voltage-gated calcium channels, as a result of neuronal membrane depolarisation (Ramakrishnan *et al.*, 2012). Neurotransmitter-containing vesicles fuse with the pre-synaptic membrane to release neurotransmitters (Sudhof, 2004), which may then bind to post-synaptic receptors, initiating (or inhibiting) intracellular processes in the post-synaptic neuron (Hudspeth *et al.*, 2013).

Synaptic vesicles are typically clustered in regions termed ‘active zones’ in axonal boutons, close to the sites where vesicles are released from the pre-synaptic neuron into the synapse (Fig. 5.11A) (Fowler and Staras, 2015). Vesicle fusion with the pre-synaptic membrane is facilitated by the SNARE protein family, which are present on both the synaptic vesicle and the pre-synaptic membrane (Ramakrishnan *et al.*, 2012). SNARE proteins tether the synaptic vesicle to the pre-synaptic membrane, thus facilitating synaptic vesicle fusion (Fig. 5.11B-D). SNAP-25 and SV2B are integral components of the pre-synaptic SNARE complex, which interact and

facilitate synaptic vesicle fusion and exocytosis (Sutton *et al.*, 1998; Lazzell *et al.*, 2004). SNAP-25 is expressed on the pre-synaptic membrane, where it is vital for vesicle fusion and exocytosis (Ramakrishnan *et al.*, 2012). Deletion of SNAP-25 from mice leads to profound dysfunction in calcium-mediated neurotransmitter exocytosis (Washbourne *et al.*, 2002). GAP43 is not directly associated with the SNARE complex but is predominantly expressed on pre-synaptic membranes, where it may influence the growth state of the presynaptic terminal (Benowitz and Routtenberg, 1997).

SNAP-25, GAP43 and SV2B were not significantly different in DLB compared to control. This was unexpected for SV2B, which had the fifth greatest fold reduction in the RNA sequencing analysis. SV2B is a synaptic vesicle protein that is predominantly expressed on glutamatergic synapses (Bragina *et al.*, 2011). Amyloid-β toxicity may be mediated by SV2B as knock-out of SV2B in amyloid-β overexpressing mice is protective against cognitive decline (Detrait *et al.*, 2014). One may speculate that reduced transcription of SV2B may reflect an attempt to attenuate SV2B-mediated amyloid-β toxicity. However, at the protein level, SV2B is not significantly different from control. A previous study has demonstrated amyloid-β may alter the translation of SV2B by acting upon a transcript variant, SV2Bb (Heese *et al.*, 2001). Therefore, one may speculate the discrepancy between transcription and expression may result from the presence of amyloid-β in the pulvinar, which may alter translation of SV2B.

The pre-synaptic proteins synaptophysin and NSF were significantly reduced in DLB compared to control. Synaptophysin and NSF both associate with the pre-synaptic SNARE complex to facilitate synaptic vesicle exocytosis (Calakos and Scheller, 1994; Rothman, 1994). The primary role of synaptophysin is thought to be in regulating neurotransmitter release and improving exocytotic efficiency (Gordon *et al.*, 2016). NSF contributes to disassembling the SNARE complex following membrane fusion and exocytosis (Fig. 5.11E) (Rizo and Xu, 2015). In contrast to SNAP-25 and SV2B, synaptophysin and NSF are not necessary for vesicle exocytosis at synapses but aid efficiency of neurotransmitter release and turnover of vesicles following exocytosis (Fig. 5.11E-F) (Rizo and Xu, 2015). Therefore, in the present study, pre-synaptic proteins necessary for synaptic vesicle exocytosis were not altered in DLB compared to control. In contrast, reductions were found in pre-synaptic proteins that aid

efficient neurotransmitter release and turnover of synaptic vesicles. Alterations to proteins related to synaptic efficiency may be the result of α-synuclein pathology in pre-synaptic regions, which may alter synaptic efficiency without eliminating the ability of neurons to communicate through synapses. A previous *in vitro* report demonstrated the addition of recombinant α-synuclein to cultured cortical neurons reduced the rate of synaptic vesicle recycling (Bate *et al.*, 2010). The pre-synaptic proteins altered in the present study are involved in the efficient recycling of synaptic vesicles, suggesting such alterations may be related to α-synuclein pathology.

Compared to control, DLB had significant reductions in all post-synaptic proteins assessed: PSD-95, gephyrin, both isoforms of GABARAP and MAP2. PSD-95 is located on the postsynaptic membrane of glutamatergic synapses (Hunt *et al.*, 1996), where it anchors neurotransmitter receptors and adhesion molecules (Keith and El-Husseini, 2008). Gephyrin has a similar role to PSD-95 on the postsynaptic membrane of inhibitory synapses, acting as a scaffold to anchor GABAergic and glycinergic receptors to the cytoskeleton (Levi *et al.*, 2004). GABARAP interacts with gephyrin and aids transport of GABAergic receptors to the post-synaptic membrane (Kneussel *et al.*, 2000). MAP2 is localised on dendritic spines, upon which postsynaptic receptors are located (Caceres *et al.*, 1983). The present results indicate reductions in post-synaptic receptor markers irrespective of their neurochemical composition, as excitatory and inhibitory post-synaptic markers are reduced.

The reductions in synaptic marker expression at the protein level are broadly consistent with those identified at the transcriptional level by RNA sequencing, and may reflect synaptic loss in the pulvinar. Pre-synaptic changes in protein expression are limited to proteins involved in the efficient recycling of synaptic vesicles following exocytosis, thus contributing to reduced refractory periods following exocytosis and correspondingly increased neuronal firing. However, the necessary components for exocytosis remain intact. In contrast, more widespread changes were observed in post-synaptic receptors. As necessary components for neurotransmitter exocytosis, such as SNAP-25 and SV2B, are intact, synaptic dysfunction appears more likely than generalised synaptic loss.

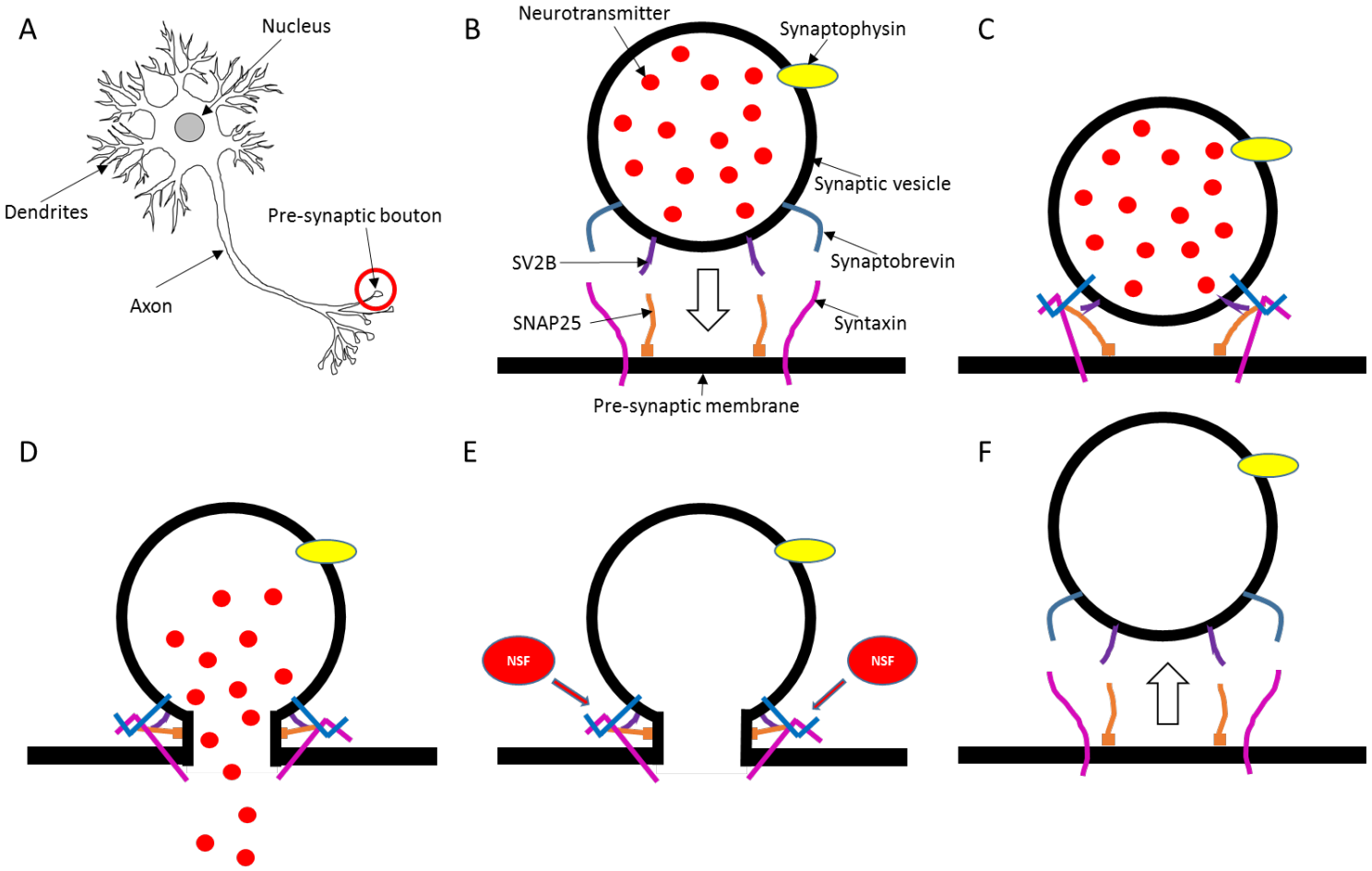


*Figure 5.11: The SNARE complex.*

*Pre-synaptic vesicles reside in the pre-synaptic bouton (A); vesicles move toward to pre-synaptic membrane (B); and are tethered by the SNARE complex (C); SNAP-25 aids vesicle fusion with the pre-synaptic membrane and contents are expelled into the synapse (D); NSF helps break down the SNARE complex (E); the vesicle is released from the pre-synaptic membrane and recycled (F).*

### 5.4.2 GABAergic marker reductions

GABARAP and GAD67 are markers of the inhibitory neurotransmitter GABA and were significantly reduced in DLB compared to control, despite no changes to GABARAP transcription on RNA sequencing, as reported in Table 5.2. GABARAP interacts with gephyrin and transports GABAergic receptors to the postsynaptic membrane (Kneussel *et al.*, 2000). GAD67 is one of two enzymes that catalyse the synthesis of GABA from glutamate (Fenalti *et al.*, 2007). The expression of GAD67 is regulated in an activity-dependent manner (Lau and Murthy, 2012) and reductions have been demonstrated to decrease inhibitory network activity in cortical regions (Lazarus *et al.*, 2015). Taken together, these results demonstrate general reductions in markers of GABAergic neurotransmission. Therefore, the present results support previous findings suggesting GABAergic dysfunction in the visual system in DLB as a potential mechanism underlying visual hallucinations (Khundakar *et al.*, 2016; Taylor *et al.*, 2016).

### 5.4.3 Selective increases in positive regulators of immune system functioning

The immune system protects the organism from a variety of diverse harm-causing agents, in addition to promoting repair and clearance of damaged tissues (Proserpio and Mahata, 2016). Positive regulators of immune system serve to activate or enhance the response of the immune system. The immune response in the brain is primarily conducted by microglia (Rivest, 2009), though astrocytes have also been demonstrated to modulate inflammation and can act to sustain inflammatory conditions (Farina *et al.*, 2007). In the context of neurodegenerative disorders, neuroinflammation is an intrinsic cellular response to neurodegenerative insult initiated to isolate and clear damaged tissues (Lopez-Valdes and Martinez-Coria, 2016).

ALDH1L1, GFAP and CHI3L1/YKL-40 are expressed on astroglia (Cahoy *et al.*, 2008). In the brain, CHI3L1/YKL-40 is predominantly expressed in astrocytes and does not co-localise with the microglial marker LN-3 (Craig-Schapiro *et al.*, 2010). However, CHI3L1/YKL-40 is specifically expressed in macrophages in the periphery (Rehli *et al.*, 2003; Coffman, 2008). Therefore, it is impossible to discount the possibility that the presently reported elevations in CHI3L1/YKL-40 result from infiltrating macrophages resulting from tissue damage or neuronal insult in DLB.

ALDH1L1, a more general astrocytic marker than GFAP or CHI3L1/YKL-40 (Cahoy *et al.*, 2008), was not elevated on RNA sequencing (Table 5.3) but was increased at the protein level. The increased protein expression but absence of increased transcription may suggest changes in the translation of ALDH1L1. DLB had a relative 24% increase in isoform 1 relative to isoform 2, perhaps suggesting ALDH1L1 is transcribed or translated differently in DLB compared to control. GFAP was increased on RNA sequencing analysis (Table 5.3) but did not show any differences between groups at the protein level. However, western blot of GFAP demonstrated numerous bands between 40 kDa and 50 kDa which made densitometric analysis difficult, and likely affected the quantification of this protein. It is notable that Chapter 4 reported increased density of GFAP-immunoreactive astrocytic profiles in a separate cohort of DLB cases compared to control. CHI3L1/YKL-40, a marker of a sub-population of astrocytes induced in inflammatory conditions (Bonneh-Barkay *et al.*, 2010a), was significantly elevated in DLB compared to control. This was consistent with the RNA sequencing data, which suggested CHI3L1/YKL-40 was the second greatest fold increase in DLB.

These findings indicate specific inflammatory changes in the pulvinar in DLB. CHI3L1/YKL-40 was negatively correlated with a number of synaptic markers. This may reflect inflammation as a result of synaptic dysfunction or vice-versa, though it is difficult to establish the direction of this relationship. CHI3L1/YKL-40 is a putative marker of inflammation (Coffman, 2008; Lee *et al.*, 2011) that is up-regulated in numerous disease states characterised by inflammation, including rheumatoid arthritis (Johansen *et al.*, 1999), active phases of inflammatory bowel diseases (Vind *et al.*, 2003), and the acute inflammatory phase of traumatic brain injury (Bonneh-Barkay *et al.*, 2010b). Therefore, the elevated expression of CHI3L1/YKL-40, and its association with synaptic protein loss, may indicate inflammatory conditions with associated synaptic loss in the pulvinar in DLB.

CHI3L1/YKL-40 has been previously shown to be decreased in the cerebrospinal fluid (CSF) of PD, MSA and DLB patients, in comparison to increased levels in tauopathy cases, which was interpreted as the result of reduced astroglial activation in synucleinopathies compared to tauopathies (Olsson *et al.*, 2013; Janelidze *et al.*, 2016). Although CSF protein levels are not necessarily representative of cerebral protein expression, these findings may indicate that CHI3L1/YKL-40 elevations are

not a global phenomenon in DLB but may be regionally specific. Therefore, the present findings may suggest inflammatory conditions in the pulvinar that are not representative of the rest of the brain in DLB. Several hypotheses have suggested the manifestation of visual hallucinations could reflect the relative selectivity of brain regions pathologically affected by changes in DLB (Collerton *et al.*, 2005b; Diederich *et al.*, 2014; Carter and Ffytche, 2015). Therefore, the identification of the pulvinar as a region with elevated levels of an inflammatory astroglial marker may indicate a selective region of impairment that may contribute to the clinical phenotype. However, as the present study only assessed the pulvinar, it is impossible to establish whether this change is selective for this region. Future studies may investigate whether other regions of the thalamus, and the brain generally, have similar elevations in CHI3L1/YKL-40 in DLB, as the relationship between CHI3L1/YKL-40 and neuroinflammation makes it a potential therapeutic target. However, further work is necessary to evaluate the role of CHI3L1/YKL-40 and inflammation in DLB.

Despite the increased transcription of complement component C3 on RNA sequencing, C3 was not changed at the protein level. The complement pathway is part of the immune system that amplifies the immune response and is implicated in several cytoprotective roles, including clearance of foreign pathogens, cell integrity and modulation of the intensity of immune responses (Holers, 2014). The cleavage of complement component C3 is a central event in the activation of the complement cascade and, therefore, in a pro-inflammatory response (Kemper and Atkinson, 2007). Complement C3 is expressed in a range of cells within the mouse brain, including a subset of pyramidal neurons in hippocampal regions (Yu *et al.*, 2002), and may be expressed in astrocytes (Zhou *et al.*, 2008). In human tissues, some fragments of complement C3 have previously been described as a component of amyloid-β plaques (Eikelenboom and Stam, 1984), suggesting they are activated, perhaps as a response to amyloid-β deposition (Eikelenboom *et al.*, 1988). Complement fragments co-localise with Lewy bodies in neurons in the substantia nigra in PD (Yamada *et al.*, 1992) but are only co-expressed with amyloid-β plaques in the neocortex in DLB, and not neocortical Lewy bodies (Rozemuller *et al.*, 2000). Increased transcription of complement C3 is, therefore, likely a pro-inflammatory response occurring as a result of pathological protein deposition in the pulvinar, as reported in Chapter 4.

Heat shock proteins bind to damaged or partially unfolded polypeptides under conditions of widespread damage to cellular proteins, such as with heat (De Maio, 1999). Under normal physiological conditions, most heat shock proteins serve to ensure the proper folding of proteins (Sherman and Goldberg, 2001). SERPNH1/HSP47 is relatively understudied but appears to be expressed in astrocytes following excitotoxic lesions and may enhance glial cell protection under adverse conditions (Acarin *et al.*, 2002). HSPA1A and HSPA1B belong to the heat shock protein 70 kDa (HSP70) family of heat shock proteins. The HSP70 family are chaperones, which promote correct folding of polypeptides upon their emergence from ribosomes under normal physiological conditions (Frydman and Hartl, 1996; Hartl and Hayer-Hartl, 2002). Under pathological conditions, HSP70 chaperones promote protein degradation through the ubiquitin-proteasome pathway (Pratt *et al.*, 2015) and may, therefore, contribute to the degradation of protein aggregates that are commonly found in neurodegenerative disorders (Sherman and Goldberg, 2001). In Lewy body disease, HSP70 chaperones co-localise with α-synuclein aggregates and may protect neurons from α-synuclein-mediated toxicity by inhibiting aggregation (Chaari *et al.*, 2013). Disaggregase components of the HSP70 protein class have been demonstrated to disassemble α-synuclein fibrils into monomers (Gao *et al.*, 2015). Therefore, the increased transcription of HSPA1A and HSPA1B may reflect a stereotyped, protective mechanism to toxic protein assemblies, such as those found in Lewy body disease. In the present study, only HSPA1B was increased at the protein level, indicating a discrepancy between HSPA1A transcription and expression, or a lack of sensitive methods to detect a change at the protein level.

### 5.4.4 General discussion

Reductions in post-synaptic proteins, without corresponding loss of pre-synaptic proteins necessary for exocytosis, may suggest neuronal loss in the pulvinar is responsible for the reduction in post-synaptic proteins (Chapter 4). The preservation of pre-synaptic proteins vital for exocytosis may indicate greater numbers of afferent connections synapse upon individual pulvinar neurons. This is possibly an adaptive mechanism to compensate for neuronal loss, though it likely reduces the sensitivity of individual pulvinar neurons. Reductions in pre-synaptic markers implicated in maintaining efficient synaptic exocytosis and vesicle recycling may suggest input to

the pulvinar is altered. Therefore, it is also possible post-synaptic protein reductions are the result of altered input due to altered pre-synaptic functioning. Equally, input to the pulvinar may be altered as a result of changes to the constituent neuronal population.

One hypothesis suggests altered retinal input, possibly secondary to pathology (Beach *et al.*, 2014), induces compensatory decreases in inhibition in the primary visual cortex (Manford and Andermann, 1998; Khundakar *et al.*, 2016; Taylor *et al.*, 2016). A study employing transcranial magnetic stimulation has demonstrated increased visual cortical excitability related to the occurrence of visual hallucinations in DLB (Taylor *et al.*, 2011). On the molecular level, decreased GABAergic transcription has been identified, which may be a stereotyped response to altered visual input (Khundakar *et al.*, 2016). The inferior and lateral pulvinar are directly connected to the primary visual cortex (Kaas and Lyon, 2007) and increased pulvinar excitability has been demonstrated to lead to increased primary visual cortical activity, without altering the physiology of the LGN (Purushothaman *et al.*, 2012). Increased excitability of the pulvinar, as a result of reduced GABAergic activity, may contribute to increased visual cortical activity in DLB. However, as the present study did not assess neurotransmitter symptoms other than GABA, it is not possible to say whether these deficits are specific. It is possible the reported GABAergic losses reflect more widespread neurotransmitter reductions in the pulvinar, possibly as a result of neuronal loss or synaptic changes, as outlined previously (Chapter 4).

The present findings on targets that positively regulate immune system functioning indicate increases in some astrocytic markers which, particularly in the case of CHI3L1/YKL-40, may suggest neuroinflammatory conditions in the pulvinar in DLB. The negative relationship between CHI3L1/YKL-40 and several synaptic proteins indicates inflammatory responses may be a response to, or potentially a potentiating factor in, the observed synaptic changes. However, it is difficult to establish the direction of these relationships. Increased levels of CHI3L1/YKL-40 have not previously been demonstrated in α-synucleinopathies, suggesting that the increase in CHI3L1/YKL-40 in the pulvinar may reflect a specific region of vulnerability in DLB. However, as the present study only investigated the pulvinar, future studies would need to address the specificity of these changes by assessing other brain regions. The up-regulation of heat shock proteins may reflect an adaptive response to protein

aggregates, which were identified and described in the histological analysis in Chapter 4.

Taken together, these results indicate synaptic and inflammatory changes in the pulvinar in DLB. Neuronal loss in the pulvinar may be responsible for the uniform reduction in post-synaptic markers, whilst pre-synaptic proteins necessary for vesicle exocytosis were preserved. The putative inflammatory marker CHI3L1/YKL-40 is found in quantities proportional to the severity of damage to the brain in studies of traumatic brain injury (Wiley *et al.*, 2015). Therefore, the most parsimonious explanation of these findings is that the expression of CHI3L1/YKL-40 is the result of neuronal or synaptic damage. This proposition is supported by the negative correlations between an array of synaptic markers and the astrocytic marker CHI3L1/YKL-40. Whether CHI3L1/YKL-40 expression is an adaptive response mechanism, a factor that exacerbates neuronal damage, or both, is an empirical question that cannot be answered by the present data.

Irrespective of the causative mechanism and the temporal sequence of the synaptic changes and inflammatory marker expression in the pulvinar, these results may indicate that the pulvinar is functionally altered in DLB. The relationship between the hypothesised pulvinar dysfunction in DLB and the manifestation of visual hallucinations may be through impaired visual attention. Impaired visual attention is thought to contribute a vulnerability to visual hallucination in DLB (Collerton *et al.*, 2005b; Diederich *et al.*, 2005; Shine *et al.*, 2011; Factor *et al.*, 2014) and focused attention upon the subject of visual hallucinations has been demonstrated to promote the disappearance of the hallucinated object (Diederich *et al.*, 2003). Therefore, the present findings of pulvinar synaptic loss and inflammation in the pulvinar in DLB, may relate to visual hallucinations through attentional dysfunction. Equally, altered excitability in the pulvinar, as a result of GABAergic dysfunction, may also alter the excitability of the primary visual cortex. Increased visual cortical excitability has previously been linked to visual hallucinations in DLB (Taylor *et al.*, 2011; Khundakar *et al.*, 2016; Taylor *et al.*, 2016). Both propositions are not mutually exclusive, and it is possible that the reported changes to the pulvinar mediate hallucinogenesis through both dysfunctional attentional mechanisms and impaired modulation of visual cortical excitability.

A weakness of the present study is that the small sample size may limit the generalisability of these findings. Pulvinar tissue with a short *post-mortem* interval was particularly difficult to obtain, though a recent study has indicated that employing this criterion in case selection may have unnecessarily limited the available tissue (Robinson *et al.*, 2016). The present study compared DLB to control cases and, unlike previous chapters, did not include AD as a disease control group. Therefore, it is difficult to ascertain whether the presently reported changes are simply related to neurodegeneration generally, or specifically related to clinical features of DLB, such as visual hallucinations. RNAseq is an expensive technique and the addition of further cases to represent an AD group would have been prohibitive for the purposes of the present analysis. An additional concern is that transcriptional changes identified from RNA sequencing did not always correspond with the expression of the protein on western blotting. In some instances, explanations have been offered for specific proteins having an evidential basis explaining transcription and expression may be discrepant. Densitometric analysis of western blot membranes has been applied in a quantitative manner in the present study. However, western blotting does not allow the quantification of absolute levels of a particular protein within a matrix, instead relying on relative comparison of the size and intensity of bands. Absolute measures of protein concentrations within samples would have been possible using more quantitative analytical techniques, such as ELISA. However, initial pilot studies in developing ELISA for the present project indicated that the volume of tissue required for each individual protein was typically much higher than that required for western blotting. Considering the small volume of tissue available per case, this would limit the number of protein targets that could be assessed. Therefore, western blot analysis was used to ensure a larger array of proteins could be investigated.

Glial markers such as GFAP, ALDH1L1 and CHI3L1 were normalised to GAPDH, a ubiquitously expressed cellular housekeeping protein. However, to evaluate whether any observed changes reflected increases in total numbers of astrocytes or increased expression of the assessed antigen within the glial population, a glial cell-specific transcript may have been used. ALDH1L1 is thought to be a superior pan-astrocytic marker than GFAP, and may have been a useful additional measure (Cahoy *et al.*, 2008). Similarly, neuron-specific markers such as GAD67 were also

normalised to GAPDH and evaluation of expression relative to a neuron-specific marker, such as NeuN (Cahoy *et al.*, 2008), may have enabled assessment of whether the assessed antigens were altered in expression whilst controlling for the confounding effects of neuronal loss as reported in chapter 4. A future study may wish to consider using cell-specific transcripts to evaluate changes in epitope expression independently of changes to cell number.

In conclusion, the present study has demonstrated reductions in synaptic proteins and increased inflammatory markers in the pulvinar of DLB patients. Synaptic changes likely alter synaptic functioning and inflammatory markers may indicate tissue damage or insult. The role of inflammation in either protecting neurons and synapses, or accentuating the damage to them, requires further study. However, the likely effect of the synaptic and inflammatory changes is that normal functioning of the pulvinar is altered. As a major function of the pulvinar is in the coordination of visual attention, this may become deficient as a result of pulvinar degeneration. Visual attentional dysfunction is a widely reported phenomenon in DLB and may contribute a vulnerability to visual hallucination. Therefore, the observed molecular changes in the pulvinar are consistent with the proposition that it is functionally altered in DLB, contributing to a vulnerability to hallucination, potentially through deficient visual attentional mechanisms.

# Chapter 6: Histological studies in the superior colliculus

## 6.1 Introduction

The superior colliculus is thought to play a vital role in orienting movements of the eyes and head to support shifts of visuo-spatial attention (Gandhi and Katnani, 2011). However, it is becoming increasingly evident that the superior colliculus has attentional functions beyond the execution of motor commands to support attention, such as target selection and the filtering of distracting stimuli (Krauzlis *et al.*, 2013).

The medial temporal visual area (area V5/MT) receives input from the inferior pulvinar in a pathway thought to originate in the superficial laminae of superior colliculus (Stepniewska *et al.*, 1999; Stepniewska *et al.*, 2000). The tectal-pulvinar-V5/MT pathway has a role in the relay of information to the cortex regarding recently executed eye movements (Bridge *et al.*, 2015). Patients with Lewy body disease have eye movement difficulties (Trick *et al.*, 1994; Terao *et al.*, 2011), which may be the result of impairment of the superior colliculus.

Impairments in attentional shifting, resulting from superior colliculus dysfunction, have been suggested to contribute to the manifestation of visual hallucinations in Lewy body disease (Diederich *et al.*, 2014). Difficulty in engaging the dorsal attentional network to attend to ambiguous visual stimuli has been suggested to contribute to the manifestation of visual hallucinations in DLB, with the superior colliculus directly implicated (Shine *et al.*, 2014). Therefore, the present study aimed to investigate the three grey matter laminae of the superior colliculus, with the aim of identifying neuropathological changes that may contribute to hallucinations in DLB.

### 6.1.1 Aims

Formalin-fixed *post-mortem* superior colliculus tissue obtained from DLB patients was compared with aged cognitively normal control and AD cases. This study aimed to:

1) Evaluate the density of neurons and glia in the individual laminae of the superior colliculus and compare these across experimental groups.
2) Compare the burden of neuropathological lesions in the different laminae of the superior colliculus across experimental groups.

3) Relate morphometric and neuropathological findings to neuropsychological data from life, where available.

## 6.2 Methods

### 6.2.1 Tissue acquisition and sampling

The superior colliculus is located on the posterior aspect of the midbrain, bordering the lateral aspects of the periaqueductal grey (Fig. 2.3) (Krauzlis *et al.*, 2013). As thalamic and midbrain blocks are cut on two different planes, and midbrain tissue is valuable in DLB cases, it was not possible to sample the entirety of the structure for stereological determination of total neuron number. Therefore, a modified protocol was used where the density of neurons was determined, as a proxy of neuronal number, on three adjacent sections.

Three groups of cases were included in this study: DLB, AD and aged control cases with low or absent levels of neurodegenerative pathology. Where possible, cases with detailed neuropsychological information from life were included to relate with pathological findings. To better evaluate relationships between neuropathological changes and visual hallucinations, two cases without a clinical history of visual hallucinations were also included. Demographic information is listed in Table 6.1.

The superior colliculus is typically divided into three grey matter laminae, the SGS, SGI and SGP, which are interspersed with predominantly fibre-rich laminae. Analyses of neuronal and glial density and neuropathology were conducted on the individual grey matter layers to enable determination of any likely physiological changes resulting from the specific degeneration of one or more particular layers, as demonstrated in Fig. 6.1.

Fixed tissue blocks containing the superior colliculus were sectioned into a series of three adjacent 30 µm-thick sections from a random starting point and stained with cresyl violet for stereological analysis. 6 µm-thick sections were obtained from three adjacent sections for densitometric analysis of protein deposits. Stereological analyses were conducted on 30 µm-thick sections stained with cresyl fast. 6 µm-thick sections were stained with antibodies against a range of protein targets (Table 6.2) using Menarini Menapath Polymer detection kits (Menarini, Berkshire, UK), as per manufacturer's instructions.

*Table 6.1: Demographic information for cases used in the superior colliculus study.*

*'PM interval' represents post-mortem interval, the interval between death and post-mortem examination, 'Braak NFT' represents the neurofibrillary pathology stage outlined in (Braak et al., 2006), 'McKeith LB' represents Lewy body pathology stage outlined in (McKeith, 2006), 'clinico-path diagnosis' represents the diagnosis reached for each individual patients by senior clinicians and a neuropathologist, with consideration given to clinical and pathological features, 'NPI(hall)' represents the hallucinations subscale of the NPI, outlined in (Cummings et al., 1994), 'UPDRS III' represents the motor subscale of the UPDRS, outlined in (Fahn and Elotion, 1987).*

| Case ID | Gender | Age at death (years) | PM interval (hours) | Braak NFT | McKeith LB | Clinico-path diagnosis | NPI (hall) | NPI interval to death (months) | UPDRS III | UPDRS interval to death (months) |
|---|---|---|---|---|---|---|---|---|---|---|
| C5 | M | 73 | 25 | 0 | None | Control | - | - | - | - |
| C22 | F | 80 | 25 | 2 | None | Control | - | - | - | - |
| C23 | F | 90 | 63 | 2 | None | Control | - | - | 7 | 21 |
| C24 | M | 91 | 72 | 1 | None | Control | - | - | 12 | 15 |
| C25 | M | 83 | 112 | 2 | None | Control | - | - | - | - |
| C26 | M | 71 | 25 | 1 | None | Control | - | - | - | - |
| C27 | M | 79 | 39 | 2 | None | Control | - | - | - | - |
| C28 | F | 93 | 12 | 3 | None | Control | - | - | - | - |
| C29 | M | 94 | 25 | 2 | None | Control | - | - | 16 | 8 |
| C30 | F | 81 | 75 | 2 | None | Control | - | - | - | - |
| C31 | M | 84 | 45 | 2 | None | Control | - | - | - | - |
| C32 | M | 78 | 64 | 2 | Brainstem | Control | - | - | - | - |
| C33 | F | 63 | 16 | 2 | None | Control | - | - | - | - |

| | | | | | | | | | | |
|---|---|---|---|---|---|---|---|---|---|---|
| Mean±SD | | 81.5±9 | 46.0±29 | 1.8±1 | | | N/A | N/A | 11.7±5 | 14.7±6 |
| D13 | M | 75 | 18 | 2 | Limbic | DLB | - | - | - | - |
| D24 | M | 77 | 29 | 2 | Neocortical | DLB | 1 | 2 | 58 | 14 |
| D6 | F | 78 | 96 | 3 | Neocortical | DLB | 6 | 1 | 14 | 1 |
| D25 | F | 91 | 84 | 5 | Limbic | DLB | 9 | 5 | 24 | 29 |
| D21 | M | 76 | 13 | 2 | Neocortical | DLB | 0 | 2 | 36 | 37 |
| D26 | M | 74 | 42 | 4 | Neocortical | DLB | 4 | 9 | 31 | 36 |
| D27 | F | 73 | 99 | 3 | Neocortical | DLB | 0 | 27 | 30 | - |
| D28 | M | 71 | 22 | 3 | Neocortical | DLB | 2 | 10 | 4 | 25 |
| D29 | F | 87 | 90 | 2 | Neocortical | DLB | 3 | - | 26 | 1 |
| D30 | M | 74 | 60 | 2 | Neocortical | DLB | - | - | 53 | 6 |
| Mean±SD | | 77.6±6 | 55.3±35 | 2.8±1 | | | 3.1±3 | 7.8±9 | 30.7±17 | 18.5±15 |
| A2 | M | 91 | 22 | 5 | None | AD | 0 | 16 | 35 | 148 |
| A9 | M | 68 | 24 | 6 | None | AD | - | - | - | - |
| A13 | M | 80 | 39 | 6 | None | AD | - | - | 3 | 31 |
| A14 | M | 87 | 21 | 6 | None | AD | 0 | 11 | 5 | 11 |
| A15 | F | 80 | 10 | 6 | Amygdala | AD | 0 | 8 | - | - |
| A16 | M | 82 | 12 | 6 | Amygdala | AD | 0 | - | - | - |
| A10 | F | 86 | 123 | 6 | Brainstem | AD | - | - | - | - |
| A17 | F | 58 | 70 | 6 | None | AD | - | - | - | - |
| A18 | M | 84 | 40 | 6 | None | AD | 2 | 10 | 17 | 14 |
| A19 | F | 89 | 11 | 6 | None | AD | - | - | - | - |
| Mean±SD | | 80.5±10 | 37.2±35 | 5.9±0 | | | 0.4±1 | 11.1±3 | 15.0±15 | 53.2±64 |

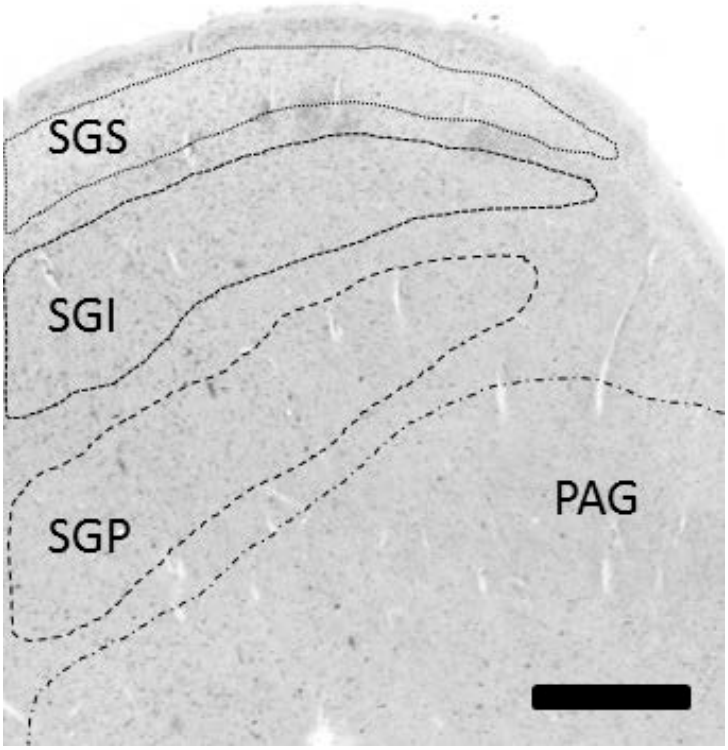


*Figure 6.1: Anatomy of the superior colliculus.*

*Photomicrograph of the superior colliculus stained with cresyl violet. The stratum griseum superficiale (SGS), stratum griseum intermedium (SGI) and stratum griseum profundum (SGP) of the superior colliculus have a distinctive laminar organisation. The periaqueductal grey (PAG) is proximal, located on the anteromedial aspect of the midbrain relative to the superior colliculus. Scale bar = 1.5 mm.*

*Table 6.2: Antibodies used in the superior colliculus study.*

| Antibody | Manufacturer | Dilution | Antigen retrieval |
|---|---|---|---|
| KM51 α-synuclein | Leica Biosystems, UK | 1:250 | EDTA pH 8.0 |
| AT8 phospho-tau | Autogen, MA, USA | 1:4000 | Citrate pH 6.0 |
| 4G8 amyloid-β | Covance, NJ, USA | 1:15000 | Formic acid |

### 6.2.2 Stereological determination of neuronal density

The SGS, SGI and SGP were identified based on their laminar location using a brain atlas (Paxinos and Huang, 2013), and each lamina was analysed individually to assess neuronal and glial cell density. Regions of interest were demarcated at 2.5x objective and cell counts were conducted at 63x oil-immersion objective using the optical disector probe. Neuronal cell counts were conducted in disector frames of 3500 $\mu m^2$ and glial cell counts were conducted in disector frames of 1900 $\mu m^2$. Section thickness did not vary across disease groups in any lamina. Mean CE values reached acceptable levels of accuracy (<0.15) in all laminae (Herculano-Houzel *et al.*, 2015).

### 6.2.3 Neuropathology

The SGS, SGI and SGP were analysed using quantitative neuropathological techniques. To quantify neuropathological lesions, images of representative parts of each lamina were taken on a Zeiss AxioVision Z.1 microscope using a Zeiss 3-chip CCD true colour camera. Stereologer software was used to delineate a region of interest with a 2.5x objective, prior to placement of disector frames in a uniform, random arrangement. This method prevented the introduction of bias by giving every area of the region of interest an equal probability of being sampled for analysis. Disector frames were captured at 10x objective for amyloid-β and tau, and at 20x objective for α-synuclein pathology, different magnifications were used based on the relative particle size and distribution of the structures measured. Images were taken within the disector frames and analysed using ImagePro Plus v.4.1 image analysis system. Using previously published techniques (Perry *et al.*, 2012; Erskine *et al.*, 2016), the mean percentage area of immunopositivity was determined by standardising RGB thresholds per antibody and applying to all sections per case. Each case thus had a mean value generated per antibody across each strata analysed.

### 6.2.4 Clinico-pathological relationships

To determine the relationships between neuropathological data and clinical features, correlational analyses were conducted with neuropsychological data obtained during life. DLB patients had been recruited for clinical research, during which they received serial assessments of cognition, motor function and visual hallucination severity and frequency at regular intervals until death (Burn *et al.*, 2003; Mosimann *et al.*, 2006). Fewer control and AD cases had been assessed for motor impairment and visual hallucinations, as these are not characteristic features of either AD or normal ageing.

The SGI and SGP have a well-described role in coordinating oculomotor functions (Krauzlis *et al.*, 2013). To investigate whether collicular degeneration is related to general motor decline, neuronal density and pathological burden in the SGI and SGP were correlated with Unified Parkinson's Disease Rating Scale Part III (UPDRS III) scores (Fahn and Elotion, 1987) in DLB cases. Only DLB cases were used for this analysis as motor features are not typically found in AD or normal ageing so no such relationship could be assessed in these groups. UPDRS Part III was available for 9/10 DLB cases. The mean interval between final UPDRS Part III and death was 20.34±6.45 months.

Due to the hypothesised role of the superior colliculus in the manifestation of visual hallucinations in Lewy body disease (Diederich *et al.*, 2014), neuronal density and pathological burden in all laminae of the superior colliculus were correlated with final NPI (hall) score (Cummings *et al.*, 1994) in DLB cases. Only DLB cases were used for this analysis as, again, visual hallucinations are not typically found in AD or normal ageing and so no relationship can be assessed. Final NPI (hall) scores were available for 8/10 DLB cases. The mean interval from final NPI assessment to death was 7.81±3.45 months.

### 6.2.5 Statistical analysis

Inspection of Q-Q plots and Shapiro-Wilk tests suggested that stereological and neuropathological data were either not normally distributed or did not have homogeneity of variance. Therefore, Kruskal-Wallis tests with post-hoc Mann-Whitney U tests were employed for all data.

## 6.3 Results

### 6.3.1 Demographics

There was no significant difference in age at death (F=0.591, p=0.560), *post-mortem* interval (F=0.761, p=0.476) or gender ($\chi^2$=0.008, p=0.996) between experimental groups (Table 6.1).

### 6.3.2 Stereology

Graphical representations of stereological data are contained in Fig. 6.2.

In the SGS, there was a significant main effect of diagnosis on neuronal density ($\chi^2$=6.58, p=0.037). Post-hoc tests showed no significant difference between control and DLB. However, AD cases had a significant reduction in neuronal density compared to control (U=27.000, p=0.018, d=1.014). There was no significant difference between DLB and AD. However, there was a trend towards a significant reduction in AD compared to DLB (p=0.070). There was no significant main effect of diagnosis on glial density. However, there was a significant main effect of diagnosis on the ratio of glia to neurons in the SGS ($\chi^2$=10.461, p=0.005). Post-hoc tests showed no significant difference between DLB and control or AD. AD cases had a significant increase in glia relative to neurons compared to control (U=13.000, p=0.001, d=1.32).

In the SGI, there was a significant main effect of diagnosis on neuronal density ($\chi^2$=13.05, p=0.001). Post-hoc tests showed DLB cases had a significant reduction in neuronal density compared to control (U=18.500, p=0.003, d=1.08). AD cases had a significant reduction in neuronal density compared to control (U=13.5, p=0.001, d=1.24). There was no significant difference between AD and DLB. There was no significant main effect of diagnosis on glial density. However, there was a significant main effect of diagnosis on the ratio of glia to neurons in the SGI ($\chi^2$=11.242, p=0.004). Post-hoc tests showed a significant increase in glia relative to neurons in DLB compared to control (U=22.000, p=0.008, d=1.09). AD cases also had a significant increase in glia relative to neurons compared to control (U=17.000, p=0.003, d=1.19). There was no significant difference in the ratio of glia to neurons between DLB and AD in the SGI.

In the SGP, there was a significant main effect of diagnosis on neuronal density ($\chi^2$=6.60, p=0.037). Post-hoc tests showed no significant difference between control and DLB. However, AD cases had a significant reduction in neuronal density compared to control (U=27.000, p=0.018, d=1.12). There was no significant difference between DLB and AD. However, there was a trend toward a significant reduction in AD compared to DLB (U=27.000, p=0.080, d=0.50). There was no significant main effect of diagnosis on glial density. However, there was a significant main effect of diagnosis on the ratio of glia to neurons in the SGP ($\chi^2$=6.381, p=0.041). Post-hoc tests showed no significant difference between DLB and control or AD. AD cases had a significant increase in glia relative to neurons compared to control (U=25.000, p=0.012, d=1.14).

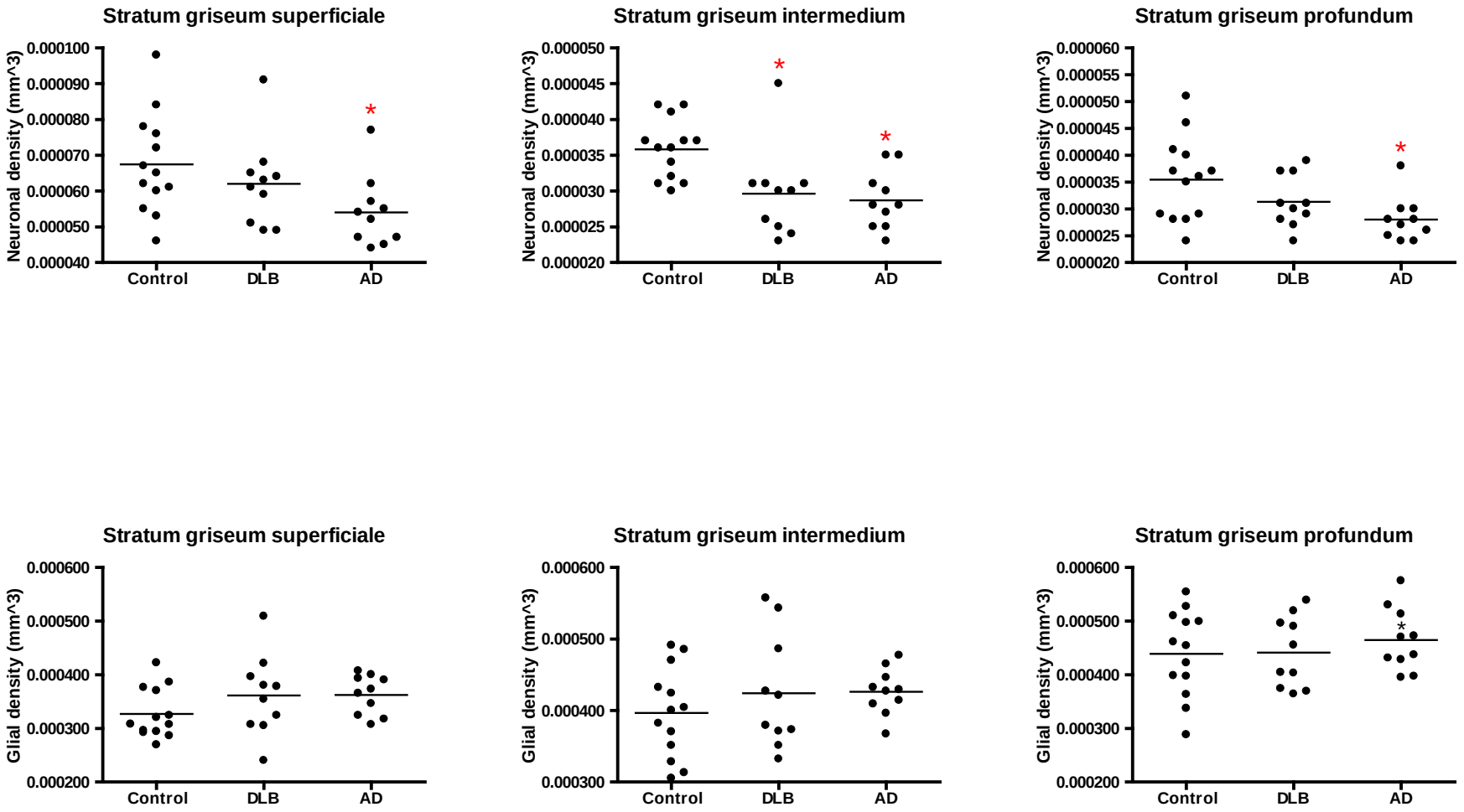


*Figure 6.2: Dot plots illustrating stereological results in the superior colliculus.*

*Stereological measures of neuronal and glial density across the three grey matter laminae of the superior colliculus. *p<0.05 compared to control.*

### 6.3.3 Neuropathology

α-synuclein pathology was present in all DLB cases. Typically, Lewy bodies and neurites were only found in the SGI and SGP, with the SGS largely spared (Fig. 6.3A-C). Significant main effects of diagnosis on α-synuclein pathology were found in the SGS ($\chi^2$=16.871, p<0.001), SGI ($\chi^2$=26.218, p<0.001) and SGP ($\chi^2$=18.426, p<0.001; Fig. 6.4). In the SGS, post-hoc analyses showed DLB cases had a greater degree of α-synuclein pathology compared to control (U=19.000, p=0.003, d=1.35) and AD (U=12.000, p=0.003, d=1.41). In the SGI, DLB cases had a greater degree of α-synuclein pathology compared to control (U=1.000, p<0.001, d=1.85) and AD (U=0.000, p<0.001, d=1.92). In the SGP, DLB cases had a greater degree of α-synuclein pathology in the SGP compared to control (U=15.500, p=0.001, d=1.27) and AD (U=27.000, p<0.001, d=1.45). α-synuclein pathology did not significantly correlate with neuronal density in the SGS (p=0.444), SGI (p=0.533) or SGP (p=0.649).

One control case, C32, had α-synuclein pathology consisting of Lewy bodies and neurites. This case also had global Lewy body pathology corresponding to the brainstem stage of the McKeith criteria (McKeith *et al.*, 2005) and Lewy body Braak stage 3 (midbrain stage) (Braak *et al.*, 2004). In contrast, no AD cases had any detectable α-synuclein pathology in the superior colliculus, despite one case (A10) having brainstem stage Lewy body pathology in the McKeith criteria (McKeith, 2006). However, under the Braak classification of Lewy body pathology, this corresponded to stage 1 (medulla oblongata) (Braak *et al.*, 2004). Therefore, α-synuclein pathology may develop in the superior colliculus at the same stage as the development of Lewy body pathology in other regions of the midbrain.

Tau pathology was observed in most cases (8/13 control, 9/10 DLB, 10/10 AD), typically in the form of neuropil threads in non-AD cases, though the pathological burden was highly variable across cases. Amyloid-β pathology was present as focal and diffuse deposits in many cases (2/13 control, 7/10 DLB, 10/10 AD), and appeared to affect all laminae of the superior colliculus (Fig. 6.3G-I). As expected on the basis of their neuropathological diagnosis, and demonstrated in Fig. 6.4, AD cases had greater levels of tau and amyloid-β than control in all laminae of the superior colliculus. DLB cases exceeded control only in tau burden in the SGI and amyloid-β burden in the SGP. Tau pathology was significantly negatively correlated

with neuronal density in the SGI (rho=-0.404, p=0.022; Fig. 6.6) and SGP (rho=-0.451, p=0.009; Fig. 6.6).

In DLB cases, there was a significant difference in the degree of α-synuclein pathology across the three laminae ($\chi^2$=12.600, p=0.002; Fig. 6.3A-C, Fig. 6.5). Post-hoc Wilcoxon signed-rank tests showed the SGI had a greater burden of α-synuclein pathology than the SGS (Z=2.803, p=0.005, d=0.85) and the SGP had a greater burden of α-synuclein pathology than the SGS (Z=2.497, p=0.013, d=1.09). There was no significant difference in the burden of α-synuclein pathology between the SGI and SGP. There were no significant correlations between α-synuclein pathology and neuronal density in any experimental group.

There was a significant difference in the degree of tau pathology across the three laminae ($\chi^2$=26.375, p<0.001; Fig. 6.3D-F, Fig. 6.5). Post-hoc tests showed the SGI had a greater burden of tau pathology than the SGS (Z=4.330, p<0.001, d=0.32) and the SGP had a greater burden of tau pathology than the SGS (Z=4.031, p<0.001, d=0.46). There was no significant difference in the burden of tau pathology between the SGI and SGP. There were no significant correlations between tau pathology and neuronal density in any experimental group. There was no significant difference in amyloid-β expression across the three laminae of the superior colliculus (Fig. 6.5). There were no significant correlations between amyloid-β pathology and neuronal density in any experimental group.

In summary, Lewy body pathology was highest across all laminae in DLB cases, and AD-type pathology was highest across all laminae in AD cases (Fig. 6.4). Lewy body and tau pathology showed distinct patterns of expression, with the SGI and SGP affected more severely than the SGS (Fig. 6.3, 6.5). Amyloid-β did not show the same topography, with all laminae affected to a similar degree (Fig. 6.3, 6.5).

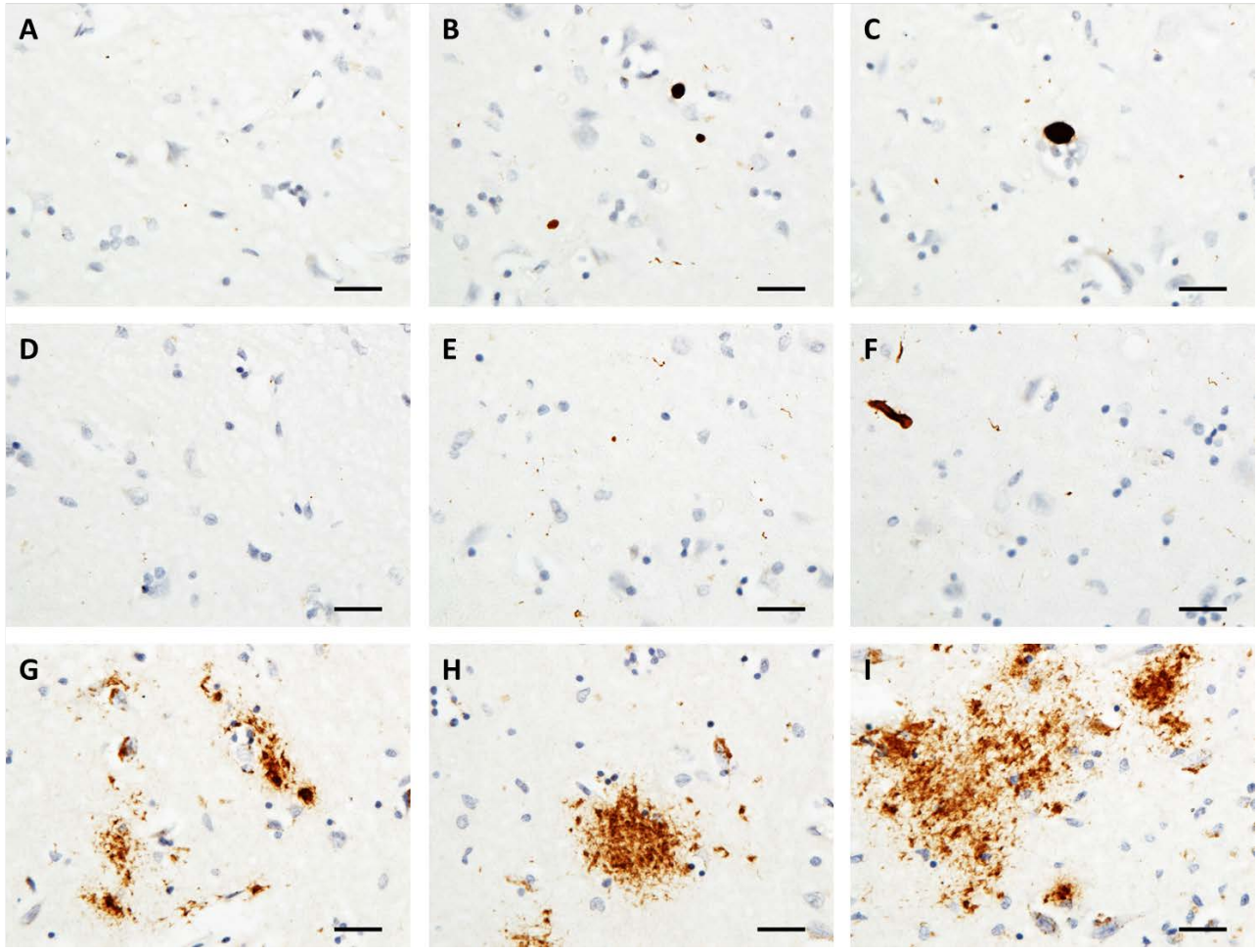


*Figure 6.3: Neuropathology in the superior colliculus.*

*Neuropathology in the different laminae of the superior colliculus in DLB case D6. α-synuclein pathology is less severe in the stratum griseum superficiale (SGS; A) than the stratum griseum intermedium (SGI; B) and stratum griseum profundum (SGP; C). Tau pathology is minimal throughout but less severe in the SGS (D) than in the SGI (E) and SGP (F). Amyloid-β is observed in the SGS (G), SGI (H) and SGP (I) and shows less regional specificity than α-synuclein and tau. Scale bar = 50 μm.*

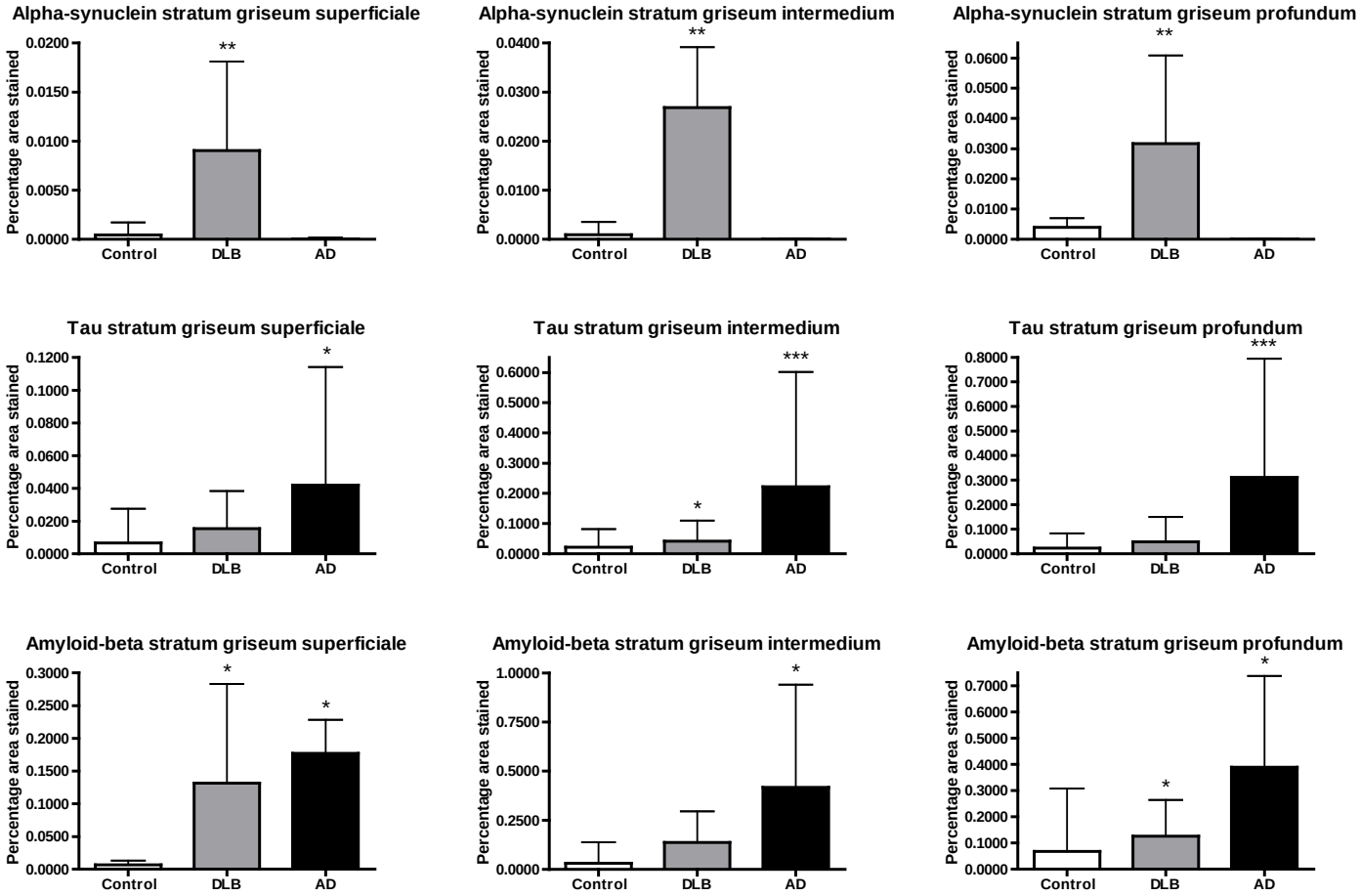


*Figure 6.4: Densitometric analysis of the superior colliculus.*

*Bars represent means and error bars represent standard deviation. *p<0.05 compared to control, **p<0.05 compared to control and AD, ***p<0.05 compared to control and DLB.*

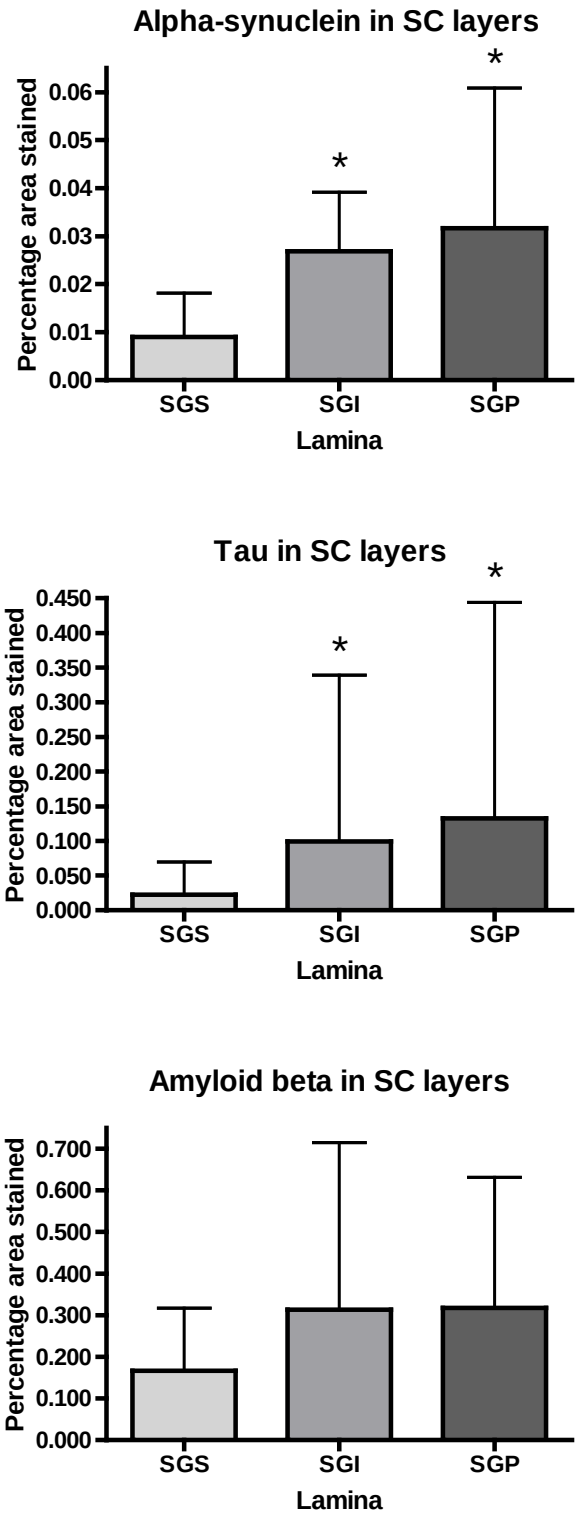


*Figure 6.5: Laminar distribution of pathology in the superior colliculus.*

*Bar charts illustrate the percentage area stained in each lamina of the superior colliculus, with bars representing means and error bars representing standard deviations. *p<0.05 compared to stratum griseum superficiale (SGS).*

### 6.3.4 Clinico-pathological correlations

There were no significant correlations between age at death, *post-mortem* interval and neuronal density in any lamina of the superior colliculus.

In DLB cases, UPDRS III was negatively correlated with tau pathological burden in the SGS (rho=-0.720, p=0.029), SGI (rho=-0.683, p=0.042) and SGP (rho=-0.700, p=0.036). However, Braak neurofibrillary pathology stage did not correlate with UPDRS III. One outlier was found to be responsible for the initial correlations and removal of this case from the analysis removed all correlations between UPDRS III and tau. UPDRS III was not significantly correlated with α-synuclein pathology in the SGS (p=0.764), SGI (p=0.606) or SGP (p=0.932). No other stereological or pathological variables correlated with UPDRS III score in DLB cases.

In DLB cases, NPI (hall) score was positively correlated with neuronal density in the SGS (rho=0.874, p=0.005; Fig. 6.6). No other stereological or pathological variables correlated with NPI (hall) score in DLB cases.

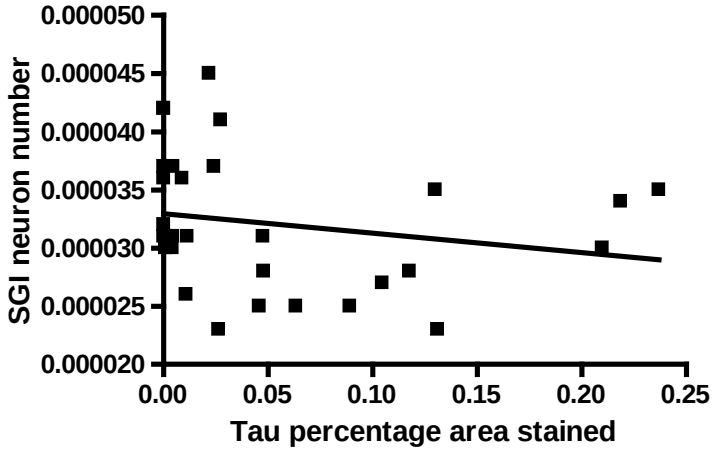


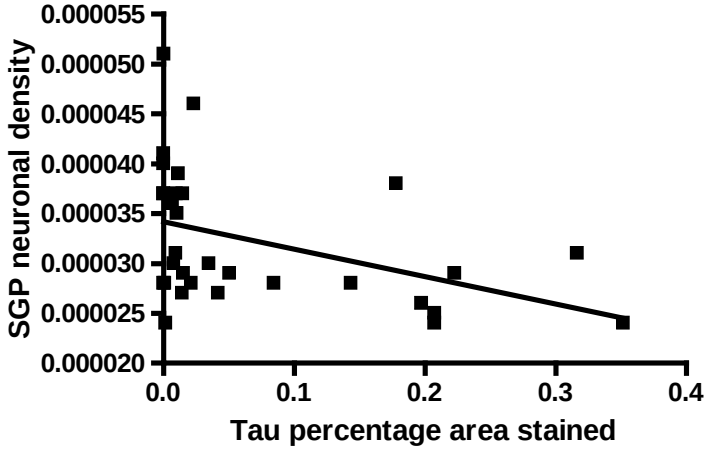


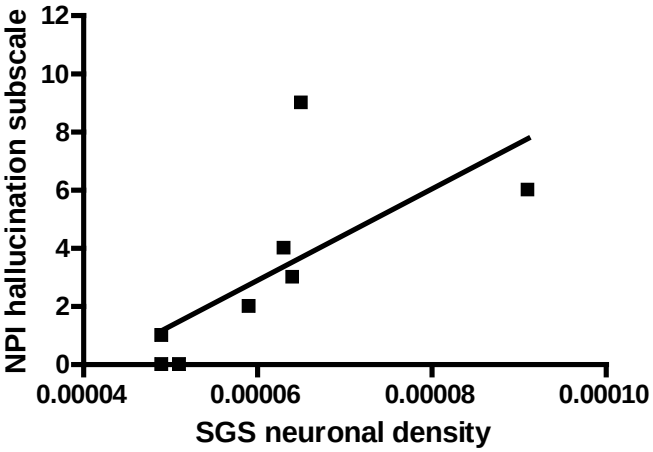


*Figure 6.6: Relationships between pathology and neuronal number and clinical features.*

*Scatterplots demonstrating the relationships between tau and neuronal density in the stratum griseum intermedium (SGI) and stratum griseum profundum (SGP), and between stratum griseum superficiale (SGS) neuronal density and NPI(hall) score.*

## 6.4 Discussion

The superior colliculus has been the subject of one previous neuropathological study that demonstrated DLB cases had moderate Lewy body pathology and mild to moderate AD-type pathology (Sierra *et al.*, 2016). However, no previous study has conducted quantitative analysis of individual laminae of the superior colliculus in the context of visual hallucinations in DLB. As the superior colliculus has been directly implicated in the visual manifestations of Lewy body disease (Diederich *et al.*, 2014; Shine *et al.*, 2014), the present study aimed to investigate whether DLB is marked by degeneration of the superior colliculus. The key findings emerging from the present study are that DLB cases have reductions in neuronal density in the SGI, in contrast to the more widespread reductions observed in all laminae in AD. Distinct topographic patterns of deposition were observed for α-synuclein and tau pathology, with the SGI and SGP affected more severely than the SGS. Lewy body pathology was not related to cellular density in any lamina in DLB but tau pathology was inversely related to neuronal density in the SGI and SGP across all cases. Motor dysfunction, as assessed by UPDRS III, was not related to any neuropathological variable in the superior colliculus. There was no relationship between Lewy body pathology and hallucination severity and frequency, as assessed by NPI (hall). However, neuronal density in the SGS was positively correlated with the severity and frequency of visual hallucinations in DLB cases.

Approximately 10% of retinal ganglion cells directly innervate the SGS (Perry and Cowey, 1984). Extra-retinal inputs to the SGS have not been examined in primates, though studies in the cat have suggested cholinergic modulation from the parabigeminal nucleus (Sherk, 1979). The medial temporal visual area (area V5/MT) receives input from the inferior pulvinar in a pathway originating in the SGS (Stepniewska *et al.*, 1999; Stepniewska *et al.*, 2000). This pathway may be involved in the non-conscious perception of motion (Lanyon *et al.*, 2009) as some neurons within the primate SGS are motion sensitive (Inayat *et al.*, 2015). There is speculation that the colliculo-pulvinar pathway may be important in saccadic suppression, the inhibition of activity in the LGN and visual cortex during the execution of saccadic eye movements (Wurtz *et al.*, 2011). The SGS also projects to other regions receiving retinal innervation, including the LGN and the pretectal nuclei (Benevento and Fallon, 1975).

The SGI and SGP are increasingly viewed as being functionally and anatomically independent from the SGS (Krauzlis *et al.*, 2013). In contrast to the predominantly retinal input of the SGS, these laminae receive inputs from wide-ranging cortical and sub-cortical regions. Inputs include motor and association sensory cortices, the hypothalamus, zona incerta, substantia nigra *pars reticulata*, locus coeruleus, dorsal raphe, pendunclopontine and deep cerebellar nuclei (Sparks and Hartwich-Young, 1989). The SGI and SGP contain retinotopic maps of the visual field and are thought to have an important role in the selection of visual targets (Sparks, 1999). However, auditory and somatosensory maps have been demonstrated in the deeper laminae of the cat superior colliculus, in addition to multi-sensory neurons that respond to input from more than one sensory modality (Wallace *et al.*, 1993). Neurons within the retinotopic area corresponding to the target of an upcoming saccade show heightened activity prior to the initiation of the saccade, suggesting the SGI and SGP are involved in the selection of saccadic targets (Glimcher and Sparks, 1992). However, neurons within the SGI also predict the target of upcoming pursuit eye movements, further indicating a role in pursuit target selection (Krauzlis and Dill, 2002). Outputs from the SGI to the mediodorsal nucleus of the thalamus, projecting to the frontal eye fields, may serve to stabilise the visual field during saccadic eye movements (Wurtz *et al.*, 2011).

Within the superior colliculus, neuropathological lesions occurred in a stereotypical manner, with higher levels of α-synuclein and tau found in the SGI and SGP compared to the SGS. Structures connected to the SGI and SGP, such as the dorsal raphe, locus coeruleus and pedunculopontine nucleus, are vulnerable to the accumulation of Lewy body and tau pathology (Rub *et al.*, 2000; Dugger *et al.*, 2012). The SGS receives predominant afferent and efferent innervation from the primary visual pathway (Krauzlis *et al.*, 2013), which does not appear to accumulate significant Lewy body or tau pathology in AD or Lewy body disease (Beach *et al.*, 2014; Ho *et al.*, 2014; Khundakar *et al.*, 2016). As tau and α-synuclein may spread throughout the brain in a manner reminiscent of prion protein, these distinct patterns of deposition may reflect greater connectivity with areas vulnerable to neuropathological lesion formation (Goedert, 2015).

The present study demonstrated neuronal loss in the superior colliculus only in the SGI in DLB. This was in contrast to AD, where neuronal density reductions were

found in all strata of the superior colliculus. The SGI has a role in selecting targets of saccadic eye movements and initiating saccades (Glimcher and Sparks, 1992; Sparks, 1999) and projects to the lateral pulvinar, where specific neuronal loss was identified in DLB and AD (chapter 4) (Benevento and Standage, 1983). In comparison to AD, DLB patients have increased saccadic latency and are more likely to perform saccades that fall short of their target (Mosimann *et al.*, 2005). Specific lesioning of the SGI in primates has been shown to increase saccadic latency and the likelihood of saccades falling short of their target (Aizawa and Wurtz, 1998). Therefore, one could speculate that the presently reported degeneration of the SGI may contribute to saccadic abnormalities in DLB. However, as no difference was observed in neuronal density in the SGI between DLB and AD, and saccadic functioning was not tested in these cases, it is difficult to definitively determine whether neuronal density reductions were specifically related to saccadic dysfunction.

Although the SGI and SGP have important roles in oculomotor function, the present study did not find the motor subscale of the UPDRS was related to neuronal density or Lewy body pathology in any lamina of the superior colliculus. This suggests degeneration of the superior colliculus is not related to parkinsonian motor dysfunction in DLB. A previous study has shown there is no relationship between UPDRS III and oculomotor dysfunction in PD, citing the potential role of non-dopaminergic pathways in oculomotor dysfunction (Pinkhardt *et al.*, 2012). Therefore, in the present study, superior colliculus degeneration may occur independently of the dopaminergic pathways that characterise the parkinsonism motor phenotype.

The significant positive correlation between neuronal density in the SGS and the severity and frequency of visual hallucinations was an unexpected finding. It is possible, however, that sparing of this lamina, perhaps in conjunction with degeneration elsewhere, contributes to a vulnerability to hallucinations. Previous studies in the LGN and primary visual cortex (Erskine *et al.*, 2016; Khundakar *et al.*, 2016) have suggested the visual system in AD shows more widespread neurodegenerative changes than in DLB. Despite this, visual hallucinations are more commonly encountered in DLB than AD (Armstrong and Kergoat, 2015), perhaps indicating the specificity of neurodegeneration in DLB may be crucial for the manifestation of visual hallucinations. However, this correlation was demonstrated in a relatively small number of DLB cases, meaning it is difficult to draw strong

conclusions about the relationship between neuronal density in the SGS and visual hallucinations.

It is possible that a dysfunctional pathway routed through the SGS contributes to visual hallucinations. The SGS is modulated by the SGI (Isa and Hall, 2009), which enhances or inhibits visual system activity in response to visual targets (Isa and Hall, 2009; Ghitani *et al.*, 2014). Specific SGI neuronal loss has been shown to lead to compensatory increases in neuronal receptive field size (Aizawa and Wurtz, 1998). As SGI neurons receive auditory, somatosensory and multisensory input, it is possible that increased receptive field sizes lead to misidentification of sensory input from other modalities. Misidentified sensory information, when fed back to the SGS, could lead to altered activity, artificially enhancing activity in particular spatial locations of the visual field. Such a proposition would be dependent upon the intactness of the SGS to facilitate the enhancement of visual responses. However, it was beyond the scope of the present study to assess receptive field sizes or the impact of SGI neuronal loss on the functional capacity of the pathway through the SGS.

The superior colliculus was not completely sampled as it is routinely dissected on two different planes, thus total neuronal number could not be estimated. The correlations between visual hallucinations and neuropathological variables also used small numbers of cases due to the small number of cases with NPI data obtained during life.

In summary, the present study revealed specific changes in the superior colliculus that may contribute to visual hallucinations and saccadic abnormalities. By demonstrating neuronal density reductions in the SGI in DLB, compared to reductions in all strata in AD, this study has added to the previous chapters by showing that DLB have relatively selective neuronal loss in the visual system compared to AD. Therefore, visual hallucinations may result from the topography of degeneration in DLB, and the resulting physiological changes to visual processing at the network level. Understanding such changes is beyond the scope of a *post-mortem* study. However, physiological studies may help establish the functional consequences of the pathological changes found here.

# Chapter 7: Discussion

## 7.1 Introduction

DLB is a progressive neurodegenerative dementia marked by three core symptoms of fluctuating cognition, parkinsonism and complex visual hallucinations (McKeith, 2006). Neuropathologically, DLB is characterised by Lewy body pathology in brainstem, limbic and neocortical regions, though intermediate levels of AD-type pathology are variably present (Attems *et al.*, 2013). 60-80% of DLB patients experience complex visual hallucinations, yet their pathological aetiology remains unknown (Burghaus *et al.*, 2012). Visual hallucinations are associated with reduced quality of life and increased rates of institutionalisation for DLB patients (Bostrom *et al.*, 2007), which contribute to caregiver distress (Ricci *et al.*, 2009).

The subcortical visual nuclei comprising the visual thalamus and superior colliculus have been implicated in several hypotheses of visual hallucinations in DLB. The cortical release hypothesis suggests a lack of input to the primary visual cortex induces compensatory increases in activity and could prime the cortical visual system for hallucination (Manford and Andermann, 1998). Deficient visual attention mechanisms have also been implicated in the manifestation of visual hallucinations in DLB (Collerton *et al.*, 2005b; Shine *et al.*, 2014). The LGN, pulvinar and superior colliculus have also been implicated in blindsight pathways suggested to be dysfunctional in PD, and may therefore contribute to visual hallucinations in Lewy body disease generally (Diederich *et al.*, 2014).

## 7.2 The lateral geniculate nucleus is relatively preserved in dementia with Lewy bodies

This study demonstrated the LGN did not exhibit α-synuclein or tau pathology in DLB, and amyloid-β did not differ significantly from control cases. Stereological analysis of neuronal and glial populations did not identify any changes in DLB cases compared to controls. In contrast, AD cases had significant increases in amyloid-β and tau pathology, accompanied with significant reductions in parvocellular neurons and gliosis in magnocellular laminae compared to controls.

The relative preservation of the LGN indicates a lack of involvement in visual hallucinations in DLB, at least at a gross structural level, though knowledge of its

functional capacity remains beyond the scope of this study. However, consistent with the present findings of histological preservation of the LGN, physiological studies in PDD (Murphy *et al.*) and DLB (Erskine *et al.*, 2016) have not revealed significant changes compared to control patients. Therefore, it is probable that degeneration in other brain regions is necessary to create a propensity toward visual hallucination. Subtle physiological changes to the retina, relayed by an intact LGN, may contribute a vulnerability to hallucination. Alternatively, a critical level of visual input may be necessary for altered mechanisms elsewhere in the brain to elicit visual hallucinations.

In AD, degeneration of the LGN may perhaps counter-intuitively prevent the generation of hallucinations by not supplying a required critical level of visual input for hallucinations to occur. Substantial neuronal loss and tau pathology was only observed in AD cases with the most severe degree of global pathological burden, perhaps indicating the LGN is affected at a relatively late stage in the progression of AD pathology.

### 7.3 The pulvinar nucleus exhibits neuronal and synaptic loss Lewy body pathology and astrogliosis in dementia with Lewy bodies

In contrast to the LGN, Lewy body pathology was present throughout the pulvinar whilst neuronal loss was restricted to the lateral sub-region. Western blot assessment of synaptic and inflammatory markers in the pulvinar, based on pathway changes identified by RNA sequencing, demonstrated reductions in synaptic markers in DLB cases compared to controls. These changes correlated with increases in inflammatory markers, particularly astrocytic proteins. In AD, neuronal loss was also identified in the lateral pulvinar. The medial sub-region of the pulvinar did not show neuronal loss in DLB but did have the highest α-synuclein pathology. In AD cases, the medial pulvinar was more severely affected by tau pathology.

The pulvinar has a vital role in controlling activity in the primary visual cortex (Purushothaman *et al.*, 2012) and visual area V4 (Zhou *et al.*, 2016) on the basis of attentional and behavioural demands. Visual attentional impairments have been suggested to create a vulnerability to visual hallucinations in DLB (Collerton *et al.*, 2005b; Shine *et al.*, 2014). The connectivity between the pulvinar and amygdala is

thought to underlie unconscious affective facial perception (Ward *et al.*, 2007) which is impaired in PD (Saenz *et al.*, 2013; Diederich *et al.*, 2014). The present findings of α-synuclein pathology, neuronal and synaptic loss and astrogliosis likely indicate altered functioning of the pulvinar in DLB. Altered visual attentional modulation may force dependence upon the self-referential default mode network, thus biasing the individual towards top-down influences in the prediction of visual stimuli (Shine *et al.*, 2014). Impaired affective facial perception circuitry may indicate wider impairments in blindsight pathways, forcing visual information to travel through the slower primary visual pathways (Diederich *et al.*, 2014). Longer latencies in visual processing may similarly bias the individual toward top-down expectancies during visual perception.

Similar to the findings from the LGN, the described changes in the pulvinar may not be solely responsible for visual hallucinations in DLB. It is likely the identified changes in the pulvinar act in concert with changes elsewhere in the brain. For example, an inherent bias toward top-down expectations may not induce visual hallucinations in isolation. Hallucinations may be dependent upon other changes to act in tandem with those identified in the pulvinar, such as altered top-down processes. Changes to the fusiform gyrus, for example, may contribute toward deficient proto-object selection, thus biasing the individual not just to top-down visual processing but also towards the selection of erroneous top-down visual objects. Our studies in the temporal lobe indicate a rostro-caudal gradient of Lewy body pathology in the fusiform gyrus in DLB, consistent with the suggestion that more complex object perception areas are impaired as a result of neurodegenerative pathology (Dey, 2015).

### 7.4 The superior colliculus has specific neuronal loss and a unique topography of α-synuclein pathology

In contrast to the LGN, Lewy body pathology was found in the superior colliculus in DLB, and neuronal loss specifically in the SGI. In DLB cases, neuronal density in the SGS was significantly correlated with clinical measures of hallucination severity and frequency. In contrast to DLB cases, neuronal loss was found in every lamina of the superior colliculus in AD. α-synuclein pathology was more severe in the SGI and SGP, with the SGS relatively spared in DLB. Tau pathology had a similar pattern of expression to α-synuclein, with the SGI and SGP more severely affected than the

SGS across all cases. In contrast, amyloid-β did not show significant lamina-specific variation in deposition in any disease group.

The superior colliculus has an important role in motion perception, visuospatial attention, visual target selection and sensory integration (Krauzlis *et al.*, 2013), which are suggested to be deficient in Lewy body disease and may contribute to the manifestation of visual hallucinations (Diederich *et al.*, 2014). Additionally, the superior colliculus is thought to be vital in switching between different neural networks. This process may be dysfunctional in DLB and contribute a vulnerability to visual hallucinations by forcing reliance on the self-referential default mode network (Shine *et al.*, 2014). As with previous findings, the changes to the superior colliculus are unlikely to elicit visual hallucinations in isolation, but likely interact with dysfunction in other regions to create a vulnerability to them.

### 7.5 Distinct vulnerability across subcortical visual structures and their relationship to visual hallucinations in dementia with Lewy bodies

The present series of studies has suggested neuronal loss and Lewy body pathology is more specific in the visual system in DLB than in AD. In particular, the secondary, rather than the primary, visual pathway is more severely affected. This is consistent with a previous study of Lewy body pathology in DLB (Yamamoto *et al.*, 2006). However, the present series of studies have also demonstrated Lewy body pathology and neuronal loss have a specific topographical distribution in secondary visual pathway structures. The LGN is a relay structure for afferent visual input, whilst the pulvinar and superior colliculus are implicated in the modulation of visual information. Therefore, the present results in DLB showing greater pathological changes in modulatory structures are consistent with physiological studies in PDD, which indicate bottom-up influences, including those routed through the LGN, are substantially less perturbed than top-down influences (Murphy *et al.*).

Neuronal loss was only found in the lateral region of the pulvinar and the SGI of the superior colliculus in DLB. The affected regions are implicated in modulating visual system activity based on salience of observed visual stimuli and impairments to these functions may contribute to the clinical phenotype in DLB. In contrast, neuronal loss was recorded in the parvocellular laminae of the LGN, the lateral region of the

pulvinar and all laminae of the superior colliculus in AD. As AD cases showed a more widespread pattern of neuronal loss, if visual hallucinations were to result purely from neuronal loss in vulnerable regions one could speculate they would be observed at least as frequently as in DLB. However, visual hallucinations are not a prominent clinical feature of AD (Burghaus *et al.*, 2012), perhaps suggesting preservation of some regions, in combination with degeneration elsewhere, may both be necessary for their manifestation.

The pulvinar and superior colliculus exhibited Lewy body pathology, which was not found in the LGN. Additionally, the pulvinar expressed increased transcription of the astrocytic marker CHI3L1/YKL-40, which has not been described in Lewy body disorders previously, and was inversely related to several synaptic markers. As CHI3L1/YKL-40 has not been previously described as elevated in DLB, it may relate to a pathological process specific to this region, rather than a global cerebral phenomenon. The relative specificity of pathological changes to the visual system in DLB compared to AD, combined with an increase in an astrocytic marker not previously described in Lewy body disorders, may suggest specific changes to the pulvinar. The specificity of such changes, in contrast to the more widespread degenerative changes in AD, may contribute to the distinct clinical phenotype of DLB, including visual hallucinations.

With respect to the hypotheses underlying visual hallucinations in DLB, these findings contribute new insights into the mechanisms underlying this phenomenon. The cortical release hypothesis (Manford and Andermann, 1998) suggests visual cortical regions become disinhibited as a result of diminished input. Whilst cortical excitability is consistent with several studies in DLB (Taylor *et al.*, 2011; Khundakar *et al.*, 2016; Taylor *et al.*, 2016), the present study may suggest visual cortical changes are not the result of altered afferent visual input through the LGN. It should be emphasised that lack of histological changes does not necessarily mean the LGN is functionally preserved. However, functional MRI in response to visual stimuli has demonstrated no changes in activity of DLB patients compared to controls (Erskine *et al.*, 2016). However, it remains possible that retinal alterations, faithfully relayed by an intact LGN, create gaps in the visual field requiring ‘filling in’ by higher visual structures. Retinal pathology transmitted by an intact LGN, in combination with deficient visual attention mechanisms resulting from pulvinar degeneration, may be

consistent with the perceptual and attentional deficit model (Collerton *et al.*, 2005b). Gaps in visual perception or corrupted visual input, relayed by an intact LGN, may contribute to incorrect proto-object selection which is then held in visual awareness by dysfunctional visual attentional mechanisms resulting from pulvinar pathology. In AD, LGN degeneration may prevent faithful relaying of visual input and thus gate against such an effect.

α-synuclein pathology and neuronal loss in the lateral pulvinar and SGI of the superior colliculus, regions involved in visual attention and target selection, appear more consistent with the hypothesis that impairments in engaging the dorsal attentional network (Shine *et al.*, 2014) contribute to visual hallucinations in DLB. Difficulty in engaging the dorsal attentional network in attending to ambiguous stimuli would force reliance on the default mode network, a self-referential system incorporating elements of memory. Therefore, in the presence of an ambiguous stimulus, instead of directing visual attention, the individual is reliant on previous experience and expectations. Such a shift toward greater top-down visual control may incorrectly match expectations with the observed stimulus, ultimately generating a hallucinatory percept. In AD, more widespread changes, particularly to regions involved in memory, may inhibit reliance upon self-referential aspects of the default mode network. In support of this proposition, a previous study has demonstrated AD patients have greater impairments in default mode network function than DLB (Franciotti *et al.*, 2013). Therefore, although AD cases manifested greater neuropathological changes to the visual thalamic circuitry than DLB, greater alterations to the default mode network may prevent visual hallucinations.

The present findings also correspond with the suggestion that individuals with Lewy body disease are ‘blind’ to blindsight (Diederich *et al.*, 2014). The superior colliculus and pulvinar are both components of blindsight pathways implicated in visual hallucinations in Lewy body disease. However, this hypothesis suggests the SGS, which directly projects to the inferior pulvinar, is impaired. Whilst this was not what was found in the present study, preservation of the SGS was significantly associated with clinical markers of visual hallucinations. Preservation of the SGS, combined with neuronal loss and pathology in the deeper modulatory laminae, may indicate this pathway is dysfunctional rather than degenerated. Dysfunction of the short latency blindsight pathways may force reliance upon the longer latency primary visual

pathway, thus biasing the individual toward top-down influence on visual perception. Dysfunctional top-down visual mechanisms, resulting from pathology elsewhere, may inaccurately predict the observed visual stimulus, which is then perceived as a hallucinatory percept.

## 7.6 Study strengths and limitations

### 7.6.1 Study strengths

Where possible, this study employed a rigorous stereological approach to estimate neuronal morphology. As tissue was sampled and cut according to stereological principles, estimates could be determined in a mathematical, rather than an assumption-based, manner. This meant that absolute measures of number could be established, rather than relying on the proxy measure of numerical density (number per area of tissue), which is vulnerable to bias resulting from factors such as tissue processing and orientation (Erskine and Khundakar, 2016).

All included cases were characterised on the basis of both clinical and neuropathological findings, thus ensuring atypical cases were not included. The NBTR dissection protocol ensures the entire brain is fixed, processed and embedded for histology, not just the blocks necessary for neuropathological diagnosis. This is a considerable strength as the LGN and pulvinar are not located on sections typically needed for neuropathological diagnosis and, were they not already processed, the tissue would likely have been fixed for a long period of time, potentially affecting antigenicity. The use of a disease-control group (AD) was also an advantage, aiding identification of specific changes in DLB, particularly those that may relate to visual hallucinations. This enabled assessment of the relative specificity of the topography of Lewy body pathology and neuronal loss in DLB, which is likely to be an important contributor to the manifestation of visual hallucinations.

Cases included in the molecular study were selectively chosen to be optimal for neurochemical analysis, ensuring the results were not affected by artefacts due to agonal state or *post-mortem* factors. The molecular analysis of the pulvinar employed whole-genome RNA sequencing, an atheoretical approach to determine relative changes in transcription. Analysis of transcriptional changes using a bioinformatics approach identified altered biological pathways without any *a priori*

hypothesis, ensuring changes were identified in an unbiased manner, irrespective of hypothesis. As the pulvinar is a relatively small structure, a limited amount of tissue was available for protein expression comparison studies. The use of western blot rather than ELISA enabled comparison of a wider range of protein targets, adding greater breadth to the study.

### 7.6.2 Study limitations

The present studies were limited by the relatively small sample sizes used. The advantages of stereological protocol, where whole structures are required to be sampled for analysis, were counterbalanced by many cases being rejected due to an incomplete sampling region. Human tissue is a valuable resource in dementia research though the fact that tissue is obtained at autopsy means that tissue is not active. Therefore, physiological changes as a result of pathology may only be inferred on the basis of known function, rather than by observation of changes in comparison to normal functioning.

A related limitation was the use of differing case cohorts in the different studies, thus precluding comparisons within cases across all structures. Only three cases (two AD and one DLB) were histologically assessed in all three regions. As before, this was typically the result of tissue availability and many cases with complete tissue for one region did not have complete tissue for another region. In the pulvinar, molecular and histological analyses were conducted on two different cohorts, with only one control case used for both analyses, thus limiting comparisons between both studies. This was the result of controlling *post-mortem* interval and tissue pH for neurochemical analyses. Furthermore, with the exception of the superior colliculus cohort, most of the cases had not received serial neuropsychological assessment during life, thus precluding comparison of the results with quantitative data on the severity and frequency of visual hallucinations. The limited number of cases with both in-depth neuropsychological test results resulted from the need for intact tissue for stereological sampling. The necessity of whole and intact structures for stereological analysis was the primary factor that limited the number of cases used, and also the quality of clinical information available. In the present studies, only few cases were found that had both intact tissue and serial neuropsychological data. Therefore,

whilst stereological analysis increased the precision of estimates of neuronal number, it also limited the ability to relate neuropathological changes to clinical features. The lack of quantitative neuropsychological data to relate to neuropathological findings, combined with the relatively small sample size, limits the generalisability of these findings to explain hallucinations in the wider DLB population.

AD cases may not have been the most appropriate disease control group, with non-hallucinating DLB cases a more suitable alternative. However, the presence of visual hallucinations as a core feature of DLB severely restricted the number of cases meeting this criterion. It was not possible to obtain enough DLB cases without a clinical history of visual hallucinations who also had complete tissue for stereological analysis. Therefore, the present results may relate more to idiosyncratic changes in DLB in general, rather than changes specific to visual hallucinations in particular. One exception was the superior colliculus study (Chapter 6) where full stereological protocol was not used, increasing the availability of cases and facilitating the inclusion of non-hallucinating DLB cases to determine relationships between neuropathological and clinical variables.

Molecular studies conducted in the pulvinar were conducted on the whole structure, rather than individual sub-nuclei. Although α-synuclein pathology and astrogliosis was found throughout the entire pulvinar, neuronal loss was only found in the lateral sub-nucleus. The sub-nuclei of the pulvinar are small and not obvious on gross visual inspection meaning sub-dissection of these structures was not possible. Furthermore, the small size of these structures would also have vastly reduced the amount of tissue available for subsequent protein expression analysis. Relative protein expression levels were assessed using western blot methodology. As noted in Chapter 5, western blot is not a directly quantitative technique, and relative assessments of the size and intensity of bands must be made. Quantitative data would have been more easily obtained using a technique such as ELISA. However, initial pilot studies indicated the use of ELISA in assessment of desired targets would require considerably more tissue than could be acquired.

Molecular studies were only conducted on the pulvinar, largely because of its size and its central role in visual function. As the LGN and superior colliculus are comparatively small structures, limiting the amount of available tissue and restricting

the breadth of analyses, we assessed these structures using purely histological methods.

## 7.7 Future directions

It is notable that the present significant results of neuronal loss using stereological sampling and rigid adherence to protocol would have been obtained even if neuronal density measures had been employed. Considering the limitations outlined in the previous section (7.6.2), if this study was to be conducted again one should focus upon obtaining a large number of cases with good clinical information rather than ensuring tissue is sufficient for stereological protocol. This would provide a better balance between the desire for accurate analysis and making results more applicable to the wider DLB population, whilst also enabling comparison between neuropathological and quantitative clinical information to evaluate clinico-pathological correlations.

As the present study has identified pathological alterations to regions that may contribute to the manifestation of visual hallucinations in DLB, further studies may examine the nature of such changes. For example, neuronal loss in the lateral pulvinar and SGI may affect particular sub-classes of neurons with specific neurochemical profiles. Identification of such specific neuronal vulnerability would aid further understanding of disease mechanisms in Lewy body disorders and potentially highlight therapeutic options based on neurochemical changes.

Considering the interconnected nature of the brain, neuronal loss in one structure is likely to have a resulting impact upon regions substantially interconnected with it. As a result, further investigation of regions with substantial connections with the lateral pulvinar and SGI of the superior colliculus, such as visual area V4 and the substantia nigra *pars reticulata*, would be useful in determining further visual system changes in DLB. Such studies would likely further our understanding of the vulnerability of the visual system to the neurodegenerative process in DLB, and the pathophysiology of visual hallucinations.

It is unlikely that neuronal loss in the lateral pulvinar and SGI are sufficient to cause visual hallucinations on their own. As noted previously, assessment of regions with

substantial connectivity with the pulvinar and superior colliculus would aid an understanding of the pathways involved in visual hallucinations. Additionally, a recurring theme of the present study is that perturbed top-down influences on vision may contribute to the phenomenon of visual hallucinations. In this regard, assessment of regions implicated in these functions, such as the frontal eye fields, cingulate gyrus and insula, which are typically affected by Lewy body pathology in DLB should be pursued. As discussed previously, the pulvinar and superior colliculus may contribute to visual hallucinations through pathways to the dorsal visual stream, particularly area V5/MT. If neuropathological changes were also found in the dorsal visual stream, it would provide further evidence for the hypotheses used to explain visual hallucinations presently, and would further implicate the tectal-pulvinar-V5/MT pathway in this phenomenon.

Cholinergic dysfunction has been described in DLB and is thought to relate to the occurrence of visual hallucinations (Perry and Perry, 1995). Therefore, future studies may wish to investigate whether neuronal loss of Lewy pathology in cholinergic nuclei is related to clinical measures of hallucinations frequency and severity. The nucleus basalis of Meynert was initially investigated as a potential part of the present study. However, in many cases the thalamic sections cut for the present study were too posterior to include the nucleus basalis of Meynert and thus this study was not conducted.

As indicated in the study limitations (7.6), the lack of stereological changes in the LGN does not necessarily indicate functional preservation. Similarly, the preservation of the SGS but association with visual hallucination severity and frequency, may indicate physiological changes. One way to assess these changes would be the use of molecular analyses, though the small size of these structures would likely limit such studies. However, a hypothesis-driven technique requiring less tissue, such as autoradiography or *in-situ* hybridisation, may be useful in this regard. Both regions receive substantial cholinergic innervation and, as a neurotransmitter typically reduced in DLB, such a study may provide useful insights into the role of the cholinergic system in visual hallucinations. Alternatively, physiological studies in DLB patients may also provide information on functional changes in the superior colliculus, notwithstanding the difficulties in resolving such small structures using imaging techniques. Such an approach has already identified the LGN does not manifest

functional changes in response to visual stimuli in DLB patients compared to control participants (Erskine *et al.*, 2016).

CHI3L1/YKL-40 protein expression was increased in the pulvinar in DLB and was inversely related to the expression of several synaptic markers. Despite previous studies finding no change in expression of this astrocytic marker in the CSF of Lewy body disorder patients (Wennstrom *et al.*, 2015), it was elevated in the pulvinar in the present study. A key finding from the present project is the relative specificity of Lewy body pathology and neuronal loss in the visual system in DLB compared to AD. Stereological studies typically report neuronal loss as being more specific throughout the brain in DLB compared to AD (Erskine and Khundakar, 2016). Therefore, one may speculate CHI3L1/YKL-40 increases are not found throughout the brain in DLB but may also be region-specific. Future studies may examine the expression of this astrocytic marker throughout the brain in DLB cases, in comparison to AD. An association between expression of CHI3L1/YKL-40 and synaptic or neuronal loss may indicate its utility as a therapeutic target in DLB.

The present study employed end-stage cases and demonstrated some regions did not show neurodegenerative changes in DLB. Therefore, a key question is why some regions did not manifest pathological changes, even after many years of symptoms. The prion-like spread hypothesis suggests misfolded α-synuclein can spread through the brain in a transsynaptic manner similar to that described previously for prion protein (Das and Zou, 2016). It is noteworthy that the retina and primary visual cortex, with which the LGN is primarily connected, do not manifest high burdens of Lewy body pathology, and the patient may die prior to pathology spreading to these regions. However, it is also possible that some neurons have reduced vulnerability to α-synuclein pathology than others. The prion-like spread hypothesis suggests α-synuclein prions are able to template the misfolding of the physiological protein into the pathogenic conformation. However, this proposal requires the normal physiological protein to be present in sufficient quantities to be templated into the pathogenic conformation. There is some evidence to indicate that regions which do not typically manifest Lewy body pathology, such as the cerebellum and visual cortex, typically express relatively low levels of physiological α-synuclein under normal conditions (Braak *et al.*, 2000). Therefore, a future direction of the present study would be to determine whether cells within the regions and sub-

regions without significant Lewy body pathology contain lower levels of physiological α-synuclein under normal conditions.

A key criticism of studies employing *post-mortem* tissue is that physiological changes cannot be observed. Future studies may wish to examine how visual functioning is perturbed in laboratory animals with α-synuclein pathology, particularly with regard to supportive visual structures in the secondary visual pathway, such as the pulvinar and superior colliculus. Murine species would not be suitable for this purpose, as they do not possess a pulvinar (Jones, 2012) and do not perform saccadic eye movements, with the superior colliculus being the primary target of retinal innervation, rather than the LGN (Hofbauer and Drager, 1985). This would indicate that non-human primates would be a better choice, despite the ethical issues related to their use. The model system used in non-human primates would also have to be carefully chosen as α-synuclein-inducing toxins, such as rotenone, act primarily on mitochondrial respiration (Xiong *et al.*, 2012). As the visual system has high metabolic demands (Chhetri and Gueven, 2016), using mitochondrial toxins would impair visual structures at an early stage (Normando *et al.*, 2016), which may not accurately reflect the clinical course of α-synucleinopathies. Therefore, a more appropriate model may be the injection of misfolded α-synuclein to pathological predilection sites, such as the dorsal motor nucleus of vagus or amygdala.

It was suggested in Chapter 6 neuronal loss in the SGI of the superior colliculus may create conditions where sensory inputs from non-visual modalities are misidentified as visual information. As the SGI is used to modulate visual information through the SGS, and ultimately the LGN and visual cortex, these changes may alter visual activity based on non-visual input. This hypothesis could be tested in DLB patients by asking patients to observe controlled visual fields, perhaps on a tablet computer. Incorporating other sensory stimuli, such as auditory and somatosensory information, alongside the visual information and subsequent patient interview of perceived images, would enable determination of whether non-visual stimuli influenced visual hallucinations or misidentification. Such work would undoubtedly be useful in verifying the present interpretation of results, and could provide novel insights into visual hallucinations.

## 7.8 Conclusions

The subcortical visual system shows relatively specific patterns of neuropathological change in DLB compared to AD. Specifically, more neurodegeneration was found in the pulvinar and superior colliculus than the LGN in DLB. Overall, these findings indicate specific impairments in structures involved in adjunctive visual functions, such as visual attention and target selection, with relative preservation of basic structures necessary for visual sensation. These findings provide anatomical evidence and support for several prominent hypotheses of visual hallucinations.

# Chapter 8: References


Aarsland, D., Andersen, K., Larsen, J.P., Lolk, A. and Kragh-Sorensen, P. (2003) 'Prevalence and characteristics of dementia in Parkinson disease: an 8-year prospective study', *Arch Neurol*, 60(3), pp. 387-92.

Aarsland, D., Ballard, C., McKeith, I., Perry, R.H. and Larsen, J.P. (2001) 'Comparison of extrapyramidal signs in dementia with Lewy bodies and Parkinson's disease', *J Neuropsychiatry Clin Neurosci*, 13(3), pp. 374-9.

Aarsland, D., Perry, R., Larsen, J.P., McKeith, I.G., O'Brien, J.T., Perry, E.K., Burn, D. and Ballard, C.G. (2005) 'Neuroleptic sensitivity in Parkinson's disease and parkinsonian dementias', *J Clin Psychiatry*, 66(5), pp. 633-7.

Aarsland, D., Tandberg, E., Larsen, J.P. and Cummings, J.L. (1996) 'Frequency of dementia in Parkinson disease', *Arch Neurol*, 53(6), pp. 538-42.

Abdelnour, C., van Steenoven, I., Londos, E., Blanc, F., Auestad, B., Kramberger, M.G., Zetterberg, H., Mollenhauer, B., Boada, M. and Aarsland, D. (2016) 'Alzheimer's disease cerebrospinal fluid biomarkers predict cognitive decline in lewy body dementia', *Mov Disord*, 31(8), pp. 1203-8.

Acarin, L., Paris, J., Gonzalez, B. and Castellano, B. (2002) 'Glial expression of small heat shock proteins following an excitotoxic lesion in the immature rat brain', *Glia*, 38(1), pp. 1-14.

Aizawa, H. and Wurtz, R.H. (1998) 'Reversible inactivation of monkey superior colliculus. I. Curvature of saccadic trajectory', *J Neurophysiol*, 79(4), pp. 2082-96.

Alladi, S., Xuereb, J., Bak, T., Nestor, P., Knibb, J., Patterson, K. and Hodges, J.R. (2007) 'Focal cortical presentations of Alzheimer's disease', *Brain*, 130(Pt 10), pp. 2636-45.

Allen, R.L., Walker, Z., D'Ath, P.J. and Katona, C.L. (1995) 'Risperidone for psychotic and behavioural symptoms in Lewy body dementia', *Lancet*, 346(8968), p. 185.

American Psychiatric, A. (2013) *Diagnostic and statistical manual of mental disorders (DSM-5®)*. American Psychiatric Pub.

Arai, M., Arai, R., Kani, K. and Jacobowitz, D.M. (1992) 'Immunohistochemical localization of calretinin in the rat lateral geniculate nucleus and its retino-geniculate projection', *Brain Res*, 596(1-2), pp. 215-22.

Arakawa, K., Tobimatsu, S., Kato, M. and Kira, J. (1999) 'Parvocellular and magnocellular visual processing in spinocerebellar degeneration and Parkinson's disease: an event-related potential study', *Clinical Neurophysiology*, 110(6), pp. 1048-57.

Archibald, N.K., Clarke, M.P., Mosimann, U.P. and Burn, D.J. (2011) 'Visual symptoms in Parkinson's disease and Parkinson's disease dementia', *Mov Disord*, 26(13), pp. 2387-95.

Arends, Y.M., Duyckaerts, C., Rozemuller, J.M., Eikelenboom, P. and Hauw, J.J. (2000) 'Microglia, amyloid and dementia in alzheimer disease. A correlative study', *Neurobiol Aging*, 21(1), pp. 39-47.

Armstrong, M.J., Litvan, I., Lang, A.E., Bak, T.H., Bhatia, K.P., Borroni, B., Boxer, A.L., Dickson, D.W., Grossman, M., Hallett, M., Josephs, K.A., Kertesz, A., Lee, S.E., Miller, B.L., Reich, S.G., Riley, D.E., Tolosa, E., Troster, A.I., Vidailhet, M. and Weiner, W.J. (2013) 'Criteria for the diagnosis of corticobasal degeneration', *Neurology*, 80(5), pp. 496-503.

Armstrong, R. and Kergoat, H. (2015) 'Oculo-visual changes and clinical considerations affecting older patients with dementia', *Ophthalmic Physiol Opt*, 35(4), pp. 352-76.

Armstrong, R.A. (2012) 'Visual signs and symptoms of dementia with Lewy bodies', *Clinical & experimental optometry : journal of the Australian Optometrical Association*, 95(6), pp. 621-30.

Asplund, C.L., Todd, J.J., Snyder, A.P. and Marois, R. (2010) 'A central role for the lateral prefrontal cortex in goal-directed and stimulus-driven attention', *Nat Neurosci*, 13(4), pp. 507-12.

Attems, J., Jellinger, K.A., Dening, T. and Thomas, A. (2013) 'Neuropathology', *Oxford textbook of old age psychiatry*, 2, pp. 87-105.

Baba, M., Nakajo, S., Tu, P.H., Tomita, T., Nakaya, K., Lee, V.M., Trojanowski, J.Q. and Iwatsubo, T. (1998) 'Aggregation of alpha-synuclein in Lewy bodies of sporadic Parkinson's disease and dementia with Lewy bodies', *Am J Pathol*, 152(4), pp. 879-84.
Bachstetter, A.D., Van Eldik, L.J., Schmitt, F.A., Neltner, J.H., Ighodaro, E.T., Webster, S.J., Patel, E., Abner, E.L., Kryscio, R.J. and Nelson, P.T. (2015) 'Disease-related microglia heterogeneity in the hippocampus of Alzheimer's disease, dementia with Lewy bodies, and hippocampal sclerosis of aging', *Acta Neuropathol Commun*, 3, p. 32.
Ballard, C., McKeith, I., Harrison, R., O'Brien, J., Thompson, P., Lowery, K., Perry, R. and Ince, P. (1997) 'A detailed phenomenological comparison of complex visual hallucinations in dementia with Lewy bodies and Alzheimer's disease', *International Psychogeriatrics*, 9(4), pp. 381-8.
Ballard, C.G., Aarsland, D., McKeith, I., O'Brien, J., Gray, A., Cormack, F., Burn, D., Cassidy, T., Starfeldt, R., Larsen, J.P., Brown, R. and Tovee, M. (2002) 'Fluctuations in attention: PD dementia vs DLB with parkinsonism', *Neurology*, 59(11), pp. 1714-20.
Bancher, C., Brunner, C., Lassmann, H., Budka, H., Jellinger, K., Wiche, G., Seitelberger, F., Grundke-Iqbal, I., Iqbal, K. and Wisniewski, H.M. (1989) 'Accumulation of abnormally phosphorylated tau precedes the formation of neurofibrillary tangles in Alzheimer's disease', *Brain Res*, 477(1-2), pp. 90-9.
Barber, R., Scheltens, P., Gholkar, A., Ballard, C., McKeith, I., Ince, P., Perry, R. and O'Brien, J. (1999) 'White matter lesions on magnetic resonance imaging in dementia with Lewy bodies, Alzheimer's disease, vascular dementia, and normal aging', *J Neurol Neurosurg Psychiatry*, 67(1), pp. 66-72.
Barbur, J.L. (2004) ''Double-blindsight' revealed through the processing of color and luminance contrast defined motion signals', *Prog Brain Res*, 144, pp. 243-59.
Barker, R.A. and Williams-Gray, C.H. (2016) 'Review: The spectrum of clinical features seen with alpha synuclein pathology', *Neuropathol Appl Neurobiol*, 42(1), pp. 6-19.
Bartels, T., Choi, J.G. and Selkoe, D.J. (2011) 'alpha-Synuclein occurs physiologically as a helically folded tetramer that resists aggregation', *Nature*, 477(7362), pp. 107-10.
Bate, C., Gentleman, S. and Williams, A. (2010) 'alpha-synuclein induced synapse damage is enhanced by amyloid-beta1-42', *Mol Neurodegener*, 5, p. 55.
Beach, T.G., Carew, J., Serrano, G., Adler, C.H., Shill, H.A., Sue, L.I., Sabbagh, M.N., Akiyama, H. and Cuenca, N. (2014) 'Phosphorylated alpha-synuclein-immunoreactive retinal neuronal elements in Parkinson's disease subjects', *Neurosci Lett*, 571, pp. 34-8.
Benarroch, E.E. (2015) 'Pulvinar: associative role in cortical function and clinical correlations', *Neurology*, 84(7), pp. 738-47.
Bendor, J.T., Logan, T.P. and Edwards, R.H. (2013) 'The function of alpha-synuclein', *Neuron*, 79(6), pp. 1044-66.
Benevento, L.A. and Fallon, J.H. (1975) 'The ascending projections of the superior colliculus in the rhesus monkey (Macaca mulatta)', *J Comp Neurol*, 160(3), pp. 339-61.
Benevento, L.A. and Standage, G.P. (1983) 'The organization of projections of the retinorecipient and nonretinorecipient nuclei of the pretectal complex and layers of the superior colliculus to the lateral pulvinar and medial pulvinar in the macaque monkey', *J Comp Neurol*, 217(3), pp. 307-36.
Benowitz, L.I. and Routtenberg, A. (1997) 'GAP-43: an intrinsic determinant of neuronal development and plasticity', *Trends Neurosci*, 20(2), pp. 84-91.
Berg, D., Postuma, R.B., Bloem, B., Chan, P., Dubois, B., Gasser, T., Goetz, C.G., Halliday, G.M., Hardy, J., Lang, A.E., Litvan, I., Marek, K., Obeso, J., Oertel, W., Olanow, C.W., Poewe, W., Stern, M. and Deuschl, G. (2014) 'Time to redefine PD? Introductory statement of the MDS Task Force on the definition of Parkinson's disease', *Mov Disord*, 29(4), pp. 454-62.
Berman, R.A. and Wurtz, R.H. (2010) 'Functional Identification of a Pulvinar Path from Superior Colliculus to Cortical Area MT', *Journal of Neuroscience*, 30(18), pp. 6342-6354.
Bertram, K. and Williams, D.R. (2012) 'Visual hallucinations in the differential diagnosis of parkinsonism', *J Neurol Neurosurg Psychiatry*, 83(4), pp. 448-52.

Beyer, M.K., Larsen, J.P. and Aarsland, D. (2007) 'Gray matter atrophy in Parkinson disease with dementia and dementia with Lewy bodies', *Neurology*, 69(8), pp. 747-54.
Bisley, J.W. and Goldberg, M.E. (2010) 'Attention, intention, and priority in the parietal lobe', *Annu Rev Neurosci*, 33, pp. 1-21.
Blanc, F., Noblet, V., Philippi, N., Cretin, B., Foucher, J., Armspach, J.P., Rousseau, F. and Alzheimer's Disease Neuroimaging, I. (2014) 'Right anterior insula: core region of hallucinations in cognitive neurodegenerative diseases', *PLoS One*, 9(12), p. e114774.
Bodis-Wollner, I., Kozlowski, P.B., Glazman, S. and Miri, S. (2014) 'alpha-synuclein in the inner retina in parkinson disease', *Ann Neurol*, 75(6), pp. 964-6.
Boeve, B.F. (2013) 'Idiopathic REM sleep behaviour disorder in the development of Parkinson's disease', *The Lancet Neurology*, 12(5), pp. 469-482.
Boeve, B.F., Silber, M.H., Ferman, T.J., Lin, S.C., Benarroch, E.E., Schmeichel, A.M., Ahlskog, J.E., Caselli, R.J., Jacobson, S., Sabbagh, M., Adler, C., Woodruff, B., Beach, T.G., Iranzo, A., Gelpi, E., Santamaria, J., Tolosa, E., Singer, C., Mash, D.C., Luca, C., Arnulf, I., Duyckaerts, C., Schenck, C.H., Mahowald, M.W., Dauvilliers, Y., Graff-Radford, N.R., Wszolek, Z.K., Parisi, J.E., Dugger, B., Murray, M.E. and Dickson, D.W. (2013) 'Clinicopathologic correlations in 172 cases of rapid eye movement sleep behavior disorder with or without a coexisting neurologic disorder', *Sleep Med*, 14(8), pp. 754-62.
Boeve, B.F., Silber, M.H., Ferman, T.J., Lucas, J.A. and Parisi, J.E. (2001) 'Association of REM sleep behavior disorder and neurodegenerative disease may reflect an underlying synucleinopathy', *Mov Disord*, 16(4), pp. 622-30.
Bohr, I.J., Ray, M.A., McIntosh, J.M., Chalon, S., Guilloteau, D., McKeith, I.G., Perry, R.H., Clementi, F., Perry, E.K., Court, J.A. and Piggott, M.A. (2005) 'Cholinergic nicotinic receptor involvement in movement disorders associated with Lewy body diseases. An autoradiography study using [(125)I]alpha-conotoxinMII in the striatum and thalamus', *Exp Neurol*, 191(2), pp. 292-300.
Bonneh-Barkay, D., Wang, G., Starkey, A., Hamilton, R.L. and Wiley, C.A. (2010a) 'In vivo CHI3L1 (YKL-40) expression in astrocytes in acute and chronic neurological diseases', *J Neuroinflammation*, 7, p. 34.
Bonneh-Barkay, D., Zagadailov, P., Zou, H., Niyonkuru, C., Figley, M., Starkey, A., Wang, G., Bissel, S.J., Wiley, C.A. and Wagner, A.K. (2010b) 'YKL-40 expression in traumatic brain injury: an initial analysis', *J Neurotrauma*, 27(7), pp. 1215-23.
Boot, B. (2013) 'The incidence and prevalence of dementia with Lewy bodies is underestimated', *Psychol Med*, 43(12), pp. 2687-8.
Bostrom, F., Jonsson, L., Minthon, L. and Londos, E. (2007) 'Patients with dementia with lewy bodies have more impaired quality of life than patients with Alzheimer disease', *Alzheimer Dis Assoc Disord*, 21(2), pp. 150-4.
Braak, H., Alafuzoff, I., Arzberger, T., Kretzschmar, H. and Del Tredici, K. (2006) 'Staging of Alzheimer disease-associated neurofibrillary pathology using paraffin sections and immunocytochemistry', *Acta Neuropathol*, 112(4), pp. 389-404.
Braak, H. and Braak, E. (1991) 'Alzheimer's disease affects limbic nuclei of the thalamus', *Acta Neuropathol*, 81(3), pp. 261-8.
Braak, H., Del Tredici, K., Gai, W.P. and Braak, E. (2000) 'Alpha-synuclein is not a requisite component of synaptic boutons in the adult human central nervous system', *J Chem Neuroanat*, 20(3-4), pp. 245-52.
Braak, H., Del Tredici, K., Rub, U., de Vos, R.A., Jansen Steur, E.N. and Braak, E. (2003) 'Staging of brain pathology related to sporadic Parkinson's disease', *Neurobiol Aging*, 24(2), pp. 197-211.
Braak, H., Ghebremedhin, E., Rub, U., Bratzke, H. and Del Tredici, K. (2004) 'Stages in the development of Parkinson's disease-related pathology', *Cell Tissue Res*, 318(1), pp. 121-34.
Bradshaw, J., Saling, M., Hopwood, M., Anderson, V. and Brodtmann, A. (2004) 'Fluctuating cognition in dementia with Lewy bodies and Alzheimer's disease is qualitatively distinct', *J Neurol Neurosurg Psychiatry*, 75(3), pp. 382-7.

Bragina, L., Fattorini, G., Giovedi, S., Melone, M., Bosco, F., Benfenati, F. and Conti, F. (2011) 'Analysis of Synaptotagmin, SV2, and Rab3 Expression in Cortical Glutamatergic and GABAergic Axon Terminals', *Front Cell Neurosci*, 5, p. 32.
Bridge, H., Leopold, D.A. and Bourne, J.A. (2015) 'Adaptive Pulvinar Circuitry Supports Visual Cognition', *Trends Cogn Sci*.
Brooks, D. and Halliday, G.M. (2009) 'Intralaminar nuclei of the thalamus in Lewy body diseases', *Brain Res Bull*, 78(2-3), pp. 97-104.
Burghaus, L., Eggers, C., Timmermann, L., Fink, G.R. and Diederich, N.J. (2012) 'Hallucinations in neurodegenerative diseases', *CNS Neurosci Ther*, 18(2), pp. 149-59.
Burn, D.J. and Jaros, E. (2001) 'Multiple system atrophy: cellular and molecular pathology', *Mol Pathol*, 54(6), pp. 419-26.
Burn, D.J., Rowan, E.N., Allan, L.M., Molloy, S., O'Brien, J.T. and McKeith, I.G. (2006) 'Motor subtype and cognitive decline in Parkinson's disease, Parkinson's disease with dementia, and dementia with Lewy bodies', *J Neurol Neurosurg Psychiatry*, 77(5), pp. 585-9.
Burn, D.J., Rowan, E.N., Minett, T., Sanders, J., Myint, P., Richardson, J., Thomas, A., Newby, J., Reid, J., O'Brien, J.T. and McKeith, I.G. (2003) 'Extrapyramidal features in Parkinson's disease with and without dementia and dementia with Lewy bodies: A cross-sectional comparative study', *Mov Disord*, 18(8), pp. 884-9.
Burre, J., Sharma, M., Tsetsenis, T., Buchman, V., Etherton, M.R. and Sudhof, T.C. (2010) 'Alpha-synuclein promotes SNARE-complex assembly in vivo and in vitro', *Science*, 329(5999), pp. 1663-7.
Burton, E.J., McKeith, I.G., Burn, D.J., Williams, E.D. and O'Brien, J.T. (2004) 'Cerebral atrophy in Parkinson's disease with and without dementia: a comparison with Alzheimer's disease, dementia with Lewy bodies and controls', *Brain*, 127(Pt 4), pp. 791-800.
Burton, H. and Jones, E.G. (1976) 'The posterior thalamic region and its cortical projection in New World and Old World monkeys', *J Comp Neurol*, 168(2), pp. 249-301.
Caceres, A., Payne, M.R., Binder, L.I. and Steward, O. (1983) 'Immunocytochemical localization of actin and microtubule-associated protein MAP2 in dendritic spines', *Proc Natl Acad Sci U S A*, 80(6), pp. 1738-42.
Cagnin, A., Gnoato, F., Jelcic, N., Favaretto, S., Zarantonello, G., Ermani, M. and Dam, M. (2013) 'Clinical and cognitive correlates of visual hallucinations in dementia with Lewy bodies', *J Neurol Neurosurg Psychiatry*, 84(5), pp. 505-10.
Cahoy, J.D., Emery, B., Kaushal, A., Foo, L.C., Zamanian, J.L., Christopherson, K.S., Xing, Y., Lubischer, J.L., Krieg, P.A., Krupenko, S.A., Thompson, W.J. and Barres, B.A. (2008) 'A transcriptome database for astrocytes, neurons, and oligodendrocytes: a new resource for understanding brain development and function', *J Neurosci*, 28(1), pp. 264-78.
Calakos, N. and Scheller, R.H. (1994) 'Vesicle-associated membrane protein and synaptophysin are associated on the synaptic vesicle', *J Biol Chem*, 269(40), pp. 24534-7.
Caminiti, S.P., Tettamanti, M., Sala, A., Presotto, L., Iannaccone, S., Cappa, S.F., Magnani, G., Perani, D. and Alzheimer's Disease Neuroimaging, I. (2016) 'Metabolic connectomics targeting brain pathology in dementia with Lewy bodies', *J Cereb Blood Flow Metab*.
Carter, R. and Ffytche, D.H. (2015) 'On visual hallucinations and cortical networks: a trans-diagnostic review', *J Neurol*, 262(7), pp. 1780-90.
Ceravolo, R., Volterrani, D., Gambaccini, G., Rossi, C., Logi, C., Manca, G., Berti, C., Mariani, G., Murri, L. and Bonuccelli, U. (2003) 'Dopaminergic degeneration and perfusional impairment in Lewy body dementia and Alzheimer's disease', *Neurol Sci*, 24(3), pp. 162-3.
Chaari, A., Hoarau-Vechot, J. and Ladjimi, M. (2013) 'Applying chaperones to protein-misfolding disorders: molecular chaperones against alpha-synuclein in Parkinson's disease', *Int J Biol Macromol*, 60, pp. 196-205.
Chang, C.C., Liu, J.S., Chang, Y.Y., Chang, W.N., Chen, S.S. and Lee, C.H. (2008) '(99m)Tc-ethyl cysteinate dimer brain SPECT findings in early stage of dementia with Lewy bodies and Parkinson's disease patients: a correlation with neuropsychological tests', *Eur J Neurol*, 15(1), pp. 61-5.

Chaudhary, H., Stefanovic, A.N., Subramaniam, V. and Claessens, M.M. (2014) 'Membrane interactions and fibrillization of alpha-synuclein play an essential role in membrane disruption', *FEBS Lett*, 588(23), pp. 4457-63.
Cheong, S.K., Tailby, C., Martin, P.R., Levitt, J.B. and Solomon, S.G. (2011) 'Slow intrinsic rhythm in the koniocellular visual pathway', *Proc Natl Acad Sci U S A*, 108(35), pp. 14659-63.
Chhetri, J. and Gueven, N. (2016) 'Targeting mitochondrial function to protect against vision loss', *Expert Opin Ther Targets*, 20(6), pp. 721-36.
Chiu, P.Y., Tsai, C.T., Chen, P.K., Chen, W.J. and Lai, T.J. (2016) 'Neuropsychiatric Symptoms in Parkinson's Disease Dementia Are More Similar to Alzheimer's Disease than Dementia with Lewy Bodies: A Case-Control Study', *PLoS One*, 11(4), p. e0153989.
Chorostecki, J., Seraji-Bozorgzad, N., Shah, A., Bao, F., Bao, G., George, E., Gorden, V., Caon, C., Frohman, E., Bhatti, M.T. and Khan, O. (2015) 'Characterization of retinal architecture in Parkinson's disease', *J Neurol Sci*, 355(1-2), pp. 44-8.
Claassen, D.O., Lowe, V.J., Peller, P.J., Petersen, R.C. and Josephs, K.A. (2011) 'Amyloid and glucose imaging in dementia with Lewy bodies and multiple systems atrophy', *Parkinsonism Relat Disord*, 17(3), pp. 160-5.
Clark, W.E. (1932) 'A MORPHOLOGICAL STUDY OF THE LATERAL GENICULATE BODY', *Br J Ophthalmol*, 16(5), pp. 264-84.
Coffman, F.D. (2008) 'Chitinase 3-Like-1 (CHI3L1): a putative disease marker at the interface of proteomics and glycomics', *Crit Rev Clin Lab Sci*, 45(6), pp. 531-62.
Collerton, D., Burn, D., McKeith, I. and O'Brien, J. (2003) 'Systematic review and meta-analysis show that dementia with Lewy bodies is a visual-perceptual and attentional-executive dementia', *Dement Geriatr Cogn Disord*, 16(4), pp. 229-37.
Collerton, D., Perry, E. and McKeith, I. (2005a) 'Still PADing along: Perception and attention remain key factors in understanding complex visual hallucinations', *Behavioral and Brain Sciences*, 28(6), pp. 776-794.
Collerton, D., Perry, E. and McKeith, L. (2005b) 'Why people see things that are not there: A novel Perception and Attention Deficit model for recurrent complex visual hallucinations', *Behavioral and Brain Sciences*, 28(6), pp. 737-+.
Colloby, S.J., Fenwick, J.D., Williams, E.D., Paling, S.M., Lobotesis, K., Ballard, C., McKeith, I. and O'Brien, J.T. (2002) 'A comparison of (99m)Tc-HMPAO SPET changes in dementia with Lewy bodies and Alzheimer's disease using statistical parametric mapping', *Eur J Nucl Med Mol Imaging*, 29(5), pp. 615-22.
Conway, K.A., Harper, J.D. and Lansbury, P.T., Jr. (2000a) 'Fibrils formed in vitro from alpha-synuclein and two mutant forms linked to Parkinson's disease are typical amyloid', *Biochemistry*, 39(10), pp. 2552-63.
Conway, K.A., Lee, S.J., Rochet, J.C., Ding, T.T., Williamson, R.E. and Lansbury, P.T., Jr. (2000b) 'Acceleration of oligomerization, not fibrillization, is a shared property of both alpha-synuclein mutations linked to early-onset Parkinson's disease: implications for pathogenesis and therapy', *Proc Natl Acad Sci U S A*, 97(2), pp. 571-6.
Cookson, M.R. (2006) 'Hero versus antihero: the multiple roles of alpha-synuclein in neurodegeneration', *Exp Neurol*, 199(2), pp. 238-42.
Corbetta, M. and Shulman, G.L. (2002) 'Control of goal-directed and stimulus-driven attention in the brain', *Nat Rev Neurosci*, 3(3), pp. 201-15.
Corneil, B.D., Olivier, E. and Munoz, D.P. (2002) 'Neck muscle responses to stimulation of monkey superior colliculus. II. Gaze shift initiation and volitional head movements', *J Neurophysiol*, 88(4), pp. 2000-18.
Corripio, I., Escarti, M.J., Portella, M.J., Perez, V., Grasa, E., Sauras, R.B., Alonso, A., Safont, G., Camacho, M.V., Duenas, R., Arranz, B., San, L., Catafau, A.M., Carrio, I. and Alvarez, E. (2011) 'Density of striatal D2 receptors in untreated first-episode psychosis: an I123-IBZM SPECT study', *Eur Neuropsychopharmacol*, 21(12), pp. 861-6.

Court, J., Spurden, D., Lloyd, S., McKeith, I., Ballard, C., Cairns, N., Kerwin, R., Perry, R. and Perry, E. (1999) 'Neuronal nicotinic receptors in dementia with Lewy bodies and schizophrenia: alpha-bungarotoxin and nicotine binding in the thalamus', *J Neurochem*, 73(4), pp. 1590-7.
Court, J.A., Ballard, C.G., Piggott, M.A., Johnson, M., O'Brien, J.T., Holmes, C., Cairns, N., Lantos, P., Perry, R.H., Jaros, E. and Perry, E.K. (2001) 'Visual hallucinations are associated with lower alpha bungarotoxin binding in dementia with Lewy bodies', *Pharmacol Biochem Behav*, 70(4), pp. 571-9.
Cowey, A. and Stoerig, P. (1989) 'Projection patterns of surviving neurons in the dorsal lateral geniculate nucleus following discrete lesions of striate cortex: implications for residual vision', *Exp Brain Res*, 75(3), pp. 631-8.
Craig-Schapiro, R., Perrin, R.J., Roe, C.M., Xiong, C., Carter, D., Cairns, N.J., Mintun, M.A., Peskind, E.R., Li, G., Galasko, D.R., Clark, C.M., Quinn, J.F., D'Angelo, G., Malone, J.P., Townsend, R.R., Morris, J.C., Fagan, A.M. and Holtzman, D.M. (2010) 'YKL-40: a novel prognostic fluid biomarker for preclinical Alzheimer's disease', *Biol Psychiatry*, 68(10), pp. 903-12.
Cremades, N., Cohen, S.I., Deas, E., Abramov, A.Y., Chen, A.Y., Orte, A., Sandal, M., Clarke, R.W., Dunne, P., Aprile, F.A., Bertoncini, C.W., Wood, N.W., Knowles, T.P., Dobson, C.M. and Klenerman, D. (2012) 'Direct observation of the interconversion of normal and toxic forms of alpha-synuclein', *Cell*, 149(5), pp. 1048-59.
Crick, F. (1984) 'Function of the thalamic reticular complex: the searchlight hypothesis', *Proc Natl Acad Sci U S A*, 81(14), pp. 4586-90.
Culo, S., Mulsant, B.H., Rosen, J., Mazumdar, S., Blakesley, R.E., Houck, P.R. and Pollock, B.G. (2010) 'Treating neuropsychiatric symptoms in dementia with Lewy bodies: a randomized controlled-trial', *Alzheimer Dis Assoc Disord*, 24(4), pp. 360-4.
Cummings, J.L., Mega, M., Gray, K., Rosenberg-Thompson, S., Carusi, D.A. and Gornbein, J. (1994) 'The Neuropsychiatric Inventory: comprehensive assessment of psychopathology in dementia', *Neurology*, 44(12), pp. 2308-14.
Cusick, C.G., Scripter, J.L., Darensbourg, J.G. and Weber, J.T. (1993) 'Chemoarchitectonic subdivisions of the visual pulvinar in monkeys and their connectional relations with the middle temporal and rostral dorsolateral visual areas, MT and DLr', *J Comp Neurol*, 336(1), pp. 1-30.
DaDalt, O. and Coughlin, J.F. (2016) 'Managing Financial Well-Being in the Shadow of Alzheimer's Disease', *Public Policy & Aging Report*, 26(1), pp. 36-38.
Danzer, K.M., Haasen, D., Karow, A.R., Moussaud, S., Habeck, M., Giese, A., Kretzschmar, H., Hengerer, B. and Kostka, M. (2007) 'Different species of alpha-synuclein oligomers induce calcium influx and seeding', *J Neurosci*, 27(34), pp. 9220-32.
Das, A.S. and Zou, W.Q. (2016) 'Prions: Beyond a Single Protein', *Clin Microbiol Rev*, 29(3), pp. 633-58.
de Jong, L.W., van der Hiele, K., Veer, I.M., Houwing, J.J., Westendorp, R.G., Bollen, E.L., de Bruin, P.W., Middelkoop, H.A., van Buchem, M.A. and van der Grond, J. (2008) 'Strongly reduced volumes of putamen and thalamus in Alzheimer's disease: an MRI study', *Brain*, 131(Pt 12), pp. 3277-85.
De Maio, A. (1999) 'Heat shock proteins: facts, thoughts, and dreams', *Shock*, 11(1), pp. 1-12.
De Reuck, J., Deramecourt, V., Cordonnier, C., Leys, D., Pasquier, F. and Maurage, C.A. (2013) 'Prevalence of cerebrovascular lesions in patients with Lewy body dementia: a neuropathological study', *Clin Neurol Neurosurg*, 115(7), pp. 1094-7.
Delli Pizzi, S., Franciotti, R., Taylor, J.P., Esposito, R., Tartaro, A., Thomas, A., Onofrj, M. and Bonanni, L. (2015a) 'Structural Connectivity is Differently Altered in Dementia with Lewy Body and Alzheimer's Disease', *Front Aging Neurosci*, 7, p. 208.
Delli Pizzi, S., Franciotti, R., Taylor, J.P., Thomas, A., Tartaro, A., Onofrj, M. and Bonanni, L. (2015b) 'Thalamic Involvement in Fluctuating Cognition in Dementia with Lewy Bodies: Magnetic Resonance Evidences', *Cereb Cortex*, 25(10), pp. 3682-9.
Delli Pizzi, S., Maruotti, V., Taylor, J.P., Franciotti, R., Caulo, M., Tartaro, A., Thomas, A., Onofrj, M. and Bonanni, L. (2014) 'Relevance of subcortical visual pathways disruption to visual symptoms in dementia with Lewy bodies', *Cortex*, 59, pp. 12-21.

Denison, R.N., Vu, A.T., Yacoub, E., Feinberg, D.A. and Silver, M.A. (2014) 'Functional mapping of the magnocellular and parvocellular subdivisions of human LGN', *Neuroimage*, 102 Pt 2, pp. 358-69.
Derrington, A.M. and Lennie, P. (1984) 'Spatial and temporal contrast sensitivities of neurones in lateral geniculate nucleus of macaque', *J Physiol*, 357, pp. 219-40.
Desgent, S. and Ptito, M. (2012) 'Cortical GABAergic interneurons in cross-modal plasticity following early blindness', *Neural Plast*, 2012, p. 590725.
Detrait, E., Maurice, T., Hanon, E., Leclercq, K. and Lamberty, Y. (2014) 'Lack of synaptic vesicle protein SV2B protects against amyloid-beta(2)(5)(-)(3)(5)-induced oxidative stress, cholinergic deficit and cognitive impairment in mice', *Behav Brain Res*, 271, pp. 277-85.
Devos, D., Tir, M., Maurage, C.A., Waucquier, N., Defebvre, L., Defoort-Dhellemmes, S. and Destee, A. (2005) 'ERG and anatomical abnormalities suggesting retinopathy in dementia with Lewy bodies', *Neurology*, 65(7), pp. 1107-10.
Dey, M., Erskine, D., Singh, P., Tsefou, E., Taylor, J.P., McKeith, I.G., Attems, J., Thomas, A.J., Khundakar, A.A., Morris, C.M., Patterson, L., Hiskett, I., Gordon, D., Hook, R., Hanson, P.S., Rushton, S., O'Brien, J.T. (2015) 'Does Abnormal Ventral Visual Stream Function Underlie Recurrent Complex Visual Hallucinations in Dementia with Lewy Bodies?', *American Journal of Neurodegenerative Diseases*, 4((S1)).
Diederich, N.J., Goetz, C.G., Raman, R., Pappert, E.J., Leurgans, S. and Piery, V. (1998) 'Poor visual discrimination and visual hallucinations in Parkinson's disease', *Clin Neuropharmacol*, 21(5), pp. 289-95.
Diederich, N.J., Goetz, C.G. and Stebbins, G.T. (2005) 'Repeated visual hallucinations in Parkinson's disease as disturbed external/internal perceptions: Focused review and a new integrative model', *Movement Disorders*, 20(2), pp. 130-140.
Diederich, N.J., Pieri, V. and Goetz, C.G. (2003) 'Coping strategies for visual hallucinations in Parkinson's disease', *Movement Disorders*, 18(7), pp. 831-832.
Diederich, N.J., Stebbins, G., Schiltz, C. and Goetz, C.G. (2014) 'Are patients with Parkinson's disease blind to blindsight?', *Brain*, 137(Pt 6), pp. 1838-49.
Donaghy, P., Thomas, A.J. and O'Brien, J.T. (2015) 'Amyloid PET Imaging in Lewy body disorders', *Am J Geriatr Psychiatry*, 23(1), pp. 23-37.
Donnemiller, E., Heilmann, J., Wenning, G.K., Berger, W., Decristoforo, C., Moncayo, R., Poewe, W. and Ransmayr, G. (1997) 'Brain perfusion scintigraphy with 99mTc-HMPAO or 99mTc-ECD and 123I-beta-CIT single-photon emission tomography in dementia of the Alzheimer-type and diffuse Lewy body disease', *Eur J Nucl Med*, 24(3), pp. 320-5.
Dorph-Petersen, K.-A., Caric, D., Saghafi, R., Zhang, W., Sampson, A.R. and Lewis, D.A. (2009) 'Volume and neuron number of the lateral geniculate nucleus in schizophrenia and mood disorders', *Acta Neuropathologica*, 117(4), pp. 369-384.
Dubois, B., Feldman, H.H., Jacova, C., Hampel, H., Molinuevo, J.L., Blennow, K., DeKosky, S.T., Gauthier, S., Selkoe, D., Bateman, R., Cappa, S., Crutch, S., Engelborghs, S., Frisoni, G.B., Fox, N.C., Galasko, D., Habert, M.O., Jicha, G.A., Nordberg, A., Pasquier, F., Rabinovici, G., Robert, P., Rowe, C., Salloway, S., Sarazin, M., Epelbaum, S., de Souza, L.C., Vellas, B., Visser, P.J., Schneider, L., Stern, Y., Scheltens, P. and Cummings, J.L. (2014) 'Advancing research diagnostic criteria for Alzheimer's disease: the IWG-2 criteria', *Lancet Neurol*, 13(6), pp. 614-29.
Dugger, B.N., Murray, M.E., Boeve, B.F., Parisi, J.E., Benarroch, E.E., Ferman, T.J. and Dickson, D.W. (2012) 'Neuropathological analysis of brainstem cholinergic and catecholaminergic nuclei in relation to rapid eye movement (REM) sleep behaviour disorder', *Neuropathol Appl Neurobiol*, 38(2), pp. 142-52.
Dugger, B.N., Tu, M., Murray, M.E. and Dickson, D.W. (2011) 'Disease specificity and pathologic progression of tau pathology in brainstem nuclei of Alzheimer's disease and progressive supranuclear palsy', *Neurosci Lett*, 491(2), pp. 122-6.
Eikelenboom, P., Hack, C.E., Rozemuller, J.M. and Stam, F.C. (1988) 'Complement activation in amyloid plaques in Alzheimer's dementia', *Virchows Archiv B*, 56(1), pp. 259-262.

Eikelenboom, P. and Stam, F.C. (1984) 'An immunohistochemical study on cerebral vascular and senile plaque amyloid in Alzheimer's dementia', *Virchows Arch B Cell Pathol Incl Mol Pathol*, 47(1), pp. 17-25.
Eliezer, D., Kutluay, E., Bussell, R., Jr. and Browne, G. (2001) 'Conformational properties of alpha-synuclein in its free and lipid-associated states', *J Mol Biol*, 307(4), pp. 1061-73.
Erickson, S.L., Melchitzky, D.S. and Lewis, D.A. (2004) 'Subcortical afferents to the lateral mediodorsal thalamus in cynomolgus monkeys', *Neuroscience*, 129(3), pp. 675-90.
Erskine, D. and Khundakar, A.A. (2016) 'Stereological approaches to dementia research using human brain tissue', *J Chem Neuroanat*.
Erskine, D., Taylor, J.P., Firbank, M.J., Patterson, L., Onofrj, M., O'Brien, J.T., McKeith, I.G., Attems, J., Thomas, A.J., Morris, C.M. and Khundakar, A.A. (2016) 'Changes to the lateral geniculate nucleus in Alzheimer's disease but not dementia with Lewy bodies', *Neuropathol Appl Neurobiol*, 42(4), pp. 366-76.
Eugene, C., Laghaei, R. and Mousseau, N. (2014) 'Early oligomerization stages for the non-amyloid component of alpha-synuclein amyloid', *J Chem Phys*, 141(13), p. 135103.
Eustache, P., Nemmi, F., Saint-Aubert, L., Pariente, J. and Peran, P. (2016) 'Multimodal Magnetic Resonance Imaging in Alzheimer's Disease Patients at Prodromal Stage', *J Alzheimers Dis*, 50(4), pp. 1035-50.
Factor, S.A., Scullin, M.K., Sollinger, A.B., Land, J.O., Wood-Siverio, C., Zanders, L., Freeman, A., Bliwise, D.L., McDonald, W.M. and Goldstein, F.C. (2014) 'Cognitive correlates of hallucinations and delusions in Parkinson's disease', *J Neurol Sci*, 347(1-2), pp. 316-21.
Fahn, S. and Elotion, R. (1987) 'UPDRS Program Members. Unified Parkinson's disease rating scale. vol 2. Florham Park'. NJ: Macmillan Healthcare Information.
Farina, C., Aloisi, F. and Meinl, E. (2007) 'Astrocytes are active players in cerebral innate immunity', *Trends Immunol*, 28(3), pp. 138-45.
Fauvet, B., Mbefo, M.K., Fares, M.B., Desobry, C., Michael, S., Ardah, M.T., Tsika, E., Coune, P., Prudent, M., Lion, N., Eliezer, D., Moore, D.J., Schneider, B., Aebischer, P., El-Agnaf, O.M., Masliah, E. and Lashuel, H.A. (2012) 'alpha-Synuclein in central nervous system and from erythrocytes, mammalian cells, and Escherichia coli exists predominantly as disordered monomer', *J Biol Chem*, 287(19), pp. 15345-64.
Fenalti, G., Law, R.H., Buckle, A.M., Langendorf, C., Tuck, K., Rosado, C.J., Faux, N.G., Mahmood, K., Hampe, C.S., Banga, J.P., Wilce, M., Schmidberger, J., Rossjohn, J., El-Kabbani, O., Pike, R.N., Smith, A.I., Mackay, I.R., Rowley, M.J. and Whisstock, J.C. (2007) 'GABA production by glutamic acid decarboxylase is regulated by a dynamic catalytic loop', *Nat Struct Mol Biol*, 14(4), pp. 280-6.
Fenelon, G., Mahieux, F., Huon, R. and Ziegler, M. (2000) 'Hallucinations in Parkinson's disease: prevalence, phenomenology and risk factors', *Brain*, 123 ( Pt 4), pp. 733-45.
Ffytche, D.H. (2005) 'Visual hallucinations and the Charles Bonnet syndrome', *Curr Psychiatry Rep*, 7(3), pp. 168-79.
ffytche, D.H. (2009) 'Visual hallucinations in eye disease', *Curr Opin Neurol*, 22(1), pp. 28-35.
Fischer, J. and Whitney, D. (2012) 'Attention gates visual coding in the human pulvinar', *Nat Commun*, 3, p. 1051.
Fowler, M.W. and Staras, K. (2015) 'Synaptic vesicle pools: Principles, properties and limitations', *Exp Cell Res*, 335(2), pp. 150-6.
Franciotti, R., Falasca, N.W., Bonanni, L., Anzellotti, F., Maruotti, V., Comani, S., Thomas, A., Tartaro, A., Taylor, J.P. and Onofrj, M. (2013) 'Default network is not hypoactive in dementia with fluctuating cognition: an Alzheimer disease/dementia with Lewy bodies comparison', *Neurobiol Aging*, 34(4), pp. 1148-58.
Frederick, J.M., Rayborn, M.E., Laties, A.M., Lam, D.M. and Hollyfield, J.G. (1982) 'Dopaminergic neurons in the human retina', *J Comp Neurol*, 210(1), pp. 65-79.
Frydman, J. and Hartl, F.U. (1996) 'Principles of chaperone-assisted protein folding: differences between in vitro and in vivo mechanisms', *Science*, 272(5267), pp. 1497-502.

Fujishiro, H., Iseki, E., Kasanuki, K., Chiba, Y., Ota, K., Murayama, N. and Sato, K. (2013) 'A follow up study of non-demented patients with primary visual cortical hypometabolism: prodromal dementia with Lewy bodies', *J Neurol Sci*, 334(1-2), pp. 48-54.
Gallagher, D.A., Parkkinen, L., O'Sullivan, S.S., Spratt, A., Shah, A., Davey, C.C., Bremner, F.D., Revesz, T., Williams, D.R., Lees, A.J. and Schrag, A. (2011) 'Testing an aetiological model of visual hallucinations in Parkinson's disease', *Brain*, 134(Pt 11), pp. 3299-309.
Galvin, J.E., Giasson, B., Hurtig, H.I., Lee, V.M. and Trojanowski, J.Q. (2000) 'Neurodegeneration with brain iron accumulation, type 1 is characterized by alpha-, beta-, and gamma-synuclein neuropathology', *Am J Pathol*, 157(2), pp. 361-8.
Gandhi, N.J. and Katnani, H.A. (2011) 'Motor functions of the superior colliculus', *Annu Rev Neurosci*, 34, pp. 205-31.
Gao, X., Carroni, M., Nussbaum-Krammer, C., Mogk, A., Nillegoda, N.B., Szlachcic, A., Guilbride, D.L., Saibil, H.R., Mayer, M.P. and Bukau, B. (2015) 'Human Hsp70 Disaggregase Reverses Parkinson's-Linked alpha-Synuclein Amyloid Fibrils', *Mol Cell*, 59(5), pp. 781-93.
Garwood, C.J., Ratcliffe, L.E., Simpson, J.E., Heath, P.R., Ince, P.G. and Wharton, S.B. (2016) 'Review: Astrocytes in Alzheimer's disease and other age-associated dementias; a supporting player with a central role', *Neuropathol Appl Neurobiol*.
Gattass, R., Galkin, T.W., Desimone, R. and Ungerleider, L.G. (2014) 'Subcortical Connections of Area V4 in the Macaque', *Journal of Comparative Neurology*, 522(8), pp. 1941-1965.
Ghitani, N., Bayguinov, P.O., Vokoun, C.R., McMahon, S., Jackson, M.B. and Basso, M.A. (2014) 'Excitatory synaptic feedback from the motor layer to the sensory layers of the superior colliculus', *J Neurosci*, 34(20), pp. 6822-33.
Giasson, B.I., Uryu, K., Trojanowski, J.Q. and Lee, V.M. (1999) 'Mutant and wild type human alpha-synucleins assemble into elongated filaments with distinct morphologies in vitro', *J Biol Chem*, 274(12), pp. 7619-22.
Gibb, W.R. and Lees, A.J. (1988) 'A comparison of clinical and pathological features of young- and old-onset Parkinson's disease', *Neurology*, 38(9), pp. 1402-6.
Gilman, S., Wenning, G.K., Low, P.A., Brooks, D.J., Mathias, C.J., Trojanowski, J.Q., Wood, N.W., Colosimo, C., Durr, A., Fowler, C.J., Kaufmann, H., Klockgether, T., Lees, A., Poewe, W., Quinn, N., Revesz, T., Robertson, D., Sandroni, P., Seppi, K. and Vidailhet, M. (2008) 'Second consensus statement on the diagnosis of multiple system atrophy', *Neurology*, 71(9), pp. 670-6.
Glimcher, P.W. and Sparks, D.L. (1992) 'Movement selection in advance of action in the superior colliculus', *Nature*, 355(6360), pp. 542-5.
Gnanalingham, K.K., Byrne, E.J., Thornton, A., Sambrook, M.A. and Bannister, P. (1997) 'Motor and cognitive function in Lewy body dementia: comparison with Alzheimer's and Parkinson's diseases', *J Neurol Neurosurg Psychiatry*, 62(3), pp. 243-52.
Goasdoue, K., Awabdy, D., Bjorkman, S.T. and Miller, S. (2016) 'Standard loading controls are not reliable for Western blot quantification across brain development or in pathological conditions', *Electrophoresis*, 37(4), pp. 630-4.
Goedert, M. (2015) 'NEURODEGENERATION. Alzheimer's and Parkinson's diseases: The prion concept in relation to assembled Abeta, tau, and alpha-synuclein', *Science*, 349(6248), p. 1255555.
Gomez-Isla, T., Price, J.L., McKeel, D.W., Jr., Morris, J.C., Growdon, J.H. and Hyman, B.T. (1996) 'Profound loss of layer II entorhinal cortex neurons occurs in very mild Alzheimer's disease', *J Neurosci*, 16(14), pp. 4491-500.
Gomperts, S.N. (2014) 'Imaging the role of amyloid in PD dementia and dementia with Lewy bodies', *Curr Neurol Neurosci Rep*, 14(8), p. 472.
Gonzalez, D., Satriotomo, I., Miki, T., Lee, K.Y., Yokoyama, T., Touge, T., Matsumoto, Y., Li, H.P., Kuriyama, S. and Takeuchi, Y. (2006) 'Changes of parvalbumin immunoreactive neurons and GFAP immunoreactive astrocytes in the rat lateral geniculate nucleus following monocular enucleation', *Neurosci Lett*, 395(2), pp. 149-54.

Gordon, S.L., Harper, C.B., Smillie, K.J. and Cousin, M.A. (2016) 'A Fine Balance of Synaptophysin Levels Underlies Efficient Retrieval of Synaptobrevin II to Synaptic Vesicles', *PLoS One*, 11(2), p. e0149457.
Gracitelli, C.P., Abe, R.Y., Diniz-Filho, A., Vaz-de-Lima, F.B., Paranhos, A., Jr. and Medeiros, F.A. (2015) 'Ophthalmology issues in schizophrenia', *Curr Psychiatry Rep*, 17(5), p. 28.
Grinberg, L.T. and Thal, D.R. (2010) 'Vascular pathology in the aged human brain', *Acta Neuropathol*, 119(3), pp. 277-90.
Grothe, M.J., Schuster, C., Bauer, F., Heinsen, H., Prudlo, J. and Teipel, S.J. (2014) 'Atrophy of the cholinergic basal forebrain in dementia with Lewy bodies and Alzheimer's disease dementia', *J Neurol*, 261(10), pp. 1939-48.
Gundersen, H.J. and Jensen, E.B. (1987) 'The efficiency of systematic sampling in stereology and its prediction', *J Microsc*, 147(Pt 3), pp. 229-63.
Gunderson, C.H. and Hoyt, W.F. (1971) 'Geniculate hemianopia: incongruous homonymous field defects in two patients with partial lesions of the lateral geniculate nucleus', *J Neurol Neurosurg Psychiatry*, 34(1), pp. 1-6.
Gurry, T., Ullman, O., Fisher, C.K., Perovic, I., Pochapsky, T. and Stultz, C.M. (2013) 'The dynamic structure of alpha-synuclein multimers', *J Am Chem Soc*, 135(10), pp. 3865-72.
Harding, A.J., Broe, G.A. and Halliday, G.M. (2002) 'Visual hallucinations in Lewy body disease relate to Lewy bodies in the temporal lobe', *Brain*, 125(Pt 2), pp. 391-403.
Harting, J.K., Huerta, M.F., Hashikawa, T. and van Lieshout, D.P. (1991) 'Projection of the mammalian superior colliculus upon the dorsal lateral geniculate nucleus: organization of tectogeniculate pathways in nineteen species', *J Comp Neurol*, 304(2), pp. 275-306.
Hartl, F.U. and Hayer-Hartl, M. (2002) 'Molecular chaperones in the cytosol: from nascent chain to folded protein', *Science*, 295(5561), pp. 1852-8.
Haug, H., Kuhl, S., Mecke, E., Sass, N.L. and Wasner, K. (1984) 'The significance of morphometric procedures in the investigation of age changes in cytoarchitectonic structures of human brain', *J Hirnforsch*, 25(4), pp. 353-74.
Heese, K., Nagai, Y. and Sawada, T. (2001) 'Identification of a new synaptic vesicle protein 2B mRNA transcript which is up-regulated in neurons by amyloid beta peptide fragment (1-42)', *Biochem Biophys Res Commun*, 289(5), pp. 924-8.
Heidebrink, J.L. (2002) 'Is dementia with Lewy bodies the second most common cause of dementia?', *J Geriatr Psychiatry Neurol*, 15(4), pp. 182-7.
Heitz, C., Noblet, V., Cretin, B., Philippi, N., Kremer, L., Stackfleth, M., Hubele, F., Armspach, J.P., Namer, I. and Blanc, F. (2015) 'Neural correlates of visual hallucinations in dementia with Lewy bodies', *Alzheimers Res Ther*, 7(1), p. 6.
Hely, M.A., Reid, W.G., Adena, M.A., Halliday, G.M. and Morris, J.G. (2008) 'The Sydney multicenter study of Parkinson's disease: the inevitability of dementia at 20 years', *Mov Disord*, 23(6), pp. 837-44.
Henderson, J.M., Carpenter, K., Cartwright, H. and Halliday, G.M. (2000) 'Loss of thalamic intralaminar nuclei in progressive supranuclear palsy and Parkinson's disease: clinical and therapeutic implications', *Brain*, 123 ( Pt 7), pp. 1410-21.
Henderson, T., Georgiou-Karistianis, N., White, O., Millist, L., Williams, D.R., Churchyard, A. and Fielding, J. (2011) 'Inhibitory control during smooth pursuit in Parkinson's disease and Huntington's disease', *Mov Disord*, 26(10), pp. 1893-9.
Hendry, S.H. and Reid, R.C. (2000) 'The koniocellular pathway in primate vision', *Annu Rev Neurosci*, 23, pp. 127-53.
Henstridge, C.M., Jackson, R.J., Kim, J.M., Herrmann, A.G., Wright, A.K., Harris, S.E., Bastin, M.E., Starr, J.M., Wardlaw, J., Gillingwater, T.H., Smith, C., McKenzie, C.A., Cox, S.R., Deary, I.J. and Spires-Jones, T.L. (2015) 'Post-mortem brain analyses of the Lothian Birth Cohort 1936: extending lifetime cognitive and brain phenotyping to the level of the synapse', *Acta Neuropathol Commun*, 3, p. 53.
Hepp, D.H., Ruiter, A.M., Galis, Y., Voorn, P., Rozemuller, A.J., Berendse, H.W., Foncke, E.M. and van de Berg, W.D. (2013) 'Pedunculopontine cholinergic cell loss in hallucinating Parkinson disease

patients but not in dementia with Lewy bodies patients', *J Neuropathol Exp Neurol*, 72(12), pp. 1162-70.
Herculano-Houzel, S., von Bartheld, C.S., Miller, D.J. and Kaas, J.H. (2015) 'How to count cells: the advantages and disadvantages of the isotropic fractionator compared with stereology', *Cell Tissue Res*, 360(1), pp. 29-42.
Hernowo, A.T., Boucard, C.C., Jansonius, N.M., Hooymans, J.M. and Cornelissen, F.W. (2011) 'Automated morphometry of the visual pathway in primary open-angle glaucoma', *Invest Ophthalmol Vis Sci*, 52(5), pp. 2758-66.
Herva, M.E. and Spillantini, M.G. (2015) 'Parkinson's disease as a member of Prion-like disorders', *Virus Res*, 207, pp. 38-46.
Hickey, T.L. and Guillery, R.W. (1979) 'Variability of laminar patterns in the human lateral geniculate nucleus', *J Comp Neurol*, 183(2), pp. 221-46.
Higashi, S., Iseki, E., Yamamoto, R., Minegishi, M., Hino, H., Fujisawa, K., Togo, T., Katsuse, O., Uchikado, H., Furukawa, Y., Kosaka, K. and Arai, H. (2007) 'Concurrence of TDP-43, tau and alpha-synuclein pathology in brains of Alzheimer's disease and dementia with Lewy bodies', *Brain Res*, 1184, pp. 284-94.
Highley, J.R., Walker, M.A., Crow, T.J., Esiri, M.M. and Harrison, P.J. (2003) 'Low medial and lateral right pulvinar volumes in schizophrenia: a postmortem study', *Am J Psychiatry*, 160(6), pp. 1177-9.
Hirai, T. and Jones, E.G. (1989) 'A new parcellation of the human thalamus on the basis of histochemical staining', *Brain Res Brain Res Rev*, 14(1), pp. 1-34.
Ho, C.Y., Troncoso, J.C., Knox, D., Stark, W. and Eberhart, C.G. (2014) 'Beta-Amyloid, Phospho-Tau and Alpha-Synuclein Deposits Similar to Those in the Brain Are Not Identified in the Eyes of Alzheimer's and Parkinson's Disease Patients', *Brain Pathology*, 24(1), pp. 25-32.
Hof, P.R. and Morrison, J.H. (1990) 'Quantitative analysis of a vulnerable subset of pyramidal neurons in Alzheimer's disease: II. Primary and secondary visual cortex', *J Comp Neurol*, 301(1), pp. 55-64.
Hofbauer, A. and Drager, U.C. (1985) 'Depth segregation of retinal ganglion cells projecting to mouse superior colliculus', *J Comp Neurol*, 234(4), pp. 465-74.
Holers, V.M. (2014) 'Complement and its receptors: new insights into human disease', *Annu Rev Immunol*, 32, pp. 433-59.
Howlett, D.R., Whitfield, D., Johnson, M., Attems, J., O'Brien, J.T., Aarsland, D., Lai, M.K., Lee, J.H., Chen, C., Ballard, C., Hortobagyi, T. and Francis, P.T. (2015) 'Regional Multiple Pathology Scores Are Associated with Cognitive Decline in Lewy Body Dementias', *Brain Pathol*, 25(4), pp. 401-8.
Hudspeth, A.J., Jessell, T.M., Kandel, E.R., Schwartz, J.H. and Siegelbaum, S.A. (2013) *Principles of neural science*.
Hugo, J. and Ganguli, M. (2014) 'Dementia and cognitive impairment: epidemiology, diagnosis, and treatment', *Clin Geriatr Med*, 30(3), pp. 421-42.
Hunt, C.A., Schenker, L.J. and Kennedy, M.B. (1996) 'PSD-95 is associated with the postsynaptic density and not with the presynaptic membrane at forebrain synapses', *J Neurosci*, 16(4), pp. 1380-8.
Hurd, M.D., Martorell, P., Delavande, A., Mullen, K.J. and Langa, K.M. (2013) 'Monetary costs of dementia in the United States', *New England Journal of Medicine*, 368(14), pp. 1326-1334.
Hyman, B.T., Phelps, C.H., Beach, T.G., Bigio, E.H., Cairns, N.J., Carrillo, M.C., Dickson, D.W., Duyckaerts, C., Frosch, M.P., Masliah, E., Mirra, S.S., Nelson, P.T., Schneider, J.A., Thal, D.R., Thies, B., Trojanowski, J.Q., Vinters, H.V. and Montine, T.J. (2012) 'National Institute on Aging-Alzheimer's Association guidelines for the neuropathologic assessment of Alzheimer's disease', *Alzheimers & Dementia*, 8(1), pp. 1-13.
Imamura, T., Ishii, K., Hirono, N., Hashimoto, M., Tanimukai, S., Kazuai, H., Hanihara, T., Sasaki, M. and Mori, E. (1999) 'Visual hallucinations and regional cerebral metabolism in dementia with Lewy bodies (DLB)', *Neuroreport*, 10(9), pp. 1903-7.
Imamura, T., Ishii, K., Sasaki, M., Kitagaki, H., Yamaji, S., Hirono, N., Shimomura, T., Hashimoto, M., Tanimukai, S., Kazui, H. and Mori, E. (1997) 'Regional cerebral glucose metabolism in dementia with

Lewy bodies and Alzheimer's disease: a comparative study using positron emission tomography', *Neurosci Lett*, 235(1-2), pp. 49-52.
Inayat, S., Barchini, J., Chen, H., Feng, L., Liu, X. and Cang, J. (2015) 'Neurons in the most superficial lamina of the mouse superior colliculus are highly selective for stimulus direction', *J Neurosci*, 35(20), pp. 7992-8003.
Irwin, D.J. (2016) 'Tauopathies as clinicopathological entities', *Parkinsonism Relat Disord*, 22 Suppl 1, pp. S29-33.
Isa, T. and Hall, W.C. (2009) 'Exploring the superior colliculus in vitro', *J Neurophysiol*, 102(5), pp. 2581-93.
Ishii, K., Hosokawa, C., Hyodo, T., Sakaguchi, K., Usami, K., Shimamoto, K., Hosono, M., Yamazoe, Y. and Murakami, T. (2015) 'Regional glucose metabolic reduction in dementia with Lewy bodies is independent of amyloid deposition', *Ann Nucl Med*, 29(1), pp. 78-83.
Ishii, K., Imamura, T., Sasaki, M., Yamaji, S., Sakamoto, S., Kitagaki, H., Hashimoto, M., Hirono, N., Shimomura, T. and Mori, E. (1998) 'Regional cerebral glucose metabolism in dementia with Lewy bodies and Alzheimer's disease', *Neurology*, 51(1), pp. 125-30.
Ishiki, A., Kamada, M., Kawamura, Y., Terao, C., Shimoda, F., Tomita, N., Arai, H. and Furukawa, K. (2016) 'Glial fibrillar acidic protein in the cerebrospinal fluid of Alzheimer's disease, dementia with Lewy bodies, and frontotemporal lobar degeneration', *J Neurochem*, 136(2), pp. 258-61.
Jahn, R., Schiebler, W., Ouimet, C. and Greengard, P. (1985) 'A 38,000-dalton membrane protein (p38) present in synaptic vesicles', *Proc Natl Acad Sci U S A*, 82(12), pp. 4137-41.
Janelidze, S., Hertze, J., Zetterberg, H., Landqvist Waldo, M., Santillo, A., Blennow, K. and Hansson, O. (2016) 'Cerebrospinal fluid neurogranin and YKL-40 as biomarkers of Alzheimer's disease', *Ann Clin Transl Neurol*, 3(1), pp. 12-20.
Janzen, J., van 't Ent, D., Lemstra, A.W., Berendse, H.W., Barkhof, F. and Foncke, E.M. (2012) 'The pedunculopontine nucleus is related to visual hallucinations in Parkinson's disease: preliminary results of a voxel-based morphometry study', *J Neurol*, 259(1), pp. 147-54.
Jayakumar, J., Dreher, B. and Vidyasagar, T.R. (2013) 'Tracking blue cone signals in the primate brain', *Clin Exp Optom*, 96(3), pp. 259-66.
Jeffries, A.M., Killian, N.J. and Pezaris, J.S. (2014) 'Mapping the primate lateral geniculate nucleus: a review of experiments and methods', *J Physiol Paris*, 108(1), pp. 3-10.
Jellinger, K., Danielczyk, W., Fischer, P. and Gabriel, E. (1990) 'Clinicopathological analysis of dementia disorders in the elderly', *J Neurol Sci*, 95(3), pp. 239-58.
Jellinger, K.A. (2003) 'Neuropathological spectrum of synucleinopathies', *Mov Disord*, 18 Suppl 6, pp. S2-12.
Jellinger, K.A. and Attems, J. (2007) 'Neuropathological evaluation of mixed dementia', *J Neurol Sci*, 257(1-2), pp. 80-7.
Jellinger, K.A. and Attems, J. (2008) 'Prevalence and impact of vascular and Alzheimer pathologies in Lewy body disease', *Acta Neuropathol*, 115(4), pp. 427-36.
Jellinger, K.A. and Attems, J. (2015) 'Challenges of multimorbidity of the aging brain: a critical update', *J Neural Transm (Vienna)*, 122(4), pp. 505-21.
Jembrek, M.J. and Vlainic, J. (2015) 'GABA Receptors: Pharmacological Potential and Pitfalls', *Curr Pharm Des*, 21(34), pp. 4943-59.
Johansen, J.S., Stoltenberg, M., Hansen, M., Florescu, A., Horslev-Petersen, K., Lorenzen, I. and Price, P.A. (1999) 'Serum YKL-40 concentrations in patients with rheumatoid arthritis: relation to disease activity', *Rheumatology (Oxford)*, 38(7), pp. 618-26.
Jones, E.G. (1998) 'A new view of specific and nonspecific thalamocortical connections', *Adv Neurol*, 77, pp. 49-71; discussion 72-3.
Jones, E.G. (2007) *The Thalamus*. Second edn. Cambridge: Cambridge University Press.
Jones, E.G. (2012) *The thalamus*. Springer Science & Business Media.
Jones, E.G. and Hendry, S.H. (1989) 'Differential Calcium Binding Protein Immunoreactivity Distinguishes Classes of Relay Neurons in Monkey Thalamic Nuclei', *Eur J Neurosci*, 1(3), pp. 222-246.

Jones, E.G., Wise, S.P. and Coulter, J.D. (1979) 'Differential thalamic relationships of sensory-motor and parietal cortical fields in monkeys', *J Comp Neurol*, 183(4), pp. 833-81.
Jorm, A.F. and Jolley, D. (1998) 'The incidence of dementia: a meta-analysis', *Neurology*, 51(3), pp. 728-33.
Josephs, K.A., Murray, M.E., Whitwell, J.L., Parisi, J.E., Petrucelli, L., Jack, C.R., Petersen, R.C. and Dickson, D.W. (2014) 'Staging TDP-43 pathology in Alzheimer's disease', *Acta Neuropathol*, 127(3), pp. 441-50.
Josephs, K.A., Murray, M.E., Whitwell, J.L., Tosakulwong, N., Weigand, S.D., Petrucelli, L., Liesinger, A.M., Petersen, R.C., Parisi, J.E. and Dickson, D.W. (2016) 'Updated TDP-43 in Alzheimer's disease staging scheme', *Acta Neuropathol*, 131(4), pp. 571-85.
Josephson, S.A. and Kirsch, H.E. (2006) 'Complex visual hallucinations as post-ictal cortical release phenomena', *Neurocase*, 12(2), pp. 107-10.
Kaas, J.H. and Lyon, D.C. (2007) 'Pulvinar contributions to the dorsal and ventral streams of visual processing in primates', *Brain Res Rev*, 55(2), pp. 285-96.
Kalia, L.V. and Kalia, S.K. (2015) 'alpha-Synuclein and Lewy pathology in Parkinson's disease', *Curr Opin Neurol*, 28(4), pp. 375-81.
Kantarci, K., Avula, R., Senjem, M.L., Samikoglu, A.R., Zhang, B., Weigand, S.D., Przybelski, S.A., Edmonson, H.A., Vemuri, P., Knopman, D.S., Ferman, T.J., Boeve, B.F., Petersen, R.C. and Jack, C.R., Jr. (2010) 'Dementia with Lewy bodies and Alzheimer disease: neurodegenerative patterns characterized by DTI', *Neurology*, 74(22), pp. 1814-21.
Kao, A.W., Racine, C.A., Quitania, L.C., Kramer, J.H., Christine, C.W. and Miller, B.L. (2009) 'Cognitive and neuropsychiatric profile of the synucleinopathies: Parkinson disease, dementia with Lewy bodies, and multiple system atrophy', *Alzheimer Dis Assoc Disord*, 23(4), pp. 365-70.
Karnath, H.O., Himmelbach, M. and Rorden, C. (2002) 'The subcortical anatomy of human spatial neglect: putamen, caudate nucleus and pulvinar', *Brain*, 125(Pt 2), pp. 350-60.
Kasai, T., Tokuda, T., Yamaguchi, N., Watanabe, Y., Kametani, F., Nakagawa, M. and Mizuno, T. (2008) 'Cleavage of normal and pathological forms of alpha-synuclein by neurosin in vitro', *Neurosci Lett*, 436(1), pp. 52-6.
Kastner, S., O'Connor, D.H., Fukui, M.M., Fehd, H.M., Herwig, U. and Pinsk, M.A. (2004) 'Functional imaging of the human lateral geniculate nucleus and pulvinar', *J Neurophysiol*, 91(1), pp. 438-48.
Keith, D. and El-Husseini, A. (2008) 'Excitation Control: Balancing PSD-95 Function at the Synapse', *Front Mol Neurosci*, 1, p. 4.
Kemper, C. and Atkinson, J.P. (2007) 'T-cell regulation: with complements from innate immunity', *Nat Rev Immunol*, 7(1), pp. 9-18.
Khundakar, A., Morris, C., Oakley, A., McMeekin, W. and Thomas, A.J. (2009) 'Morphometric analysis of neuronal and glial cell pathology in the dorsolateral prefrontal cortex in late-life depression', *Br J Psychiatry*, 195(2), pp. 163-9.
Khundakar, A.A., Hanson, P.S., Erskine, D., Lax, N.Z., Roscamp, J., Karyka, E., Tsefou, E., Singh, P., Cockell, S.J., Gribben, A., Ramsay, L., Blain, P.G., Mosimann, U.P., Lett, D.J., Elstner, M., Turnbull, D.M., Xiang, C.C., Brownstein, M.J., O'Brien, J.T., Taylor, J.P., Attems, J., Thomas, A.J., McKeith, I.G. and Morris, C.M. (2016) 'Analysis of primary visual cortex in dementia with Lewy bodies indicates GABAergic involvement associated with recurrent complex visual hallucinations', *Acta Neuropathol Commun*, 4(1), p. 66.
Kim, H.J., Jeon, B.S. and Jellinger, K.A. (2015) 'Diagnosis and differential diagnosis of MSA: boundary issues', *J Neurol*, 262(8), pp. 1801-13.
Kim, H.J., Lee, J.E., Shin, S.J., Sohn, Y.H. and Lee, P.H. (2011) 'Analysis of the substantia innominata volume in patients with Parkinson's disease with dementia, dementia with lewy bodies, and Alzheimer's disease', *J Mov Disord*, 4(2), pp. 68-72.
Kneussel, M., Haverkamp, S., Fuhrmann, J.C., Wang, H., Wassle, H., Olsen, R.W. and Betz, H. (2000) 'The gamma-aminobutyric acid type A receptor (GABAAR)-associated protein GABARAP interacts

with gephyrin but is not involved in receptor anchoring at the synapse', *Proc Natl Acad Sci U S A*, 97(15), pp. 8594-9.
Knopman, D.S., Parisi, J.E., Salviati, A., Floriach-Robert, M., Boeve, B.F., Ivnik, R.J., Smith, G.E., Dickson, D.W., Johnson, K.A., Petersen, L.E., McDonald, W.C., Braak, H. and Petersen, R.C. (2003) 'Neuropathology of cognitively normal elderly', *J Neuropathol Exp Neurol*, 62(11), pp. 1087-95.
Kodama, T. and Honda, Y. (1996) 'Acetylcholine releases of mesopontine PGO-on cells in the lateral geniculate nucleus in sleep-waking cycle and serotonergic regulation', *Prog Neuropsychopharmacol Biol Psychiatry*, 20(7), pp. 1213-27.
Kovacs, G.G., Alafuzoff, I., Al-Sarraj, S., Arzberger, T., Bogdanovic, N., Capellari, S., Ferrer, I., Gelpi, E., Kovari, V., Kretzschmar, H., Nagy, Z., Parchi, P., Seilhean, D., Soininen, H., Troakes, C. and Budka, H. (2008) 'Mixed brain pathologies in dementia: the BrainNet Europe consortium experience', *Dement Geriatr Cogn Disord*, 26(4), pp. 343-50.
Kovacs, G.G., Wagner, U., Dumont, B., Pikkarainen, M., Osman, A.A., Streichenberger, N., Leisser, I., Verchere, J., Baron, T., Alafuzoff, I., Budka, H., Perret-Liaudet, A. and Lachmann, I. (2012) 'An antibody with high reactivity for disease-associated alpha-synuclein reveals extensive brain pathology', *Acta Neuropathol*, 124(1), pp. 37-50.
Kovari, E., Horvath, J. and Bouras, C. (2009) 'Neuropathology of Lewy body disorders', *Brain Res Bull*, 80(4-5), pp. 203-10.
Krauzlis, R. and Dill, N. (2002) 'Neural correlates of target choice for pursuit and saccades in the primate superior colliculus', *Neuron*, 35(2), pp. 355-63.
Krauzlis, R.J., Lovejoy, L.P. and Zenon, A. (2013) 'Superior colliculus and visual spatial attention', *Annu Rev Neurosci*, 36, pp. 165-82.
Kromer, R., Buhmann, C., Hidding, U., Keseru, M., Keseru, D., Hassenstein, A. and Stemplewitz, B. (2016) 'Evaluation of Retinal Vessel Morphology in Patients with Parkinson's Disease Using Optical Coherence Tomography', *PLoS One*, 11(8), p. e0161136.
Kruger, R., Vieira-Saecker, A.M., Kuhn, W., Berg, D., Muller, T., Kuhnl, N., Fuchs, G.A., Storch, A., Hungs, M., Woitalla, D., Przuntek, H., Epplen, J.T., Schols, L. and Riess, O. (1999) 'Increased susceptibility to sporadic Parkinson's disease by a certain combined alpha-synuclein/apolipoprotein E genotype', *Ann Neurol*, 45(5), pp. 611-7.
Kuljis, R.O. (1994) 'Lesions in the pulvinar in patients with Alzheimer's disease', *J Neuropathol Exp Neurol*, 53(2), pp. 202-11.
Kuruva, C.S. and Reddy, P.H. (2016) 'Amyloid beta modulators and neuroprotection in Alzheimer's disease: a critical appraisal', *Drug Discov Today*.
Kusumi, I., Boku, S. and Takahashi, Y. (2015) 'Psychopharmacology of atypical antipsychotic drugs: From the receptor binding profile to neuroprotection and neurogenesis', *Psychiatry Clin Neurosci*, 69(5), pp. 243-58.
Langkammer, C., Ropele, S., Pirpamer, L., Fazekas, F. and Schmidt, R. (2014) 'MRI for iron mapping in Alzheimer's disease', *Neurodegener Dis*, 13(2-3), pp. 189-91.
Lanyon, L.J., Giaschi, D., Young, S.A., Fitzpatrick, K., Diao, L., Bjornson, B.H. and Barton, J.J. (2009) 'Combined functional MRI and diffusion tensor imaging analysis of visual motion pathways', *J Neuroophthalmol*, 29(2), pp. 96-103.
Lau, C.G. and Murthy, V.N. (2012) 'Activity-dependent regulation of inhibition via GAD67', *J Neurosci*, 32(25), pp. 8521-31.
Lazarus, M.S., Krishnan, K. and Huang, Z.J. (2015) 'GAD67 deficiency in parvalbumin interneurons produces deficits in inhibitory transmission and network disinhibition in mouse prefrontal cortex', *Cereb Cortex*, 25(5), pp. 1290-6.
Lazzell, D.R., Belizaire, R., Thakur, P., Sherry, D.M. and Janz, R. (2004) 'SV2B regulates synaptotagmin 1 by direct interaction', *J Biol Chem*, 279(50), pp. 52124-31.
Lee, B.B., Creutzfeldt, O.D. and Elepfandt, A. (1979) 'The responses of magno- and parvocellular cells of the monkey's lateral geniculate body to moving stimuli', *Exp Brain Res*, 35(3), pp. 547-57.

Lee, C.G., Da Silva, C.A., Dela Cruz, C.S., Ahangari, F., Ma, B., Kang, M.J., He, C.H., Takyar, S. and Elias, J.A. (2011) 'Role of chitin and chitinase/chitinase-like proteins in inflammation, tissue remodeling, and injury', *Annu Rev Physiol*, 73, pp. 479-501.
Lee, H.G., Jo, J., Hong, H.H., Kim, K.K., Park, J.K., Cho, S.J. and Park, C. (2016) 'State-of-the-art housekeeping proteins for quantitative western blotting: Revisiting the first draft of the human proteome', *Proteomics*, 16(13), pp. 1863-7.
Lee, J.E., Park, H.J., Park, B., Song, S.K., Sohn, Y.H., Lee, J.D. and Lee, P.H. (2010) 'A comparative analysis of cognitive profiles and white-matter alterations using voxel-based diffusion tensor imaging between patients with Parkinson's disease dementia and dementia with Lewy bodies', *Journal of Neurology Neurosurgery and Psychiatry*, 81(3), pp. 320-326.
Leuba, G. and Saini, K. (1995) 'Pathology of subcortical visual centres in relation to cortical degeneration in Alzheimer's disease', *Neuropathol Appl Neurobiol*, 21(5), pp. 410-22.
Levi, S., Logan, S.M., Tovar, K.R. and Craig, A.M. (2004) 'Gephyrin is critical for glycine receptor clustering but not for the formation of functional GABAergic synapses in hippocampal neurons', *J Neurosci*, 24(1), pp. 207-17.
Li, J.C., Sampson, G.P. and Vidyasagar, T.R. (2007) 'Interactions between luminance and colour channels in visual search and their relationship to parallel neural channels in vision', *Exp Brain Res*, 176(3), pp. 510-8.
Lippa, C.F., Smith, T.W. and Perry, E. (1999) 'Dementia with Lewy bodies: choline acetyltransferase parallels nucleus basalis pathology', *J Neural Transm (Vienna)*, 106(5-6), pp. 525-35.
Litvan, I., Goldman, J.G., Troster, A.I., Schmand, B.A., Weintraub, D., Petersen, R.C., Mollenhauer, B., Adler, C.H., Marder, K., Williams-Gray, C.H., Aarsland, D., Kulisevsky, J., Rodriguez-Oroz, M.C., Burn, D.J., Barker, R.A. and Emre, M. (2012) 'Diagnostic criteria for mild cognitive impairment in Parkinson's disease: Movement Disorder Society Task Force guidelines', *Mov Disord*, 27(3), pp. 349-56.
Lobotesis, K., Fenwick, J.D., Phipps, A., Ryman, A., Swann, A., Ballard, C., McKeith, I.G. and O'Brien, J.T. (2001) 'Occipital hypoperfusion on SPECT in dementia with Lewy bodies but not AD', *Neurology*, 56(5), pp. 643-9.
Lopez-Valdes, H.E. and Martinez-Coria, H. (2016) 'The Role of Neuroinflammation in Age-Related Dementias', *Rev Invest Clin*, 68(1), pp. 40-8.
Love, M.I., Huber, W. and Anders, S. (2014) 'Moderated estimation of fold change and dispersion for RNA-seq data with DESeq2', *Genome Biol*, 15(12), p. 550.
Love, S. and Miners, J.S. (2016) 'Cerebral Hypoperfusion and the Energy Deficit in Alzheimer's Disease', *Brain Pathology*, 26(5), pp. 607-17.
Lu, Z.L. and Dosher, B.A. (1998) 'External noise distinguishes attention mechanisms', *Vision Res*, 38(9), pp. 1183-98.
Luck, S.J. and Gold, J.M. (2008) 'The construct of attention in schizophrenia', *Biol Psychiatry*, 64(1), pp. 34-9.
Luco, C., Hoppe, A., Schweitzer, M., Vicuna, X. and Fantin, A. (1992) 'Visual field defects in vascular lesions of the lateral geniculate body', *J Neurol Neurosurg Psychiatry*, 55(1), pp. 12-5.
Lysakowski, A., Standage, G.P. and Benevento, L.A. (1986) 'Histochemical and architectonic differentiation of zones of pretectal and collicular inputs to the pulvinar and dorsal lateral geniculate nuclei in the macaque', *J Comp Neurol*, 250(4), pp. 431-48.
Mackenzie, I.R. (2000) 'Activated microglia in dementia with Lewy bodies', *Neurology*, 55(1), pp. 132-4.
Madras, B.K. (2013) 'History of the discovery of the antipsychotic dopamine D2 receptor: a basis for the dopamine hypothesis of schizophrenia', *J Hist Neurosci*, 22(1), pp. 62-78.
Mai, J.K., Majtanik, M. and Paxinos, G. (2016) *Atlas of the human brain*. Academic Press.
Makin, S.M., Redman, J., Mosimann, U.P., Dudley, R., Clarke, M.P., Colbourn, C. and Collerton, D. (2013) 'Complex visual hallucinations and attentional performance in eye disease and dementia: a test of the Perception and Attention Deficit model', *Int J Geriatr Psychiatry*, 28(12), pp. 1232-8.

Mandelkow, E.M. and Mandelkow, E. (2012) 'Biochemistry and cell biology of tau protein in neurofibrillary degeneration', *Cold Spring Harb Perspect Med*, 2(7), p. a006247.
Mandler, M., Walker, L., Santic, R., Hanson, P., Upadhaya, A.R., Colloby, S.J., Morris, C.M., Thal, D.R., Thomas, A.J., Schneeberger, A. and Attems, J. (2014) 'Pyroglutamylated amyloid-beta is associated with hyperphosphorylated tau and severity of Alzheimer's disease', *Acta Neuropathol*, 128(1), pp. 67-79.
Manford, M. and Andermann, F. (1998) 'Complex visual hallucinations. Clinical and neurobiological insights', *Brain*, 121 ( Pt 10), pp. 1819-40.
Marra, C., Quaranta, D., Profice, P., Pilato, F., Capone, F., Iodice, F., Di Lazzaro, V. and Gainotti, G. (2012) 'Central cholinergic dysfunction measured "in vivo" correlates with different behavioral disorders in Alzheimer's disease and dementia with Lewy body', *Brain Stimul*, 5(4), pp. 533-8.
Martin, P.R., Blessing, E.M., Buzas, P., Szmajda, B.A. and Forte, J.D. (2011) 'Transmission of colour and acuity signals by parvocellular cells in marmoset monkeys', *J Physiol*, 589(Pt 11), pp. 2795-812.
Masland, R.H. (2012) 'The neuronal organization of the retina', *Neuron*, 76(2), pp. 266-80.
Masliah, E., Rockenstein, E., Veinbergs, I., Sagara, Y., Mallory, M., Hashimoto, M. and Mucke, L. (2001) 'beta-amyloid peptides enhance alpha-synuclein accumulation and neuronal deficits in a transgenic mouse model linking Alzheimer's disease and Parkinson's disease', *Proc Natl Acad Sci U S A*, 98(21), pp. 12245-50.
Maurage, C.A., Ruchoux, M.M., de Vos, R., Surguchov, A. and Destee, A. (2003) 'Retinal involvement in dementia with Lewy bodies: a clue to hallucinations?', *Ann Neurol*, 54(4), pp. 542-7.
May, P.J. (2006) 'The mammalian superior colliculus: laminar structure and connections', *Prog Brain Res*, 151, pp. 321-78.
Mazoyer, B., Zago, L., Mellet, E., Bricogne, S., Etard, O., Houde, O., Crivello, F., Joliot, M., Petit, L. and Tzourio-Mazoyer, N. (2001) 'Cortical networks for working memory and executive functions sustain the conscious resting state in man', *Brain Res Bull*, 54(3), pp. 287-98.
McAleese, K.E., Walker, L., Erskine, D., Thomas, A.J., McKeith, I.G. and Attems, J. (2016) 'TDP-43 pathology in Alzheimer's disease, dementia with Lewy bodies and ageing', *Brain Pathol*.
McCann, H., Cartwright, H. and Halliday, G.M. (2016) 'Neuropathology of alpha-synuclein propagation and braak hypothesis', *Mov Disord*, 31(2), pp. 152-60.
McKeith, I., Fairbairn, A., Perry, R., Thompson, P. and Perry, E. (1992) 'Neuroleptic sensitivity in patients with senile dementia of Lewy body type', *Bmj*, 305(6855), pp. 673-8.
McKeith, I., Mintzer, J., Aarsland, D., Burn, D., Chiu, H., Cohen-Mansfield, J., Dickson, D., Dubois, B., Duda, J.E., Feldman, H., Gauthier, S., Halliday, G., Lawlor, B., Lippa, C., Lopez, O.L., Carlos Machado, J., O'Brien, J., Playfer, J., Reid, W. and International Psychogeriatric Association Expert Meeting on, D.L.B. (2004) 'Dementia with Lewy bodies', *Lancet Neurol*, 3(1), pp. 19-28.
McKeith, I., O'Brien, J., Walker, Z., Tatsch, K., Booij, J., Darcourt, J., Padovani, A., Giubbini, R., Bonuccelli, U., Volterrani, D., Holmes, C., Kemp, P., Tabet, N., Meyer, I. and Reininger, C. (2007) 'Sensitivity and specificity of dopamine transporter imaging with 123I-FP-CIT SPECT in dementia with Lewy bodies: a phase III, multicentre study', *Lancet Neurol*, 6(4), pp. 305-13.
McKeith, I., Taylor, J.P., Thomas, A., Donaghy, P. and Kane, J. (2016) 'Revisiting DLB Diagnosis: A Consideration of Prodromal DLB and of the Diagnostic Overlap With Alzheimer Disease', *J Geriatr Psychiatry Neurol*, 29(5), pp. 249-53.
McKeith, I.G. (2000) 'Clinical Lewy body syndromes', *Ann N Y Acad Sci*, 920, pp. 1-8.
McKeith, I.G. (2006) 'Consensus guidelines for the clinical and pathologic diagnosis of dementia with Lewy bodies (DLB): report of the Consortium on DLB International Workshop', *J Alzheimers Dis*, 9(3 Suppl), pp. 417-23.
McKeith, I.G., Ballard, C.G., Perry, R.H., Ince, P.G., O'Brien, J.T., Neill, D., Lowery, K., Jaros, E., Barber, R., Thompson, P., Swann, A., Fairbairn, A.F. and Perry, E.K. (2000) 'Prospective validation of consensus criteria for the diagnosis of dementia with Lewy bodies', *Neurology*, 54(5), pp. 1050-8.
McKeith, I.G., Dickson, D.W., Lowe, J., Emre, M., O'Brien, J.T., Feldman, H., Cummings, J., Duda, J.E., Lippa, C., Perry, E.K., Aarsland, D., Arai, H., Ballard, C.G., Boeve, B., Burn, D.J., Costa, D., Del Ser, T.,

Dubois, B., Galasko, D., Gauthier, S., Goetz, C.G., Gomez-Tortosa, E., Halliday, G., Hansen, L.A., Hardy, J., Iwatsubo, T., Kalaria, R.N., Kaufer, D., Kenny, R.A., Korczyn, A., Kosaka, K., Lee, V.M., Lees, A., Litvan, I., Londos, E., Lopez, O.L., Minoshima, S., Mizuno, Y., Molina, J.A., Mukaetova-Ladinska, E.B., Pasquier, F., Perry, R.H., Schulz, J.B., Trojanowski, J.Q. and Yamada, M. (2005) 'Diagnosis and management of dementia with Lewy bodies: third report of the DLB Consortium', *Neurology*, 65(12), pp. 1863-72.
McKeith, I.G., Galasko, D., Kosaka, K., Perry, E.K., Dickson, D.W., Hansen, L.A., Salmon, D.P., Lowe, J., Mirra, S.S., Byrne, E.J., Lennox, G., Quinn, N.P., Edwardson, J.A., Ince, P.G., Bergeron, C., Burns, A., Miller, B.L., Lovestone, S., Collerton, D., Jansen, E.N., Ballard, C., de Vos, R.A., Wilcock, G.K., Jellinger, K.A. and Perry, R.H. (1996) 'Consensus guidelines for the clinical and pathologic diagnosis of dementia with Lewy bodies (DLB): report of the consortium on DLB international workshop', *Neurology*, 47(5), pp. 1113-24.
McKeith, I.G., Rowan, E., Askew, K., Naidu, A., Allan, L., Barnett, N., Lett, D., Mosimann, U.P., Burn, D. and O'Brien, J.T. (2006) 'More severe functional impairment in dementia with lewy bodies than Alzheimer disease is related to extrapyramidal motor dysfunction', *Am J Geriatr Psychiatry*, 14(7), pp. 582-8.
McKhann, G.M., Knopman, D.S., Chertkow, H., Hyman, B.T., Jack, C.R., Kawas, C.H., Klunk, W.E., Koroshetz, W.J., Manly, J.J., Mayeux, R., Mohs, R.C., Morris, J.C., Rossor, M.N., Scheltens, P., Carrillo, M.C., Thies, B., Weintraub, S. and Phelps, C.H. (2011) 'The diagnosis of dementia due to Alzheimer's disease: Recommendations from the National Institute on Aging-Alzheimer's Association workgroups on diagnostic guidelines for Alzheimer's disease', *Alzheimers & Dementia*, 7(3), pp. 263-269.
Mega, M.S., Lee, L., Dinov, I.D., Mishkin, F., Toga, A.W. and Cummings, J.L. (2000) 'Cerebral correlates of psychotic symptoms in Alzheimer's disease', *J Neurol Neurosurg Psychiatry*, 69(2), pp. 167-71.
Meppelink, A.M., Koerts, J., Borg, M., Leenders, K.L. and van Laar, T. (2008) 'Visual object recognition and attention in Parkinson's disease patients with visual hallucinations', *Mov Disord*, 23(13), pp. 1906-12.
Merigan, W.H. and Maunsell, J.H. (1993) 'How parallel are the primate visual pathways?', *Annu Rev Neurosci*, 16, pp. 369-402.
Metzler-Baddeley, C., Baddeley, R.J., Lovell, P.G., Laffan, A. and Jones, R.W. (2010) 'Visual impairments in dementia with Lewy bodies and posterior cortical atrophy', *Neuropsychology*, 24(1), pp. 35-48.
Middeldorp, J. and Hol, E.M. (2011) 'GFAP in health and disease', *Prog Neurobiol*, 93(3), pp. 421-443.
Miners, J.S., Renfrew, R., Swirski, M. and Love, S. (2014a) 'Accumulation of alpha-synuclein in dementia with Lewy bodies is associated with decline in the alpha-synuclein-degrading enzymes kallikrein-6 and calpain-1', *Acta Neuropathol Commun*, 2, p. 164.
Miners, S., Moulding, H., de Silva, R. and Love, S. (2014b) 'Reduced vascular endothelial growth factor and capillary density in the occipital cortex in dementia with Lewy bodies', *Brain Pathol*, 24(4), pp. 334-43.
Minoshima, S., Foster, N.L., Sima, A.A., Frey, K.A., Albin, R.L. and Kuhl, D.E. (2001) 'Alzheimer's disease versus dementia with Lewy bodies: cerebral metabolic distinction with autopsy confirmation', *Ann Neurol*, 50(3), pp. 358-65.
Mondon, K., Gochard, A., Marque, A., Armand, A., Beauchamp, D., Prunier, C., Jacobi, D., de Toffol, B., Autret, A., Camus, V. and Hommet, C. (2007) 'Visual recognition memory differentiates dementia with Lewy bodies and Parkinson's disease dementia', *J Neurol Neurosurg Psychiatry*, 78(7), pp. 738-41.
Montero, V.M. (2000) 'Attentional activation of the visual thalamic reticular nucleus depends on 'top-down' inputs from the primary visual cortex via corticogeniculate pathways', *Brain Res*, 864(1), pp. 95-104.
Monti, J.M. (2011) 'Serotonin control of sleep-wake behavior', *Sleep Med Rev*, 15(4), pp. 269-81.

Montine, T.J., Phelps, C.H., Beach, T.G., Bigio, E.H., Cairns, N.J., Dickson, D.W., Duyckaerts, C., Frosch, M.P., Masliah, E., Mirra, S.S., Nelson, P.T., Schneider, J.A., Thal, D.R., Trojanowski, J.Q., Vinters, H.V. and Hyman, B.T. (2012) 'National Institute on Aging-Alzheimer's Association guidelines for the neuropathologic assessment of Alzheimer's disease: a practical approach', *Acta Neuropathol*, 123(1), pp. 1-11.
Moon, W.J., Kim, H.J., Roh, H.G., Choi, J.W. and Han, S.H. (2012) 'Fluid-attenuated inversion recovery hypointensity of the pulvinar nucleus of patients with Alzheimer disease: its possible association with iron accumulation as evidenced by the t2(*) map', *Korean J Radiol*, 13(6), pp. 674-83.
Moreno-Ramos, T., Benito-Leon, J., Villarejo, A. and Bermejo-Pareja, F. (2013) 'Retinal nerve fiber layer thinning in dementia associated with Parkinson's disease, dementia with Lewy bodies, and Alzheimer's disease', *J Alzheimers Dis*, 34(3), pp. 659-64.
Morris, J.C. and Cummings, J. (2005) 'Mild cognitive impairment (MCI) represents early-stage Alzheimer's disease', *J Alzheimers Dis*, 7(3), pp. 235-9; discussion 255-62.
Mosimann, U.P., Mather, G., Wesnes, K.A., O'Brien, J.T., Burn, D.J. and McKeith, I.G. (2004) 'Visual perception in Parkinson disease dementia and dementia with Lewy bodies', *Neurology*, 63(11), pp. 2091-6.
Mosimann, U.P., Muri, R.M., Burn, D.J., Felblinger, J., O'Brien, J.T. and McKeith, I.G. (2005) 'Saccadic eye movement changes in Parkinson's disease dementia and dementia with Lewy bodies', *Brain*, 128(Pt 6), pp. 1267-76.
Mosimann, U.P., Rowan, E.N., Partington, C.E., Collerton, D., Littlewood, E., O'Brien, J.T., Burn, D.J. and McKeith, I.G. (2006) 'Characteristics of visual hallucinations in Parkinson disease dementia and dementia with lewy bodies', *Am J Geriatr Psychiatry*, 14(2), pp. 153-60.
Mouton, P.R. (2011) *Unbiased stereology: a concise guide*. JHU Press.
Mouton, P.R. (2013) *Neurostereology: unbiased stereology of neural systems*. John Wiley & Sons.
Mueser, K.T., Bellack, A.S. and Brady, E.U. (1990) 'Hallucinations in schizophrenia', *Acta Psychiatr Scand*, 82(1), pp. 26-9.
Mukaetova-Ladinska, E.B., Andras, A., Milne, J., Abdel-All, Z., Borr, I., Jaros, E., Perry, R.H., Honer, W.G., Cleghorn, A., Doherty, J., McIntosh, G., Perry, E.K., Kalaria, R.N. and McKeith, I.G. (2013) 'Synaptic proteins and choline acetyltransferase loss in visual cortex in dementia with Lewy bodies', *J Neuropathol Exp Neurol*, 72(1), pp. 53-60.
Muller, J.R., Philiastides, M.G. and Newsome, W.T. (2005) 'Microstimulation of the superior colliculus focuses attention without moving the eyes', *Proc Natl Acad Sci U S A*, 102(3), pp. 524-9.
Munhoz, R.P. and Teive, H.A. (2014) 'REM sleep behaviour disorder: how useful is it for the differential diagnosis of parkinsonism?', *Clin Neurol Neurosurg*, 127, pp. 71-4.
Munkle, M.C., Waldvogel, H.J. and Faull, R.L. (2000) 'The distribution of calbindin, calretinin and parvalbumin immunoreactivity in the human thalamus', *J Chem Neuroanat*, 19(3), pp. 155-73.
Murphy, N., Killen, A., Graziadio, S., Peraza-Rodriguez, L., Baker, M., Elder, G.J., Thomas, A., McKeith, I., Rochester, L. and Taylor, J.-P. 'Early Bottom-up Visual Information Processing in Hallucinating Patients with Parkinson's Disease with Dementia: A preliminary visual evoked potential study', American Journal of Neurodegenerative Disease: Proceedings of the International Dementia with Lewy Bodies Conference 2015
Nagahama, Y., Okina, T., Suzuki, N. and Matsuda, M. (2010) 'Neural correlates of psychotic symptoms in dementia with Lewy bodies', *Brain*, 133(Pt 2), pp. 557-67.
Nakagawa, S. and Tanaka, S. (1984) 'Retinal projections to the pulvinar nucleus of the macaque monkey: a re-investigation using autoradiography', *Exp Brain Res*, 57(1), pp. 151-7.
Nedelska, Z., Schwarz, C.G., Boeve, B.F., Lowe, V.J., Reid, R.I., Przybelski, S.A., Lesnick, T.G., Gunter, J.L., Senjem, M.L., Ferman, T.J., Smith, G.E., Geda, Y.E., Knopman, D.S., Petersen, R.C., Jack, C.R., Jr. and Kantarci, K. (2015) 'White matter integrity in dementia with Lewy bodies: a voxel-based analysis of diffusion tensor imaging', *Neurobiol Aging*, 36(6), pp. 2010-7.

Nelson, P.T., Jicha, G.A., Kryscio, R.J., Abner, E.L., Schmitt, F.A., Cooper, G., Xu, L.O., Smith, C.D. and Markesbery, W.R. (2010) 'Low sensitivity in clinical diagnoses of dementia with Lewy bodies', *J Neurol*, 257(3), pp. 359-66.
Neumann, M., Adler, S., Schluter, O., Kremmer, E., Benecke, R. and Kretzschmar, H.A. (2000) 'Alpha-synuclein accumulation in a case of neurodegeneration with brain iron accumulation type 1 (NBIA-1, formerly Hallervorden-Spatz syndrome) with widespread cortical and brainstem-type Lewy bodies', *Acta Neuropathol*, 100(5), pp. 568-74.
Neuropathology Group. Medical Research Council Cognitive, F. and Aging, S. (2001) 'Pathological correlates of late-onset dementia in a multicentre, community-based population in England and Wales. Neuropathology Group of the Medical Research Council Cognitive Function and Ageing Study (MRC CFAS)', *Lancet*, 357(9251), pp. 169-75.
Nordstrom, A.L., Farde, L., Eriksson, L. and Halldin, C. (1995) 'No elevated D2 dopamine receptors in neuroleptic-naive schizophrenic patients revealed by positron emission tomography and [11C]N-methylspiperone', *Psychiatry Res*, 61(2), pp. 67-83.
Normando, E.M., Davis, B.M., De Groef, L., Nizari, S., Turner, L.A., Ravindran, N., Pahlitzsch, M., Brenton, J., Malaguarnera, G., Guo, L., Somavarapu, S. and Cordeiro, M.F. (2016) 'The retina as an early biomarker of neurodegeneration in a rotenone-induced model of Parkinson's disease: evidence for a neuroprotective effect of rosiglitazone in the eye and brain', *Acta Neuropathol Commun*, 4(1), p. 86.
Nowacka, B., Lubinski, W., Honczarenko, K., Potemkowski, A. and Safranow, K. (2015) 'Bioelectrical function and structural assessment of the retina in patients with early stages of Parkinson's disease (PD)', *Doc Ophthalmol*, 131(2), pp. 95-104.
O'Brien, J.T., Colloby, S.J., Pakrasi, S., Perry, E.K., Pimlott, S.L., Wyper, D.J., McKeith, I.G. and Williams, E.D. (2008) 'Nicotinic alpha4beta2 receptor binding in dementia with Lewy bodies using 123I-5IA-85380 SPECT demonstrates a link between occipital changes and visual hallucinations', *Neuroimage*, 40(3), pp. 1056-63.
O'Connor, D.H., Fukui, M.M., Pinsk, M.A. and Kastner, S. (2002) 'Attention modulates responses in the human lateral geniculate nucleus', *Nat Neurosci*, 5(11), pp. 1203-9.
Ogren, M. and Hendrickson, A. (1976) 'Pathways between striate cortex and subcortical regions in Macaca mulatta and Saimiri sciureus: evidence for a reciprocal pulvinar connection', *Exp Neurol*, 53(3), pp. 780-800.
Oikawa, T., Nonaka, T., Terada, M., Tamaoka, A., Hisanaga, S.I. and Hasegawa, M. (2016) 'alpha-Synuclein fibrils exhibit gain-of-toxic-function, promoting tau aggregation and inhibiting microtubule assembly', *J Biol Chem*.
Olsson, B., Constantinescu, R., Holmberg, B., Andreasen, N., Blennow, K. and Zetterberg, H. (2013) 'The glial marker YKL-40 is decreased in synucleinopathies', *Mov Disord*, 28(13), pp. 1882-5.
Onofrj, M., Taylor, J.P., Monaco, D., Franciotti, R., Anzellotti, F., Bonanni, L., Onofrj, V. and Thomas, A. (2013) 'Visual hallucinations in PD and Lewy body dementias: old and new hypotheses', *Behav Neurol*, 27(4), pp. 479-93.
Pachalska, M., Bidzan, L., Bidzan, M. and Goral-Polrola, J. (2015) 'Vascular Factors and Cognitive Dysfunction in Alzheimer Disease', *Med Sci Monit*, 21, pp. 3483-9.
Papapetropoulos, S., McCorquodale, D.S., Gonzalez, J., Jean-Gilles, L. and Mash, D.C. (2006) 'Cortical and amygdalar Lewy body burden in Parkinson's disease patients with visual hallucinations', *Parkinsonism Relat Disord*, 12(4), pp. 253-6.
Paskavitz, J.F., Lippa, C.F., Hamos, J.E., Pulaski-Salo, D. and Drachman, D.A. (1995) 'Role of the dorsomedial nucleus of the thalamus in Alzheimer's disease', *J Geriatr Psychiatry Neurol*, 8(1), pp. 32-7.
Paslawski, W., Andreasen, M., Nielsen, S.B., Lorenzen, N., Thomsen, K., Kaspersen, J.D., Pedersen, J.S. and Otzen, D.E. (2014) 'High stability and cooperative unfolding of alpha-synuclein oligomers', *Biochemistry*, 53(39), pp. 6252-63.

Pasquier, J., Michel, B.F., Brenot-Rossi, I., Hassan-Sebbag, N., Sauvan, R. and Gastaut, J.L. (2002) 'Value of (99m)Tc-ECD SPET for the diagnosis of dementia with Lewy bodies', *Eur J Nucl Med Mol Imaging*, 29(10), pp. 1342-8.
Patterson, B.W., Elbert, D.L., Mawuenyega, K.G., Kasten, T., Ovod, V., Ma, S., Xiong, C., Chott, R., Yarasheski, K., Sigurdson, W., Zhang, L., Goate, A., Benzinger, T., Morris, J.C., Holtzman, D. and Bateman, R.J. (2015) 'Age and amyloid effects on human central nervous system amyloid-beta kinetics', *Ann Neurol*, 78(3), pp. 439-53.
Paxinos, G. and Huang, X.-F. (2013) *Atlas of the human brainstem*. Elsevier.
Percival, K.A., Koizumi, A., Masri, R.A., Buzas, P., Martin, P.R. and Grunert, U. (2014) 'Identification of a pathway from the retina to koniocellular layer K1 in the lateral geniculate nucleus of marmoset', *J Neurosci*, 34(11), pp. 3821-5.
Perneczky, R., Drzezga, A., Boecker, H., Forstl, H., Kurz, A. and Haussermann, P. (2008) 'Cerebral metabolic dysfunction in patients with dementia with Lewy bodies and visual hallucinations', *Dement Geriatr Cogn Disord*, 25(6), pp. 531-8.
Perriol, M.P., Dujardin, K., Derambure, P., Marcq, A., Bourriez, J.L., Laureau, E., Pasquier, F., Defebvre, L. and Destee, A. (2005) 'Disturbance of sensory filtering in dementia with Lewy bodies: comparison with Parkinson's disease dementia and Alzheimer's disease', *J Neurol Neurosurg Psychiatry*, 76(1), pp. 106-8.
Perry, E.K., Haroutunian, V., Davis, K.L., Levy, R., Lantos, P., Eagger, S., Honavar, M., Dean, A., Griffiths, M., McKeith, I.G. and et al. (1994) 'Neocortical cholinergic activities differentiate Lewy body dementia from classical Alzheimer's disease', *Neuroreport*, 5(7), pp. 747-9.
Perry, E.K., Johnson, M., Ekonomou, A., Perry, R.H., Ballard, C. and Attems, J. (2012) 'Neurogenic abnormalities in Alzheimer's disease differ between stages of neurogenesis and are partly related to cholinergic pathology', *Neurobiol Dis*, 47(2), pp. 155-62.
Perry, E.K. and Perry, R.H. (1995) 'Acetylcholine and hallucinations: disease-related compared to drug-induced alterations in human consciousness', *Brain Cogn*, 28(3), pp. 240-58.
Perry, E.K., Smith, C.J., Court, J.A. and Perry, R.H. (1990a) 'Cholinergic nicotinic and muscarinic receptors in dementia of Alzheimer, Parkinson and Lewy body types', *J Neural Transm Park Dis Dement Sect*, 2(3), pp. 149-58.
Perry, R.H., Irving, D., Blessed, G., Fairbairn, A. and Perry, E.K. (1990b) 'Senile dementia of Lewy body type. A clinically and neuropathologically distinct form of Lewy body dementia in the elderly', *J Neurol Sci*, 95(2), pp. 119-39.
Perry, V.H. and Cowey, A. (1984) 'Retinal ganglion cells that project to the superior colliculus and pretectum in the macaque monkey', *Neuroscience*, 12(4), pp. 1125-37.
Petrova, M., Mehrabian-Spasova, S., Aarsland, D., Raycheva, M. and Traykov, L. (2015) 'Clinical and Neuropsychological Differences between Mild Parkinson's Disease Dementia and Dementia with Lewy Bodies', *Dement Geriatr Cogn Dis Extra*, 5(2), pp. 212-20.
Pievani, M., de Haan, W., Wu, T., Seeley, W.W. and Frisoni, G.B. (2011) 'Functional network disruption in the degenerative dementias', *Lancet Neurol*, 10(9), pp. 829-43.
Piggott, M.A., Ballard, C.G., Dickinson, H.O., McKeith, I.G., Perry, R.H. and Perry, E.K. (2007) 'Thalamic D2 receptors in dementia with Lewy bodies, Parkinson's disease, and Parkinson's disease dementia', *Int J Neuropsychopharmacol*, 10(2), pp. 231-44.
Piggott, M.A., Marshall, E.F., Thomas, N., Lloyd, S., Court, J.A., Jaros, E., Burn, D., Johnson, M., Perry, R.H., McKeith, I.G., Ballard, C. and Perry, E.K. (1999) 'Striatal dopaminergic markers in dementia with Lewy bodies, Alzheimer's and Parkinson's diseases: rostrocaudal distribution', *Brain*, 122 ( Pt 8), pp. 1449-68.
Pinkhardt, E.H., Jurgens, R., Lule, D., Heimrath, J., Ludolph, A.C., Becker, W. and Kassubek, J. (2012) 'Eye movement impairments in Parkinson's disease: possible role of extradopaminergic mechanisms', *BMC Neurol*, 12, p. 5.
Plassman, B.L., Langa, K.M., Fisher, G.G., Heeringa, S.G., Weir, D.R., Ofstedal, M.B., Burke, J.R., Hurd, M.D., Potter, G.G., Rodgers, W.L., Steffens, D.C., Willis, R.J. and Wallace, R.B. (2007) 'Prevalence of

dementia in the United States: the aging, demographics, and memory study', *Neuroepidemiology*, 29(1-2), pp. 125-32.
Polymeropoulos, M.H., Lavedan, C., Leroy, E., Ide, S.E., Dehejia, A., Dutra, A., Pike, B., Root, H., Rubenstein, J., Boyer, R., Stenroos, E.S., Chandrasekharappa, S., Athanassiadou, A., Papapetropoulos, T., Johnson, W.G., Lazzarini, A.M., Duvoisin, R.C., Di Iorio, G., Golbe, L.I. and Nussbaum, R.L. (1997) 'Mutation in the alpha-synuclein gene identified in families with Parkinson's disease', *Science*, 276(5321), pp. 2045-7.
Popken, G.J., Leggio, M.G., Bunney, W.E. and Jones, E.G. (2002) 'Expression of mRNAs related to the GABAergic and glutamatergic neurotransmitter systems in the human thalamus: normal and schizophrenic', *Thalamus & Related Systems*, 1(4), pp. 349-369.
Postuma, R.B., Berg, D., Stern, M., Poewe, W., Olanow, C.W., Oertel, W., Obeso, J., Marek, K., Litvan, I., Lang, A.E., Halliday, G., Goetz, C.G., Gasser, T., Dubois, B., Chan, P., Bloem, B.R., Adler, C.H. and Deuschl, G. (2015) 'MDS clinical diagnostic criteria for Parkinson's disease', *Mov Disord*, 30(12), pp. 1591-601.
Pratt, W.B., Gestwicki, J.E., Osawa, Y. and Lieberman, A.P. (2015) 'Targeting Hsp90/Hsp70-based protein quality control for treatment of adult onset neurodegenerative diseases', *Annu Rev Pharmacol Toxicol*, 55, pp. 353-71.
Price, J.L., Davis, P.B., Morris, J.C. and White, D.L. (1991) 'The distribution of tangles, plaques and related immunohistochemical markers in healthy aging and Alzheimer's disease', *Neurobiol Aging*, 12(4), pp. 295-312.
Prince, M., Guerchet, M. and Prina, M. (2013) *The global impact of dementia 2013-2050*. Alzheimer's Disease International.
Proserpio, V. and Mahata, B. (2016) 'Single-cell technologies to study the immune system', *Immunology*, 147(2), pp. 133-40.
Prusiner, S.B. and Kingsbury, D.T. (1985) 'Prions - Infectious Pathogens Causing the Spongiform Encephalopathies', *Crc Critical Reviews in Clinical Neurobiology*, 1(3), pp. 181-200.
Purushothaman, G., Marion, R., Li, K. and Casagrande, V.A. (2012) 'Gating and control of primary visual cortex by pulvinar', *Nat Neurosci*, 15(6), pp. 905-12.
Rabinovici, G.D., Jagust, W.J., Furst, A.J., Ogar, J.M., Racine, C.A., Mormino, E.C., O'Neil, J.P., Lal, R.A., Dronkers, N.F., Miller, B.L. and Gorno-Tempini, M.L. (2008) 'Abeta amyloid and glucose metabolism in three variants of primary progressive aphasia', *Ann Neurol*, 64(4), pp. 388-401.
Rahimi, J. and Kovacs, G.G. (2014) 'Prevalence of mixed pathologies in the aging brain', *Alzheimers Res Ther*, 6(9), p. 82.
Rahimi, J., Milenkovic, I. and Kovacs, G.G. (2015) 'Patterns of Tau and α-Synuclein Pathology in the Visual System', *J Parkinsons Dis*, 5(2), pp. 333-340.
Ramakrishnan, N.A., Drescher, M.J. and Drescher, D.G. (2012) 'The SNARE complex in neuronal and sensory cells', *Mol Cell Neurosci*, 50(1), pp. 58-69.
Ray, M., Bohr, I., McIntosh, J.M., Ballard, C., McKeith, I., Chalon, S., Guilloteau, D., Perry, R., Perry, E., Court, J.A. and Piggott, M. (2004) 'Involvement of alpha6/alpha3 neuronal nicotinic acetylcholine receptors in neuropsychiatric features of Dementia with Lewy bodies: [(125)I]-alpha-conotoxin MII binding in the thalamus and striatum', *Neurosci Lett*, 372(3), pp. 220-5.
Reese, B.E. (2011) 'Development of the retina and optic pathway', *Vision research*, 51(7), pp. 613-32.
Rehli, M., Niller, H.H., Ammon, C., Langmann, S., Schwarzfischer, L., Andreesen, R. and Krause, S.W. (2003) 'Transcriptional regulation of CHI3L1, a marker gene for late stages of macrophage differentiation', *J Biol Chem*, 278(45), pp. 44058-67.
Respondek, G., Roeber, S., Kretzschmar, H., Troakes, C., Al-Sarraj, S., Gelpi, E., Gaig, C., Chiu, W.Z., van Swieten, J.C., Oertel, W.H. and Hoglinger, G.U. (2013) 'Accuracy of the National Institute for Neurological Disorders and Stroke/Society for Progressive Supranuclear Palsy and neuroprotection and natural history in Parkinson plus syndromes criteria for the diagnosis of progressive supranuclear palsy', *Mov Disord*, 28(4), pp. 504-9.

Ricci, M., Guidoni, S.V., Sepe-Monti, M., Bomboi, G., Antonini, G., Blundo, C. and Giubilei, F. (2009) 'Clinical findings, functional abilities and caregiver distress in the early stage of dementia with Lewy bodies (DLB) and Alzheimer's disease (AD)', *Arch Gerontol Geriatr*, 49(2), pp. e101-4.
Richard, I.H., Papka, M., Rubio, A. and Kurlan, R. (2002) 'Parkinson's disease and dementia with Lewy bodies: one disease or two?', *Mov Disord*, 17(6), pp. 1161-5.
Rivest, S. (2009) 'Regulation of innate immune responses in the brain', *Nat Rev Immunol*, 9(6), pp. 429-39.
Rizo, J. and Xu, J. (2015) 'The Synaptic Vesicle Release Machinery', *Annu Rev Biophys*, 44, pp. 339-67.
Robertson, A.D., Messner, M.A., Shirzadi, Z., Kleiner-Fisman, G., Lee, J., Hopyan, J., Lang, A.E., Black, S.E., MacIntosh, B.J. and Masellis, M. (2016) 'Orthostatic hypotension, cerebral hypoperfusion, and visuospatial deficits in Lewy body disorders', *Parkinsonism Relat Disord*, 22, pp. 80-6.
Robinson, A.C., Palmer, L., Love, S., Hamard, M., Esiri, M., Ansorge, O., Lett, D., Attems, J., Morris, C., Troakes, C., Selvackadunco, S., King, A., Al-Sarraj, S. and Mann, D.M. (2016) 'Extended post-mortem delay times should not be viewed as a deterrent to the scientific investigation of human brain tissue: a study from the Brains for Dementia Research Network Neuropathology Study Group, UK', *Acta Neuropathol*, 132(5), pp. 753-755.
Romanski, L.M., Giguere, M., Bates, J.F. and Goldman-Rakic, P.S. (1997) 'Topographic organization of medial pulvinar connections with the prefrontal cortex in the rhesus monkey', *J Comp Neurol*, 379(3), pp. 313-32.
Rothman, J.E. (1994) 'Intracellular membrane fusion', *Adv Second Messenger Phosphoprotein Res*, 29, pp. 81-96.
Rothman, K.J. (1990) 'No adjustments are needed for multiple comparisons', *Epidemiology*, 1(1), pp. 43-6.
Rozemuller, A.J., Eikelenboom, P., Theeuwes, J.W., Jansen Steur, E.N. and de Vos, R.A. (2000) 'Activated microglial cells and complement factors are unrelated to cortical Lewy bodies', *Acta Neuropathol*, 100(6), pp. 701-8.
Rub, U., Del Tredici, K., Schultz, C., Ghebremedhin, E., de Vos, R.A., Jansen Steur, E. and Braak, H. (2002) 'Parkinson's disease: the thalamic components of the limbic loop are severely impaired by alpha-synuclein immunopositive inclusion body pathology', *Neurobiol Aging*, 23(2), pp. 245-54.
Rub, U., Del Tredici, K., Schultz, C., Thal, D.R., Braak, E. and Braak, H. (2000) 'The evolution of Alzheimer's disease-related cytoskeletal pathology in the human raphe nuclei', *Neuropathol Appl Neurobiol*, 26(6), pp. 553-67.
Ruffmann, C., Calboli, F.C., Bravi, I., Gveric, D., Curry, L.K., de Smith, A., Pavlou, S., Buxton, J.L., Blakemore, A.I., Takousis, P., Molloy, S., Piccini, P., Dexter, D.T., Roncaroli, F., Gentleman, S.M. and Middleton, L.T. (2016) 'Cortical Lewy bodies and Abeta burden are associated with prevalence and timing of dementia in Lewy body diseases', *Neuropathol Appl Neurobiol*, 42(5), pp. 436-50.
Rye, D.B. (1997) 'Contributions of the pedunculopontine region to normal and altered REM sleep', *Sleep*, 20(9), pp. 757-88.
Saalmann, Y.B., Pinsk, M.A., Wang, L., Li, X. and Kastner, S. (2012) 'The Pulvinar Regulates Information Transmission Between Cortical Areas Based on Attention Demands', *Science*, 337(6095), pp. 753-756.
Saenz, A., Doe de Maindreville, A., Henry, A., de Labbey, S., Bakchine, S. and Ehrle, N. (2013) 'Recognition of facial and musical emotions in Parkinson's disease', *Eur J Neurol*, 20(3), pp. 571-7.
Saito, Y., Kawai, M., Inoue, K., Sasaki, R., Arai, H., Nanba, E., Kuzuhara, S., Ihara, Y., Kanazawa, I. and Murayama, S. (2000) 'Widespread expression of alpha-synuclein and tau immunoreactivity in Hallervorden-Spatz syndrome with protracted clinical course', *J Neurol Sci*, 177(1), pp. 48-59.
Saito, Y., Ruberu, N.N., Sawabe, M., Arai, T., Kazama, H., Hosoi, T., Yamanouchi, H. and Murayama, S. (2004) 'Lewy body-related alpha-synucleinopathy in aging', *J Neuropathol Exp Neurol*, 63(7), pp. 742-9.

Sartucci, F., Borghetti, D., Bocci, T., Murri, L., Orsini, P., Porciatti, V., Origlia, N. and Domenici, L. (2010) 'Dysfunction of the magnocellular stream in Alzheimer's disease evaluated by pattern electroretinograms and visual evoked potentials', *Brain Res Bull*, 82(3-4), pp. 169-76.
Sato, T., Hanyu, H., Hirao, K., Shimizu, S., Kanetaka, H. and Iwamoto, T. (2007) 'Deep gray matter hyperperfusion with occipital hypoperfusion in dementia with Lewy bodies', *Eur J Neurol*, 14(11), pp. 1299-301.
Schall, J.D. (1995) 'Neural basis of saccade target selection', *Rev Neurosci*, 6(1), pp. 63-85.
Scharre, D.W., Chang, S.I., Nagaraja, H.N., Park, A., Adeli, A., Agrawal, P., Kloos, A., Kegelmeyer, D., Linder, S., Fritz, N., Kostyk, S.K. and Kataki, M. (2016) 'Paired Studies Comparing Clinical Profiles of Lewy Body Dementia with Alzheimer's and Parkinson's Diseases', *J Alzheimers Dis*, 54(3), pp. 995-1004.
Schmeichel, A.M., Buchhalter, L.C., Low, P.A., Parisi, J.E., Boeve, B.W., Sandroni, P. and Benarroch, E.E. (2008) 'Mesopontine cholinergic neuron involvement in Lewy body dementia and multiple system atrophy', *Neurology*, 70(5), pp. 368-73.
Schmid, M.C., Mrowka, S.W., Turchi, J., Saunders, R.C., Wilke, M., Peters, A.J., Ye, F.Q. and Leopold, D.A. (2010) 'Blindsight depends on the lateral geniculate nucleus', *Nature*, 466(7304), pp. 373-7.
Schneider, J.A., Arvanitakis, Z., Bang, W. and Bennett, D.A. (2007) 'Mixed brain pathologies account for most dementia cases in community-dwelling older persons', *Neurology*, 69(24), pp. 2197-204.
Schneider, K.A. and Kastner, S. (2009) 'Effects of sustained spatial attention in the human lateral geniculate nucleus and superior colliculus', *J Neurosci*, 29(6), pp. 1784-95.
Seidel, K., Mahlke, J., Siswanto, S., Kruger, R., Heinsen, H., Auburger, G., Bouzrou, M., Grinberg, L.T., Wicht, H., Korf, H.W., den Dunnen, W. and Rub, U. (2015) 'The brainstem pathologies of Parkinson's disease and dementia with Lewy bodies', *Brain Pathology*, 25(2), pp. 121-35.
Selemon, L.D. and Begovic, A. (2007) 'Stereologic analysis of the lateral geniculate nucleus of the thalamus in normal and schizophrenic subjects', *Psychiatry Res*, 151(1-2), pp. 1-10.
Sharma, M., Burre, J. and Sudhof, T.C. (2011) 'CSPalpha promotes SNARE-complex assembly by chaperoning SNAP-25 during synaptic activity', *Nat Cell Biol*, 13(1), pp. 30-9.
Sherk, H. (1979) 'Connections and visual-field mapping in cat's tectoparabigeminal circuit', *J Neurophysiol*, 42(6), pp. 1656-68.
Sherman, M.Y. and Goldberg, A.L. (2001) 'Cellular defenses against unfolded proteins: a cell biologist thinks about neurodegenerative diseases', *Neuron*, 29(1), pp. 15-32.
Shimizu, S., Hanyu, H., Hirao, K., Sato, T., Iwamoto, T. and Koizumi, K. (2008) 'Value of analyzing deep gray matter and occipital lobe perfusion to differentiate dementia with Lewy bodies from Alzheimer's disease', *Ann Nucl Med*, 22(10), pp. 911-6.
Shine, J.M., Halliday, G.M., Naismith, S.L. and Lewis, S.J. (2011) 'Visual misperceptions and hallucinations in Parkinson's disease: dysfunction of attentional control networks?', *Mov Disord*, 26(12), pp. 2154-9.
Shine, J.M., O'Callaghan, C., Halliday, G.M. and Lewis, S.J. (2014) 'Tricks of the mind: Visual hallucinations as disorders of attention', *Prog Neurobiol*, 116, pp. 58-65.
Shipp, S. (2003) 'The functional logic of cortico-pulvinar connections', *Philos Trans R Soc Lond B Biol Sci*, 358(1438), pp. 1605-24.
Sierra, M., Gelpi, E., Marti, M.J. and Compta, Y. (2016) 'Lewy- and Alzheimer-type pathologies in midbrain and cerebellum across the Lewy body disorders spectrum', *Neuropathol Appl Neurobiol*, 42(5), pp. 451-62.
Siew, L.K., Love, S., Dawbarn, D., Wilcock, G.K. and Allen, S.J. (2004) 'Measurement of pre- and post-synaptic proteins in cerebral cortex: effects of post-mortem delay', *J Neurosci Methods*, 139(2), pp. 153-9.
Silva, M.F., Faria, P., Regateiro, F.S., Forjaz, V., Januario, C., Freire, A. and Castelo-Branco, M. (2005) 'Independent patterns of damage within magno-, parvo- and koniocellular pathways in Parkinson's disease', *Brain*, 128(Pt 10), pp. 2260-71.

Sincich, L.C., Park, K.F., Wohlgemuth, M.J. and Horton, J.C. (2004) 'Bypassing V1: a direct geniculate input to area MT', *Nat Neurosci*, 7(10), pp. 1123-8.
Sinclair, L.I., Tayler, H.M. and Love, S. (2015) 'Synaptic protein levels altered in vascular dementia', *Neuropathol Appl Neurobiol*, 41(4), pp. 533-43.
Soares, J.G., Gattass, R., Souza, A.P., Rosa, M.G., Fiorani, M., Jr. and Brandao, B.L. (2001) 'Connectional and neurochemical subdivisions of the pulvinar in Cebus monkeys', *Vis Neurosci*, 18(1), pp. 25-41.
Sofroniew, M.V. (2009) 'Molecular dissection of reactive astrogliosis and glial scar formation', *Trends Neurosci*, 32(12), pp. 638-47.
Sommer, M.A. and Wurtz, R.H. (2004) 'What the brain stem tells the frontal cortex. I. Oculomotor signals sent from superior colliculus to frontal eye field via mediodorsal thalamus', *J Neurophysiol*, 91(3), pp. 1381-402.
Sosa-Ortiz, A.L., Acosta-Castillo, I. and Prince, M.J. (2012) 'Epidemiology of dementias and Alzheimer's disease', *Arch Med Res*, 43(8), pp. 600-8.
Sparks, D.L. (1999) 'Conceptual issues related to the role of the superior colliculus in the control of gaze', *Curr Opin Neurobiol*, 9(6), pp. 698-707.
Sparks, D.L. and Hartwich-Young, R. (1989) 'The deep layers of the superior colliculus', *Rev Oculomot Res*, 3, pp. 213-255.
Spillantini, M.G., Schmidt, M.L., Lee, V.M., Trojanowski, J.Q., Jakes, R. and Goedert, M. (1997) 'Alpha-synuclein in Lewy bodies', *Nature*, 388(6645), pp. 839-40.
Sprague, J.M. (1966) 'Interaction of cortex and superior colliculus in mediation of visually guided behavior in the cat', *Science*, 153(3743), pp. 1544-7.
Sprengelmeyer, R., Young, A.W., Mahn, K., Schroeder, U., Woitalla, D., Buttner, T., Kuhn, W. and Przuntek, H. (2003) 'Facial expression recognition in people with medicated and unmedicated Parkinson's disease', *Neuropsychologia*, 41(8), pp. 1047-1057.
Stepniewska, I., Qi, H.X. and Kaas, J.H. (1999) 'Do superior colliculus projection zones in the inferior pulvinar project to MT in primates?', *Eur J Neurosci*, 11(2), pp. 469-80.
Stepniewska, I., Ql, H.X. and Kaas, J.H. (2000) 'Projections of the superior colliculus to subdivisions of the inferior pulvinar in New World and Old World monkeys', *Vis Neurosci*, 17(4), pp. 529-49.
Steriade, M. (1996) 'Arousal: revisiting the reticular activating system', *Science*, 272(5259), pp. 225-6.
Steriade M, J.E., McCormick DA (1997) *Thalamus*. Oxford: Elsevier.
Stoerig, P. and Cowey, A. (1997) 'Blindsight in man and monkey', *Brain*, 120 ( Pt 3), pp. 535-59.
Streiner, D.L. and Norman, G.R. (2011) 'Correction for multiple testing: is there a resolution?', *Chest*, 140(1), pp. 16-8.
Sudhof, T.C. (2004) 'The synaptic vesicle cycle', *Annu Rev Neurosci*, 27, pp. 509-47.
Sudhof, T.C. (2013) 'Neurotransmitter release: the last millisecond in the life of a synaptic vesicle', *Neuron*, 80(3), pp. 675-90.
Sutton, R.B., Fasshauer, D., Jahn, R. and Brunger, A.T. (1998) 'Crystal structure of a SNARE complex involved in synaptic exocytosis at 2.4 A resolution', *Nature*, 395(6700), pp. 347-53.
Taipa, R., Pinho, J. and Melo-Pires, M. (2012) 'Clinico-pathological correlations of the most common neurodegenerative dementias', *Front Neurol*, 3, p. 68.
Tamietto, M. and de Gelder, B. (2010) 'Neural bases of the non-conscious perception of emotional signals', *Nat Rev Neurosci*, 11(10), pp. 697-709.
Taylor, J.P., Firbank, M., Barnett, N., Pearce, S., Livingstone, A., Mosimann, U., Eyre, J., McKeith, I.G. and O'Brien, J.T. (2011) 'Visual hallucinations in dementia with Lewy bodies: transcranial magnetic stimulation study', *Br J Psychiatry*, 199(6), pp. 492-500.
Taylor, J.P., Firbank, M. and O'Brien, J.T. (2016) 'Visual cortical excitability in dementia with Lewy bodies', *Br J Psychiatry*, 208(5), pp. 497-8.
Taylor, J.P., Firbank, M.J., He, J.B., Barnett, N., Pearce, S., Livingstone, A., Vuong, Q., McKeith, I.G. and O'Brien, J.T. (2012) 'Visual cortex in dementia with Lewy bodies: magnetic resonance imaging study', *British Journal of Psychiatry*, 200(6), pp. 491-498.

Teaktong, T., Piggott, M.A., McKeith, I.G., Perry, R.H., Ballard, C.G. and Perry, E.K. (2005) 'Muscarinic M2 and M4 receptors in anterior cingulate cortex: relation to neuropsychiatric symptoms in dementia with Lewy bodies', *Behav Brain Res*, 161(2), pp. 299-305.
Terao, Y., Fukuda, H., Yugeta, A., Hikosaka, O., Nomura, Y., Segawa, M., Hanajima, R., Tsuji, S. and Ugawa, Y. (2011) 'Initiation and inhibitory control of saccades with the progression of Parkinson's disease - changes in three major drives converging on the superior colliculus', *Neuropsychologia*, 49(7), pp. 1794-806.
Thal, D.R., Rub, U., Orantes, M. and Braak, H. (2002) 'Phases of A beta-deposition in the human brain and its relevance for the development of AD', *Neurology*, 58(12), pp. 1791-1800.
Tiraboschi, P., Hansen, L.A., Alford, M., Merdes, A., Masliah, E., Thal, L.J. and Corey-Bloom, J. (2002) 'Early and widespread cholinergic losses differentiate dementia with Lewy bodies from Alzheimer disease', *Arch Gen Psychiatry*, 59(10), pp. 946-51.
Tiraboschi, P., Salmon, D.P., Hansen, L.A., Hofstetter, R.C., Thal, L.J. and Corey-Bloom, J. (2006) 'What best differentiates Lewy body from Alzheimer's disease in early-stage dementia?', *Brain*, 129(Pt 3), pp. 729-35.
Tofaris, G.K. and Spillantini, M.G. (2007) 'Physiological and pathological properties of alpha-synuclein', *Cell Mol Life Sci*, 64(17), pp. 2194-201.
Tosto, G., Monsell, S.E., Hawes, S.E., Bruno, G. and Mayeux, R. (2015) 'Progression of Extrapyramidal Signs in Alzheimer's Disease: Clinical and Neuropathological Correlates', *J Alzheimers Dis*, 49(4), pp. 1085-93.
Trick, G.L., Kaskie, B. and Steinman, S.B. (1994) 'Visual impairment in Parkinson's disease: deficits in orientation and motion discrimination', *Optom Vis Sci*, 71(4), pp. 242-5.
Uchiyama, M., Nishio, Y., Yokoi, K., Hosokai, Y., Takeda, A. and Mori, E. (2015) 'Pareidolia in Parkinson's disease without dementia: A positron emission tomography study', *Parkinsonism Relat Disord*, 21(6), pp. 603-9.
Ungerleider, L.G., Galkin, T.W., Desimone, R. and Gattass, R. (2014) 'Subcortical Projections of Area V2 in the Macaque', *Journal of Cognitive Neuroscience*, 26(6), pp. 1220-1233.
Ungerleider LG, M.M. (1982) 'Two cortical visual streams', in Inge DJ, G.M.M.R. (ed.) *Analysis of visual behaviour*. Cambridge, MA: MIT Press, pp. 549-586.
United Nations. Department of, E. (2010) *World population ageing 2009*. United Nations Publications.
Urwyler, P., Nef, T., Killen, A., Collerton, D., Thomas, A., Burn, D., McKeith, I. and Mosimann, U.P. (2014) 'Visual complaints and visual hallucinations in Parkinson's disease', *Parkinsonism Relat Disord*, 20(3), pp. 318-22.
Urwyler, P., Nef, T., Muri, R., Archibald, N., Makin, S.M., Collerton, D., Taylor, J.P., Burn, D., McKeith, I. and Mosimann, U.P. (2016) 'Visual Hallucinations in Eye Disease and Lewy Body Disease', *Am J Geriatr Psychiatry*, 24(5), pp. 350-8.
van den Berge, S.A., Kevenaar, J.T., Sluijs, J.A. and Hol, E.M. (2012) 'Dementia in Parkinson's Disease Correlates with alpha-Synuclein Pathology but Not with Cortical Astrogliosis', *Parkinsons Dis*, 2012, p. 420957.
Vann Jones, S.A. and O'Brien, J.T. (2014) 'The prevalence and incidence of dementia with Lewy bodies: a systematic review of population and clinical studies', *Psychol Med*, 44(4), pp. 673-83.
Vind, I., Johansen, J.S., Price, P.A. and Munkholm, P. (2003) 'Serum YKL-40, a potential new marker of disease activity in patients with inflammatory bowel disease', *Scand J Gastroenterol*, 38(6), pp. 599-605.
von Gunten, A., Kovari, E., Bussiere, T., Rivara, C.B., Gold, G., Bouras, C., Hof, P.R. and Giannakopoulos, P. (2006) 'Cognitive impact of neuronal pathology in the entorhinal cortex and CA1 field in Alzheimer's disease', *Neurobiol Aging*, 27(2), pp. 270-7.
Wakabayashi, K., Hayashi, S., Yoshimoto, M., Kudo, H. and Takahashi, H. (2000) 'NACP/α-synuclein-positive filamentous inclusions in astrocytes and oligodendrocytes of Parkinson's disease brains', *Acta Neuropathologica*, 99(1), pp. 14-20.

Wakabayashi, K., Yoshimoto, M., Fukushima, T., Koide, R., Horikawa, Y., Morita, T. and Takahashi, H. (1999) 'Widespread occurrence of alpha-synuclein/NACP-immunoreactive neuronal inclusions in juvenile and adult-onset Hallervorden-Spatz disease with Lewy bodies', *Neuropathol Appl Neurobiol*, 25(5), pp. 363-8.
Walker, M.P., Ayre, G.A., Cummings, J.L., Wesnes, K., McKeith, I.G., O'Brien, J.T. and Ballard, C.G. (2000a) 'The Clinician Assessment of Fluctuation and the One Day Fluctuation Assessment Scale. Two methods to assess fluctuating confusion in dementia', *Br J Psychiatry*, 177, pp. 252-6.
Walker, M.P., Ayre, G.A., Cummings, J.L., Wesnes, K., McKeith, I.G., O'Brien, J.T. and Ballard, C.G. (2000b) 'Quantifying fluctuation in dementia with Lewy bodies, Alzheimer's disease, and vascular dementia', *Neurology*, 54(8), pp. 1616-25.
Walker, Z., Costa, D.C., Janssen, A.G., Walker, R.W., Livingstone, G. and Katona, C.L. (1997) 'Dementia with lewy bodies: a study of post-synaptic dopaminergic receptors with iodine-123 iodobenzamide single-photon emission tomography', *Eur J Nucl Med*, 24(6), pp. 609-14.
Walker, Z., McKeith, I., Rodda, J., Qassem, T., Tatsch, K., Booij, J., Darcourt, J. and O'Brien, J. (2012) 'Comparison of cognitive decline between dementia with Lewy bodies and Alzheimer's disease: a cohort study', *BMJ open*, 2, p. e000380.
Wallace, M.T., Meredith, M.A. and Stein, B.E. (1993) 'Converging influences from visual, auditory, and somatosensory cortices onto output neurons of the superior colliculus', *J Neurophysiol*, 69(6), pp. 1797-809.
Ward, R., Calder, A.J., Parker, M. and Arend, I. (2007) 'Emotion recognition following human pulvinar damage', *Neuropsychologia*, 45(8), pp. 1973-8.
Ward, R., Danziger, S., Owen, V. and Rafal, R. (2002) 'Deficits in spatial coding and feature binding following damage to spatiotopic maps in the human pulvinar', *Nat Neurosci*, 5(2), pp. 99-100.
Warren, N.M., Piggott, M.A., Lees, A.J. and Burn, D.J. (2007) 'Muscarinic receptors in the thalamus in progressive supranuclear palsy and other neurodegenerative disorders', *J Neuropathol Exp Neurol*, 66(5), pp. 399-404.
Washbourne, P., Thompson, P.M., Carta, M., Costa, E.T., Mathews, J.R., Lopez-Bendito, G., Molnar, Z., Becher, M.W., Valenzuela, C.F., Partridge, L.D. and Wilson, M.C. (2002) 'Genetic ablation of the t-SNARE SNAP-25 distinguishes mechanisms of neuroexocytosis', *Nat Neurosci*, 5(1), pp. 19-26.
Watson, R., Blamire, A.M., Colloby, S.J., Wood, J.S., Barber, R., He, J. and O'Brien, J.T. (2012) 'Characterizing dementia with Lewy bodies by means of diffusion tensor imaging', *Neurology*, 79(9), pp. 906-14.
Watson, R., Blamire, A.M. and O'Brien, J.T. (2009) 'Magnetic resonance imaging in lewy body dementias', *Dement Geriatr Cogn Disord*, 28(6), pp. 493-506.
Weber, T., Zemelman, B.V., McNew, J.A., Westermann, B., Gmachl, M., Parlati, F., Sollner, T.H. and Rothman, J.E. (1998) 'SNAREpins: minimal machinery for membrane fusion', *Cell*, 92(6), pp. 759-72.
Weddell, R.A. (2004) 'Subcortical modulation of spatial attention including evidence that the Sprague effect extends to man', *Brain Cogn*, 55(3), pp. 497-506.
Wennstrom, M., Surova, Y., Hall, S., Nilsson, C., Minthon, L., Hansson, O. and Nielsen, H.M. (2015) 'The Inflammatory Marker YKL-40 Is Elevated in Cerebrospinal Fluid from Patients with Alzheimer's but Not Parkinson's Disease or Dementia with Lewy Bodies', *PLoS One*, 10(8), p. e0135458.
Whitwell, J.L., Weigand, S.D., Shiung, M.M., Boeve, B.F., Ferman, T.J., Smith, G.E., Knopman, D.S., Petersen, R.C., Benarroch, E.E., Josephs, K.A. and Jack, C.R., Jr. (2007) 'Focal atrophy in dementia with Lewy bodies on MRI: a distinct pattern from Alzheimer's disease', *Brain*, 130(Pt 3), pp. 708-19.
Wiley, C.A., Bonneh-Barkay, D., Dixon, C.E., Lesniak, A., Wang, G., Bissel, S.J. and Kochanek, P.M. (2015) 'Role for mammalian chitinase 3-like protein 1 in traumatic brain injury', *Neuropathology*, 35(2), pp. 95-106.
Wilke, M., Turchi, J., Smith, K., Mishkin, M. and Leopold, D.A. (2010) 'Pulvinar Inactivation Disrupts Selection of Movement Plans', *Journal of Neuroscience*, 30(25), pp. 8650-8659.
Winner, B., Jappelli, R., Maji, S.K., Desplats, P.A., Boyer, L., Aigner, S., Hetzer, C., Loher, T., Vilar, M., Campioni, S., Tzitzilonis, C., Soragni, A., Jessberger, S., Mira, H., Consiglio, A., Pham, E., Masliah, E.,

Gage, F.H. and Riek, R. (2011) 'In vivo demonstration that alpha-synuclein oligomers are toxic', *Proc Natl Acad Sci U S A*, 108(10), pp. 4194-9.
Wolfe, J.M., Butcher, S.J., Lee, C. and Hyle, M. (2003) 'Changing your mind: on the contributions of top-down and bottom-up guidance in visual search for feature singletons', *J Exp Psychol Hum Percept Perform*, 29(2), pp. 483-502.
Wong-Riley, M., Antuono, P., Ho, K.C., Egan, R., Hevner, R., Liebl, W., Huang, Z., Rachel, R. and Jones, J. (1997) 'Cytochrome oxidase in Alzheimer's disease: biochemical, histochemical, and immunohistochemical analyses of the visual and other systems', *Vision Res*, 37(24), pp. 3593-608.
World Health, O. (2012) *Dementia: a public health priority*. World Health Organization.
Wurtz, R.H., Joiner, W.M. and Berman, R.A. (2011) 'Neuronal mechanisms for visual stability: progress and problems', *Philos Trans R Soc Lond B Biol Sci*, 366(1564), pp. 492-503.
Xiong, N., Long, X., Xiong, J., Jia, M., Chen, C., Huang, J., Ghoorah, D., Kong, X., Lin, Z. and Wang, T. (2012) 'Mitochondrial complex I inhibitor rotenone-induced toxicity and its potential mechanisms in Parkinson's disease models', *Crit Rev Toxicol*, 42(7), pp. 613-32.
Xu, X., Ichida, J.M., Allison, J.D., Boyd, J.D., Bonds, A.B. and Casagrande, V.A. (2001) 'A comparison of koniocellular, magnocellular and parvocellular receptive field properties in the lateral geniculate nucleus of the owl monkey (Aotus trivirgatus)', *J Physiol*, 531(Pt 1), pp. 203-18.
Xuereb, J.H., Perry, R.H., Candy, J.M., Perry, E.K., Marshall, E. and Bonham, J.R. (1991) 'Nerve cell loss in the thalamus in Alzheimer's disease and Parkinson's disease', *Brain*, 114 ( Pt 3), pp. 1363-79.
Yamada, T., McGeer, P.L. and McGeer, E.G. (1992) 'Lewy bodies in Parkinson's disease are recognized by antibodies to complement proteins', *Acta Neuropathol*, 84(1), pp. 100-4.
Yamamoto, R., Iseki, E., Marui, W., Togo, T., Katsuse, O., Kato, M., Isojima, D., Akatsu, H., Kosaka, K. and Arai, H. (2005) 'Non-uniformity in the regional pattern of Lewy pathology in brains of dementia with Lewy bodies', *Neuropathology*, 25(3), pp. 188-94.
Yamamoto, R., Iseki, E., Murayama, N., Minegishi, M., Marui, W., Togo, T., Katsuse, O., Kato, M., Iwatsubo, T., Kosaka, K. and Arai, H. (2006) 'Investigation of Lewy pathology in the visual pathway of brains of dementia with Lewy bodies', *J Neurol Sci*, 246(1-2), pp. 95-101.
Yamamoto, R., Iseki, E., Murayama, N., Minegishi, M., Marui, W., Togo, T., Katsuse, O., Kosaka, K., Kato, M., Iwatsubo, T. and Arai, H. (2007) 'Correlation in Lewy pathology between the claustrum and visual areas in brains of dementia with Lewy bodies', *Neurosci Lett*, 415(3), pp. 219-24.
Yarnall, A.J., Breen, D.P., Duncan, G.W., Khoo, T.K., Coleman, S.Y., Firbank, M.J., Nombela, C., Winder-Rhodes, S., Evans, J.R., Rowe, J.B., Mollenhauer, B., Kruse, N., Hudson, G., Chinnery, P.F., O'Brien, J.T., Robbins, T.W., Wesnes, K., Brooks, D.J., Barker, R.A. and Burn, D.J. (2014) 'Characterizing mild cognitive impairment in incident Parkinson disease: the ICICLE-PD study', *Neurology*, 82(4), pp. 308-16.
Yee, R.D. (1983) 'Eye movement recording as a clinical tool', *Ophthalmology*, 90(3), pp. 211-22.
Yi, H.A., Moller, C., Dieleman, N., Bouwman, F.H., Barkhof, F., Scheltens, P., van der Flier, W.M. and Vrenken, H. (2016) 'Relation between subcortical grey matter atrophy and conversion from mild cognitive impairment to Alzheimer's disease', *J Neurol Neurosurg Psychiatry*, 87(4), pp. 425-32.
Yokota, O., Davidson, Y., Arai, T., Hasegawa, M., Akiyama, H., Ishizu, H., Terada, S., Sikkink, S., Pickering-Brown, S. and Mann, D.M. (2010) 'Effect of topographical distribution of alpha-synuclein pathology on TDP-43 accumulation in Lewy body disease', *Acta Neuropathol*, 120(6), pp. 789-801.
Yoshizawa, H., Vonsattel, J.P. and Honig, L.S. (2013) 'Early neuropsychological discriminants for Lewy body disease: an autopsy series', *J Neurol Neurosurg Psychiatry*, 84(12), pp. 1326-30.
Yu, J.X., Bradt, B.M. and Cooper, N.R. (2002) 'Constitutive expression of proinflammatory complement components by subsets of neurons in the central nervous system', *J Neuroimmunol*, 123(1-2), pp. 91-101.
Yucel, Y.H., Zhang, Q., Gupta, N., Kaufman, P.L. and Weinreb, R.N. (2000) 'Loss of neurons in magnocellular and parvocellular layers of the lateral geniculate nucleus in glaucoma', *Arch Ophthalmol*, 118(3), pp. 378-84.

Zahirovic, I., Wattmo, C., Torisson, G., Minthon, L. and Londos, E. (2016) 'Prevalence of Dementia With Lewy Body Symptoms: A Cross-Sectional Study in 40 Swedish Nursing Homes', *J Am Med Dir Assoc*.
Zakharov, S.D., Hulleman, J.D., Dutseva, E.A., Antonenko, Y.N., Rochet, J.C. and Cramer, W.A. (2007) 'Helical alpha-synuclein forms highly conductive ion channels', *Biochemistry*, 46(50), pp. 14369-79.
Zhang, P., Zhou, H., Wen, W. and He, S. (2015) 'Layer-specific response properties of the human lateral geniculate nucleus and superior colliculus', *Neuroimage*, 111, pp. 159-66.
Zhou, H., Schafer, R.J. and Desimone, R. (2016) 'Pulvinar-Cortex Interactions in Vision and Attention', *Neuron*, 89(1), pp. 209-20.
Zhou, J., Fonseca, M.I., Pisalyaput, K. and Tenner, A.J. (2008) 'Complement C3 and C4 expression in C1q sufficient and deficient mouse models of Alzheimer's disease', *J Neurochem*, 106(5), pp. 2080-92.
Zikou, A.K., Kitsos, G., Tzarouchi, L.C., Astrakas, L., Alexiou, G.A. and Argyropoulou, M.I. (2012) 'Voxel-based morphometry and diffusion tensor imaging of the optic pathway in primary open-angle glaucoma: a preliminary study', *AJNR Am J Neuroradiol*, 33(1), pp. 128-34.
Zinner-Feyerabend, M. and Braak, E. (1991) 'Glutamic acid decarboxylase (GAD)-immunoreactive structures in the adult human lateral geniculate nucleus', *Anat Embryol (Berl)*, 183(2), pp. 111-7.